RESEARCH

UDOT CONNECTING COMMUNITIES

Utah Department of Transportation - Research Division
4501 South 2700 West, Box 148410 - Salt Lake City, Utah 84114-8410

Report No. UT-09.11

IMPLEMENTATION OF THE MECHANISTIC-EMPIRICAL PAVEMENT DESIGN GUIDE IN UTAH: VALIDATION, CALIBRATION, AND DEVELOPMENT OF THE UDOT MEPDG USER'S GUIDE

Prepared For:

Utah Department of Transportation
Research Division

Submitted By:

Applied Research Associates, Inc.

Authored By:

Michael I. Darter, P.E.
Leslie Titus-Glover
Harold L. Von Quintus, P.E.

October 2009

INSIDE COVER

DISCLAIMER

The authors alone are responsible for the preparation and accuracy of the information, data, analysis, discussions, recommendations, and conclusions presented herein. The contents do not necessarily reflect the views, opinions, endorsements, or policies of the Utah Department of Transportation and the US Department of Transportation. The Utah Department of Transportation makes no representation or warranty of any kind, and assumes no liability therefore.

THIS PAGE INTENTIONALLY LEFT BLANK

1. Report No.	2. Government Accession No.	3. Recipient's Catalog No.
UT- 09.11		

4. Title and Subtitle	5. Report Date
IMPLEMENTATION OF THE MECHANISTIC-EMPIRICAL PAVEMENT DESIGN GUIDE IN UTAH: VALIDATION, CALIBRATION, AND DEVELOPMENT OF THE UDOT MEPDG USER'S GUIDE	October 2009
	6. Performing Organization Code
7. Authors	8. Performing Organization Report No.
Michael I. Darter, Leslie Titus-Glover, and Harold L. Von Quintus	
9. Performing Organization Name and Address	10. Work Unit No. (TRAIS)
Applied Research Associates, Inc. 100 Trade Centre Dr., Suite 200 Champaign, IL 61820-7233	5H06221H
	11. Contract or Grant No.
	069083
12. Sponsoring Agency Name and Address	13. Type of Report and Period Covered
Utah Department of Transportation Research Division 4501 South 2700 West Salt Lake City, UT 84114-8410	Final Research Report October 2005 to June 2009
	14. Sponsoring Agency Code
	PIC No. UT03.203

15. Supplementary Notes

This report was prepared in cooperation with the Utah Department of Transportation.

16. Abstract

Highway agencies across the nation are moving towards implementation of the new AASHTO Mechanistic-Empirical Pavement Design Guide (MEPDG) for pavement design. The objective of this project was to implement the MEPDG into the daily operations of the Utah Department of Transportation (UDOT). The implementation of the MEPDG as a UDOT standard required modifications in some UDOT pavement design protocols (i.e., lab testing procedures, equipment, and protocols, traffic data reporting, software issues, design output interpretation, and others). A key requirement is validation of the MEPDG's nationally calibrated pavement distress and smoothness prediction models when applied under Utah conditions and performing local calibration if needed. This was accomplished using data from Long Term Pavement Performance (LTPP) projects located in Utah and UDOT pavement management system (PMS) pavement sections. The nationally calibrated MEPDG models were evaluated. With the exception of the new hot-mix asphalt (HMA) pavement total rutting model, all other models were found to be reasonable. The rutting model was locally calibrated to increase goodness of fit and remove significant bias. Due to the nature of the data used in model validation, it is recommended that further MEPDG model validation be accomplished in the future using a database that contains HMA pavement and jointed plain concrete pavement (JPCP) exhibiting moderate to severe deterioration. This report represents Phase II of the UDOT MEPDG implementation study and builds on the Phase I study report completed in 2005 for UDOT. The *Draft User's Guide for UDOT Mechanistic-Empirical Pavement Design* (UDOT Research Report No. UT-09.11a, dated October 2009) incorporates the findings of this report as inputs and pavement design guidelines for Utah for use by UDOT's pavement design engineers during trial implementation of the MEPDG.

17. Key Words	18. Distribution Statement	23. Registrant's Seal
Pavement, mechanistic, design, concrete, asphalt, calibration, MEPDG, user's guide	UDOT Research Division 4501 South 2700 West, Box 148410 Salt Lake City, UT 84114-8410 http://www.udot.utah.gov/go/research	

19. Security Classification (of this report)	20. Security Classification (of this page)	21. No. of Pages	22. Price
Unclassified	Unclassified	210	

THIS PAGE INTENTIONALLY LEFT BLANK

ACKNOWLEDGMENTS

This research was made possible with funding from the Utah Department of Transportation (UDOT). The authors express their deep gratitude to UDOT whose staff assisted the ARA staff in many ways. We are particularly grateful to Mr. Steve Anderson (pavement design), Mr. Todd Hadden (traffic data), Mr. Tim Biel (materials), Mr. Kevin Van Frank (materials), Mr. Gary Kuhl (pavement management system and traffic data), Mr. John Butterfield (materials), and Mr. Doug Anderson (research) for their extensive assistance throughout the project.

THIS PAGE INTENTIONALLY LEFT BLANK

TABLE OF CONTENTS

LIST OF FIGURES ..... **xi**

LIST OF TABLES ..... **xiii**

EXECUTIVE SUMMARY **1**

Introduction 1
Research Methodology 1
Research Results 2
Summary and Conclusions 4

1.0 INTRODUCTION **5**

1.1 Background 5
1.2 Scope 11
1.3 Organization of Report 12

2.0 NEW HMA AND NEW JPCP PERFORMANCE PREDICTION MODELS **13**

2.1 New and Reconstructed HMA Pavements 13
2.2 New JPCP 19

3.0 FRAMEWORK FOR MEPDG MODEL VALIDATION AND RECALIBRATION **25**

3.1 Step 1: Select Hierarchical Input Level 25
3.2 Step 2: Experimental Factorial & Matrix or Sampling Template 29
3.3 Step 3: Estimate Minimum Sample Size (Number of Pavement Projects) Required for Each Distress/IRI Prediction Model Validation and Local Calibration 30
3.4 Step 4: Select Projects 31
3.5 Step 5: Extract and Evaluate Distress and Project Data 32
3.6 Step 6: Conduct Field and Forensic Investigations 45
3.7 Steps 7 through 10: Assess Local Bias and Standard Error of the Estimate from Global Calibration Factors and Eliminate/Reduce Standard Error of the Estimate and Local Bias of Distress Prediction Models 45
3.8 Step 11: Interpretation of Results and Deciding on Adequacy of Calibration Factors 52

4.0 VALIDATION/RECALIBRATION OF SELECTED MEPDG MODELS **53**

4.1 New HMA Pavement Models 53
4.2 New JPCP 67

TABLE OF CONTENTS, CONTINUED

5.0 SENSITIVITY ANALYSIS OF LOCALLY CALIBRATED MEPDG MODELS 75

5.1 Scope of Sensitivity Analysis 75
5.2 Selected HMA Pavement Baseline Designs 75
5.3 Sensitivity Analysis Results for Locally Calibrated Rutting Model 75
5.4 Summary 81

6.0 SUMMARY, CONCLUSIONS, AND RECOMMENDATIONS 83

6.1 Summary 83
6.2 Conclusions and Recommendations 85
6.3 Draft User's Guide and Future Updates 85

REFERENCES 87

APPENDIX A. DISTRESS AND IRI DATA PLOTS FOR HMA SURFACED PAVEMENTS 89

APPENDIX B. DISTRESS AND IRI DATA PLOTS FOR JPC SURFACED PAVEMENTS 119

APPENDIX C. MEPDG INPUT DATA 141

APPENDIX D. SUMMARY OF TRAFFIC DATA 183

APPENDIX E. SUBGRADE SOIL PROPERTIES CHARACTERIZATION 193

LIST OF FIGURES

Figure 1. Map showing the locations of many of the LTPP test pavements used for calibration of the MEPDG. 6
Figure 2. Map showing the location of HMA surfaced pavement projects identified for local calibration/validation. 36
Figure 3. Map showing the location of JPCP projects identified for local calibration/validation. 36
Figure 4. UDOT PMS pavement distress data entry form, highlighting units of measurement and reporting. 38
Figure 5. Plot of UDOT PMS versus LTPP measured rutting for the projects listed in Table 9. 40
Figure 6. Histogram showing distribution of measured alligator cracking. 54
Figure 7. Histogram showing distribution of measured transverse "thermal" cracking. 55
Figure 8. Histogram showing distribution of measured total rutting for all projects used in analysis. 59
Figure 9. Plot of measured versus MEPDG predicted HMA pavement total rutting. . 59
Figure 10. Plot of measured versus MEPDG predicted HMA pavement total rutting for LTPP projects only (viscosity graded binders). 61
Figure 11. Plot of measured versus MEPDG predicted HMA pavement total rutting for UDOT PMS projects only (SuperPave binders). 62
Figure 12. Plot of measured versus locally calibrated model predicted HMA pavement total rutting. 64
Figure 13. Histogram showing distribution of measured IRI for HMA. 65
Figure 14. Plot of measured versus MEPDG predicted HMA pavement IRI. 66
Figure 15. Histogram showing distribution of measured percent slabs cracked. 68
Figure 16. Plot of measured versus MEPDG predicted JPCP percent slabs with transverse cracking. 68
Figure 17. Histogram showing distribution of measured transverse joint faulting for all projects evaluated. 70
Figure 18. Plot of measured versus MEPDG predicted JPCP faulting. 70
Figure 19. Histogram showing distribution of measured JPCP IRI. 72
Figure 20. Plot of measured versus MEPDG predicted JPCP pavement IRI. 72
Figure 21. Plot showing the effect of base type on predicted rutting. 77
Figure 22. Plot showing the effect of climate on predicted rutting. 78
Figure 23. Plot showing the effect of HMA thickness on predicted rutting. 80
Figure 24. Plot showing the effect of subgrade type on predicted rutting. 80
Figure 25. Plot showing the effect of HMA air voids on predicted rutting. 81

THIS PAGE INTENTIONALLY LEFT BLANK

LIST OF TABLES

Table 1. Improvements to original AASHTO pavement performance prediction models by the MEPDG. 7
Table 2. Timeline of key AASHTO design and pavement technology development leading to the MEPDG. 9
Table 3. Recommended hierarchical inputs levels for the key data required by the MEPDG for new HMA and HMA overlaid pavements. 27
Table 4. Recommended hierarchical inputs levels for the key data required by the MEPDG for new JPCP and JPCP subjected to CPR. 28
Table 5. Simplified sampling template for the validation and local calibration of new and rehabilitated HMA surfaced pavements. 30
Table 6. Simplified sampling template for the validation and local calibration of new and rehabilitated JPCP. 30
Table 7. Estimated number of pavement projects required for the validation and local calibration (obtained from AASHTO 2008). 31
Table 8. HMA and JPCP projects identified for validation and local calibration (LTPP 2008 and UDOT PMS projects). 33
Table 9. Rutting data used for developing transformation relationship. 40
Table 10. Comparison of range of distress/IRI values with design criteria or threshold values. 44
Table 11. Predominant sources of data used for MEPDG performance models verification in Utah. 46
Table 12. Shortlist of HMA and HMA overlaid HMA pavement projects with adequate performance included in analysis. 47
Table 13. Shortlist of JPCP projects with adequate performance included in analysis. 48
Table 14. Simplified sampling template for the validation and local calibration of new and rehabilitated HMA surfaced pavements. 49
Table 15. Simplified sampling template for the validation and local calibration of new and rehabilitated JPCP. 49
Table 16. Summary of national calibration under NCHRP 1-40D new HMA pavement and new JPCP model statistics. 50
Table 17. Comparison of measured and predicted transverse cracking (percentage of all measurements). 54
Table 18. Comparison of measured and predicted transverse cracking (all pavements). 56
Table 19. Comparison of measured and predicted transverse cracking (by binder type). 56
Table 20. Statistical comparison of measured and predicted rutting data. 60
Table 21. Statistical comparison of measured and predicted rutting data for LTPP projects only (viscosity graded binders). 61
Table 22. Statistical comparison of measured and predicted rutting data for UDOT PMS projects only (SuperPave binders). 62

LIST OF TABLES, CONTINUED

Table 23. Statistical comparison of measured and recalibrated rutting model predicted rutting data. 64
Table 24. Statistical comparison of measured and MEPDG predicted IRI data. 66
Table 25. Statistical comparison of measured and MEPDG predicted transverse slab cracking data. 69
Table 26. Statistical comparison of measured and MEPDG predicted transverse joint faulting data. 71
Table 27. Statistical comparison of measured and MEPDG predicted JPCP IRI data. ... 73
Table 28. Input parameters of interest used in the HMA models sensitivity analysis... 76
Table 29. Input parameters of interest used in the HMA models sensitivity analysis... 77

EXECUTIVE SUMMARY

Introduction

Many highway agencies across the U.S. are in the process of implementing the recently completed American Association of State and Highway Transportation Officials (AASHTO) Mechanistic-Empirical Pavement Design Guide, Interim Edition: A Manual of Practice (MEPDG).

The Utah Department of Transportation (UDOT) initiated research studies in 2003 to begin this process. The goals of the UDOT MEPDG implementation project were to (1) determine the suitability of the MEPDG for Utah, (2) define needed modifications to the MEPDG (including pavement performance prediction models) if required, (3) improve materials characterization and obtain necessary new equipment, (4) prioritize and implement needed modifications incrementally based on their impact on pavement design, and (5) provide training to UDOT staff on the use of the MEPDG.

In order to fully achieve these goals, a major effort was required to validate the nationally calibrated "global calibration" MEPDG models for Utah conditions and then perform local calibration of the national models as needed to make them suitable for Utah conditions. This work required the consideration of all inputs to the MEPDG to establish the most appropriate methodology to obtain them for design.

Research Methodology

This project was conducted in two phases. Phase I involved (1) identification and detailed description of the Long Term Pavement Performance (LTPP) projects to be used for model validation and local calibration, (2) identification of gaps in assembled LTPP projects, (3) verification of the MEPDG version 0.8 models and design procedure, (4) sensitivity analysis using version 0.8 of the MEPDG, (5) comparison of the MEPDG and the existing UDOT pavement design methods, and (6) development of scope of future work required for full implementation of the MEPDG in Utah. A three-volume, unpublished report was prepared under Phase I and presented to UDOT in 2005.

Phase II involved validation of the nationally calibrated MEPDG models (version 1.0) using LTPP and UDOT pavement management system (PMS) projects. Specifically, work done included (1) identifying suitable HMA and JPCP projects, (2) assembling all relevant data for the projects identified and developing a project database, (3) coding up the assembled data into the MEPDG, running the MEPDG, and developing a database of MEPDG outputs (predicted pavement distress and smoothness) and measured pavement distress and smoothness, and (4) determining the national models goodness of fit and possible bias in predicted distress and smoothness.

Based on the outcome of the validation effort, models found to be inadequate (i.e., poor goodness of fit or biased predictions of distress and IRI or both) were recalibrated using Utah specific pavement projects to improve goodness of fit and remove bias.

This study focused on four pavement types:

1. New or reconstructed hot-mix asphalt (HMA) pavement.
2. HMA overlaid existing HMA pavement.
3. New or reconstructed jointed plain concrete pavement (JPCP).
4. Older JPCP subjected to concrete pavement restoration (CPR). CPR often includes several types of treatments such as full-depth repairs, load transfer restoration, etc. but must always include diamond grinding to make it possible to design with the MEPDG.

This report documents all work done under both Phases I and II performed for UDOT.

Research Results

Results for the validation and local calibration effort are summarized in the following sections.

New HMA and HMA Overlaid HMA Pavements

- Alligator fatigue cracking: Due to the nature of alligator cracking data available a non statistical approach for validating this model was adopted. Alligator cracking model validation showed that the national model predicted alligator cracking relatively well in Utah conditions. However, the alligator cracking model could not be evaluated for pavements exhibiting significant amounts of the distress as projects experiencing significant deterioration were not available. There is need to identify and include HMA projects with moderate to severe levels of alligator cracking and include them in future validation studies.
- Transverse "thermal" cracking: Due to the nature of transverse cracking data available, a non statistical approach for validating this model was adopted. The non-statistical comparison of predicted and measured transverse cracking data showed that for the relatively younger pavements constructed using UDOT SuperPave binders, the national model predicted transverse cracking well. For the older LTPP pavements constructed using conventional asphalt binders (AC-10 and AC-20) the national model was very inadequate. The project team decided not to recalibrate this model since it seemed to predict transverse cracking well for the current UDOT HMA designs using SuperPave. There is, however, need for continuing monitoring of the existing UDOT pavements with SuperPave mixes to determine if the national model will be able to predict transverse cracking once they start to deteriorate and exhibit this distress. Also,

developing UDOT mix specific HMA input properties (i.e., creep compliance and tensile strength) used for predicting HMA transverse cracking will increase model prediction capability.

- Rutting: The MEPDG national rutting model predicted rutting adequately for older pavements constructed using viscosity graded asphalt mixes. The same model, however, poorly predicted rutting with significant bias when applied to newer HMA pavement designs with SuperPave HMA mixes. Therefore, there was a need for local calibration of the national model to enable it to predict rutting much more accurately under current Utah HMA pavement design (including HMA mix design) and construction conditions. Local calibration was done and produced new local calibration coefficients for all three rutting submodels (HMA, base, and subgrade). The new local calibration coefficients based on HMA thickness are as follows:

Pavement Type	**Rutting Submodels Local Calibration Coefficients**		
	HMA (β_{r1})	**Base (β_{B1})**	**Subgrade (β_{s1})**
New HMA	0.560	0.604	0.400
HMA overlaid HMA	0.560	0.604	0.400

  Local calibration significantly improved on the model accuracy and removed all significant bias. A sensitivity analysis performed showed the locally calibrated model to be reasonable.
- HMA International Roughness Index (IRI): There was good correlation between measured and MEPDG predicted IRI and standard error of estimate (SEE) was approximately the same as that reported for the national MEPDG IRI model. Although there was some bias in predicted IRI, the bias was deemed as not significant.

New JPCP and JPCP Subjected to CPR

Results for the nationally calibrated MEPDG models validation and local calibration effort in Utah for JPCP are summarized as follows:

- Transverse "fatigue" cracking in the slab: A full evaluation of this model was conducted. Results showed very adequate goodness of fit and no significant bias in predicted transverse cracking.
- Transverse joint faulting: The MEPDG model predicted faulting reasonably well with an adequate goodness of fit and no significant bias in predicted faulting.
- IRI: Predicted IRI using the nationally calibrated MEPDG model showed the model predicting IRI well under Utah conditions with an adequate goodness of fit and no significant bias in predicted IRI.

Summary and Conclusions

The MEPDG models were reviewed thoroughly for use under Utah conditions using both LTPP and UDOT PMS projects.

The review of the MEPDG models indicated that with the exception of the HMA rutting model, all the models evaluated predicted distress/IRI reasonably. However, for some models the range of distress data used in evaluation was limited. This raises concern about their ability to predict higher levels of distress reasonably.

Therefore, based on the analysis performed, the following conclusions are drawn:

- Full validation of the MEPDG distress and IRI models needs to be a continuous process to fully consider the impacts of current pavement design, materials, and construction practices on model adequacy. By doing so, projects from which moderate to high levels of distress currently are obtained, which tend to be older and mostly were constructed using outdated pavement design features and materials types (e.g., Marshall versus SuperPave HMA mixes), will gradually be removed from the project database.

- The mix of original MEPDG and locally calibrated models presented in this report appear to predict distress/IRI reasonably well, within the limitations such as:
    a. HMA transverse cracking using Level 3 inputs does not predict transverse cracking adequately for conventional asphalt binders and thus only lab tested HMA creep compliance and tensile strength must be used in predicting transverse cracking in order to obtain reasonable predictions.
    b. The HMA rutting model must be used only with the local calibration coefficients specified.
    c. The HMA pavement alligator fatigue cracking is valid only for low levels of cracking.
    d. The national and locally calibrated models are valid only for the limited conditions under which they were evaluated.

The *Draft User's Guide for UDOT Mechanistic-Empirical Pavement Design* is presented in a companion UDOT research report (Report No. UT-09.11a) dated October 2009. The Draft User's Guide presents an input by input overview and recommendations for designing pavements in Utah. The Draft User's Guide was developed using version 1.0 of the MEPDG software. Future updates of this software are expected. This, along with UDOT's experience with the MEPDG, will lead to future updates of the UDOT MEPDG Draft User's Guide which will be published by UDOT as a standalone document.

1.0 INTRODUCTION

1.1 Background

1.1.1 Initial Development

The 1962, 1972, 1986, and 1993 versions of the American Association of State Highway and Transportation Officials (AASHTO) Guide for the Design of Pavement Structures have been the primary document used to design new and rehabilitated highway pavements in the United States for many decades (AASHTO 1972, AASHTO 1986, AASHTO 1993). Design algorithms and procedures presented in these Guides were based on empirical relationships derived from the American Association of State Highway Officials (AASHO) Road Test in the late 1950's. The AASHO Road Test comprised of (1) the design and construction of a limited number of flexible and rigid pavement sections at a location in northern Illinois and (2) subjecting the test pavements to repeated truck traffic over a 2 year period while monitoring performance in the form of pavement distress and smoothness loss (HRB 1962). Using the data assembled from the Road Test, empirical models relating key pavement properties and traffic to performance were developed. The models developed and modified over the years have formed the empirical basis for pavement design in the U.S. over the past five decades.

Significant progress and advancement have been made since the AASHO Road Test in (1) understanding the mechanisms that cause pavement distress and deterioration, (2) simulating pavement responses to repeated traffic and environmental loading, and (3) relating pavement responses directly to distress development and progression. These advancements have increased the ability to develop a mechanistic based pavement design procedure that far more properly relates applied traffic loads to pavement responses leading to more accurate prediction of deterioration. This approach also better simulates the interaction between paving material properties and environment over time. As a consequence, in the mid 1990's, the AASHTO Joint Task Force on Pavements (JTFP), initiated National Cooperative Highway Research Program (NCHRP) Project 1-37A: *Development of the 2002 Guide for the Design of New and Rehabilitated Pavement Structures: Phase II* to develop a mechanistic based design procedure for new and rehabilitated pavement structures. After six years of development and testing, NCHRP Project 1-37A in 2004 produced a new mechanistic based pavement design procedure called the Mechanistic-Empirical Pavement Design Guide (MEPDG). The MEPDG consisted of (1) a Guide for mechanistic-empirical pavement design and analysis, (2) companion software and a software user manual, and (3) MEPDG implementation and training materials. Pavement types covered by the MEPDG include new and rehabilitated flexible and rigid pavements.

The MEPDG basically contains several modules used for simulating all the interacting processes that lead to pavement fatigue cracking, permanent deformation, joint

faulting, low temperature cracking distress development and progression and associated smoothness loss. The main modules are:

- Traffic (used to model total truck traffic growth, truck class distribution, various volume adjustments, axles per truck type, and axle load distribution).
- Climate (the Integrated Climatic Model is used to model temperature and moisture within the pavement structure and subgrade).
- Materials characterization (several models are used to model gain in Portland cement concrete [PCC] strength, changes in PCC modulus, changes in HMA dynamic modulus with variation in temperature and binder aging, and so on).
- Pavement responses (layer elastic and finite-element based analysis module used to compute critical pavement responses, i.e., stresses, strains, and deflections).
- Distress prediction (transfer models used to estimate damage and other critical parameters that are then used to predict key distress types.
- Smoothness prediction models for IRI.

Outputs from the MEPDG distress prediction modules (i.e., predicted distress and smoothness) were calibrated using data from hundreds of flexible, rigid, and rehabilitated pavement test sections contained in the Long-Term Pavement Performance (LTPP) program.

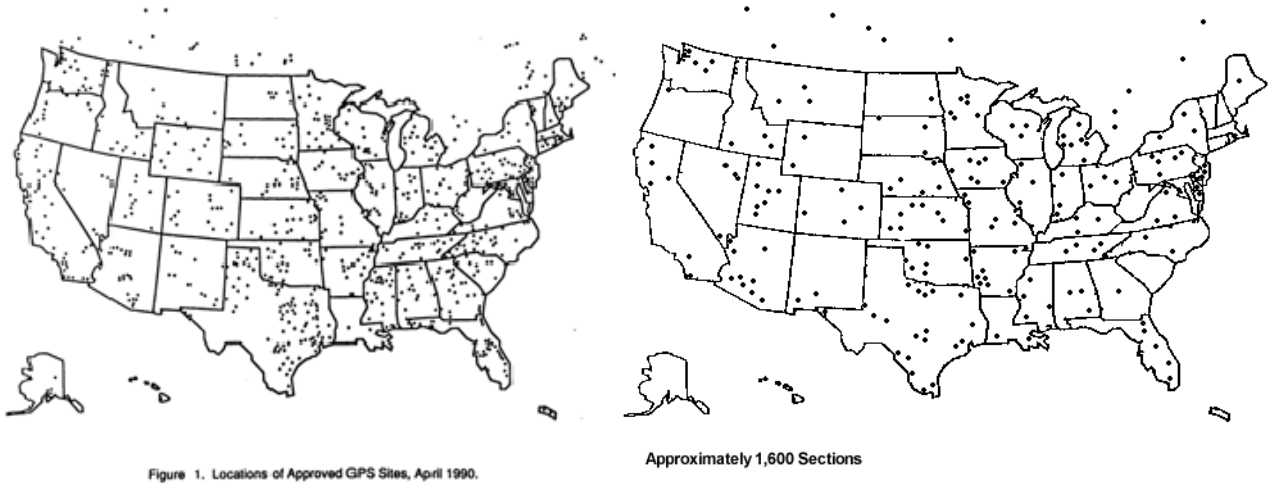

GPS Sections SPS Sections

Figure 1. Map showing the locations of many of the LTPP test pavements used for calibration of the MEPDG.

The MEPDG differs from previous AASHTO pavement design Guides by not providing a design pavement thickness as its main output. Design is based on a new philosophy that estimates damage incrementally, accumulates damage and predicts distress and smoothness over time. Once distress/smoothness is predicted at a given reliability level over time, estimates of predicted distress/IRI are compared to distress/IRI threshold values used to set a given design criteria. Designs with predicted distress/IRI less than the threshold values are deemed as adequate. Pavements not deemed adequate are redesigned. Key differences between the MEPDG and previous AASHTO pavement design Guides are presented in Table 1.

Table 1. Improvements to original AASHTO pavement performance prediction models by the MEPDG.

Performance Prediction	**Past AASHTO Pavement Design Guides**	**MEPDG Improvements**
Type of Pavement	• All flexible pavement types are designed by a single "flexible" pavement model • All rigid pavement types are designed by a single "rigid" pavement model.	Developed separate models for each combination of major pavement type and key distress. Replaced overall pavement condition with smoothness measured using International Roughness Index (IRI). Incorporated the Integrated Climatic Model (ICM) into the design process using weather station data.
Pavement Rehabilitation	Extrapolation from new design only.	Specific design models and methodology for HMA and PCC overlays and CPR.
Climate Across the United States	Models are only valid for northern Illinois (wet-freeze climate)	Calibrated models using project specific climate data obtained from over 800 weather stations located throughout the U.S.
Traffic Loadings	Uses equivalent single axle load concept (ESAL)	Consider individual axle type and actual loading for each axle type along with tire and axle characteristics such as spacing, location, pressure and so on.
Subgrade	Implicit is the soil at the AASHTO Road Test, IL (A-6, silty sand material)	Considers project specific subgrade along with its properties such as gradation, Atterberg limits, saturation, density, hydraulic conductivity, and resilient modulus.
Pavement Structure	Pavement structure is defined only by the structural number, SN for flexible pavements and PCC layer thickness, D for rigid pavements	Define pavement structure using all layer types and thicknesses (i.e., surface HMA or PCC, granular or stabilized base and subbase types, subgrade, and bedrock).
Database to Validate Models	AASHTO Road Test (limited to the site conditions of Northern Illinois)	Used national pavement and climate databases such as LTPP and National Climatic Data Center (NCDC) data.
Characterizing Pavement Condition	Present Serviceability Rating (PSR) only (subjective user serviceability)	Considers far more objective measures of pavement condition: smoothness (IRI) and individual surface distresses.

1.1.2 Follow Up Work to Verify and Validate the MEPDG

Following the completion of NCHRP Project 1-37A, the AASHTO JTFP developed a plan for the adoption and implementation of the MEPDG by State highway agencies (SHA). Key components of this plan were:

1. Conduct an independent, third-party review to test the MEPDG's underlying assumptions, evaluate its engineering reasonableness and design reliability, and identify opportunities for its implementation in day-to-day design production work.
2. Develop a MEPDG engineering user manual and MEPDG local calibration guide.
3. Provide technical assistance to incorporate findings and recommendations provided by the independent review panel into the MEPDG.

The three key components of the AASHTO JTFP's implementation plan proceeded under the following NCHRP projects:

- NCHRP 01-40A: Independent Review of the Recommended Mechanistic-Empirical Design Guide and Software.
- NCHRP 01-40B: User Manual and Local Calibration Guide for the Mechanistic-Empirical Pavement Design Guide and Software.
- NCHRP 01-40D (01&02): Technical Assistance to NCHRP and NCHRP Project 1-40A: Versions 0.9 and 1.0 of the M-E Pavement Design Software.

The completion of all or substantial portions of the above referenced projects resulted in the development of the following products:

- NCHRP Research Results Digest 307: Independent Review of the Mechanistic-Empirical Pavement Design Guide and Software (1-40A).
- Mechanistic-Empirical Pavement Design Guide, AASHTO Interim Edition: A Manual of Practice (1-40B).
- MEPDG Local Calibration Guide (1-40B).
- NCHRP Research Results Digest 308: Changes to the Mechanistic-Empirical Pavement Design Guide Software through Version 0.900 (1-40D).
- Version 1.0 of MEPDG software (1-40D).

A timeline of key pavement technology development leading to the MEPDG is presented in Table 2.

Table 2. Timeline of key AASHTO design and pavement technology development leading to the MEPDG.

Time	Key Development in Pavement Technology
1958-60	AASHO Road Test
1962	First Interim AASHO Pavement Design Guide developed
1960's	Continuation of development of mechanistic concepts of previous decades and usage of high speed computers to obtain structural responses (e.g., elastic layered, finite element)
1972	Interim AASHTO Pavement Design Guide updated
1970's & 80's	Continuation of development of mechanistic concepts and material characterization, development of climatic models (e.g., ICM)
1986	Updated AASHTO Pavement Design Guide released with recommendation to move to mechanistic based design
1989	20-year LTPP program begins
1993	Revised overlay design procedures in AASHTO Pavement Design Guide
1996	National pavement engineering meeting recommended initiation of mechanistic design procedure
1998-2004	NCHRP 1-37A completed (mechanistic-empirical design, MEPDG)
200506	NCHRP 1-40A (independent review of the MEPDG)
2006-07	NCHRP 1-40D Revision and recalibration of MEPDG models
2006-08	NCHRP 1-40B Manual on local calibration
2003-present	Many State highway agencies begin the process of MEPDG implementation
2007	NCHRP 1-40D substantially completed with the development of Version 1.0 of MEPDG software
2007	Balloting and acceptance of MEPDG as an Interim AASHTO Guide
2008	Publication of Mechanistic-Empirical Pavement Design Guide, AASHTO Interim Edition: A Manual of Practice by AASHTO
2009	(1)Initiation of DARWin-ME v2.0 software intended to migrate the research software, resulting from the NCHRP Projects 1-37A and 1-40, to production software for use by the transportation community (2)Several NCHRP projects aimed at enhancing MEPDG models continue

1.1.3 Future Developments Related to MEPDG

Enhancing MEPDG Technology

Since the completion of NCHRP Project 1-37A and completion of substantial portions of NCHRP Projects 1-40D and 1-40B, the NCHRP has initiated several research projects aimed at enhancing various aspects of the MEPDG. A summary of these completed and ongoing projects is presented as follows:

- NCHRP 1-39: Traffic Data Collection, Analysis, and Forecasting for Mechanistic Pavement Design.
- NCHRP 1-41: Models for Predicting Reflection Cracking of Hot-Mix Asphalt Overlays.
- NCHRP 1-42A: Models for Predicting Top-Down Cracking of Hot-Mix Asphalt Layers.
- NCHRP 9-38: Endurance Limit of Hot-Mix Asphalt Mixtures to Prevent Fatigue Cracking in Flexible Pavements.
- NCHRP 9-30A: Calibration of Rutting Models for HMA Structural and Mix Design.

MEPDG Implementation

Utah was one of the first states to implement the original AASHTO Interim Design Guide in the early 1960's which required the entire decade. Utah was then one of the first States to begin implementation of the new AASHTO MEPDG in 2003. The main goals of the UDOT MEPDG implementation process were to (1) determine the suitability of the MEPDG for Utah, (2) define needed modifications to the MEPDG (including pavement performance prediction models) if required, (3) improve materials characterization and obtain necessary new equipment, (4) prioritize and implement needed modifications incrementally based on their impact on pavement design, (5) provide training to UDOT staff on the use of the MEPDG, and identify benefits from implementation of the MEPDG.

In order to fully achieve these goals, a validation of the nationally calibrated "global calibration" MEPDG models for Utah site, design, and construction conditions must be achieved. If any of the models are biased, they must be calibrated to remove the bias (over or under prediction of distress and IRI).

This project was conducted in two phases. Phase I involved (1) identification and detailed description of the LTPP projects to be used for model validation and local calibration, (2) identification of gaps in assembled LTPP projects, (3) verification of the MEPDG version 0.8 models and design procedure, (4) sensitivity analysis using version

0.8 of the MEPDG, (5) comparison of the MEPDG and the existing UDOT pavement design methods, and (6) development of scope of future work required for full implementation of the MEPDG in Utah. A three-volume, unpublished report was prepared under Phase I and presented to UDOT in 2005.

Phase II involved validation of the nationally calibrated MEPDG models (version 1.0) using LTPP and UDOT pavement management system (PMS) projects. Specifically, work done included (1) identifying suitable HMA and JPCP projects, (2) assembling all relevant data for the projects identified and developing a project database, (3) coding up the assembled data into the MEPDG, running the MEPDG, and developing a database of MEPDG outputs (predicted pavement distress and smoothness) and measured pavement distress and smoothness, and (4) determining the national models goodness of fit and possible bias in predicted distress and smoothness.

This report documents all work done under both Phases I and II performed for UDOT.

1.2 Scope

A range of new and rehabilitated pavements were of interest to UDOT and were included in the local validation and calibration.

1. New or reconstructed hot-mix asphalt (HMA) pavement.
2. HMA overlaid existing HMA pavement.
3. New or reconstructed jointed plain concrete pavement (JPCP).
4. JPCP subjected to concrete pavement restoration (CPR) that includes diamond grinding.

For the pavement types selected, the following performance indicators and thus, MEPDG prediction models, were of interest to UDOT as these represent the predominant structural and functional distresses that occur in Utah:

- HMA surfaced pavements.
    - Total rut depth.
    - Transverse "thermal" cracking.
    - Load related fatigue alligator cracking, bottom initiated cracks.
    - Smoothness (measured as International Roughness Index [IRI]).
- JPC surfaced pavements.
    - Mean transverse joint faulting.
    - Load related fatigue transverse slab cracking (includes both bottom and surface initiated cracks).
    - Smoothness (IRI).

1.3 Organization of Report

This report presents the results of validation and local calibration of selected MEPDG models for HMA surfaced pavements and JPCP in Utah. Chapter 2 describes the MEPDG models selected for validation and local calibration if needed. Chapter 3 describes the framework for model validation and local calibration.

Chapter 4 describes the model validation and recalibration effort. Sensitivity of the recalibrated models is presented in Chapter 5. Chapter 6 discusses the summary and conclusions from this study. Appendix A and B presents plots of measured distress/IRI over time. Appendix C presents detailed description of projects used in analysis while Appendix D presents a summary of initial truck traffic and truck traffic growth for the selected projects. Appendix E presents an example of soil data obtained from Utah specific county soil maps and used for obtaining project specific soil information required by the MEPDG.

The *Draft User's Guide for UDOT Mechanistic-Empirical Pavement Design* is presented in a companion UDOT research report (Report No. UT-09.11a) dated October 2009. The Draft User's Guide presents an input by input overview and recommendations for designing pavements in Utah. The Draft User's Guide was developed using version 1.0 of the MEPDG software. Future updates of this software are expected. This, along with UDOT's experience with the MEPDG, will lead to future updates of the UDOT MEPDG Draft User's Guide which will be published by UDOT as a standalone document.

2.0 NEW HMA AND NEW JPCP PERFORMANCE PREDICTION MODELS

A brief description of the MEPDG models used to predict performance is presented in this chapter. Detailed descriptions of these models and the entire MEPDG design procedure have been presented in several publications, including AASHTO's MEPDG Manual of Practice (AASHTO 2008), MEPDG reports developed under NCHRP Project 1-37A (ARA 2004) and NCHRP 1-40D (AASHTO 2008, Darter et al. 2007).

2.1 New and Reconstructed HMA Pavements

2.1.1 Alligator Cracking

Alligator cracking initiates at the bottom of the HMA layers and propagates to the surface with repeated application of heavy truck axles. Alligator cracking prediction in the MEPDG begins with the computation incrementally of HMA bottom up fatigue damage. This is done using a grid pattern throughout the HMA layers at critical depths to determine the location within the HMA layer subjected to the highest amount of horizontal tensile strain—the mechanistic parameters used to relate applied loading to fatigue damage. An incremental damage index, ΔDI, is calculated by dividing the actual number of axle loads by the allowable number of axle loads (note that computation of damage is based on Miner's hypothesis) within a specific time increment and axle load interval for each axle type (Miner 1945). The cumulative damage index for each critical location is determined by summing the incremental damage over time and traffic using equation 1 (AASHTO 2008):

$$DI = \sum (\Delta DI)_{j,m,l,p,T} = \sum \left(\frac{n}{N_{f-HMA}} \right)_{j,m,l,p,T} \quad (1)$$

where:

n	=	Actual number of axle load applications within a specific time period
j	=	Axle load interval
m	=	Axle load type (single, tandem, tridem, quad, or special axle configuration)
l	=	Truck type using the truck classification groups included in the MEPDG
p	=	Month
T	=	Median temperature for the five temperature intervals or quintiles used to subdivide each month, °F
$N_{f\text{-}HMA}$	=	Allowable number of axle load applications for a flexible pavement and HMA overlays to fatigue cracking

The allowable number of axle load applications needed for the incremental damage index computation is shown in equation 2 (AASHTO 2008).

$$N_{f-HMA} = k_{f1}(C)(C_H)\beta_{f1}(\varepsilon_t)^{k_{f2}\beta_{f2}}(E_{HMA})^{k_{f3}\beta_{f3}} \quad (2)$$

where:

$N_{f\text{-}HMA}$	=	Allowable number of axle load applications for a flexible pavement and HMA overlays to fatigue cracking
ε_t	=	Tensile strain at critical locations and calculated by the structural response model, in/in
E_{HMA}	=	Dynamic modulus of the HMA measured in compression, psi
k_{f1}, k_{f2}, k_{f3}	=	Global field calibration parameters (from the NCHRP 1-40D re-calibration; k_{f1} = 0.007566, k_{f2} = -3.9492, and k_{f3} = -1.281)
β_{f1}, β_{f2}, β_{f3}	=	Local or mixture specific field calibration constants; for the global calibration effort, these constants were set to 1.0

$$C = 10^M \quad (3)$$

$$M = 4.84\left(\frac{V_{be}}{V_a + V_{be}} - 0.69\right) \quad (4)$$

V_{be}	=	Effective asphalt content by volume, percent
V_a	=	Percent air voids in the HMA mixture (in situ only, not mixture design)
C_H	=	Thickness correction term as follows:

$$C_H = \frac{1}{0.000398 + \frac{0.003602}{1 + e^{(11.02 - 3.49 H_{HMA})}}} \quad (5)$$

H_{HMA}	=	Total HMA thickness, in

Alligator cracking is calculated from the cumulative damage over time (equation 1) using the relationship presented as equation 6 (AASHTO 2008).

$$FC_{Bottom} = \left(\frac{1}{60}\right)\left(\frac{C_4}{1 + e^{(C_1 C_1^* + C_2 C_2^* Log(DI_{Bottom}))}}\right) \quad (6)$$

where:

FC_{Bottom}	=	Area of alligator cracking that initiates at the bottom of the HMA layers, percent of total lane area
DI_{Bottom}	=	Cumulative damage index at the bottom of the HMA layers
$C_{1,2,4}$	=	Transfer function regression constants; C_4= 6,000; C_1=1.00; and C_2=1.00

$$C_1^* = -2C_2^* \tag{7}$$

$$C_2^* = -2.40874 - 39.748\left(1 + H_{HMA}\right)^{-2.856} \tag{8}$$

where: H_{HMA} = Total HMA thickness, in

2.1.2 Transverse Cracking (Low Temperature Induced)

For the MEPDG, the amount of crack propagation induced by a given thermal cooling cycle is predicted using the Paris law of crack propagation (AASHTO 2008).

$$\Delta C = A\left(\Delta K\right)^n \tag{9}$$

where:

ΔC	=	Change in the crack depth due to a cooling cycle
ΔK	=	Change in the stress intensity factor due to a cooling cycle
A, n	=	Fracture parameters for the HMA mixture

Experimental results indicate that reasonable estimates of A and n can be obtained from the indirect tensile creep-compliance and strength of the HMA in accordance with equations 10 and 11 (AASHTO 2008).

$$A = 10^{k_t \beta_t \left(4.389 - 2.52\, Log\left(E_{HMA} \sigma_m n\right)\right)} \tag{10}$$

where:

$$n = 0.8\left[1 + \frac{1}{m}\right] \tag{11}$$

k_t	=	Coefficient determined through global calibration for each input level (Level 1 = 5.0; Level 2 = 1.5; and Level 3 = 3.0)
E_{HMA}	=	HMA indirect tensile modulus, psi
σ_m	=	Mixture tensile strength, psi
m	=	The m-value derived from the indirect tensile creep compliance curve measured in the laboratory
β_t	=	Local or mixture calibration factor

Stress intensity factor, K, was incorporated in the MEPDG through the use of a simplified equation developed from theoretical finite element studies (equation 12).

$$K = \sigma_{tip}\left(0.45 + 1.99\left(C_o\right)^{0.56}\right) \tag{12}$$

where:

σ_{tip}	=	Far-field stress from pavement response model at depth of crack tip, psi
C_o	=	Current crack length, ft

The amount of transverse cracking is predicted by the MEPDG using an assumed relationship between the probability distribution of the log of the crack depth to HMA layer thickness ratio and the percent of cracking. Equation 13 shows the expression used to determine the amount of thermal cracking (AASHTO 2008).

$$TC = \beta_{t1} N\left[\frac{1}{\sigma_d} Log\left(\frac{C_d}{H_{HMA}}\right)\right] \tag{13}$$

Where:

TC	=	Thermal cracking, ft/mi
β_{t1}	=	Regression coefficient determined through global calibration (400)
$N[z]$	=	Standard normal distribution evaluated at [z]
σ_d	=	Standard deviation of the log of the depth of cracks in the pavement (0.769), in
C_d	=	Crack depth, in
H_{HMA}	=	Thickness of HMA layers, in

2.1.3 Rutting

Rutting is caused by the plastic or permanent vertical deformation in the HMA, unbound base/subbase layers, and subgrade/foundation soil. For the MEPDG, rutting is predicted by calculating incrementally the plastic vertical strain accumulated in each pavement layer due to applied axle loading. In other words, rutting is the sum of all plastic vertical strain at the mid-depth of each pavement layer within the pavement structure, accumulated over a given analysis period. The rate of pavement layer plastic deformation could vary significantly over a given time increment since (1) the pavement layer properties (HMA and unbound aggregate material and subgrade) do change with temperature (summer versus winter months) and moisture (wet versus dry) and (2) applied traffic could also be very different.

The MEPDG model for calculating total rutting is based on the universal "strain hardening" relationship developed from data obtained from repeated load permanent

deformation triaxial tests of both HMA mixtures and unbound aggregate materials and subgrade soils in the laboratory. The laboratory derived relationship was then calibrated to match field measured rut depth.

For all HMA mixtures types, the MEPDG field calibrated form of the laboratory derived relationship from repeated load permanent deformation tests is shown in equation 14.

$$\Delta_{p(HMA)} = \varepsilon_{p(HMA)} h_{HMA} = \beta_{1r} k_z \varepsilon_{r(HMA)} 10^{k_{1r}} n^{k_{2r}\beta_{2r}} T^{k_{3r}\beta_{3r}} \quad (14)$$

where:

$\Delta_{p(HMA)}$	=	Accumulated permanent or plastic vertical deformation in the HMA layer/sublayer, in
$\varepsilon_{p(HMA)}$	=	Accumulated permanent or plastic axial strain in the HMA layer/sublayer, in/in
$\varepsilon_{r(HMA)}$	=	Resilient or elastic strain calculated by the structural response model at the mid-depth of each HMA sublayer, in/in
$h_{(HMA)}$	=	Thickness of the HMA layer/sublayer, in
n	=	Number of axle load repetitions
T	=	Mix or pavement temperature, °F
k_z	=	Depth confinement factor
$k_{1r,2r,3r}$	=	Global field calibration parameters (from the NCHRP 1-40D recalibration; k_{1r} = -3.35412, k_{2r} = 0.4791, k_{3r} = 1.5606)
β_{1r}, β_{2r}, β_{3r},	=	Local or mixture field calibration constants; for the global calibration, these constants were all set to 1.0

$$k_z = (C_1 + C_2 D) 0.328196^{D} \quad (15)$$

$$C_1 = -0.1039 (H_{HMA})^2 + 2.4868 H_{HMA} - 17.342 \quad (16)$$

$$C_2 = 0.0172 (H_{HMA})^2 - 1.7331 H_{HMA} + 27.428 \quad (17)$$

D	=	Depth below the surface, in
H_{HMA}	=	Total HMA thickness, in

Equation 18 shows the field-calibrated mathematical equation used to calculate plastic vertical deformation within all unbound pavement sublayers and the foundation or embankment soil.

$$\Delta_{p(soil)} = \beta_{s1} k_{s1} \varepsilon_v h_{soil} \left(\frac{\varepsilon_o}{\varepsilon_r} \right) e^{-\left(\frac{\rho}{n}\right)^{\beta}} \quad (18)$$

where:

$\Delta_{p(Soil)}$	=	Permanent or plastic deformation for the layer/sublayer, in.
n	=	Number of axle load applications
ε_o	=	Intercept determined from laboratory repeated load permanent deformation tests, in/in
ε_r	=	Resilient strain imposed in laboratory test to obtain material properties ε_o, β, and ρ, in/in
ε_v	=	Average vertical resilient or elastic strain in the layer/sublayer and calculated by the structural response model, in/in
h_{Soil}	=	Thickness of the unbound layer/sublayer, in
k_{s1}	=	Global calibration coefficients; k_{s1}=1.673 for granular materials and 1.35 for fine-grained materials
β_{s1}	=	Local calibration constant for the rutting in the unbound layers (base or subgrade); the local calibration constant was set to 1.0 for the global calibration effort. Note that β_{s1} represents subgrade layer while β_{B1} represents base layer

$$Log\beta = -0.61119 - 0.017638(W_c) \tag{19}$$

$$\rho = 10^9\left(\frac{C_o}{\left(1-\left(10^9\right)^{\beta}\right)}\right)^{\frac{1}{\beta}} \tag{20}$$

$$C_o = Ln\left(\frac{a_1 M_r^{b_1}}{a_9 M_r^{b_9}}\right) = 0.0075 \tag{21}$$

W_c	=	Water content, percent
M_r	=	Resilient modulus of the unbound layer or sublayer, psi
$a_{1,9}$	=	Regression constants; a_1=0.15 and a_9=20.0
$b_{1,9}$	=	Regression constants; b_1=0.0 and b_9=0.0

2.1.4 Smoothness (IRI)

The design premise included in the MEPDG for predicting smoothness degradation is that the development of surface distress will result in a reduction in smoothness (increasing IRI). Equations 22 and 23 were developed using data from the LTPP program and are embedded in the MEPDG to predict the IRI over time for new HMA pavements (AASHTO 2008).

$$IRI = IRI_o + 0.0150(SF) + 0.400(FC_{Total}) + 0.0080(TC) + 40.0(RD) \tag{22}$$

where:

IRI_o	=	Initial IRI after construction, in/mi
SF	=	Site factor, refer to equation 23

FC_{Total}	=	Area of fatigue cracking (combined alligator, longitudinal, and reflection cracking in the wheel path), percent of total lane area. All load related cracks are combined on an area basis – length of cracks is multiplied by 1 foot to convert length into an area basis
TC	=	Length of transverse cracking (including the reflection of transverse cracks in existing HMA pavements), ft/mi.
RD	=	Average rut depth, in

The site factor (SF) is calculated in accordance with the following equation.

$$SF = FROSTH + SWELLP*AGE^{1.5} \quad (23)$$

where:

FROSTH	=	LN([PRECIP+1]*FINES*[FI+1])
SWELLP	=	LN([PRECIP+1]*CLAY*[PI+1])
FINES	=	FSAND + SILT
AGE	=	pavement age, years
PI	=	subgrade soil plasticity index
PRECIP	=	mean annual precipitation, in.
FI	=	mean annual freezing index, deg. F Days
FSAND	=	amount of fine sand particles in subgrade (percent of particles between 0.074 and 0.42 mm)
SILT	=	amount of silt particles in subgrade (percent of particles between 0.074 and 0.002 mm)
CLAY	=	amount of clay size particles in subgrade (percent of particles less than 0.002 mm)

2.2 New JPCP

2.2.1 Transverse Slab Cracking

The MEPDG considers both JPCP bottom-up and top-down modes of transverse "slab" cracking. Under typical service conditions, the potential for either mode of cracking is present in all slabs. Any given slab may crack either from bottom-up or top-down, but not both. Therefore, the predicted bottom-up and top-down cracking are not particularly meaningful by themselves, and combined cracking is reported excluding the possibility of both modes of cracking occurring on the same slab. The percentage of slabs with transverse cracks (including all severities) in a given traffic lane is used as the measure of transverse cracking and is predicted using the following globally calibrated equation for both bottom-up and top-down cracking (AASHTO 2008):

$$CRK = \frac{1}{1 + \left(DI_F\right)^{-1.98}} \tag{24}$$

where:

CRK = Predicted amount of bottom-up or top-down cracking (fraction).
DI_F = Fatigue damage calculated using the procedure described in this section.

The general expression for fatigue damage accumulations considering all critical factors for JPCP transverse cracking is as follows (based on Miner's hypothesis) (Miner 1945):

$$DI_F = \sum \frac{n_{i,j,k,l,m,n,o}}{N_{i,j,k,l,m,n,o}} \tag{25}$$

where:

DI_F = Total fatigue damage (top-down or bottom-up)
$n_{i,j,k,\ldots}$ = Applied number of load applications at condition *i, j, k, l, m, n*
$N_{i,j,k,\ldots}$ = Allowable number of load applications at condition *i, j, k, l, m, n*
i = Age (accounts for change in PCC modulus of rupture and elasticity, slab/base contact friction, traffic loads)
j = Month (accounts for change in base elastic modulus and effective dynamic modulus of subgrade reaction)
k = Axle type (single, tandem, and tridem for bottom-up cracking; short, medium, and long wheelbase for top-down cracking)
l = Load level (incremental load for each axle type)
m = Equivalent temperature difference between top and bottom PCC surfaces.
n = Traffic offset path
o = Hourly truck traffic fraction

The applied number of load applications ($n_{i,j,k,l,m,n}$) is the actual number of axle type k of load level l that passed through traffic path n under each condition (age, season, and temperature difference). The allowable number of load applications is the number of load cycles at which fatigue failure is expected on average and is a function of the applied stress and PCC strength. The allowable number of load applications is determined using the following globally calibrated PCC fatigue equation:

$$\log\left(N_{i,j,k,l,m,n}\right) = C_1 \cdot \left(\frac{MR_i}{\sigma_{i,j,k,l,m,n}}\right)^{C_2} \tag{26}$$

Where:

$N_{i,j,k,\ldots}$ = Allowable number of load applications at condition *i, j, k, l, m, n.*
MR_i = PCC modulus of rupture at age *i*, psi.
$\sigma_{i,j,k,.}$ = Applied stress at condition *i, j, k, l, m, n*
C_1 = Calibration constant, 2.0

C_2 = Calibration constant, 1.22

The fatigue damage calculation is a process of summing damage from each damage increment. Once top-down and bottom-up damage are estimated, the corresponding cracking is computed using equation 24 and the total combined cracking determined using equation 27.

$$TCRACK = \left(CRK_{Bottom-up} + CRK_{Top-down} - CRK_{Bottom-up} \cdot CRK_{Top-down}\right) \cdot 100 \qquad (27)$$

where:

$TCRACK$ = Total transverse cracking (percent, all severities).
$CRK_{Bottop-up}$ = Predicted amount of bottom-up transverse cracking (fraction).
$CRK_{Top-down}$ = Predicted amount of top-down transverse cracking (fraction).

It is important to note that equation 27 assumes that a slab may crack from either bottom-up or top-down, but not both.

2.2.2 Transverse Joint Faulting

The mean transverse joint faulting is predicted incrementally on a monthly basis. The magnitude of increment is based on current faulting level, the number of axle loads applied, pavement design features, material properties, and climatic conditions. Total faulting is determined as a sum of faulting increments from all previous months (i.e., since traffic opening) using the following equations (AASHTO 2008):

$$Fault_m = \sum_{i=1}^{m} \Delta Fault_i \qquad (28)$$

$$\Delta Fault_i = C_{34} * (FAULTMAX_{i-1} - Fault_{i-1})^2 * DE_i \qquad (29)$$

$$FAULTMAX_i = FAULTMAX_0 + C_7 * \sum_{j=1}^{m} DE_j * Log(1 + C_5 * 5.0^{EROD})^{C_6} \qquad (30)$$

$$FAULTMAX_0 = C_{12} * \delta_{curling} * \left[Log(1 + C_5 * 5.0^{EROD}) * Log(\frac{P_{200} * WetDays}{P_s}) \right]^{C_6} \qquad (31)$$

where:

$Fault_m$	=	Mean joint faulting at the end of month m, in.
$\Delta Fault_i$	=	Incremental change (monthly) in mean transverse joint faulting during month i, in.
$FAULTMAX_i$	=	Maximum mean transverse joint faulting for month i, in.
$FAULTMAX_0$	=	Initial maximum mean transverse joint faulting, in.
$EROD$	=	Base/subbase erodibility factor.

DE_i = Differential density of energy of subgrade deformation accumulated during month i.

$\delta_{curling}$ = Maximum mean monthly slab corner upward deflection PCC due to temperature curling and moisture warping.

P_S = Overburden on subgrade, lb.

P_{200} = Percent subgrade material passing No. 200 sieve.

$WetDays$ = Average annual number of wet days (greater than 0.1 inch rainfall).

$C_{1,2,3,4,5,6,7,12,34}$ = Global calibration constants

Calibration Coefficients	New JPCP	JPCP subjected to CPR
C1	1.0184	0.6
C2	0.91656	1.2
C3	0.0021848	0.002125
C4	0.000884	0.000884
C5	250	400
C6	0.4	0.4
C7	1.83312	1.83312

Note that C_{12} and C_{34} are defined by equations 32 and 33.

$$C_{12} = C_1 + C_2 * FR^{0.25} \quad (32)$$

$$C_{34} = C_3 + C_4 * FR^{0.25} \quad (33)$$

FR = Base freezing index defined as percentage of time the top base temperature is below freezing (32 °F) temperature.

Since the maximum faulting development occurs during nighttime when the PCC slab is curled upward and joints are opened and the load transfer efficiencies are lower, only axle load repetitions applied from 8 p.m. to 8 a.m. are considered in the faulting analysis.

2.2.3 Smoothness (IRI)

In the MEPDG, JPCP smoothness is predicted as a function of the initial as-constructed smoothness and any change in pavement longitudinal profile over time and traffic due to distress development and progression and foundation movements. The IRI model was calibrated and validated using LTPP data that represented variety of design, materials, foundations, and climatic conditions. The following is the final globally calibrated model (AASHTO 2008, LTPP 2008):

$$IRI = IRI_I + C1*CRK + C2*SPALL + C3*TFAULT + C4*SF \quad (34)$$

Where:

IRI	=	Predicted IRI, in/mi
IRI_I	=	Initial smoothness measured as IRI, in/mi
CRK	=	Percent slabs with transverse cracks (all severities)
SPALL	=	Percentage of joints with spalling (medium and high severities)
TFAULT	=	Total joint faulting cumulated per mi, in
C1	=	0.8203
C2	=	0.4417
C3	=	0.4929
C4	=	25.24
SF	=	Site factor

$$SF = AGE\ (1+0.5556*FI)\ (1+P_{200})*10^{-6} \tag{35}$$

where:

AGE	=	Pavement age, yr.
FI	=	Freezing index, °F-days.
P_{200}	=	Percent subgrade material passing No. 200 sieve.

The transverse cracking and faulting are obtained using the MEPDG models described earlier. The transverse joint spalling is determined in accordance with equation 36, which was calibrated using LTPP and other data (AASHTO 2008):

$$\text{SPALL} = \left[\frac{\text{AGE}}{\text{AGE} + 0.01}\right]\left[\frac{100}{1 + 1.005^{(-12*\text{AGE} + \text{SCF})}}\right] \tag{36}$$

Where:

SPALL	=	Percentage joints spalled (medium- and high-severities)
AGE	=	Pavement age since construction, years
SCF	=	Scaling factor based on site-, design-, and climate-related

$$SCF = -1400 + 350 \bullet AC_{PCC} \bullet (0.5 + PREFORM) + 3.4\, f'c \bullet 0.4 - 0.2\ (FT_{cycles} \bullet AGE) + 43\ H_{PCC} - 536\ WC_{PCC} \tag{37}$$

AC_{PCC}	=	PCC air content, percent
AGE	=	Time since construction, years
PREFORM	=	1 if preformed sealant is present; 0 if not
f'c	=	PCC compressive strength, psi
FT_{cycles}	=	Average annual number of freeze-thaw cycles
H_{PCC}	=	PCC slab thickness, in
WC_{PCC}	=	PCC water/cement ratio

THIS PAGE INTENTIONALLY LEFT BLANK

3.0 FRAMEWORK FOR MEPDG MODEL VALIDATION AND RECALIBRATION

The framework for MEPDG models validation and local calibration for Utah outlined in this chapter was based closely on guidelines presented in NCHRP Project 1-40B Draft MEPDG Local Calibration Guide (Von Quintus et al. 2008). In all, model validation and local calibration consists of 11 steps. A detailed description of all 11 steps as applied in this study is presented in this chapter along with Chapters 4 and 5.

3.1 Step 1: Select Hierarchical Input Level

The AASHTO MEPDG Manual of Practice (Interim Edition) describes hierarchical input levels as follows (AASHTO 2008):

- Level 1 inputs provide for the highest level of accuracy and, thus, would have the lowest level of uncertainty or error. Level 1 material inputs require laboratory or field testing, such as the dynamic modulus testing of hot-mix asphalt concrete, site-specific axle load spectra data collections, or nondestructive deflection testing.
- Level 2 inputs provide an intermediate level of accuracy and would be closest to the typical procedures used with earlier editions of the AASHTO Guide. Level 2 inputs typically would be user-selected, possibly from an agency database, could be derived from a limited testing program, or could be estimated through correlations.
- Level 3 inputs provide the lowest level of accuracy. Inputs typically would be user-selected values or typical averages for the region.

For models, validation and local calibration, the MEPDG Local Calibration Guide recommends selecting an appropriate mix of MEPDG hierarchical input levels (1 through 3) consistent with agency's day-to-day practices for characterizing pavement inputs for design. Also, in general, inputs found to be highly sensitive to MEPDG distress/IRI predictions are characterized as accurately as possible.

Thus to select the right mix of hierarchical input levels, the project team conducted a thorough review of UDOT pavement design policy (e.g., HMA binder type, PCC mix type, base type and thickness, and so on), traffic data collection, materials characterization, and subgrade soil characterization practices as well as sources of data required by the MEPDG but not collected directly by UDOT (e.g., climate). The goal was to determine at what hierarchical input level current and future data collection practices fall into. Also, results of Utah specific sensitivity analysis performed as part of Phase I of this study was reviewed to determine inputs that most impact distress/IRI

prediction under Utah conditions. The results of the reviews are summarized below and presented in Tables 3 and 4:

- Traffic.
    - Saito and Jin (2009) report that UDOT collects truck traffic data among other vehicles types at automatic traffic recorder (ATR) stations. UDOT has three different types of ATR stations that measure (1) volume only, (2) volume by length, and (3) volume by vehicle class. As of 2008/2009, UDOT has a total of 90 working ATR stations across the state from which valuable truck traffic type and volume data were collected.
    - Seegmiller (2006) reports that Utah currently has 15 permanent WIM sites (i.e., 9 piezoelectric sites and 6 load cell sites). All sites are under the jurisdiction of UDOT with the exception of the I-80 Evanston and I-70 Loma sites, which are maintained by the Wyoming and Colorado Departments of Transportation, respectively. Data collected at each WIM site include a listing of time and date for each vehicle, as well as detailed classification data, vehicle length, aggregate vehicle weight, disaggregate axle spacing, and disaggregate axle weight for each vehicle that crosses the WIM location.
    - Combining information from the ATR and WIM sites in Utah provided traffic data in sufficient detail for the MEPDG (i.e., historical and current truck traffic type and volume, axle load distribution, vehicle class distribution, axle spacing and dimensions, and so on).
    - Thus, in general MEPDG traffic inputs in Utah can be obtained at level 1 or 2.
- Materials.
    - Materials along with foundation/subgrade soils data collection practices in Utah is currently in transition as UDOT upgrades its lab testing facilities in order to be able to perform most of the testing required to characterize HMA and PCC. Notable and significant upgrades include establishing equipment, protocols, etc., required for testing HMA dynamic modulus and indirect tensile strength and PCC coefficient of thermal expansion (CTE). The UDOT materials lab has the facilities for characterizing unbound granular materials and chemically treated materials at levels 1 or 2 (i.e., resilient modulus, compressive strength, maximum density, optimum moisture content, and so on). For this study, however, material testing information was mainly available at level 3 as most of the testing for material characterization in the past was done at level 3.

Table 3. Recommended hierarchical inputs levels for the key data required by the MEPDG for new HMA and HMA overlaid pavements.

MEPDG Input Variable	Sensitivity to Predicted Distress/Smoothness				Typical UDOT Data Collection Practice	Recommended Hierarchical Input Level	
	Alligator Cracking	Rutting	Transverse Cracking	IRI		Ideal	Selected
HMA thickness	XXX	XX	X	XX	Level 1	Level 1 or 2	Level 1
HMA coefficient of thermal contraction			XX		Level 3	Level 3	Level 2 & 3
HMA dynamic modulus	XX	XXX			Level 3 (i.e., using HMA mixture gradation and binder grade and Witzak's Model)	Level 1 or 2	Level 2
HMA air voids in situ (at placement)	XXX	XXX	XX		Level 3 (estimates from past construction projects QA/QC testing)	Level 1 or 2	Level 3
Effective HMA binder content	XXX	XX	XX	X		Level 1 or 2	Level 3
HMA creep compliance	XX	XXX	XXX		Level 3 (based on binder type)	Level 1 or 2	Level 1
HMA tensile strength			XXX			Level 1 or 2	Level 3
Base type/modulus	XXX	XX			Level 3 (based on material type)	Level 1 or 2	Level 2
Base thickness	X				Level 1	Level 3	Level 1
Subgrade type/modulus	XX	XX			Level 1 (backcalculated using deflection testing data)	Level 3	Level 1
Ground water table	X	X			Level 2 (from USDA-NRSC soil reports)	Level 3	Level 3
Climate	XX	XX	XXX	X	Level 2 (from NCDC database)	Level 1 or 2	Level 2
Truck volume	XXX	XXX			Level 1 (estimates from onsite traffic counting devices)	Level 1 or 2	Level 2
Truck axle load distribution	X	X				Level 3	Level 2
Tire load, contact area, and pressures	XX	XXX			Level 3	Level 1 or 2	Level 3
Truck speed	XX	XXX			Level 3	Level 1 or 2	Level 3
Truck wander	XX	XX			Level 3	Level 1 or 2	Level 3
Initial IRI				XXX	Level 2 (estimates from past construction projects QA/QC testing or through backcasting)	Level 1 or 2	Level 2

Key: X Factor has small effect on distress/IRI
XX Factor has moderate effect on distress/IRI
XXX Factor has large effect on distress/IRI

Table 4. Recommended hierarchical inputs levels for the key data required by the MEPDG for new JPCP and JPCP subjected to CPR.

MEPDG Input Variable	Sensitivity to Predicted Distress/Smoothness			Typical UDOT Data Collection Practice	Recommended Hierarchical Input Level	
	Faulting	Transverse Cracking	IRI		Ideal	Selected
PCC thickness	XX	XXX	XX	Level 1	Level 1	Level 1
PCC modulus of rupture & elasticity		XXX	X	Level 2 (correlation with compressive strength)	Level 1	Level 2 & 3
PCC Coefficient of thermal expansion	XXX	XXX	XXX	Level 1 (lab testing)	Level 1	Level 1 & 3 (current data available)
Joint spacing	XX	XXX	XX	Level 1	Level 1	Level 1
Lane to PCC shoulder long tern load transfer efficiency	XXX		XXX			Level 3
Edge support	XX	XXX	XX	Level 1	Level 1	Level 1
Permanent curl/warp	XXX	XXX	XXX			Level 3
Base type	XXX	XXX	X	Level 1	Level 1	Level 1
Climate	XXX	XXX	XXX	Level 2 (from NCDC database)	Level 1	Level 2
Subgrade type/modulus	X	XX	X	Level 1 (backcalculated using deflection testing data)	Level 3	Level 1
Truck axle load distribution	X	XXX	X	Level 1 (estimates from onsite traffic counting devices)	Level 1	Level 1
Truck Volume	XXX	XXX	XXX		Level 1	Level 1
Tire pressure		X		Level 3	Level 3	Level 3
Truck lateral offset	XX	XXX	XX	Level 3	Level 1	Level 3
Truck wander		XX		Level 3	Level 3	Level 3
Initial IRI			XXX		Level 2 (estimates from past construction projects QA/QC testing or through backcasting)	Level 1 or 2

Key: X Factor has small effect on distress/IRI
XX Factor has moderate effect on distress/IRI
XXX Factor has large effect on distress/IRI

- Climate
    - Horel et al. (2003) reports the deployment of automated Road Weather Information System (RWIS) stations (typically consisting of conventional weather sensors on a 33 ft tower with additional sensors embedded in the surface and subsurface of the roadway) throughout the western states of the U.S. The RWIS weather stations are basically a key part of winter maintenance system (i.e., snow removal and ice prevention). UDOT has to date deployed throughout the state over 30 RWIS stations. Data collected and accessed by UDOT from the RWIS stations include temperature, wind speed, relative humidity, dew point, visibility, and precipitation.

      Although significant portions of the data collected by the RWIS stations can eventually be used by the MEPDG to characterize climate condition for pavement design, the RWIS climate data in its current form is not configured and formatted in a manner that makes it useful to the MEPDG. Making the RWIS climate data useable would require as a minimum (1) obtaining all relevant climate and RWIS station location information, (2) reviewing the climate data for anomalies, inconsistencies, and errors, (3) cleaning up the data as needed, and (4) creating MEPDG specific climate files that can be used to create virtual weather stations as needed. The work just described was outside the scope of this project.

      Thus, for pavement design, climate data was obtained from the National Oceanic and Atmospheric Administration (NOAA) NCDC archive of climate data. Specifically for Utah, there are approximately 25 weather stations within or around the State from which climate data was obtained to create project specific level 2 climate inputs.

3.2 Step 2: Experimental Factorial & Matrix or Sampling Template

A sampling template was created for the validation and local calibration effort. The goal was to create a matrix for selecting a mix of projects that reflect current and future UDOT pavement design features, material types, and site conditions. Climate was included by obtaining projects from all four regions of the State. The primary variables in the matrix were HMA and PCC thickness, base type, and subgrade type. Specific to JPCP, design features (such as dowel diameter, edge support, and so on) with significant impact on distress/IRI were included.

In theory, an adequate number of pavement projects should be selected to populate the sampling matrix (i.e., a full or fractional factorial). Along with a balanced factorial must be replicate pavement projects within each populated cell. Tables 5 and 6 shows the sampling matrix created for MEPDG models validation and local calibration in Utah.

Table 5. Simplified sampling template for the validation and local calibration of new and rehabilitated HMA surfaced pavements.

HMA Thickness, in	Base Thickness, in	Base and Subgrade Type					
		Coarse (A-1 through A-3) & Granular Base			Fine (A-4 through A-7) & Granular Base		
4 to 8	< 6						
	≥ 6						
≥ 8	< 6						
	≥ 6						

Table 6. Simplified sampling template for the validation and local calibration of new and rehabilitated JPCP.

PCC Thickness, in	Dowel Diameter, in	Edge Support	Joint Spacing, ft	Subgrade Type			
				Coarse (A-1 through A-3)		Fine (A-4 through A-7)	
				Base Type			
				LCB	Granular	LCB	Granular
≤ 10	No dowels	None	<15				
			≥15				
		Tied PCC	<15				
			≥15				
	Doweled	None	<15				
			≥15				
		Tied PCC	<15				
			≥15				
> 10	No dowels	None	<15				
			≥15				
		Tied PCC	<15				
			≥15				
	Doweled	None	<15				
			≥15				
		Tied PCC	<15				
			≥15				

LCB = lean concrete base

3.3 Step 3: Estimate Minimum Sample Size (Number of Pavement Projects) Required for Each Distress/IRI Prediction Model Validation and Local Calibration

Under this step, the project team estimated the minimum number of projects required for MEPDG distress/IRI models validation and local validation. Information required for determining minimum number of projects include model error (i.e., SEE), confidence level for statistical analysis, and performance indicators threshold value at typical agency design reliability level. For this project the following was assumed:

- Design reliability level: 90 percent.
- Confidence interval: 90 percent.
- MEPDG nationally calibrated models SEE: see Table 7.
- Performance indicator threshold value: see Table 7.

Table 7. Estimated number of pavement projects required for the validation and local calibration (obtained from AASHTO 2008).

Pavement Type	Performance Indicator	Perf. Indicator Threshold (@ 90 Percent Reliability) (σ)	Standard Error of Estimate (SEE)	Minimum No. of Projects Required for Validation & Local Calibration	Minimum Number of Projects Required for Each Pavement Type (n)*
New HMA and HMA overlaid HMA	Alligator cracking	20 percent lane area	5.01 percent	16	18
	Transverse "thermal" cracking	Crack spacing > 100 ft. of 630 ft/mi	150 ft/mi**	18	
	Rutting	0.4 in	0.107 in	14	
	IRI	169 in / mi	18.9 in/mi	80	
New JPCP and CPR	Faulting	< 0.15 in	0.033 in	21	21
	Transverse Cracking	< 10 percent slabs	4.52 percent	5	
	IRI	169 in/mi	17.1 in/mi	98	

* $n = \left(\frac{Z_{\alpha/2}\sigma}{E}\right)^2$, where $Z_{\alpha/2}$ = 1.601 (for a 90 percent confidence interval), σ = performance indicator threshold (design criteria), and E = tolerable bias at 90 percent reliability (1.601*SEE).
**Estimated from other MEPDG implementation projects.

Table 7 summarizes the estimated minimum number of pavement projects required for the validation and local calibration effort for each distress/IRI model of interest. Note that all HMA (flexible) pavements and JPCP surfaced pavement projects were combined to determine total number of projects available as they were being used to essentially validate and calibrate the same models.

Finally, in selecting the overall minimum number of pavement HMA and JPCP projects required, the performance indicator IRI was excluded. This is because the accuracy of the IRI models depends very much on the accuracy of other pavement distress predictions. Sampling a vast number of projects to validate the IRI models is therefore not necessary if the individual distress prediction models are judged to be accurate and reasonable.

3.4 Step 4: Select Projects

The MEPDG Local Calibration Guide recommends that for the projects selected for validation and local calibration, distress/IRI should cover a reasonable range of values that is typical for Utah and must be representative of Utah pavement design and construction practices and site conditions. Thus, some of the selected pavements projects should be in poor, moderate, and good condition and must be well distributed throughout the State.

The first step in project selection was to identify as many potential projects as possible that could be used to satisfy the recommendations presented above. A total of 60 LTPP

and UDOT PMS projects were identified for possible inclusion in the project database. A breakdown of the projects was as follows:

- New HMA (including HMA pavements with thin overlays): 26 projects.
- HMA overlaid existing HMA: 4 projects.
- New JPCP (including JPCP over existing HMA, LCB and unbonded JPCP): 21 projects.
- JPCP subjected to CPR: 9 projects.

Note that existing HMA pavements overlaid with thin (< 1.0-in) HMA overlays were considered new designs, as thin overlays are essentially maintenance events.

The number of identified projects was in excess of the 18 HMA and 21 JPCP projects required (see Table 7). A detailed description of the projects identified is presented in Table 8. Figures 2 and 3 show the locations of the identified projects in Utah.

3.5 Step 5: Extract and Evaluate Distress and Project Data

The MEPDG local calibration guide groups this step into the following four activities:

- Extract and review distress/IRI data for each identified project.
- Compare performance indicator magnitudes to the design threshold values (see Table 7).
- Evaluate the distress data to identify anomalies and outliers.
- Determine MEPDG inputs.

However, before the four activities listed above were done, the project team reviewed thoroughly all the identified projects to determine which projects had adequate amounts of distress/IRI data and other relevant MEPDG inputs for analysis. Projects without the required input data were removed from further consideration.

3.5.1 Extract and Review Distress/IRI Data for Each Selected Project

Distress and IRI data of interest was obtained from the LTPP database for LTPP projects and UDOT local PMS performance data files for UDOT PMS projects (LTPP 2008). This was a major work activity with UDOT staff assisting. Distress and IRI data from both databases were reviewed for accuracy, reasonableness, and consistency. Key issue considered was whether the raw data as measured and reported could be converted into the MEPDG reporting units for each performance indicator.

Since MEPDG performance indicators measuring units was obtained from LTPP database, by default all the LTPP projects had distress/IRI measured and reported in units that could be converted into units compatible with the MEPDG.

Table 8. HMA and JPCP projects identified for validation and local calibration (LTPP 2008 and UDOT PMS projects).

Project ID*	Rehab (Yes or No)	Rehab Date	Existing Pavement Constr. Date	Pavement Type	Location
49_0803	No		1997	New HMA	SR-35, Start of section is 0.6 miles east of bridge crossing Provo River, Wasatch County
49_0804	No		1997	New HMA	SR-35, Start of section is 0.6 miles east of bridge crossing Provo River, Wasatch County
49_1001_1	No		1980	New HMA	US-191, Start of section is 2.4 miles north of the US-191 and US-163 intersection, San Juan County
49_1004_2	Yes	1978	1971	HMA over HMA	US-89, Start of section is 6.0 miles north of junction SR-20 and 15.9 miles south of junction SR-62, Garfield County
49_1005_1	Yes	1984	1970	HMA over HMA	US-89, Start of section is 0.239 miles north of junction with SR-109, Davis County
49_1006	Yes	1988	1971	HMA over HMA	SR-28, Start of section is 2.354 miles north of the junction with SR-89 and 3.104 miles south of the entrance road to Fayette, Sanpete County
49_1007_1	Yes	1988	1979	HMA over HMA	US-6, Start of section is 3.398 miles north of the 1st street north overcrossing in Price and 0.158 miles south of the Price River Bridge, Carbon County
49_1008_1	No		1976	New HMA	US-89, Start of section is 0.852 miles north of the I-70 overcrossing and 0.571 miles south of Salina Creek Bridge, Sevier County
49_1008_2	Yes	1990	1976	HMA over HMA	
49_1017_1	No		1966	New HMA	US-89, Start of section is 0.275 miles North of Sevier River Bridge and 2.178 miles south of junction with SR-4, Sevier County
49_3010	No		1978	New JPCP	I-15, Start of section is 1.394 miles north of Paragonah overcrossing and 10.806 miles south of Panquitch overcrossing, Iron county
49_3011	No		1986	New JPCP	I-15, Start of section is 14.55 miles north of exit 207 (Mills overpass). Exit 222 (Nephi overpass) is 1.65 miles north of the start of section, Juab County
49_3015_1	No		1985	New JPCP	I-215, Start of section is 0.4 miles southbound of the RR overpass just after exiting I-15. Exit 28 (Redwood Road) is 0.6 miles southbound of the start of section, Salt Lake County
49_7082	No		1990	New JPCP	I-15, Start of section is 4.26 miles north of Riverside/Logan exit (exit 387, SR-30 east). Exit 394 (SR-13 south, Plymount) is 2.8 miles north of the start of section, Box Elder County
49_7083_1	No		1989	New JPCP	I-70, Start of section is 1.9 miles east of the west Richfield exit (exit 35) and 1.5 miles west of the east Richfield exit (exit 38), Sevier County
49_7085_1	No		1991	New JPCP	US-40, Start of section is 8.2 miles eastbound (south) of the Park City exit, Wasatch County
49_7086	No		1991	New JPCP	SR-154, Start of section is 0.5 miles south of 2100 S. street and 3100 S. street is 0.7 miles south of the start of section, Salt Lake county

*Project names with the prefix 49 indicate LTPP projects while those with the prefix CPR, JPCP, or HMA are UDOT PMS projects.

Table 8. HMA and JPCP projects identified for validation and local calibration, continued (LTPP 2008 and UDOT PMS projects).

Project ID*	Rehab (Y/N)	Rehab Date	Existing Pavement Constr. Date	Pavement Type	Location
CPR1	Yes	2001	–	CPR of JPCP	I-80, State Street to 2300 East, Salt Lake County
CPR2	Yes	2004	–	CPR of JPCP	I-15 Diamond grind at Levan Ridge South of Nephi, Juab County
CPR3	Yes	2005	1986	CPR of JPCP	I-70, North Richfield to Sigard, Sevier County
CPR4	Yes	2006	1997	CPR of JPCP	SR-120, MP 1 to MP 3, Sevier County
CPR5	Yes	2005	–	CPR of JPCP	I-84, Riverdale to Uintah Junction, Weber County
CPR6	Yes	1998	–	CPR of JPCP	I-15, Hot Springs to Brigham, Box Elder County
CPR7**	Yes	2002	–	CPR	I-215, 5600 S to 4500 S. Salt Lake East Side, Salt Lake County
CPR8**	Yes	2006	–	CPR of JPCP	I-15, S Nephi to N. Nephi, Juab County
CPR9	Yes	2004	1983	CPR of JPCP	I-70, Clear Creek Canyon MP 7 to 17, Sevier County
JPCP1	No	–	1972	New JPCP	I-15, Pages Lane Lagoon, Davis County
JPCP10	No	–	2001	New JPCP	US-89 & SR-50, Salina Main Street, Sevier County
JPCP11	No	–	1984	New JPCP	I-15, Scipio to Juab countyline, Millard County
JPCP13	No	–	1987	New JPCP	I-70, Belknap to Elsenor, Sevier County
JPCP14	No	–	1987	New JPCP	I-70, Elsenor to South Richfield, Sevier County
JPCP15	No	–	1986	New JPCP	25569, North Richfield to Sigard, Sevier County
JPCP16	No	–	1975	New JPCP	I-15, Plymouth to Idaho, Box Elder County
JPCP17	No	–	1982	New JPCP	I-15, Riverside to Plymouth, Box Elder County
JPCP2	No	–	1996	New Doweled JPCP	I-84, Morgan to Summit county, Morgan County
JPCP3	No	–	1976	New JPCP	I-80, Wahsatch to WY State line, Summit County
JPCP4	No	–	1976	New JPCP	I-80, Wahsatch to Castle Rock, Summit County
JPCP5	No	–	2001	New JPCP	I-15, 10800 South to 500 N. SLC valley, Salt Lake County
JPCP6***	No	–	2004	Unbonded JPCP overlay of JPCP	I-215, Redwood Rd. to 4700 South, Salt Lake West Side Belt, Salt Lake County
JPCP7***	No	–	Missing	New JPCP over existing HMA	I-80, Wyoming state line to Castle Rock, Summit County
HMA_R1 01	No	–	2001	New HMA	SR-226, Snow Basin Rd., Weber County
HMA_R1 02	No	–	2002	New HMA	US-89, Logan Canyon; Tony Grove to Franklin Basin, Cache County

*Project names with the prefix 49 indicate LTPP projects while those with the prefix CPR, JPCP, or HMA are UDOT PMS projects.
**Including dowels bar retrofit.
***Considered new JPCP design.

Table 8. HMA and JPCP projects identified for validation and local calibration, continued (LTPP 2008 and UDOT PMS projects).

Project ID*	Rehab (Y/N)	Rehab Date	Existing Pavement Construction Date	Pavement Type	Location
HMA_R1 03	No	–	2002	New HMA	SR-104, Wilson Lane in Ogden (SR-126) to I-15, Weber County
HMA_R1 04	Yes	–	1998	New HMA over fractured PCC (C&S)	I-15, 450 North to Hot Springs, Weber County
HMA_R2 02	No	–	1993	New HMA	SR-224, SR-224, Bear Hollow to 248, Summit County
HMA_R2 03	No	–	2002	New HMA	SR-71, 700 East; 6300 S. to 6000 S., Salt Lake County
HMA_R2 04	No	–	2002	New HMA	SR-36, Mills Junction to I-80, Tooele County
HMA_R3 01	No	–	1986	New HMA	SR-73, Tickville Wash to Fairfield, Utah County
HMA_R3 02	No	–	1996	New HMA	SR-73, Tickville Wash to SR-68, Utah County
HMA_R3 03	Yes	–	2003	New HMA over fractured PCC (C&S)	I-15, Point of Mountain to Lehi, Utah County
HMA_R3 04	Yes	–	2003	New HMA over fractured PCC (rubblized)	I-15, Sevier River to Mills, Juab County
HMA_R4 01	No	–	2002	New HMA	US-89, Centerfield to Gunnison, Sanpete County
HMA_R4 02	No	–	2002	New HMA	SR-10, Huntington to Poison Springs Bench, Emery County
HMA_R4 03	No	–	2002	New HMA	SR-56, I-15 to Iron Springs, Iron County
HMA_R4 04 (NB)	No	–	2006	New HMA	US-191, Moab to I-70 at Crescent Junction, Grand County
HMA_R4 04 (SB)	No	–	2006	New HMA	US-191, Moab to I-70 at Crescent Junction, Grand County
HMA_OVLY_1	Yes	2006	1970	HMA over HMA	I-15, Arizona State Line to Bluff Street MP 0-6, Washington County
HMA_OVLY_2	Yes	2002	–	HMA over HMA	I-15, Dog Valley through Baker Canyon, Millard County
HMA_OVLY_3	Yes	2002	–	HMA over HMA	US-191, Junction SR-211 to RP 93 North of Monticello, San Juan County
HMA_OVLY_4	Yes	2004	–	HMA over HMA	SR-10, Fremont junction to Quitchupah Hill, Emery, Sevier County

*Project names with the prefix 49 indicate LTPP projects while those with the prefix CPR, JPCP, or HMA are UDOT PMS projects.

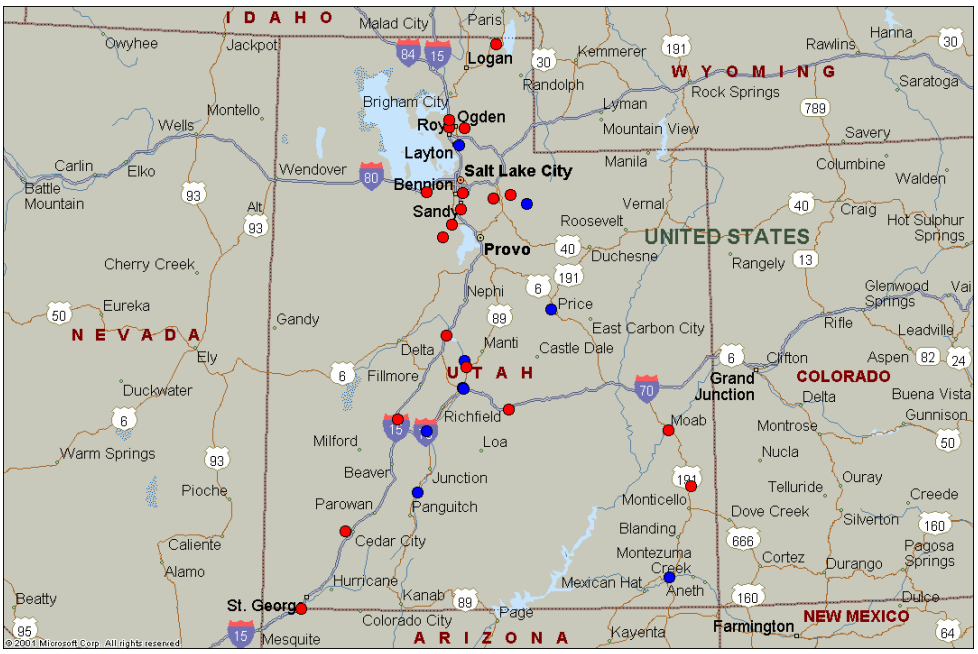

Figure 2. Map showing the location of HMA surfaced pavement projects identified for local calibration/validation.

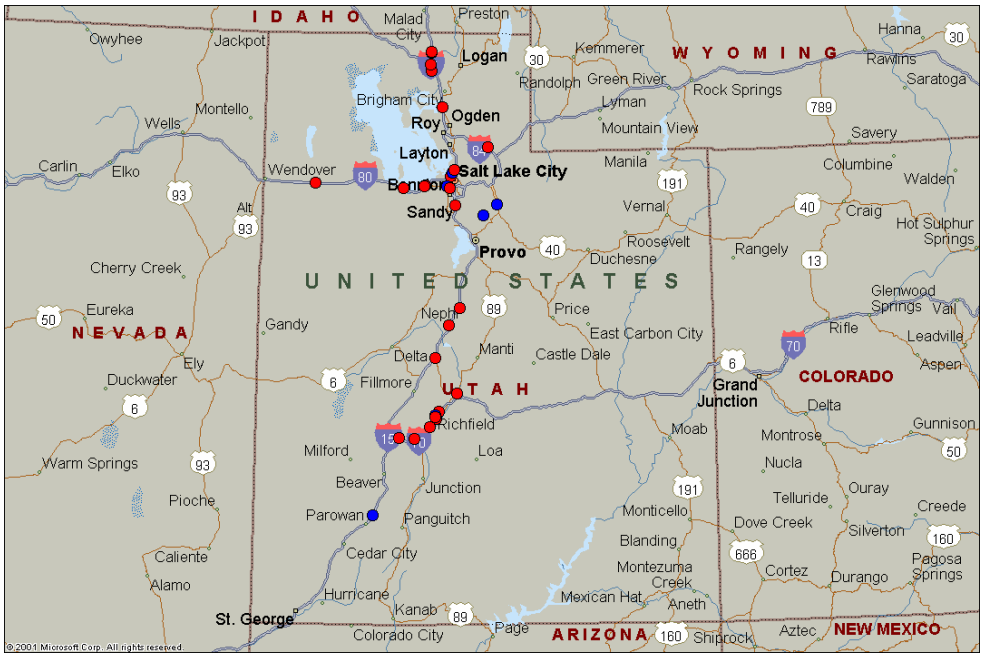

Figure 3. Map showing the location of JPCP projects identified for local calibration/validation.

Data Collection and Reporting

The review of the LTPP measured distress/IRI data showed distress/IRI data consistent with the MEPDG as expected (LTPP 2008). The review of the UDOT measured distress/IRI data indicated the following:

- HMA surfaced pavements.
    - Alligator cracking called wheelpath cracking by UDOT has a definition close enough to that of LTPP. Wheelpath cracking is reported at 3 severity levels (low, medium, and high) and for each severity level is reported as length of cracking per 500 ft length of highway.
    - Transverse cracking has a definition close enough to that of LTPP. Transverse cracking is reported at 3 severity levels (low, medium, and high) and for each severity level is reported as the number of cracks per 500 ft length of highway.
    - Rutting has a definition close enough to that of LTPP. However, UDOT rutting measurement is quite different from that of LTPP. LTPP measures rutting in two ways, namely by recording maximum rut depth to the nearest millimeter (0.04-in), at 15.25-m (50-ft) intervals for each wheel path (along a typical 500-ft LTPP pavement section), as measured with a 1.2-m (6-ft) straight edge or wire. UDOT uses a van mounted 3-point laser profiler to obtain the transverse profile of the pavement at regular intervals (typically a tenth of a mile). Maximum rut depth is then computed using the transverse profile obtained. UDOT rut depth measurement changed in 2008 to include full transverse profile and calculation of maximum rut depth in each wheel path. After adding the 2008 data on to each project rut history, there was no reason to believe that this produced a significant difference. For LTPP, rutting is reported for each individual point (50-ft apart) along the pavement section for the left and right wheelpaths separately. For UDOT PMS sections, mean left and right wheelpath rutting is reported for every tenth of a mile (approximately 500-ft) along a given project.
    - IRI measurement and reporting was similar to that of the LTPP.
- JPCP
    - UDOT measures transverse joint faulting using a high-speed profiler using a 3-point laser system. Faulting data is collected in the outer lane. Although UDOT reports faulting at 3 severity levels (determined by the height of the fault, i.e. less than 0.3 inch = low severity and greater than 0.5 inch = high severity), the laser system used for measurements records only faults that are greater than or equal to 0.1 in. LTPP, however, records faulting 0.3-m (1-ft) and 0.75-m (2.5-ft) from the outside slab edge (approximately the outer wheel path). For both the 1-ft and 2.5-ft

locations, faulting is measured several times and the mean value is reported to the nearest millimeter (0.04-in).

- Transverse cracking is reported by UDOT as shattered slabs or transverse cracking. A shattered panel is when a JPCP slab panel is broken into 3 or more pieces with boundaries of each piece defined by cracks or joints. Shattered slabs may be caused by several crack types including transverse cracking. Transverse cracking has a definition close enough to that of LTPP. It is reported at 3 severity levels (low, medium, and high). Transverse cracking is reported as number of cracks per 40 slab panels. Shattered slabs is reported as the number of shattered panels per 40 slab panels.
- IRI measurement and reporting was similar to that of the LTPP.

The UDOT PMS pavement distress data entry form, highlighting units of measurement and reporting, is shown in Figure 4.

Processing LTPP and UDOT Performance Data for MEPDG

The raw LTPP and UDOT PMS distress/IRI data were processed and converted into units of measurement consistent with the MEPDG. Details of the conversion are presented in Appendix A and B for HMA and JPCP, respectively.

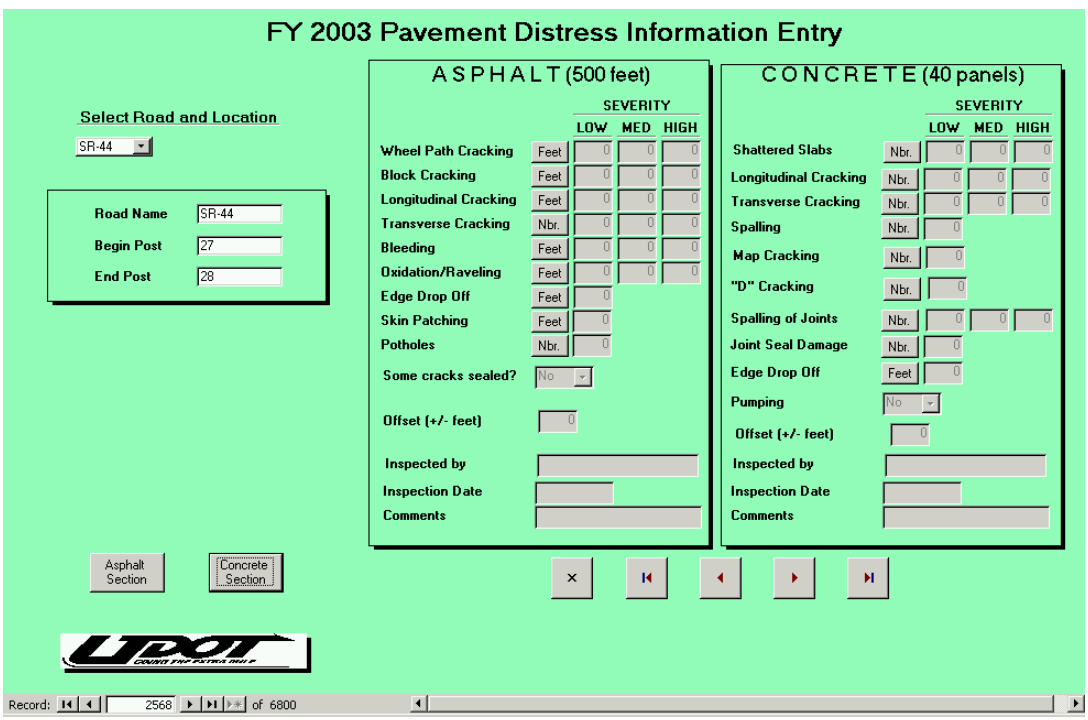

Figure 4. UDOT PMS pavement distress data entry form, highlighting units of measurement and reporting.

Potential problems regarding compatibility of UDOT and LTPP distress/IRI measurements were identified and are summarized as follows:

- HMA.
    - Alligator cracking: UDOT reported alligator cracking as length per 500 ft of pavement (outer lane). As the MEPDG requires a measurement unit of percent lane area, the UDOT measure had to be converted to percent lane area by assuming an average width of alligator cracking of 1-ft.
    - Transverse cracking: UDOT reported transverse cracking as number of cracks per 500 ft of pavement (outer lane). As the MEPDG requires a measurement unit of linear length in feet per mile, the UDOT measure had to be converted to linear length in feet per mile by assuming that (1) all the transverse cracks are full-width and (2) lane width is 12-ft.
    - Rutting: UDOT measures rutting using a three point laser system at approximately 0.1 mile (528-ft) intervals. LTPP uses a straightedge or a wire line and measures the distress at 50-ft intervals. Measurement method and frequency are significantly different for LTPP and UDOT resulting in differences in the measured distress. There was a need, therefore, to transform measured UDOT PMS rutting to be in conformity with LTPP measured rutting data. Transformation of the UDOT rutting measurements was done empirically and involved the following steps:
        - Determine LTPP projects for which there is corresponding UDOT PMS measured rutting data available (see Table 9).
        - Plot UDOT PMS versus LTPP measured rutting for the projects identified in step 1 (see Figure 5).
        - Develop a relationship between the two rutting measurements (see Figure 5).

      A simple exponential relationship between measured UDOT PMS and LTPP rutting data was observed and established as shown in Figure 5. This relationship was applied to all UDOT PMS rutting measurements to make them compatible with LTPP measurements. The transformed UDOT PMS rutting and LTPP rutting data were used for model evaluation.
    - IRI: UDOT and LTPP IRI measurements were similar. There was therefore no need for modifying the UDOT data.

Table 9. Rutting data used for developing transformation relationship.

LTPP ID	Rutting, in		
	Year	UDOT	LTPP
1001	1999	0.28	0.43
1001	2000	0.28	0.39
1001	2004		0.45
1004	2004	0.05	0.10
1006	1999	0.12	0.14
1006	2000	0.17	0.17
1006	2002	0.11	0.14
1006	2002	0.11	0.12
1008	1999		0.43
1008	2000		0.42
1017	1999	0.11	0.19
1017	2000	0.14	0.18
1017	2001		0.18

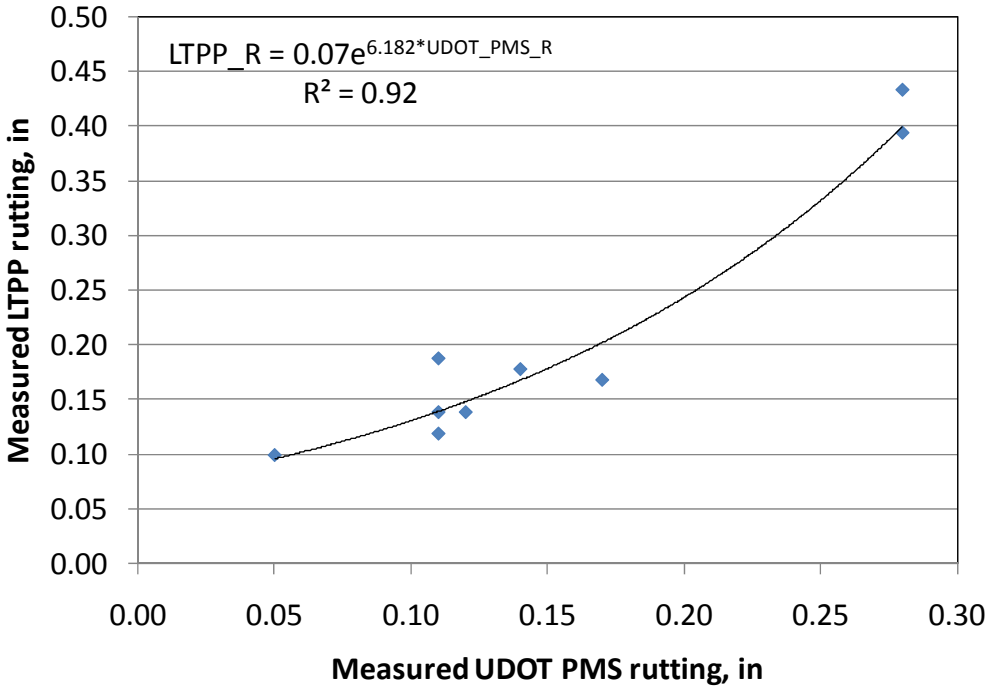

Figure 5. Plot of UDOT PMS versus LTPP measured rutting for the projects listed in Table 9.

- JPCP
  - Transverse cracking: UDOT reported transverse "slab" cracking in two ways (1) number of transverse cracks per 40 panels and (2) number of shattered slabs per 40 panels. Without having detailed information from distress survey maps or video to determine exactly which panels were cracked or shattered and why, the project team had to make the following assumptions:
    - When multiple transverse cracks occurred on a given panel, the panel was classified as a shattered slab.
    - All shattered slabs experienced at least one transverse crack.
    - Thus, summing the total number of shattered panels and transverse cracks resulted in the total number of panels with transverse cracking. Dividing this number by 40 panels and multiplying by 100 resulted in the percentage of slabs with transverse cracking as required by the MEPDG.
  - Faulting: UDOT measures faulting using a three point laser system at approximately 0.1 mile (528-ft) intervals. LTPP uses a Georgia faultmeter and measures the distress at each joint within the typical 500-ft LTPP pavement sections. The mean faulting is computed for all joints. Faulting is measured at 1-ft and 2.5 ft from the slab edge. UDOT reports faulting as follows:

Faulting Category	Measurement Reporting (Outer Wheelpath)
1*	Number of joints with faulting < 0.1 in
1	Number of joints with faulting > 0.1 in and < 0.3 in
2	Number of joints with faulting > 0.3 in and < 0.5 in
3	Number of joints with faulting > 0.5 in

*Faulting measurements were not reported for this category as the UDOT measuring equipment does not report faulting less than 0.1-in.

Faulting measurement method and frequency are significantly different for LTPP and UDOT resulting in differences in the measured distress. There was a need, therefore, to transform measured UDOT PMS faulting to be in conformity with LTPP measured faulting data. Transformation of the UDOT rutting measurements was done empirically and involved the following steps:

- Determine LTPP projects for which there is corresponding UDOT PMS measured faulting data available.
- Using the relationship presented below determine mean values of faulting for each UDOT reporting category for which total UDOT faulting has similar magnitude as the LTPP faulting.

$$MFLT = \frac{\left(N1_F * F1 + N2_F * F2 + N3_F * F3 + N4_F * F4\right)}{TJTS} \quad (38)$$

where

MFLT	=	mean transverse joint faulting, in
$N1_F$	=	number of joints with faulting < 0.1 in
$N2_F$	=	number of joints with faulting > 0.1 in and < 0.3 in
$N3_F$	=	number of joints with faulting > 0.3 in and < 0.5 in
$N4_F$	=	number of joints with faulting > 0.5 in
F1	=	mean faulting for joints with low faulting
F2	=	mean faulting for joints with low faulting
F3	=	mean faulting for joints with moderate faulting
F4	=	mean faulting for joints with high faulting
TJTS	=	total number of joints = $N1_F + N2_F + N3_F + N4_F$

Mean faults were as reported below:

Faulting Category	Measurement Reporting (Outer Wheelpath)	Assumed Mean Faulting Value, in
1*	Number of joints with faulting < 0.1 in	0.067**
1	Number of joints with faulting > 0.1 in and < 0.3 in	0.067**
2	Number of joints with faulting > 0.3 in and < 0.5 in	0.35
3	Number of joints with faulting > 0.5 in	0.5

*Joints with less than 0.1 in faulting. UDOT does not report faulting for these joints.
**This 0.067 in value is the assumed weighted mean faulting for all joints less than 0.3 in faulting.

The transformed UDOT PMS faulting and LTPP faulting data were used for validation and local calibration.

- IRI: UDOT and LTPP IRI measurements were similar. There was therefore no need for modifying the UDOT data.

In general, the project team was able to use measured LTPP and UDOT distress/IRI data from the same projects where available to test the reasonableness of assumptions made and to ensure that the reported distress/IRI from both sources was as close as possible. This ensured as much compatibility between the two data sources as possible.

3.5.2 Compare Performance Indicator Magnitudes to the Design Threshold (Trigger) Values

A comparison of the magnitudes of time-series distress/IRI from the identified LTPP and UDOT PMS projects with design threshold values for each distress type and IRI was done. This was to determine whether distress/IRI from the identified projects covered the range of distress/IRI typical for Utah. Table 10 summarizes the results of the comparison and showed the following:

- All distress and IRI data covered typical values reported for Utah pavements including design threshold values.
- With the exception of alligator cracking, the mean distress/IRI was mostly 40 to 62 percent of the design threshold value. For alligator cracking this value was approximately 10 percent. This suggests that for both HMA and JPC surfaced pavements, the identified pavements were mostly in relatively better condition than the design threshold values. This is typical for in-service pavements, as moderately to badly deteriorated pavements are rehabilitated as soon as possible.
- A review of the max distress/IRI values showed that for all the distress/IRI, maximum distress/IRI was greater than that of the design threshold values. Thus, the range of distress/IRI values from the identified projects covered UDOT design threshold values.

Finally, although the MEPDG local calibration Guide recommends the use of approximately the same number of repeated measures of distress/IRI from each project for validation and recalibration, in practice different projects tend to have very different repeated measures of distress/IRI (e.g., 10 observations over 10 years versus two or three observations over 10 years). The imbalance in the number of repeated observations of distress/IRI across projects was resolved by weighting the time series observation obtained from each project during analysis and effectively reducing the combined effect/weight of distress/IRI from each project to 1.0.

3.5.3 Evaluate Distress/IRI Data to Identify Anomalies and Outliers

Time series plots of distress and IRI data for each LTPP and UDOT PMS project were reviewed prior to determining MEPDG inputs. Review was limited to visual inspection of time series plots showing the progression of distress and IRI to (1) determine if observed trends in distress/IRI progression were reasonable, (2) identify potential anomalies (e.g., significant decrease in distress/IRI magnitude indicating an occurrence of significant rehabilitation or maintenance event), and (3) identify potential outliers. The plots reviewed are presented in Appendix A and B for HMA and HMA overlaid HMA pavements and JPCP and JPCP subjected to CPR, respectively.

Table 10. Comparison of range of distress/IRI values with design criteria or threshold values.

Pavement Type	Distress or Performance Indicator	Design Criteria	Max. Values Statistics				
			Average Max. Value	Lowest Max. Value	Largest Max. Value	Average Value is What Percentage of Design Criteria	Standard Deviation of Max. Values
HMA and HMA overlaid HMA	Alligator cracking, percent lane area	10	0.96	0	28.4	9.6	4.7
	Transverse "thermal" cracking, ft/mi	630 (equiv to crack spacing > 100 ft)	350	0	6118	55.5	1003
	Rutting, in	0.4	0.16	0.013	0.443	40.0	0.096
	IRI, in/mi	169	95.6	42.0	229.6	56.8	39.4
JPCP	Transverse cracking, percent slabs cracked	< 10	5.6	0	87.5	56.0	16.2
	Transverse joint faulting, in	< 0.15	0.074	0	0.228	49.3	0.076
	IRI, in/mi	169	115	57	232	68.0	44

The results of this exercise were as follows:

- Projects exhibiting unreasonable trends in distress/IRI progression were removed and not used for analysis. It must be noted that each distress type and IRI were treated separately and thus removal of a project from say the rutting database does not imply that it was also removed from the transverse cracking database.
- Individual distress/IRI data points identified as outliers and erroneous were removed. Examples include zero measurements that could represent non-entry values and significantly high or low distress/IRI values deemed unreasonable.
- Individual distress/IRI data points measured after the performance of a significant maintenance or rehabilitation event that altered the design of the pavement significantly were removed.

3.5.4 Determining MEPDG Inputs

Several categories of input data are required by the MEPDG. For this project, data was primarily obtained from two sources: LTPP and UDOT traffic, materials, performance,

etc., databases. Additional data to complement these data sources was obtained from the MEPDG, NCDC, and the United States Department of Agriculture (USDA) Natural Resources Conservation Service (NRCS) Soil Survey Geographic (SSURGO) database. A detailed summary of data sources used for analysis is presented in Table 11. Detailed description of all key data variables used for validation and local calibration is presented in Appendix C. Projects without key input information were removed from the project database.

Following the data assembly, review, and cleanup effort, a final selection of projects with adequate detailed information for validation and local calibration was completed. A summary of the final selection of projects is presented in Tables 12 and 13 for HMA pavements and JPCP, respectively. The populated sampling templates (see step 2) are presented in Tables 14 and 15.

3.6 Step 6: Conduct Field and Forensic Investigations

The inputs obtained from the various databases along with default MEPDG and UDOT inputs were deemed reasonable and thus no field or forensic investigation was warranted.

3.7 Steps 7 through 10: Assess Local Bias and Standard Error of the Estimate from Global Calibration Factors and Eliminate/Reduce Standard Error of the Estimate and Local Bias of Distress Prediction Models

This section presents a summary of procedures used in models validation and local calibration. Several methods (statistical or otherwise) were used singly or in combination to validate the MEPDG models for Utah conditions. Statistical methods were used in situations were measured distress/IRI was mostly non-zero, otherwise a non statistical approach to model validation was applied. Model validation consisted of the following steps:

1. Execute the MEPDG for each selected LTPP and UDOT PMS project (see Tables 12 and 13) and predict pavement distresses and IRI over time (typically 20 to 40 years).
2. Extract predicted distress and IRI data from the MEPDG outputs that match age of measured LTPP and UDOT PMS distress/IRI.
3. Perform statistical or non statistical analysis to validate model.

Details of the statistical or non statistical analysis as needed to validate models are presented in the following sections.

Table 11. Predominant sources of data used for MEPDG performance models verification in Utah.

Input Group		Input Parameter	Validation Input Level Used	Data Source
Truck Traffic		Axle load distributions (single, tandem, tridem, and quad)	Level 1	LTPP and UDOT traffic databases
		Truck volume distribution	Level 1	LTPP and UDOT traffic databases
		Lane & directional truck distributions	Level 1	
		Tire pressure	Level 3	UDOT and MEPDG defaults
		Axle configuration, tire spacing	Level 3	
		Truck wander	Level 3	
Climate		Temperature, wind speed, cloud cover, precipitation, relative humidity	Level 1 (MEPDG weather stations)	MEPDG data obtained from NCDC data files
Material Properties	Unbound Layers & Subgrade	Resilient modulus – subgrade	Level 1; Backcalculation	LTPP and UDOT FWD deflection test data files
		Resilient modulus – unbound granular and chemically treated base/subbase layers	Level 3	MEPDG defaults
		Unbound base/ subgrade soil classification	Level 1 & 3	LTPP, UDOT, and USDA-NRCS soil data files
		Moisture-density relationships & other volumetric properties	Level 3	LTPP database and MEPDG defaults
		Soil-water characteristic relationships	Level 3	MEPDG defaults
		Saturated hydraulic conductivity	Level 3	MEPDG defaults
	HMA	HMA dynamic modulus	Level 2	LTPP and UDOT materials database
		HMA creep compliance & indirect tensile strength	Levels 3	MEPDG defaults
		Volumetric properties	Level 3	Typical UDOT as-placed defaults
		HMA coefficient of thermal contraction	Level 3	MEPDG defaults
	PCC	PCC elastic modulus	Level 2 &3	LTPP materials database & typical UDOT defaults
		PCC flexural strength	Level 2 &3	
		PCC coefficient of thermal expansion	Level 1, 2 & 3	
All Materials		Unit Weight	Level 1	LTPP
		Poisson's Ratio	Level 2 &3	MEPDG defaults
		Other thermal properties; conductivity, heat capacity, surface absorptivity	Level 3	MEPDG defaults

FWD = Falling Weight Deflectometer

Table 12. Shortlist of HMA and HMA overlaid HMA pavement projects with adequate performance included in analysis.

Pavement Type	Project ID	Included in Project Database?			
		Alligator Cracking	Transverse Cracking	Rutting	IRI
New HMA	LTPP 0803	X	X	X	X
	LTPP 0804	X	X	X	X
	LTPP 1001	X	X	X	X
	LTPP 1004	X		X	
	LTPP 1005	X	X	X	X
	LTPP 1006	X	X	X	X
	LTPP 1007	X	X	X	X
	LTPP 1008		X	X	X
	LTPP 1017				X
	HMA_R1 01	X	X	X	X
	HMA_R1 02	X	X	X	X
	HMA_R1 03	X	X	X	X
	HMA_R1 04	X	X	X	
	HMA_R2 01	X	X	X	
	HMA_R2 02	X	X	X	
	HMA_R2 03	X	X	X	X
	HMA_R2 04	X	X	X	X
	HMA_R3 01	X	X	X	X
	HMA_R3 02	X	X	X	X
	HMA_R3 03	X	X	X	
	HMA_R3 04	X		X	
	HMA_R4 01		X	X	
	HMA_R4 02	X	X	X	X
	HMA_R4 03	X	X	X	X
	HMA_R4 04 (NB)	X	X	X	X
	HMA_R4 04 (SB)	X	X	X	X
HMA overlaid HMA	HMA_OVLY_1				
	HMA_OVLY_2	X	X	X	X
	HMA_OVLY_3	X	X		X
	HMA_OVLY_4	X	X	X	X
Total number of projects available		26	24	25	23
Total number of projects required		16	18	14	–

Table 13. Shortlist of JPCP projects with adequate performance included in analysis.

Pavement Type	Project ID	Included in Project Database?		
		Transverse Cracking	Faulting	IRI
JPCP subjected to CPR including diamond grinding	CPR1			
	CPR2	X	X	X
	CPR3		X	
	CPR4	X	X	
	CPR5	X	X	
	CPR6	X	X	X
	CPR7	X	X	X
	CPR8	X	X	X
New JPCP	49_3010	X	X	X
	49_3011	X	X	X
	49_3015_1	X	X	X
	49_7082	X	X	X
	49_7083_1			X
	49_7085_1	X	X	X
	49_7086	X	X	X
	JPCP1			
	JPCP2	X	X	X
	JPCP3			
	JPCP4			
	JPCP5	X	X	
	JPCP6	X	X	X
	JPCP7			
	JPCP10	X	X	X
	JPCP11			
	JPCP13			
	JPCP14	X	X	X
	JPCP15			
	JPCP16	X	X	X
	JPCP17			
Total number of projects available		18	19	16
Total number of projects required		5	21	–

Table 14. Simplified sampling template for the validation and local calibration of new and rehabilitated HMA surfaced pavements.

HMA Thickness, in	Base Thickness, in	Base and Subgrade Type	
		Coarse (A-1 through A-3) & Granular Base	Fine (A-4 through A-7) & Granular Base
4 to 8	< 6	1001	
	≥ 6	0803 0804 1017 HMA_R2 01 HMA_R2 03	HMA_R1 01 HMA_R1 02 HMA_R1 03 HMA_R2 04 HMA_R3 01 HMA_R3 02 HMA_R4 01 HMA_R4 03 HMA_R4 04 (NB) HMA_R4 04 (SB)
≥ 8	< 6		1007 1008
	≥ 6	1004 1005 1006 HMA_OVLY_1 HMA_R2 02	HMA_OVLY_2 HMA_OVLY_3 HMA_OVLY_4 HMA_R3 03 HMA_R4 02

Table 15. Simplified sampling template for the validation and local calibration of new and rehabilitated JPCP.

PCC Thickness, in	Dowel Diameter, in	Edge Support	Joint Spacing, ft	Subgrade Type			
				Coarse (A-1 through A-3)		Fine (A-4 through A-7)	
				Base Type			
				LCB	Granular	LCB	Granular
≤ 10	No dowels	None	<15	7085			
			≥15			CPR5	
		Tied PCC	<15	7082		CPR3 JPCP14 JPCP16	CPR4
			≥15	3010		CPR2 CPR6	
	Doweled	None	<15				
			≥15				
		Tied PCC	<15				
			≥15	CPR7 CPR8		JPCP6	
> 10	No dowels	None	<15	7086			
			≥15				
		Tied PCC	<15	3015 7083			
			≥15			3011	
	Doweled	None	<15				
			≥15				
		Tied PCC	<15				
			≥15	JPCP2	JPCP5		JPCP10

3.7.1 Statistical Method for Model Validation

Evaluate Goodness of Fit

The goodness of fit of a given MEPDG distress/IRI prediction model was assessed by determining model coefficient of determination (R^2) and standard error estimate (SEE) when tested with Utah data and determining the reasonableness of both diagnostic statistics by comparing their values with those obtained from national calibration under NCHRP 1-40D (see Table 16). Engineering judgment was then used to determine the reasonableness of both diagnostic statistics.

Models exhibiting a poor R^2 (i.e., R^2 less than 50 percent) or excessive SEE (significantly higher than the values presented in Table 16) were deemed to be inadequate for Utah conditions.

Table 16. Summary of national calibration under NCHRP 1-40D new HMA pavement and new JPCP model statistics.

Pavement Type	Performance Model	Model Statistics		
		Coefficient of Determination, R^2	Standard Error of Estimate, SEE	Number of Data Points, N
New HMA	Alligator cracking	0.275	5.01 percent	405
	Transverse "thermal" cracking	Level 1*: 0.344 Level 2*: 0.218 Level 3*: 0.057	–	–
	Rutting	0.58	0.107 in	334
	IRI	0.56	18.9 in/mi	1926
New JPCP	Transverse "slab" cracking	0.85	4.52 percent	1505
	Transverse joint faulting	0.58	0.033 in	1239
	IRI	0.60	17.1 in/mi	163

*Level of inputs used for calibration.

Evaluate Bias

Bias was defined as the consistent under- or over-prediction of distress/IRI. Bias was determined by performing linear regression using measured and MEPDG predicted distress/IRI and performing the following two hypothesis tests. A significance level, α, of 0.05 or 5 percent was assumed for all hypothesis testing.

- Hypothesis 1: Determine whether the linear regression model developed using measured and MEPDG predicted distress/IRI has an intercept of zero:

a. Using the results of the linear regression analysis, test the following null and alternative hypotheses to determine if the fitted linear regression model has an intercept of zero:
    i. H_0: Model intercept = 0.
    ii. H_A: Model intercept ≠ 0.

    A rejection of the null hypothesis (p-value < 0.05) would imply the linear model had an intercept significantly different from zero at the 5 percent significant level. This indicates that using the distress/IRI model for within the range of very low measured distress/IRI values will produce biased predictions.

- Hypothesis 2: Determine whether the linear regression model developed using measured and MEPDG predicted distress/IRI has a slope of 1.0:
    a. Using the results of the linear regression analysis, test the following null and alternative hypothesis to determine if the fitted linear regression model has an slope of 1.0:
        i. H_0: Model slope = 1.0.
        ii. H_A: Model slope ≠ 1.0.

    A rejection of the null hypothesis (p-value < 0.05) would imply that the linear model has a slope significantly different from 1.0 at the 5 percent significant level. This indicates that using the distress/IRI model outside of the range of measured distress/IRI used for analysis will produce biased predictions.

A third hypothesis test (paired t-test) was done to determine whether the measured and MEPDG predicted distress/IRI represented the same population of distress/IRI. The paired t-test was performed as follows:

- Hypothesis 3: Paired t-test.
    a. Perform a paired t-test to test the following null and alternative hypothesis:
        i. H_0: Mean measured distress/IRI = mean predicted distress/IRI.
        ii. H_A: Mean measured distress/IRI ≠ mean predicted distress/IRI.

    A rejection of the null hypothesis (p-value < 0.05) would imply the measured and MEPDG distress/IRI are from different populations. This indicates that for the range of distress/IRI used in analysis, the MEPDG model will produce biased predictions.

A rejection of any of the three null hypotheses indicates bias in predicted distress/IRI. Models that successfully passed all three tests were deemed to be not biased.

The presence of bias did not necessarily imply that the prediction model was inadequate. It basically means that there is some bias along the range of measured distress/IRI values evaluated. For example, the IRI models may produce perfect

predictions for the typical IRI range of 30 to 250 in/mi. The same model will, however, produce biased predictions for measured IRI values close to zero.

3.7.2 Non Statistical Method for Model Validation

For situations where measured distress/IRI was mostly zero, a simple visual comparison was made of measured and predicted distress/IRI categorized into as many groups as needed. The range of each group was determined based on engineering judgment. The goal was to determine how often measured and predicted distress/IRI remained in the same group. Measured and predicted distress remaining in the same group implied reasonable goodness of fit and no bias, while measured and predicted distress residing in different groups suggest otherwise.

The results of both the non-statistical and statistical analysis as appropriately applied were used to validate the MEPDG distress/IRI models. Where the MEPDG models were deemed inadequate for Utah conditions the models were locally calibrated.

3.7.3 Local Calibration of MEPDG Models

Local calibration was done using both linear and non-linear regression procedures in the SAS Institute Inc. software and consisted of the following steps (SAS 2004):

1. Determine MEPDG models global calibration coefficients that can be modified as part of local calibration (see Chapter 2).
2. Develop inputs for local calibration.
3. Perform optimization in SAS (linear and non-linear regression) to select local calibration coefficients that maximize R^2 and minimize SEE.
4. Validate the locally calibrated models (i.e., check for goodness of fit and bias).
5. Perform limited sensitivity analysis.
6. Develop final locally calibrated model coefficients based on the outcomes of steps 3 through 5.

Detailed description of Steps 7 through 10 is presented in Chapter 4.

3.8 Step 11: Interpretation of Results and Deciding on Adequacy of Calibration Factors

Under this step, the project team conducted a limited sensitivity analysis of the locally calibrated models to determine (1) reasonableness of predictions and (2) how predictions differ with the MEPDG nationally calibrated models. Based on this sensitivity analysis, adjustments were made to the locally calibrated models as needed. Results are presented in Chapter 5.

4.0 VALIDATION/RECALIBRATION OF SELECTED MEPDG MODELS

The MEPDG nationally calibrated models validation and local calibration effort for Utah is presented in this chapter. All statistical analysis presented in this chapter was done using the SAS statistical software (version 8). (SAS 2004)

4.1 New HMA Pavement Models

4.1.1 HMA Alligator Cracking

Validation

Figure 6 presents a histogram of all measured (including time series) alligator cracking for the UDOT PMS and LTPP projects evaluated and included in analysis. The plot shows that 160 of the 162 measured alligator cracking (percent lane area) had a value less that 2 percent. The remaining 2 measurements had a value ranging from 2 to 4 percent. The information in Figure 6 shows that the majority of the pavement projects used in analysis had minimal or no alligator cracking. Applying conventional statistical analysis including hypothesis testing to such data typically produces meaningless diagnostic statistics as the measured alligator cracking values are mostly zero. Thus, a non-statistical comparison of measured and predicted alligator cracking was done. For this comparison, alligator cracking was categorized into eight groups as shown in Table 17.

The goal was to determine how often measured and predicted alligator cracking fell in the same grouping. The range of each group was determined using engineering judgment. Results of the comparison are presented in Table 17. A review of the information presented in Table 17 showed the following:

- Ninety five percent of all data points (155 of the 162 data points) fell within the same measured and predicted alligator cracking grouping.
- Three percent (5 of the 162 data points) fell within an adjacent grouping (i.e., measured grouping 0 to 2 against predicted grouping 2 to 5 and measured grouping 2 to 5 against predicted grouping 0 to 2).
- For the remaining 2 data points, for a measured grouping 0 to 2, the MEPDG predictions fell in predicted grouping 5 to 10.

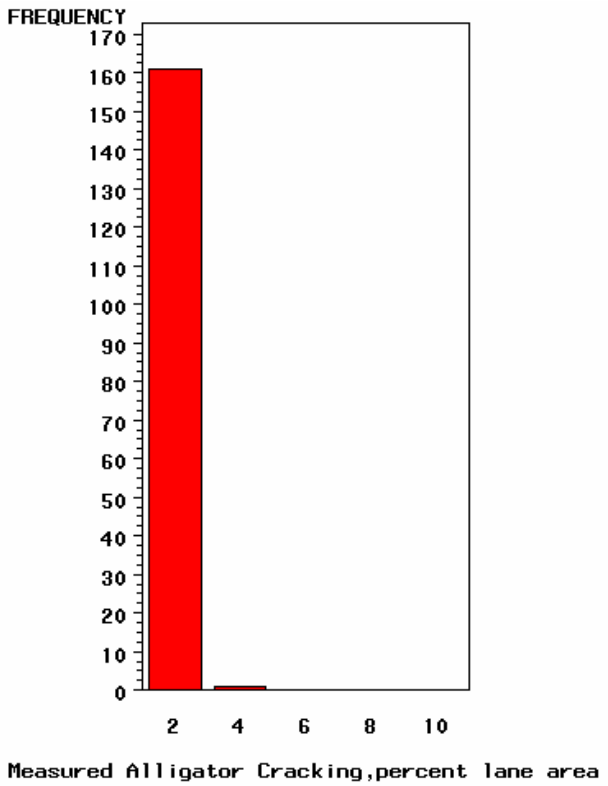

Figure 6. Histogram showing distribution of measured alligator cracking.

Table 17. Comparison of measured and predicted transverse cracking (percentage of all measurements).

Measured Alligator Cracking, percent lane area	**MEPDG Predicted Alligator Cracking, percent lane area**							
	0-2	2-5	5-10	10-20	20-40	40-60	60-80	80-100
0-2	155	4	2	0	0	0	0	0
2-5	1	0	0	0	0	0	0	0
5-10	0	0	0	0	0	0	0	0
10-20	0	0	0	0	0	0	0	0
20-40	0	0	0	0	0	0	0	0
40-60	0	0	0	0	0	0	0	0
60-80	0	0	0	0	0	0	0	0
80-100	0	0	0	0	0	0	0	0

Based on the results presented in Table 17, the following is concluded:

- The MEPDG predicts alligator cracking relatively well for the range of alligator cracking values reviewed.
- There is a need for further evaluation of this model using projects exhibiting higher levels of the distress.

Local Calibration

Local calibration was not required at this time.

4.1.2 HMA Transverse Cracking

Validation

Figure 7 presents a histogram of all measured (including time series) transverse cracking for the UDOT PMS and LTPP projects included in the analysis.

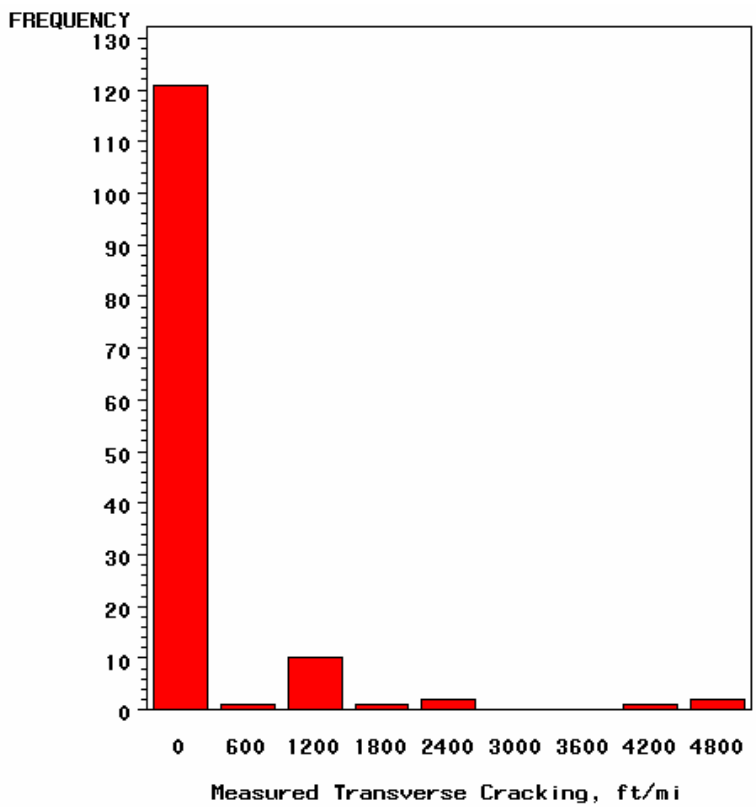

Figure 7. Histogram showing distribution of measured transverse "thermal" cracking.

Information provided in Figure 7 shows a wide distribution of transverse cracking but with most of the measured cracking being zero. A more detailed review of the information presented in Figure 7 and the LTPP and UDOT PMS project database indicated the following:

- Transverse cracking was exhibited mostly by the older pavements (constructed in the 1960's through 1980's). All of these projects were LTPP.
- The 1960's through 1980's HMA pavements were constructed mostly with conventional asphalt binders (i.e., AC-10, AC-20, and PEN 85-100).
- Pavements constructed in the 1990's and 2000's used SuperPave binders (LTPP SPS-8 and UDOT PMS projects). These pavements are relatively younger and exhibit little to no transverse cracking to date.

A thorough validation of the transverse cracking model using non statistical methods was done using (1) all the projects included in the project database and (2) separately for each binder type (conventional versus Superpave). Results are presented in Tables 18 and 19.

Table 18. Comparison of measured and predicted transverse cracking (all pavements).

MEPDG Measured Transverse Cracking, ft/mi	**MEPDG Predicted Transverse Cracking, ft/mi**			
	0-250	**250-500**	**500-1000**	**1000-2000**
0-250	120	0	0	0
250-500	1	0	0	0
500-1000	3	0	0	0
1000-2000	14	0	0	0

Table 19. Comparison of measured and predicted transverse cracking (by binder type).

Binder Type	**MEPDG Measured Transverse Cracking, ft/mi**	**MEPDG Predicted Transverse Cracking, ft/mi**			
		0-250	**250-500**	**500-1000**	**1000-2000**
Conventional binder (AC-10 & AC-20) (Older LTPP projects)	0-250	4	0	0	0
	250-500	1	0	0	0
	500-1000	3	0	0	0
	1000-2000	14	0	0	0
SuperPave binder (LTPP 0803 & 0804 and UDOT PMS projects)	0-250	116	0	0	0
	250-500	0	0	0	0
	500-1000	0	0	0	0
	1000-2000	0	0	0	0

Results of the model validation presented in Table 18 showed that 120 out of 138 measured and predicted transverse cracking data fell within the same grouping. Although this outcome appeared reasonable, a more detailed analysis by binder type indicates that all the SuperPave projects (116 data points) measured and predicted transverse cracking data fell in the same grouping (see Table 19). Thus, the MEPDG transverse cracking model appeared to predict transverse cracking well for new SuperPave binders and not so well for the conventional binders (where the model significantly under predicted transverse cracking).

Although no specific reason could be assigned to why the SuperPave binder projects predicted transverse cracking better than conventional mixes, the following can be theorized:

- Transverse cracking prediction was done using Level 3 inputs of MEPDG HMA creep compliance and tensile strength values (for each binder type). There is the possibility that default MEPDG HMA creep compliance and tensile strength values are more reasonable for SuperPave binders than conventional binders.
- The SuperPave projects were all relatively young. It is possible that the MEPDG model will significantly under predict cracking in the future once these pavements age and exhibit significant amounts of cracking. This essentially means the model itself is inadequate.

There will be need for additional work to answer the questions of reasonableness of inputs and the model adequacy.

Local Calibration

Considering that current UDOT HMA pavement design policy recommends the use of only SuperPave binders it was concluded that a local calibration effort is not necessary at this stage.

A comprehensive examination of older pavements with SuperPave binders exhibiting transverse cracking is, however, needed. This assessment should include determining whether (1) the defaults MEPDG HMA inputs are adequate (compare lab tested values to defaults and create UDOT specific defaults as needed) and (2) if the MEPDG transverse cracking model is adequate (using lab tested HMA inputs determine model adequacy).

A decision on local calibration can be made after the comprehensive assessment of this model adequacy.

4.1.3 HMA Rutting

Validation

Figure 8 presents a histogram of all measured (including time series) rutting data for the UDOT PMS and LTPP HMA pavement projects used in analysis. The projects included both new HMA and HMA overlaid HMA pavements. The plot shows data ranging from 0.05 to 0.35 in and a mean of 0.17 in. Evaluating such data statistically should produce reasonable and meaningful diagnostic statistics that can then be used to assess model's goodness of fit and bias. Thus, a statistical comparison of measured and MEPDG predicted rutting was performed. The results are presented in Figure 9 and Table 20 and they show the following:

- Significant bias in predicted rutting as indicated by the results of hypothesis testing of items (2) and (3) in Table 20. It is also obvious from Figure 9 that the MEPDG over predicts rutting.
- A poor correlation between measured and MEPDG predicted rutting (judging by the R^2 in Table 20).
- SEE in Table 20 is significantly higher than that reported for the national MEPDG rutting model.

Considering the biased predictions, poor R^2, and very high SEE, local calibration of the nationally calibrated MEPDG rutting model to improve its prediction accuracy in Utah was warranted.

Local Calibration

Local calibration involved (1) investigating the causes of poor goodness of fit and bias of the MEPDG nationally calibrated models and (2) modifying the local calibration coefficients of the HMA, base, and subgrade rutting sub models (see Chapter 2) as needed based on information derived from (1) to improve goodness of fit and reduce or eliminate bias. Specifically, state/regional local calibration coefficients β_{1r}, β_{2r}, and β_{3r} for the HMA sub model and unbound base and subgrade sub model coefficients β_{S1} and β_{S2} were modified as needed to improve predicted rutting.

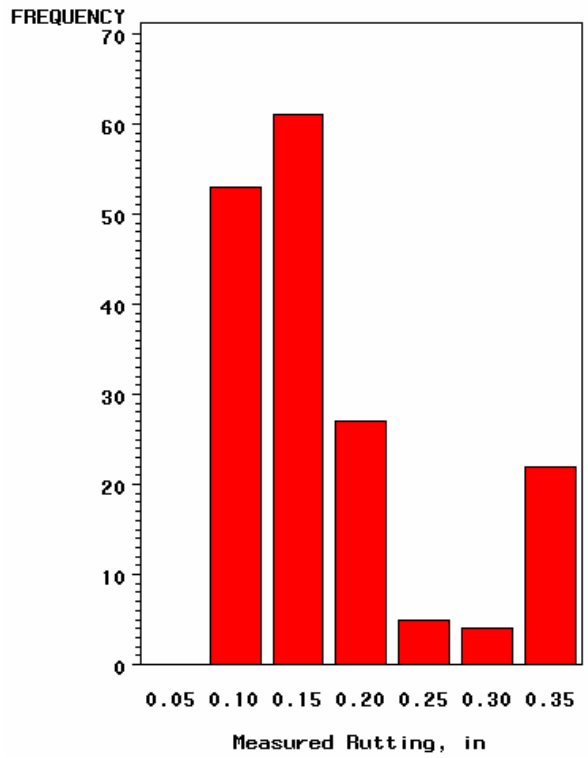

Figure 8. Histogram showing distribution of measured total rutting for all projects used in analysis.

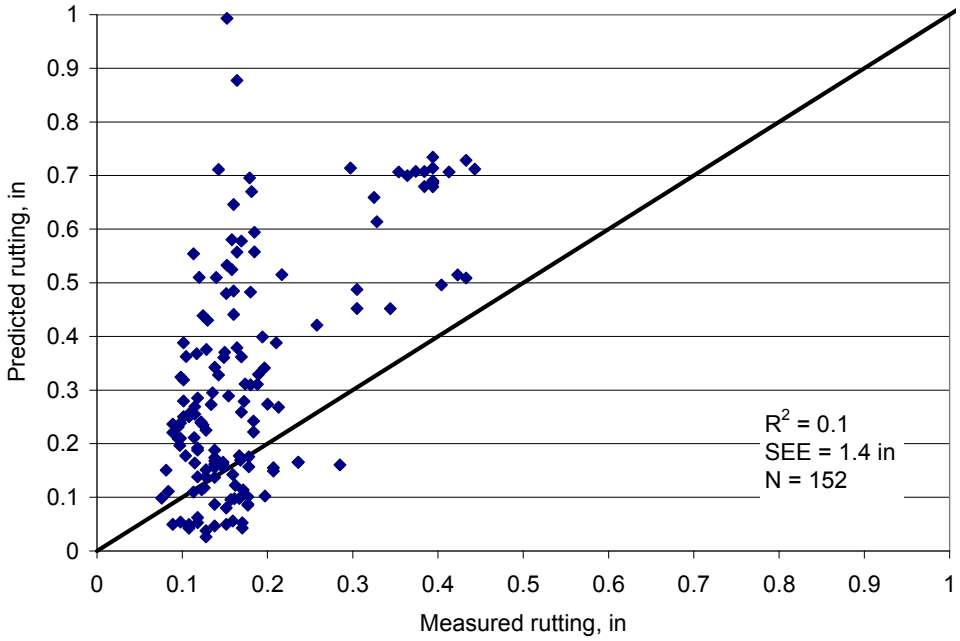

Figure 9. Plot of measured versus MEPDG predicted HMA pavement total rutting.

Table 20. Statistical comparison of measured and predicted rutting data.

Goodness of Fit N = 152 R^2 = 0.101 SEE = 1.4 in							
Hypothesis Testing							
Hypothesis	**Degrees of Freedom**	**Parameter Estimate**	**Std. Error**	**t Value**	**p-value (Pr > |t|)**	**95 Percent Confidence Limits**	
(1) Ho: Intercept = 0	1	-0.463	0.246	-1.88	0.0625	-0.951	0.245
(2) Ho: Slope = 1.0	1	2.922	0.548	5.33	0.0006	1.839	4.004
(3) Ho: Measured Rutting – MEPDG Predicted Rutting = 0	152			2.22	0.0281		

Investigation of Causes of Poor Goodness of Fit and Bias

The project team investigated the possible causes of poor goodness of fit and bias in predicted rutting by determining:

1. General reasonableness of rutting predictions for each submodel (HMA, base, and subgrade).
2. Specifically, for the HMA rutting submodel, the reasonableness of rutting predictions for pavements constructed using viscosity grade (mostly AC-10 and AC-20) asphalt binders and SuperPave grade asphalt binders.

Results from the investigations above are summarized below:

1. A review of predicted rutting for all three submodels show reasonable trends for predicted rutting. On average 48 percent of total rutting was located in the HMA layer, 15 percent in the granular base layer, and the remaining 37 percent in the subgrade.
2. The nationally calibrated rutting model predicted rutting adequately for older pavements constructed using viscosity graded binders (mostly AC-10 and AC-20) as shown by the information presented in Table 21 and Figure 10.
3. For more recently constructed HMA pavements, constructed based on current UDOT HMA mix design policy (i.e., UDOT PMS projects using SuperPave binders), the national rutting models predicted rutting poorly (see Table 22 and Figure 11). The reasons for thus may include the following:
    a. The national rutting model was calibrated using mostly older pavements constructed using viscosity graded binders rather than SuperPave binder.

b. Over prediction of subgrade rutting as local experience indicates that there is mostly little or no rutting occurring in the subgrade.
c. Since most of the SuperPave projects were obtained from the UDOT PMS database and thus measured rutting was adjusted to make it compatible with LTPP rutting measurements, a higher level of variability along with reduced goodness of fit is expected.

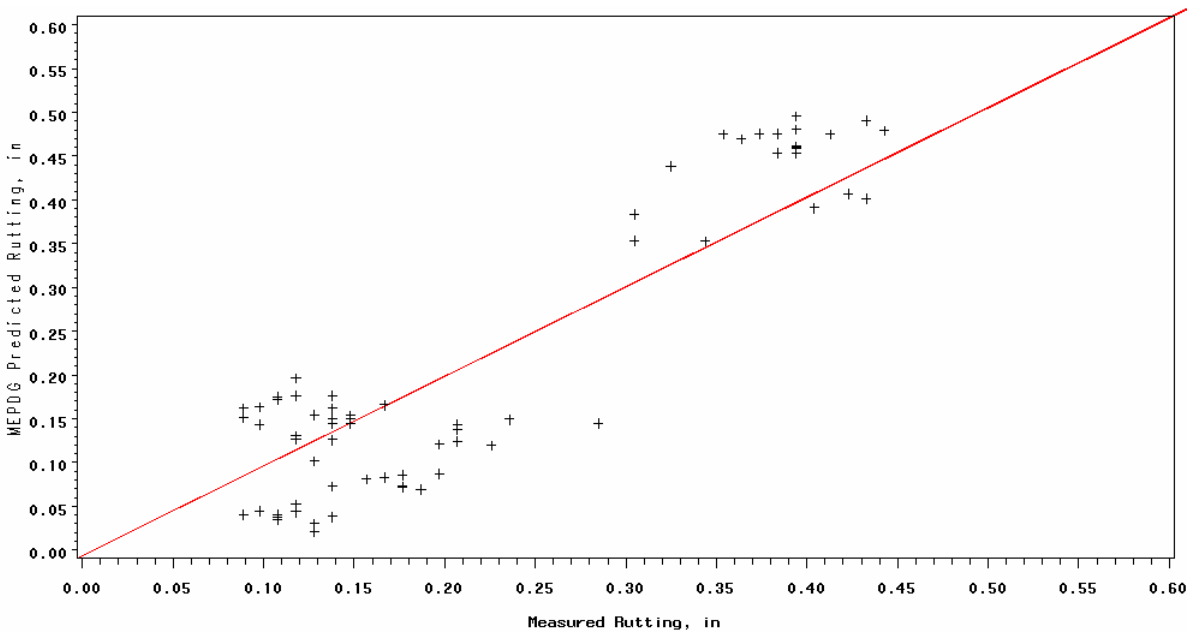

Figure 10. Plot of measured versus MEPDG predicted HMA pavement total rutting for LTPP projects only (viscosity graded binders).

Table 21. Statistical comparison of measured and predicted rutting data for LTPP projects only (viscosity graded binders).

Goodness of Fit N = 68 R^2 = 0.84 SEE = 0.066 in		
Hypothesis Testing		
Hypothesis	**Degrees of Freedom**	**p-value (Pr > |t|)**
(1) Ho: Intercept = 0	1	0.0008
(2) Ho: Slope = 1.0	1	0.2283
(3) Ho: Measured Rutting – MEPDG Predicted Rutting = 0	68	0.6566

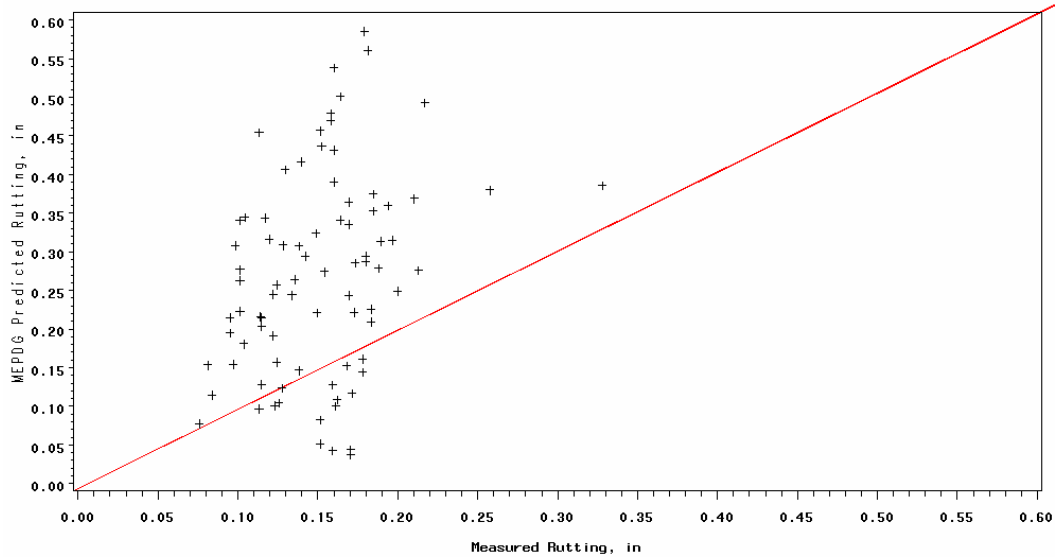

Figure 11. Plot of measured versus MEPDG predicted HMA pavement total rutting for UDOT PMS projects only (SuperPave binders).

Table 22. Statistical comparison of measured and predicted rutting data for UDOT PMS projects only (SuperPave binders).

Goodness of Fit N = 86 R^2 = 0.097 SEE = 0.15498		
Hypothesis Testing		
Hypothesis	**DF**	**p-value (Pr > |t|)**
(1) Ho: Intercept = 0	1	0.0822
(2) Ho: Slope = 1.0	1	< 0.0001
(3) Ho: Measured Rutting – MEPDG Predicted Rutting = 0	86	< 0.0001

Thus, although the nationally calibrated rutting model was found to be adequately predicting rutting for the older UDOT HMA pavement designs, there was a need for local calibration to make the rutting model suitable for analyzing newer HMA pavement designs in Utah. The local calibration performed as part of this research was limited in the sense that it was based only the UDOT PMS HMA projects (coded using mostly level 3 inputs and adjusted measured rutting data). A more through local calibration exercise in the future may be warranted using more accurate levels 1 and 2 input data.

Local Calibration of Rutting Submodels

Local calibration was performed using all the selected UDOT PMS projects described earlier. Model local coefficients were determined through optimization using SAS statistical software. The locally calibrated model including new model coefficients are as presented below:

$$\Delta_{p(total)} = \beta_{1r} k_z \varepsilon_{r(HMA)} 10^{k_{1r}} n^{k_{2r}\beta_{2r}} T^{k_{3r}\beta_{3r}} + \beta_{B1} k_{B1} \varepsilon_{vbase} h_{base} \left(\frac{\varepsilon_o}{\varepsilon_r}\right) e^{-\left(\frac{\rho}{n}\right)^{\beta}} + \beta_{s1} k_{s1} \varepsilon_{vsubgrade} h_{subgrade} \left(\frac{\varepsilon_o}{\varepsilon_r}\right) e^{-\left(\frac{\rho}{n}\right)^{\beta}} \quad (38)$$

All other variables are as previously defined in Chapter 2 (equations 14 through 21). Locally calibrated rutting model coefficients are as follows:

HMA	Base	Subgrade
k_{1r} = -3.35412 k_{2r} = 0.4791 k_{3r} = 1.5606 β_{1r} = 0.560 β_{2r} = 1.000 β_{3r} = 1.000	k_{B1} = 2.03 β_{B1} = 0.604	k_{S1} = 1.35 β_{S1} = 0.400

A statistical comparison of measured and predicted rutting from the locally calibrated rutting model was done to determine goodness of fit and bias. The results are presented in Figure 12 and Table 23 and show the following:

- A poor correlation between measured and MEPDG predicted rutting. This was mostly due to the nature of the measured rutting data (obtained from UDOT PMS database, measured using laser system, and converted to LTPP standards).
- SEE approximately the same as that reported for the national MEPDG rutting model.
- No significant bias in predicted rutting as indicated by the results of hypothesis (1), (2), and (3).

A limited sensitivity analysis of the locally calibrated rutting model is presented in Chapter 5. The sensitivity analysis basically compares the new locally calibrated model to the nationally calibrated model and assesses reasonableness of trends. The locally calibrated model removes bias that was presented in the nationally calibrated MEPDG rutting model.

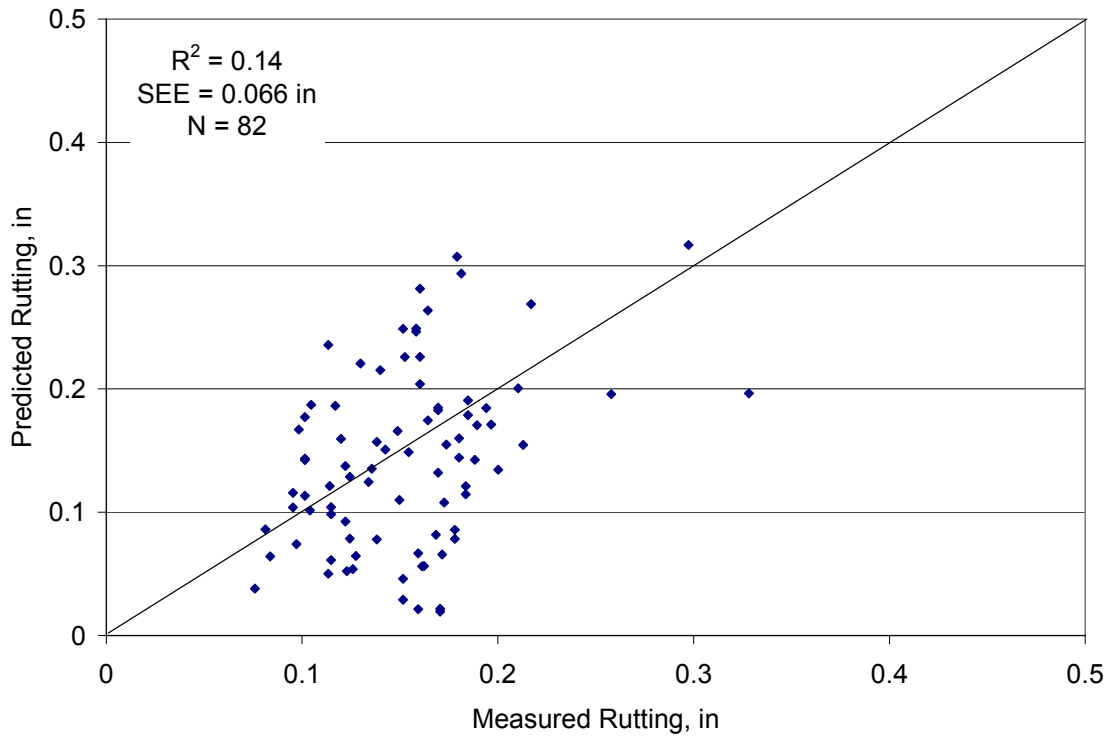

Figure 12. Plot of measured versus locally calibrated model predicted HMA pavement total rutting.

Table 23. Statistical comparison of measured and recalibrated rutting model predicted rutting data.

Goodness of Fit N = 82 R^2 = 0.144 SEE = 0.066 in							
Hypothesis Testing							
Hypothesis	**Degrees of Freedom**	**Parameter Estimate**	**Std. Error**	**t Value**	**p-value (Pr > |t|)**	**95 Percent Confidence Limits**	
(1) Ho: Intercept = 0	1	0.047	0.0266	1.79	0.078	-0.00541	0.1006
(2) Ho: Slope = 1.0	1	0.908	0.0466	19.47	0.054	0.8159	1.0017
(3) Ho: Measured Rutting – MEPDG Predicted Rutting = 0	82			-1.38	0.1716		

4.1.4 HMA Smoothness (IRI)

Validation

Figure 13 presents a histogram of all measured (including time series) IRI for the UDOT PMS and LTPP projects included in the analysis. The plot shows that the IRI data ranges from approximately 38.7 to 230 in/mi and a mean of 81.7 in/mi. A statistical comparison of the measured and MEPDG predicted IRI was performed to validate the nationally calibrated MEPDG model. Note that rutting is a key input for the MEPDG IRI model. For model validation, the locally calibrated rutting model was used to estimate rutting inputs. The results are presented in Figure 14 and Table 24.

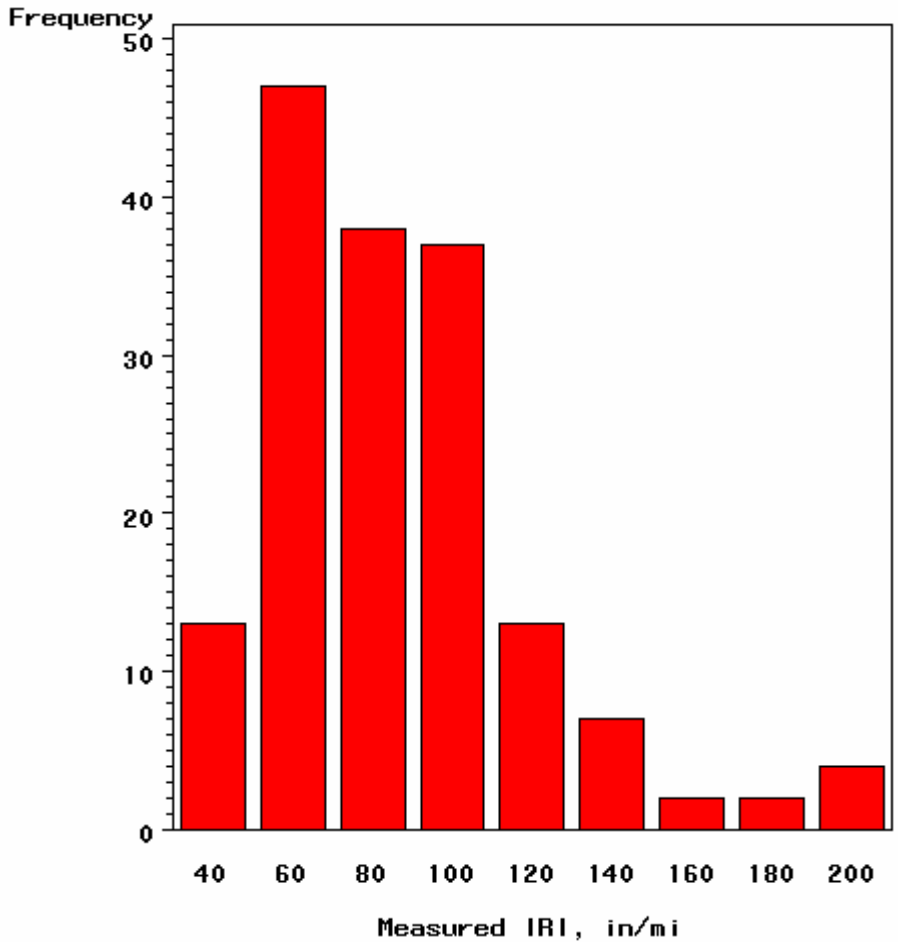

Figure 13. Histogram showing distribution of measured IRI for HMA.

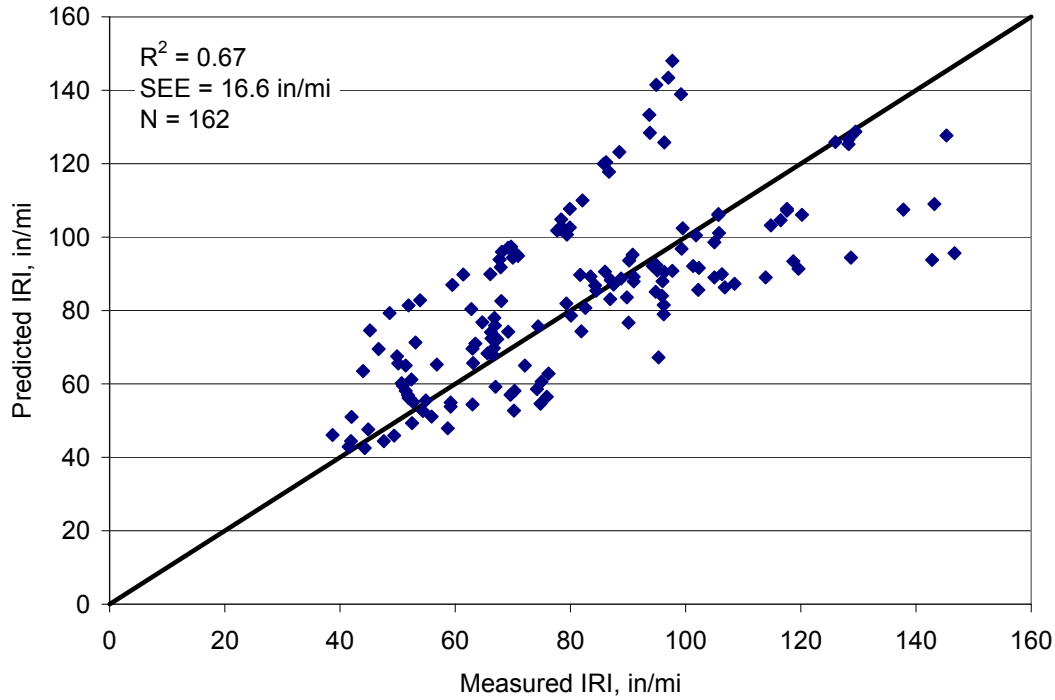

Figure 14. Plot of measured versus MEPDG predicted HMA pavement IRI.

Table 24. Statistical comparison of measured and MEPDG predicted IRI data.

Goodness of Fit N = 162 R2 = 0.67 SEE = 16.6 in/mi							
Hypothesis Testing							
Hypothesis	**Degrees of Freedom**	**Parameter Estimate**	**Std. Error**	**t Value**	**p-value (Pr > |t|)**	**95 Percent Confidence Limits**	
(1) Ho: Intercept = 0	1	29.2	3.53	8.27	<0.0001	22.24	36.19
(2) Ho: Slope = 1.0	1	0.9784	0.0165	1.70	0.1944	0.945	1.011
(3) Ho: Measured IRI – MEPDG Predicted IRI = 0	163			1.35	0.1790		

The results presented in Figure 14 and Table 24 indicate the following:

- Goodness of fit for the locally calibrated model was deemed adequate as there was a good correlation between measured and MEPDG predicted IRI and locally calibrated model SEE is slightly less than that reported for the national MEPDG IRI model.

- Overall t-test and slope of the MEPDG IRI versus measured IRI curve indicated that within the range of typical IRI (i.e. 30 to 250 in/mi) the nationally calibrated models predictions were adequate.
- There was some bias in predicted IRI at measured IRI values close to zero. This was, however, deemed as not relevant as it is expected that extrapolating the IRI model to predict IRI at values close to zero would lead to erroneous results as pavements never exhibit such low IRI values and the model was certainly not developed to predict IRI at such magnitudes.

Recalibration

Recalibration was not warranted based on the validation test results.

4.2 New JPCP

4.2.1 Transverse Slab Cracking

Validation

Figure 15 presents a histogram of all measured (including time series) PCC slab transverse cracking for the UDOT PMS and LTPP projects included in the analysis. Note that both CPR and new JPCP projects are combined for this analysis. As shown in Figure 15, 80 out of the 87 reported measurements of percent slabs cracked were less than 5 percent and mostly zero. However, there were sufficient amounts of non-zero measurements of transverse cracking distress available to evaluate and validate the MEPDG JPCP transverse cracking model using statistical methods. The results are presented in Figure 16 and Table 25 and show the following:

- A very good correlation between measured and MEPDG predicted cracking.
- SEE approximately the same as that of the national MEPDG JPC cracking model.
- No significant bias in predicted cracking as indicated by the results of hypothesis (1), (2), and (3).

Therefore it can be concluded that the MEPDG JPCP transverse cracking model predicted the distress adequately without significant bias.

Recalibration

Recalibration of this model was not needed.

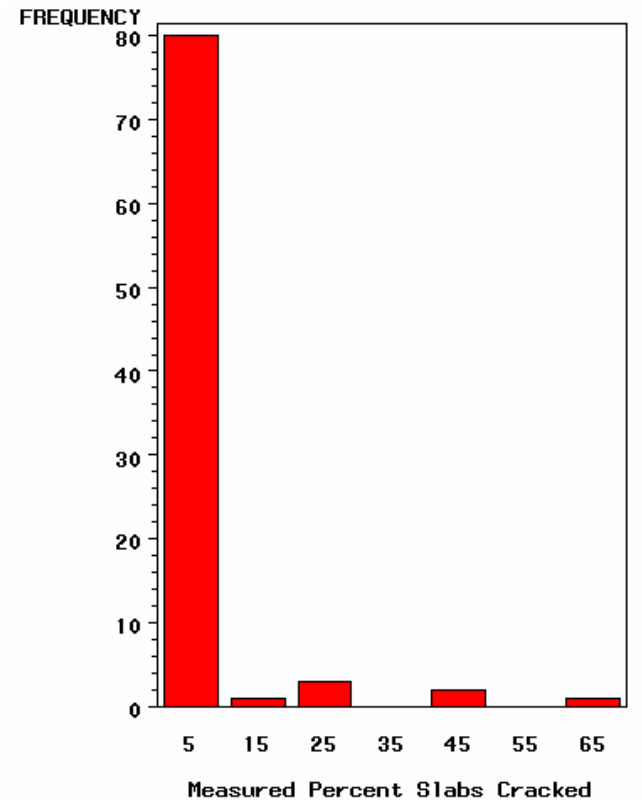

Figure 15. Histogram showing distribution of measured percent slabs cracked.

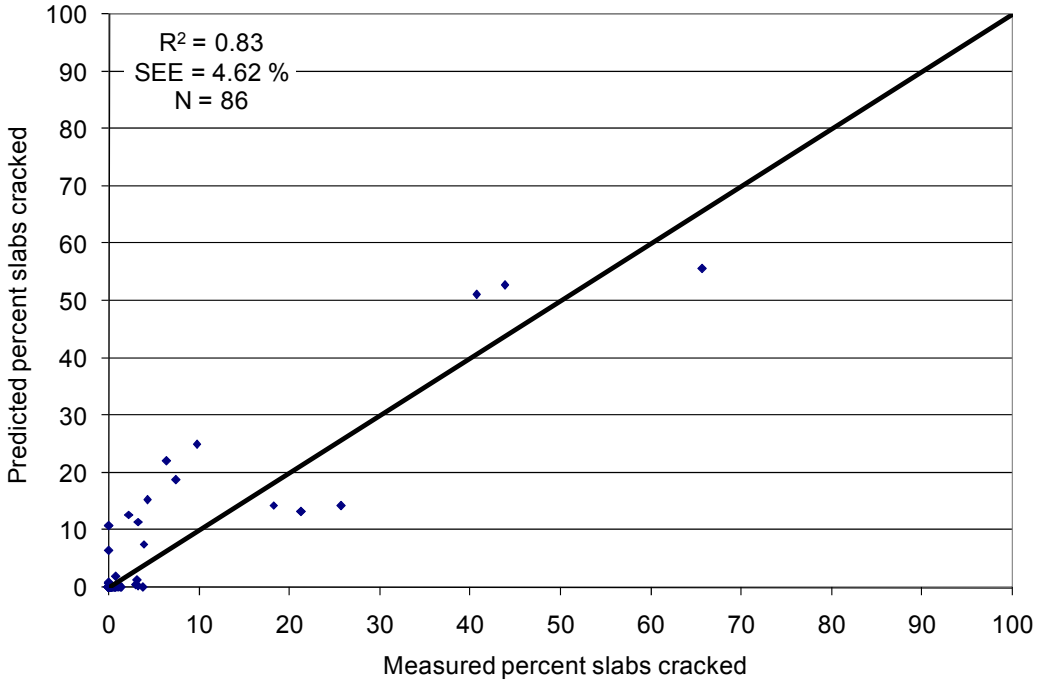

Figure 16. Plot of measured versus MEPDG predicted JPCP percent slabs with transverse cracking.

Table 25. Statistical comparison of measured and MEPDG predicted transverse slab cracking data.

Goodness of Fit N = 86 R^2 = 0.83 SEE = 4.62 percent							
Hypothesis Testing							
Hypothesis	**Degrees of Freedom**	**Parameter Estimate**	**Std. Error**	**t Value**	**p-value (Pr > |t|)**	**95 Percent Confidence Limits**	
(1) Ho: Intercept = 0	1	0.906	0.511	1.77	0.0798	-0.1101	1.9221
(2) Ho: Slope = 1.0	1	0.987	0.045	0.08	0.7845	0.8967	1.0782
(3) Ho: Measured Slab Cracking – MEPDG Predicted Cracking = 0	86			1.60	0.1143		

4.2.2 Transverse Joint Faulting

Validation

Figure 17 presents a histogram of all measured (including time series) mean transverse joint faulting for all the UDOT PMS and LTPP projects included in analysis. Note that both CPR and new JPCP projects were combined for this analysis. Also, default MEPDG models calibration coefficients for CPR and new JPCP are different as presented in Chapter 2. The plot shows that the measured mean joint faulting ranges from 0 to 0.26 in, with a mean of 0.04 in.

Evaluating the data presented in Figure 17 should produce reasonable and meaningful diagnostic statistics as the measured distress was mostly non-zero. Thus, a statistical comparison of measured and MEPDG predicted transverse joint faulting was done. The results are presented in Figure 18 and Table 26 and show the following:

- A fair correlation between measured and MEPDG predicted faulting.
- SEE slightly higher than that reported for the national MEPDG faulting model.
- No significant bias in predicted faulting as indicated by the results of hypothesis (1), (2), and (3).

Therefore it was concluded that the MEPDG mean joint faulting model's goodness of fit was adequate and model predictions had no significant bias.

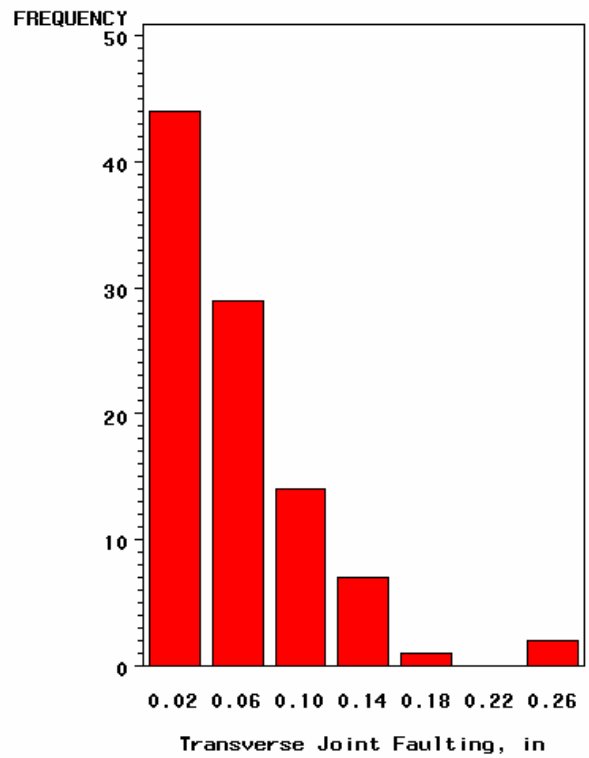

Figure 17. Histogram showing distribution of measured transverse joint faulting for all projects evaluated.

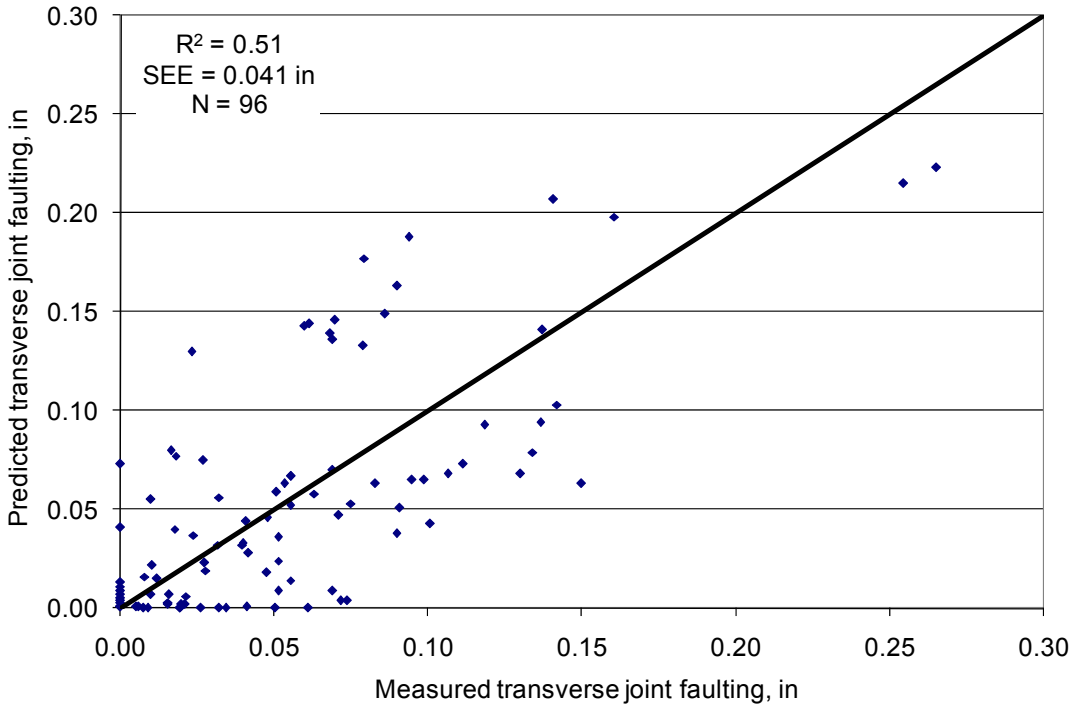

Figure 18. Plot of measured versus MEPDG predicted JPCP faulting.

Table 26. Statistical comparison of measured and MEPDG predicted transverse joint faulting data.

Goodness of Fit							
N = 96 R^2 = 0.51 SEE = 0.041 in							
Hypothesis Testing							
Hypothesis	**Degrees of Freedom**	**Parameter Estimate**	**Std. Error**	**t Value**	**p-value (Pr > |t|)**	**95 Percent Confidence Limits**	
(1) Ho: Intercept = 0	1	0.00901	0.00606	1.49	0.1402	-0.00302	0.02104
(2) Ho: Slope = 1.0	1	0.90331	0.05573	3.01	0.0859	0.79269	1.01393
(3) Ho: Measured Faulting – MEPDG Predicted Faulting = 0	96			-0.26	0.7945		

Recalibration

Recalibration of this model was not needed.

4.2.3 JPCP Smoothness (IRI)

Validation

Figure 19 presents a histogram of all the measured (including time series) IRI data for the selected UDOT PMS and LTPP projects included in analysis. Note that both CPR and new JPCP projects are combined for this analysis. The plot shows that the measured IRI ranges from 60 to 165 in/mi with a mean of 93 in/mi. A statistical comparison of the measured and MEPDG predicted IRI was performed. The results are presented in Figure 20 and Table 27 and showed the following:

- A very good correlation between measured and MEPDG predicted IRI.
- SEE less than that reported for the national MEPDG JPCP IRI model.
- No significant bias in predicted JPCP IRI as indicated by the results of hypothesis (1), (2), and (3).

Therefore it was concluded that the MEPDG IRI model's goodness of fit was adequate and model predictions had no significant bias.

Recalibration

There was no need for JPCP IRI prediction model local calibration.

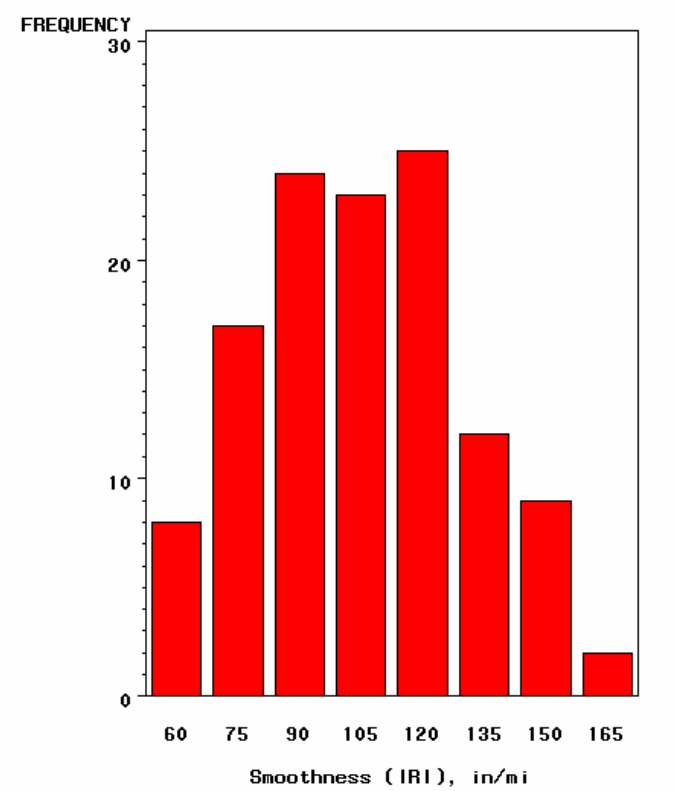

Figure 19. Histogram showing distribution of measured JPCP IRI.

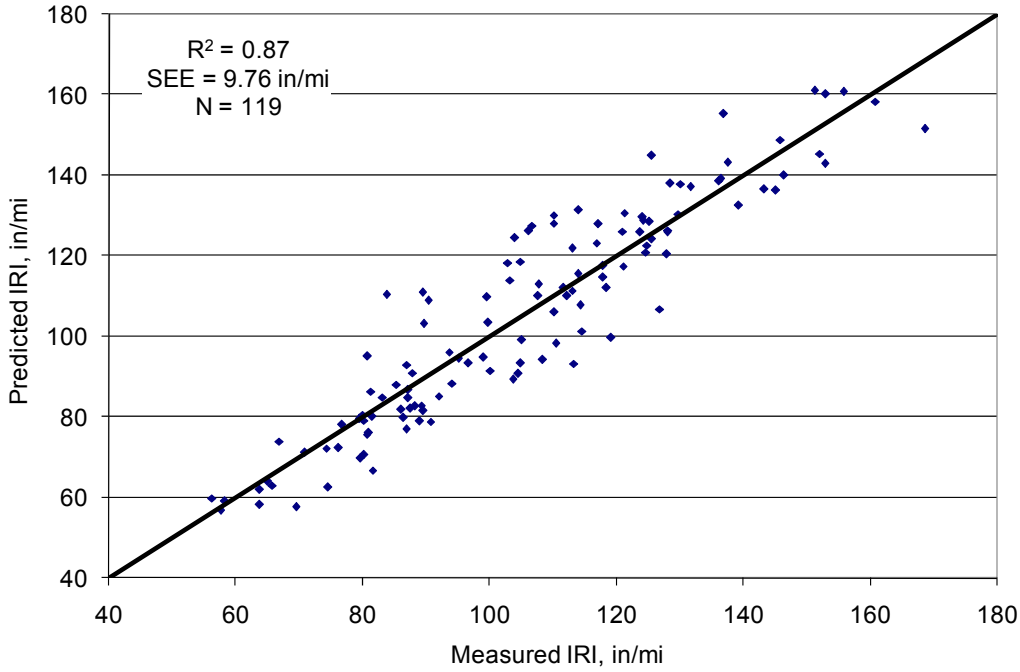

Figure 20. Plot of measured versus MEPDG predicted JPCP pavement IRI.

Table 27. Statistical comparison of measured and MEPDG predicted JPCP IRI data.

Goodness of Fit

N = 119
R^2 = 0.87
SEE = 9.76 in/mi

Hypothesis Testing

Hypothesis	DF	Parameter Estimate	Std. Error	t Value	p-value (Pr > |t|)	95 Percent Confidence Limits	
(1) Ho: Intercept = 0	1	-0.6915	3.8793	-0.18	0.8588	-8.3737	6.9906
(2) Ho: Slope = 1.0	1	1.00255	0.0082	0.10	0.7569	0.9863	1.0188
(3) Ho: Measured IRI – MEPDG Predicted IRI = 0	119			0.26	0.7947		

THIS PAGE INTENTIONALLY LEFT BLANK

5.0 SENSITIVITY ANALYSIS OF LOCALLY CALIBRATED MEPDG MODELS

5.1 Scope of Sensitivity Analysis

A sensitivity analysis is the process of varying model input parameters (subgrade type, base type, HMA as-placed air voids, etc.) over a practical range and observing the relative change in model response (e.g., HMA rutting and IRI). By doing this for typical Utah conditions, the locally calibrated MEPDG models can be evaluated for reasonableness (i.e., do pavement deterioration predictions from these models reflect actual observed pavement deterioration).

5.2 Selected HMA Pavement Baseline Designs

A representative baseline new HMA pavement design developed for use in sensitivity analysis is described in Table 28. The baseline design was typical of Utah site conditions and UDOT pavement design and construction practices.

The baseline new HMA pavement design was used to perform a comprehensive sensitivity analysis by varying the values of key inputs over a practical range and determining their impact on predicted distress/IRI. The key input parameters of interest varied as part of the sensitivity analysis are summarized in Table 29.

5.3 Sensitivity Analysis Results for Locally Calibrated Rutting Model

The results of the sensitivity analysis are presented in the following sections.

5.3.1 Effect of Base Type

Two base types—dense graded aggregate base (DGAB) (A-1-a) and lean concrete base (LCB)—were considered to determine the impact of base type on predicted rutting. Both base types were 4.7-in thick and had the following modulus values:

- LCB: 2,000,000 psi.
- DGAB: 40,000 psi.

The effect of base type on predicted rutting is shown in Figure 21. The information presented shows HMA pavements with unbound aggregate bases experience higher levels of rutting than pavements with LCB. This is as expected. Compared to the nationally calibrated MEPDG models, the recalibrated models predicted less amount of rutting. An evaluation of the trend in predicted rutting using the locally calibrated

model showed reasonable predictions that were in agreement with the trends in pavement deterioration observed in Utah.

Table 28. Input parameters of interest used in the HMA models sensitivity analysis.

Data Category	Description	Value
General information	Design life	25 years
Traffic	Initial two-way AADTT	466
	Number of lanes in design direction	1
	Percent of trucks in design direction	50
	Percent of trucks in design lane	100
	Truck traffic growth	4 percent, compound
Climate	Latitude (degrees)	38.95
	Longitude (degrees)	-111.86
	Elevation (ft)	5200
	Depth of water table (ft)	25
Surface layer	Material type	Asphalt concrete
	Layer thickness (in)	9
	Effective binder content (percent)	11
	Air voids (percent)	8.5
	Total unit weight (pcf)*	148
	Cumulative percent retained 3/4 inch sieve	0
	Cumulative percent retained 3/8 inch sieve	12
	Cumulative percent retained No. 4 sieve	37.5
	percent Passing #200 sieve	9.9
	AC viscosity grade	AC 10
Base layer	Unbound material	A-1-a
	Thickness(in)	4.7
	Modulus (input) (psi)	40,000
	Plasticity index, PI	1
	Passing no. 200 sieve (percent)	12.2
	Passing no. 4 sieve (percent)	56.5
	D60 (mm)	12.4
Subgrade	Unbound material	A-4
	Thickness(in)	Semi-infinite
	Modulus (input) (psi)	16,500
	Plasticity index, PI	10
	Passing no. 200 sieve (percent)	61.1
	Passing no. #4 sieve (percent)	91.5
	D60 (mm)	0.075

* pcf = pounds per cubic foot

Table 29. Input parameters of interest used in the HMA models sensitivity analysis.

MEPDG Input Parameter	Levels of Input
Base type	LCB (elastic modulus = 2,000,000 psi), Granular base (A-1-a, resilient modulus = 40,000 psi)
Climate	Logan, Cedar City, Moab, Salt Lake City, Price, Vernal
HMA thickness	3-, 6-, 9-in
Subgrade type	A-1-a (resilient modulus = 29,500 psi), A-4 (resilient modulus = 16,500 psi), A-7-6 (resilient modulus = 11,500 psi)
HMA air voids	4.5, 6.5, 8.5 percent
HMA binder type	AC-10, PG70-16, PG64-34

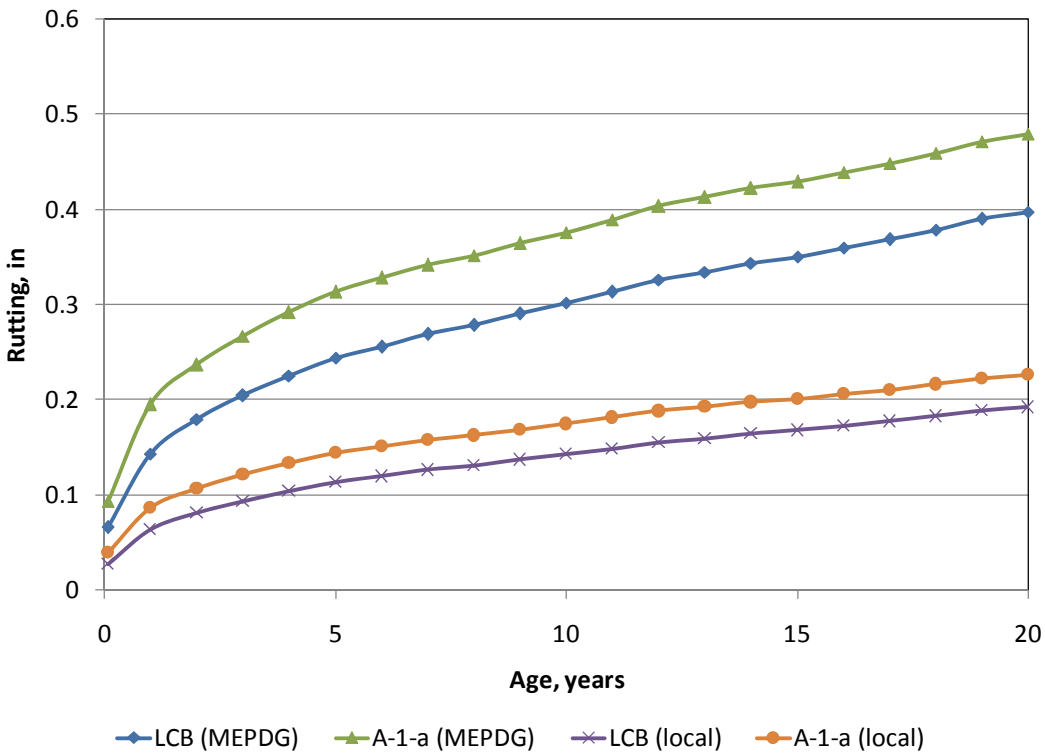

Figure 21. Plot showing the effect of base type on predicted rutting.

5.3.2 Effect of Climate

The effect of climate on locally calibrated rutting model predictions was determined by selecting representative weather stations from the north (Salt Lake City), central (Moab), and south (Cedar City) parts of Utah.

The objective was to determine (1) whether the effect of climate on the recalibrated models was reasonable and (2) how it compared with the nationally calibrated models. Climatic conditions were simulated using approximately 9 years of climate data (i.e., temperature, precipitation, cloud cover, sunshine, and so on) collected from weather stations located in these regions of Utah. The exact locations of these cities across Utah are shown in Appendix C. The result of the sensitivity analysis is presented in Figure 22.

The overall trend observed in predicted rutting for the locally calibrated model is similar to that of the nationally calibrated model.

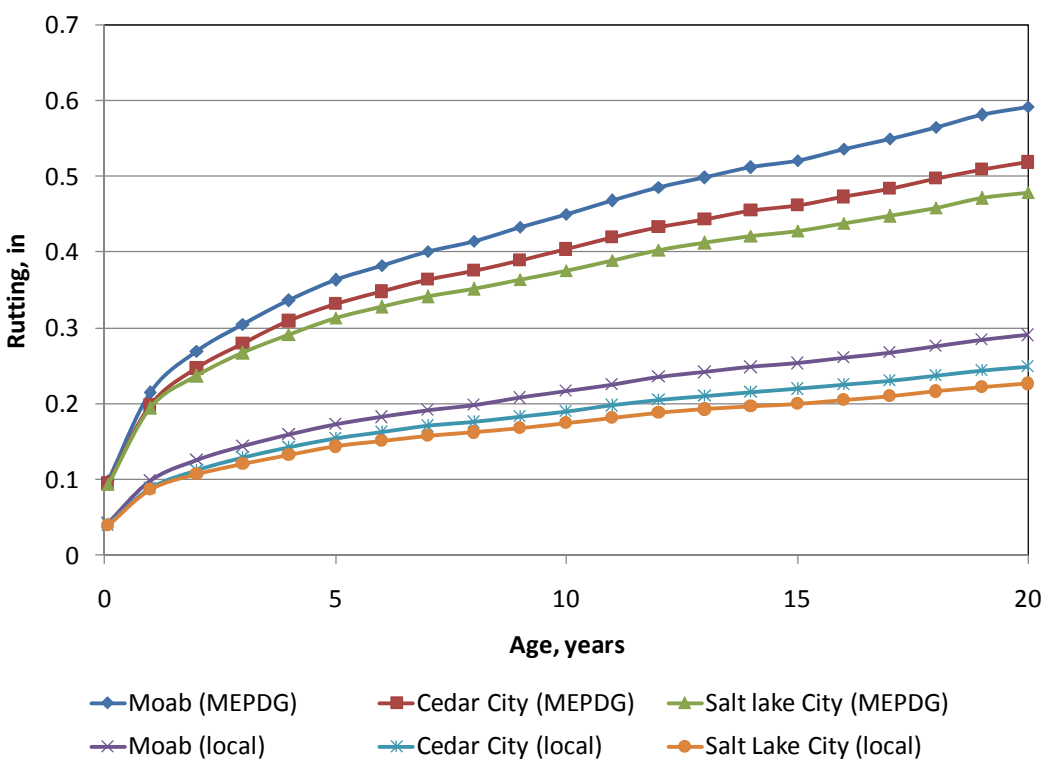

Figure 22. Plot showing the effect of climate on predicted rutting.

5.3.3 Effect of HMA Thickness

HMA thickness had a large effect on rutting for both the nationally and locally calibrated models. This effect is shown in Figure 23 for HMA thickness ranging from 3 to 9 in. The trends shown by the locally calibrated models were reasonable and as expected. The locally calibrated models were thus deemed reasonable.

5.3.4 Effect of Subgrade Type

The effect of subgrade type (AASHTO Classification) on predicted rutting was determined by simulating a new HMA pavement constructed over a fine-grained (A-7-6) and coarse grained (A-1-a) soil foundation. The baseline subgrade soil type (A-4) was also considered. The subgrade soil properties represented by these two soil types used in sensitivity analysis are summarized below:

- Coarse-grained soil (A-1-a):
    - Resilient modulus: 29,500 psi.
    - Percent passing the No. 200 sieve size: 8.7 percent.
    - Maximum dry density: 127.2 pcf.
    - Optimum moisture content: 7.4 percent.
    - Hydraulic conductivity: 0.051 ft/hr
- Fine-grained soil (A-7-6):
    - Resilient modulus: 11,500 psi
    - Percent passing the No. 200 sieve size: 79.1 percent.
    - Maximum dry density: 97.7 pcf.
    - Optimum moisture content: 22.2 percent.
    - Hydraulic conductivity: 0.000089 ft/hr

The most significant property affecting rutting development is the resilient modulus which affects stress, strains, and deformations in the pavement and subgrade. As the subgrade modulus decreases, vertical strain at the top of the subgrade increases. Figure 24 presents the effect of subgrade soil type (A-1-a, A-4, and A-7-6) on predicted rutting. In general, lowering the subgrade modulus led to higher estimates of rutting. The trends shown by the locally calibrated rutting model were reasonable and as expected.

5.3.5 Effect of HMA In-Situ Air Voids

Changes in HMA air voids has a considerable effect on rutting since air voids does affect HMA dynamic modulus, a key input for estimating permanent strain within the HMA layer. Figure 25 shows the effect of the air voids in the HMA layer on predicted rutting. As can be noted, an increase of in situ air void content in the HMA layer results in an increase in rutting. Trends shown by the locally calibrated model were reasonable and as expected. The locally calibrated models were thus deemed reasonable.

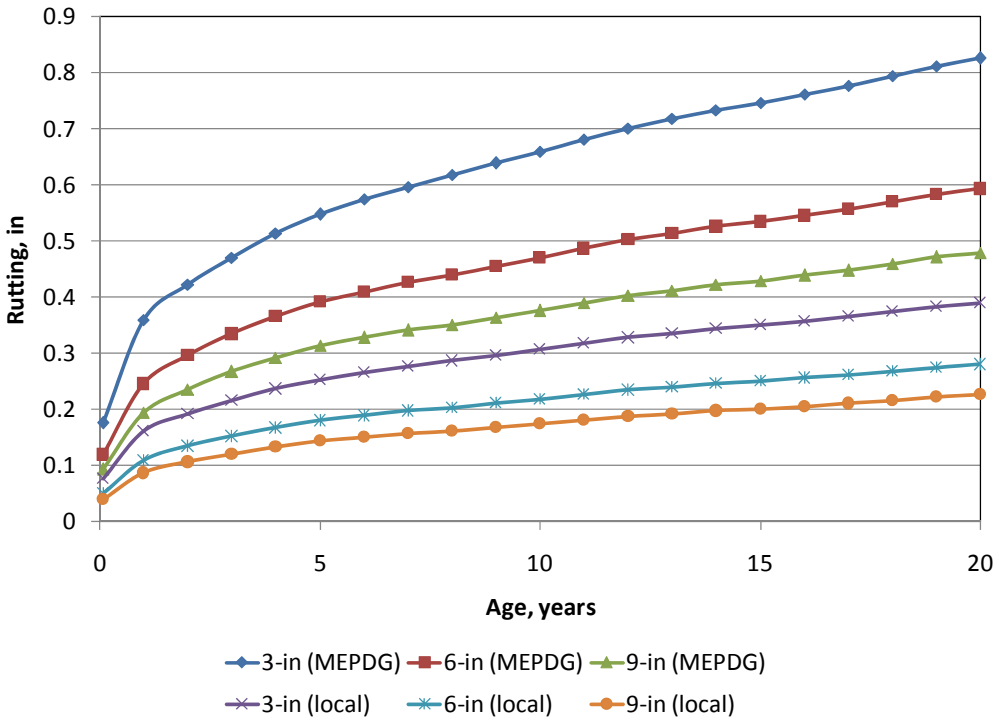

Figure 23. Plot showing the effect of HMA thickness on predicted rutting.

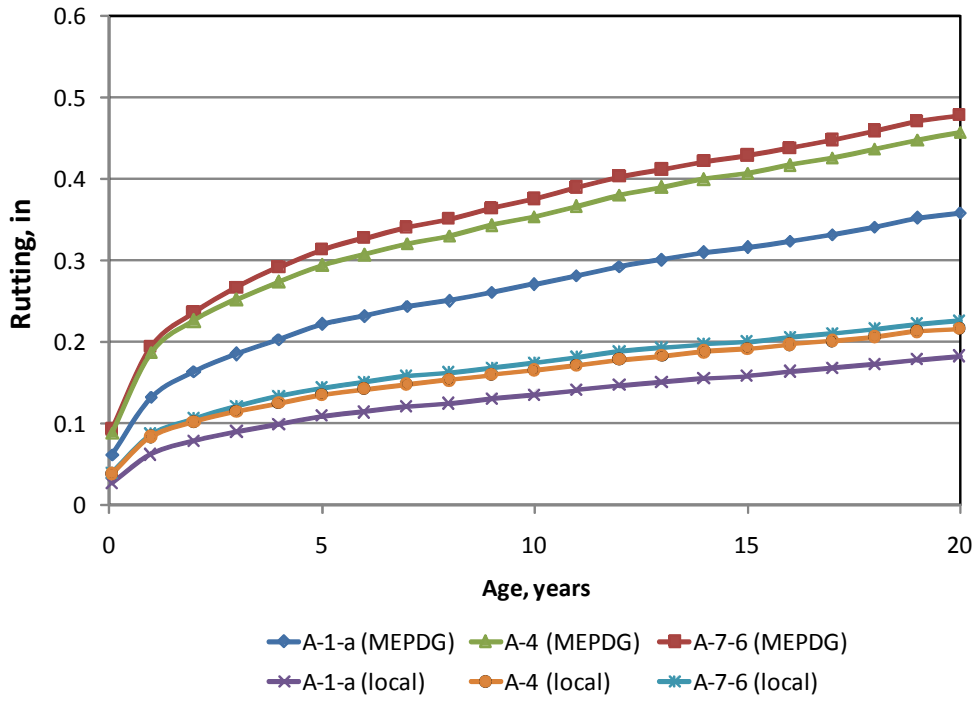

Figure 24. Plot showing the effect of subgrade type on predicted rutting.

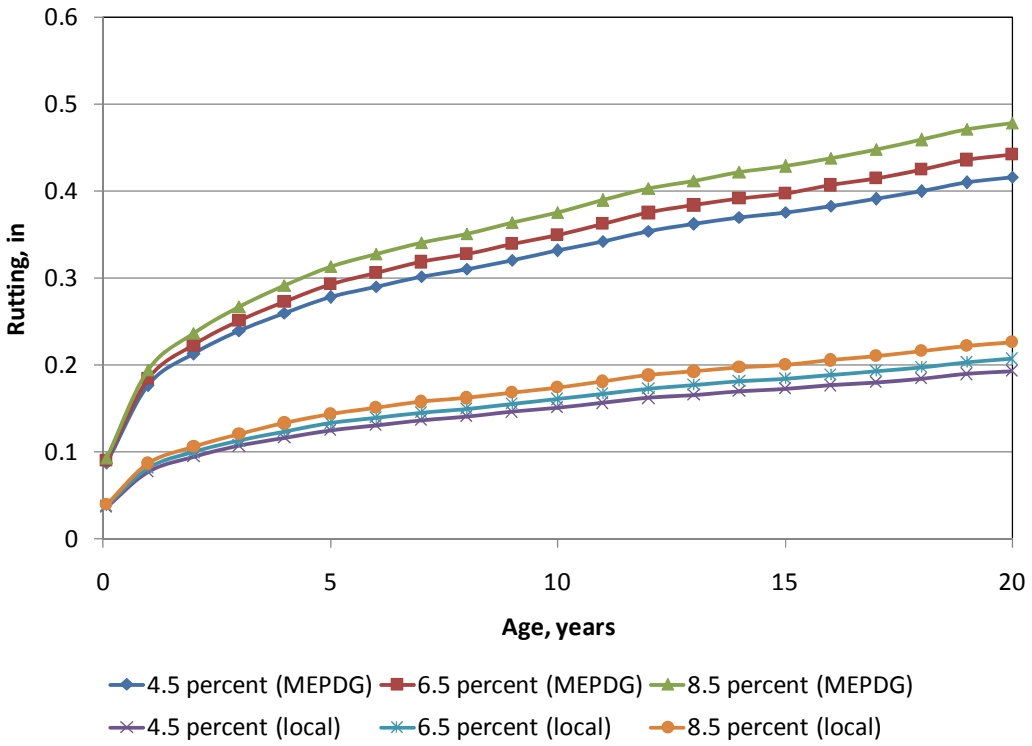

Figure 25. Plot showing the effect of HMA air voids on predicted rutting.

5.4 Summary

In general, the locally calibrated rutting model predicted less rutting than the national model. This is in agreement with trends shown in the plot of predicted rutting using the nationally calibrated model versus measured rutting, where the national model was observed to significantly over predict rutting (see Figure 9).

THIS PAGE INTENTIONALLY LEFT BLANK

6.0 SUMMARY, CONCLUSIONS, AND RECOMMENDATIONS

6.1 Summary

6.1.1 New HMA and HMA Overlaid HMA Pavements

Results for the nationally calibrated MEPDG models validation and local calibration effort in Utah for HMA are summarized as follows:

- Alligator fatigue cracking: Due to the nature of alligator cracking data available a non statistical approach for validating this model was adopted. Alligator cracking model validation showed that the national model predicted alligator cracking relatively well in Utah conditions. However, the alligator cracking model could not be evaluated for pavements exhibiting significant amounts of the distress as projects experiencing significant deterioration were not available. There is need to identify and include HMA projects with moderate to severe levels of alligator cracking and include them in future validation studies.

- Transverse "thermal" cracking: Due to the nature of transverse cracking data available, a non statistical approach for validating this model was adopted. The non-statistical comparison of predicted and measured transverse cracking data showed that for the relatively younger pavements constructed using UDOT SuperPave binders, the national model predicted transverse cracking well. For the older LTPP pavements constructed using conventional asphalt binders (AC-10 and AC-20) the national model was very inadequate. The project team decided not to recalibrate this model since it seemed to predict transverse cracking well for the current UDOT HMA designs using SuperPave. There is, however, need for continuing monitoring of the existing UDOT pavements with SuperPave mixes to determine if the national model will be able to predict transverse cracking once they start to deteriorate and exhibit this distress. Also, developing UDOT mix specific HMA input properties (i.e., creep compliance and tensile strength) used for predicting HMA transverse cracking will increase model prediction capability.

- Rutting: The MEPDG national rutting model predicted rutting adequately for older pavements constructed using viscosity graded asphalt mixes. The same model, however, poorly predicted rutting with significant bias when applied to newer HMA pavement designs with SuperPave HMA mixes. Therefore, there was a need for local calibration of the national model to enable it to predict rutting much more accurately under current Utah HMA pavement design (including HMA mix design) and construction conditions. Local calibration was

done and produced new local calibration coefficients for all three rutting submodels (HMA, base, and subgrade). The new local calibration coefficients based on HMA thickness are as follows:

Pavement Type	Rutting Submodels Local Calibration Coefficients		
	HMA (β_{1r})	Base (β_{B1})	Subgrade (β_{s1})
New HMA	0.560	0.604	0.400
HMA overlaid HMA	0.560	0.604	0.400

Local calibration significantly improved on the model accuracy and removed all significant bias. A sensitivity analysis performed showed the locally calibrated model to be reasonable.

- HMA IRI: There was good correlation between measured and MEPDG predicted IRI and SEE was approximately the same as that reported for the national MEPDG IRI model. Although there was some bias in predicted IRI, the bias was deemed as not significant.

6.1.2 New JPCP and JPCP Subjected to CPR

Results for the nationally calibrated MEPDG models validation and local calibration effort in Utah for JPCP are summarized as follows:

- Transverse "fatigue" cracking in the slab: A full evaluation of this model was conducted. Results showed very adequate goodness of fit and no significant bias in predicted transverse cracking.

- Transverse joint faulting: The MEPDG model predicted faulting reasonably well with an adequate goodness of fit and no significant bias in predicted faulting.

- IRI: Predicted IRI using the nationally calibrated MEPDG model showed the model predicting IRI well under Utah conditions with an adequate goodness of fit and no significant bias in predicted IRI.

6.1.3 Materials and Traffic Data Used in Models Validation and Local Calibration

Materials inputs used for all LTPP and Utah PMS sections are included in various sections throughout this report and appendices. These inputs from HMA and JPCP projects scattered throughout the State provide an excellent resource for typical and default materials inputs for pavement design.

Traffic inputs for all sections are available in electronic file format and have been provided to UDOT for use as a resource for typical and default traffic inputs for pavement design.

6.2 Conclusions and Recommendations

The MEPDG models were reviewed thoroughly for use under Utah conditions using both LTPP and UDOT PMS projects.

The review of the MEPDG models indicated that with the exception of the HMA rutting model, all the models evaluated predicted distress/IRI reasonably. However, for some models the range of distress data used in evaluation was limited. This raises questions about their ability to predict higher levels of distress reasonably.

Therefore, based on the analysis performed, the following conclusions are drawn:

- Evaluating all the MEPDG distress and IRI models needs to be a continuous process over time to fully consider the impacts of current pavement design and construction practices on model adequacy. By doing so, projects from which moderate to high levels of distress are currently obtained, which tend to be older and mostly were constructed using outdated pavement design features and materials types (e.g., Marshall versus SuperPave HMA mixes), will gradually be removed from the project database. They will be replaced by projects that are currently relatively younger and exhibit little to no distress but are designed based on current UDOT procedures.

- The mix of original MEPDG and locally calibrated models presented in this report appear to predict distress/IRI reasonably well in Utah. They must be used, however, within the limitations such as:
    - HMA transverse cracking using Level 3 inputs does not predict transverse cracking adequately for conventional asphalt binders and thus only lab tested HMA creep compliance and tensile strength must be used in predicting transverse cracking in order to obtain more reasonable results.
    - The HMA rutting model must be used only with the local calibration coefficients specified.
    - The HMA pavement alligator fatigue cracking is valid only for low levels of cracking.
    - The national and locally calibrated models are valid only for the limited conditions under which they were evaluated.

6.3 Draft User's Guide and Future Updates

The *Draft User's Guide for UDOT Mechanistic-Empirical Pavement Design* is presented in a companion UDOT research report (Report No. UT-09.11a) dated October 2009. The

Draft User's Guide presents an input by input overview and recommendations for designing pavements in Utah. The Draft User's Guide was developed using version 1.0 of the MEPDG software. Future updates of this software are expected. This, along with UDOT's experience with the MEPDG, will lead to future updates of the UDOT MEPDG Draft User's Guide which will be published by UDOT as a standalone document.

REFERENCES

AASHTO. 1972. *Interim Guide for Design of Pavement Structures*. American Association of State Highway and Transportation Officials, Washington, D.C.

AASHTO. 1986. *Guide for Design of Pavement Structures*. American Association of State Highway and Transportation Officials, Washington, D.C.

AASHTO. 1993. *Guide for Design of Pavement Structures*. American Association of State Highway and Transportation Officials, Washington, D.C.

AASHTO. 2008. *Mechanistic-Empirical Pavement Design Guide, Interim Edition: A Manual of Practice*. American Association of State and Highway Transportation Officials, Washington, D.C.

ARA. 2004. *Guide for Mechanistic-Empirical Design of New and Rehabilitated Pavement Structures (NCHRP Project 1-37A).* Online Version (http://www.trb.org/mepdg), July 2004.

Darter, M.I., J. Mallela, L. Titus-Glover, C. Rao, G. Larson, A. Gotlif, H.L. Von Quintus, L. Khazanovich, M.W. Witczak, M. El-Basyouny, S. El-Badawy, A. Zborowski, and C. Zapata. 2007. "Changes to the Mechanistic-Empirical Pavement Design Guide Software through Version 0.900." *NCHRP Research Digest 308*. National Cooperative Highway Research Program, Transportation Research Board, Washington, D.C.

Darter, M.I., L. Titus-Glover, H.L. Von Quintus. 2009. *Draft User's Guide for UDOT Mechanistic-Empirical Pavement Design*. Research Report No. UT-09.11a, Utah Department of Transportation, Salt Lake City.

Horel, J., M. Splitt, and S. Conger. "Application of Road Weather Information Systems in the Western United States". Downloaded from website with URL: http://www.met.utah.edu/jhorel/html/mesonet/rwis.pdf. Website visited on September 1, 2003.

HRB. 1962. *The AASHO Road Test*, Report 5: Pavement Research; Report 6*: Special Studies;* and Report 7: Summary Report, Highway Research Board, Washington, D.C.

LTPP. 2008. Data Release Version 22. Federal Highway Administration, Washington, D.C.

Miner, M.A. 1945. "Cumulative Damage in Fatigue," *Transactions.* American Society of Mechanical Engineers, Vol. 67, pp. A159-A164.

Saito, M., and T.G. Jin. 2009. *Evaluating the Accuracy Level of Truck Traffic Data on State Highways*. Research Report No. UT-09.02. Utah Department of Transportation, Salt Lake City.

SAS Institute Inc. 2004. SAS 9.1.3 Help and Documentation, SAS Institute, Cary, NC.

Seegmiller, L.W. 2006. "Utah Commercial Motor Vehicle Weigh-in-Motion Data Analysis and Calibration Methodology." Master's thesis, Department of Civil and Environmental Engineering, Brigham Young University.

Von Quintus, H.L., M.I. Darter, and J. Mallela. Local Calibration Guidance for the Recommended Guide for Mechanistic-Empirical Design of New and Rehabilitated Pavement Structures, NCHRP Project 1-40B, Transportation Research Board, Washington, DC., April 2008.

APPENDIX A. DISTRESS AND IRI DATA PLOTS FOR HMA SURFACED PAVEMENTS

Table A-1. Summary of LTPP distress/IRI data processing for HMA and HMA overlaid HMA pavements.

Performance Indicator	Raw LTPP Measurement	Conversion Procedure & MEPDG Data Description
Alligator cracking	Reported as affected area at each severity level in sq. meters	Convert to MEPDG reporting standards which is percent lane area with alligator cracking (all severities) as follows: $$PCRK = \frac{(C_{Low} + C_{Moderate} + C_{High}) * 100}{L * W}$$ where PCRK = percent lane area with alligator cracking, percent C_{Low} = total area of low severity alligator cracking, m^2 $C_{Moderate}$ = total area of moderate severity alligator cracking, m^2 C_{High} = total area of high severity alligator cracking, m^2 L = section length, m (typically 152-m (500-ft) for LTPP) W = lane width, m (typically 3.65-m (12-ft) for LTPP)
Transverse cracking	Reported as length of transverse cracks at each severity level (typically for a 500-ft pavement section for LTPP)	Convert to MEPDG reporting standards which is length of transverse cracking (in feet) per mile of pavement as follows: $$TC = (TC_{Low} + TC_{Moderate} + TC_{High}) * \frac{5280}{L}$$ where TC = total length of transverse cracking, ft/mi TC_{Low} = length of low severity transverse cracking per section length, ft $TC_{Moderate}$ = length of moderate severity transverse cracking per section length, ft TC_{High} = length of high severity transverse cracking per section length, ft L = section length, ft (typically 500-ft for LTPP)

Table A-1. Summary of LTPP distress/IRI data processing for HMA and HMA overlaid HMA pavements, continued.

Performance Indicator	Raw LTPP Measurement	Conversion Procedure & MEPDG Data Description
Rutting	Reported as the mean of measurements of maximum rut depth (measured at 15.25-m intervals with a 1.2-m straight edge) for each wheel path	Convert to MEPDG reporting standards which is mean rut depth in inches (for both wheelpaths) as follows: $$MRUT = (R_{LWP} + R_{RWP}) * \frac{0.5}{25.4}$$ where MRUT = mean rutting in the left and right wheelpaths over the entire pavement section, in R_{LWP} = mean rutting in the left wheelpath over the entire pavement section, mm R_{RWP} = mean rutting in the right wheelpath over the entire pavement section, mm
IRI	Reported as the mean of measurements of IRI for each wheel path	Convert to MEPDG reporting standards which is mean IRI in inches per mile (for both wheelpaths) as follows: $$MIRI = (IRI_{LWP} + IRI_{RWP}) * 0.5 * 63.4$$ where MIRI = mean IRI in the left and right wheelpaths, in/mi IRI_{LWP} = mean IRI in the left wheelpath, m/km IRI_{RWP} = mean IRI in the right wheelpath, m/km

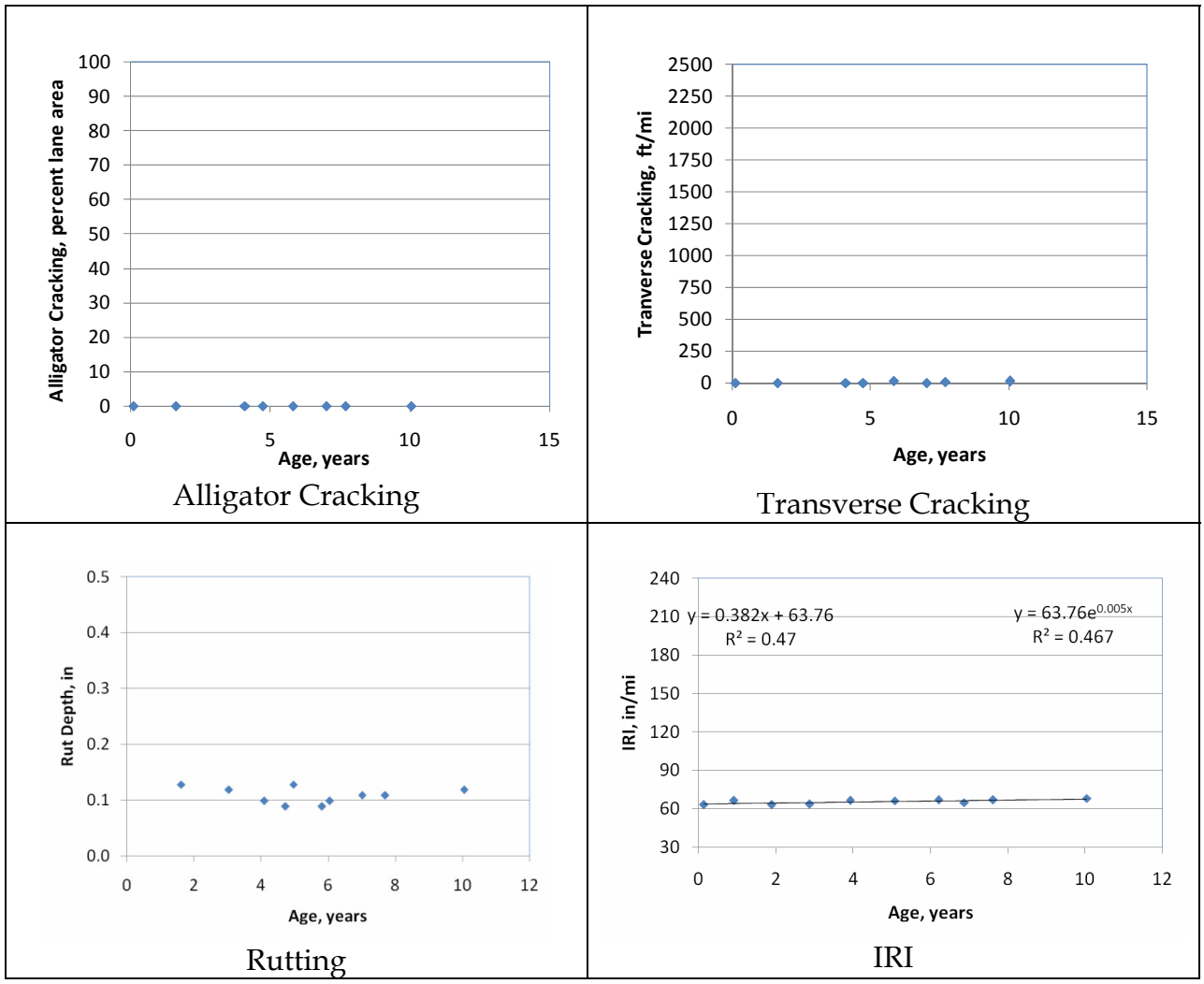

Figure A-1. Distress & IRI data plots for project LTPP 0803.

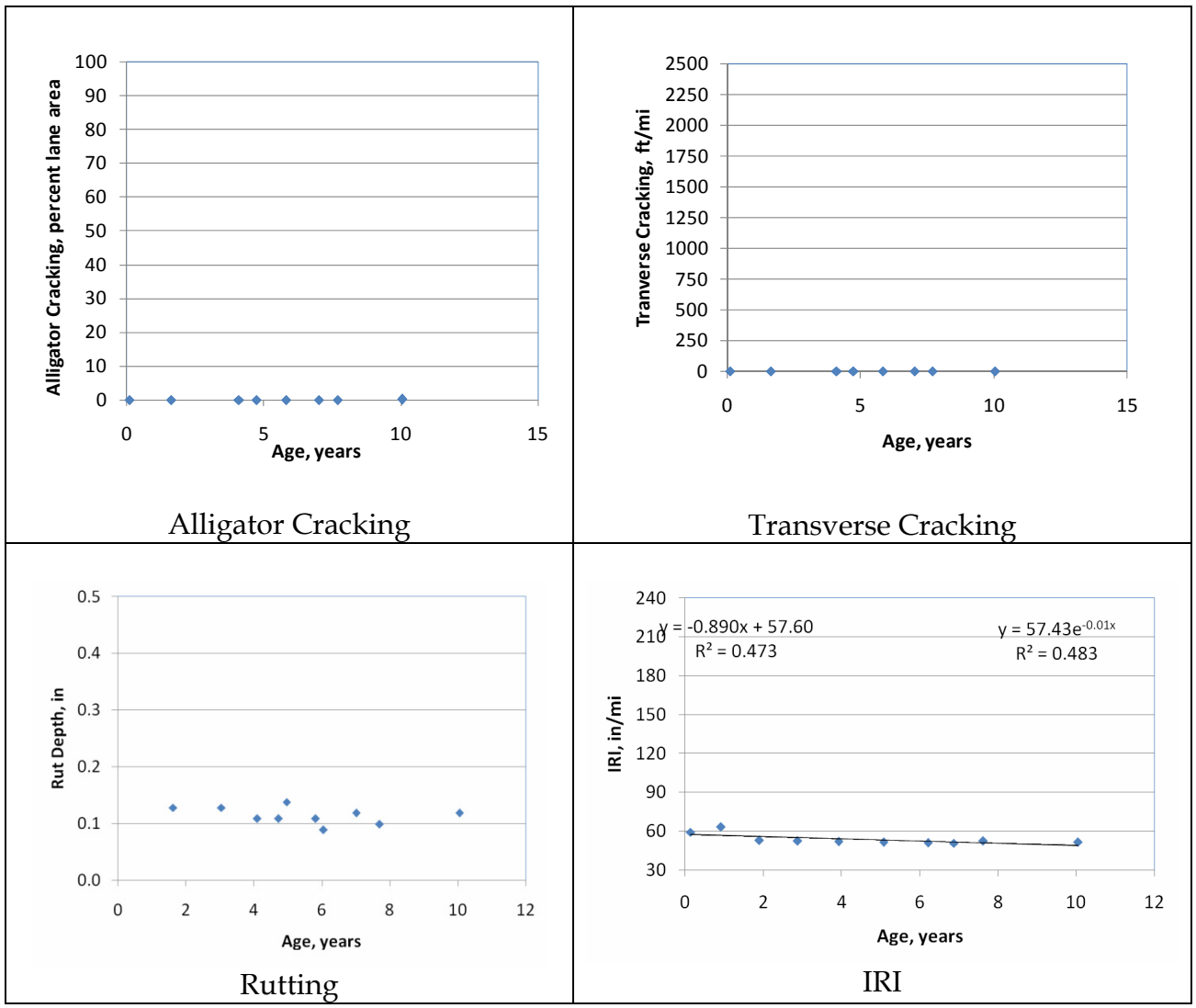

Figure A-2. Distress & IRI data plots for project LTPP 0804.

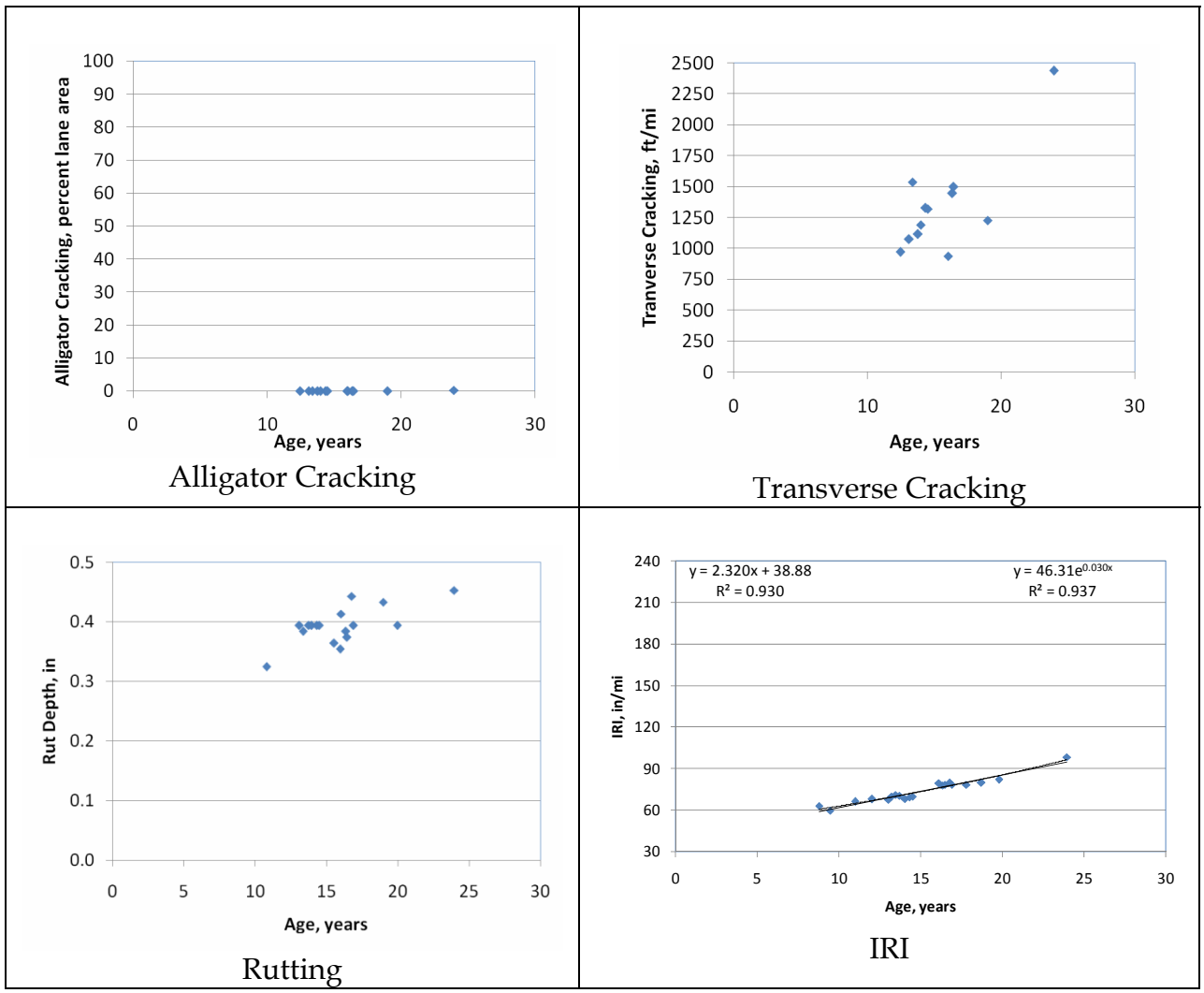

Figure A-3. Distress & IRI data plots for project LTPP 1001.

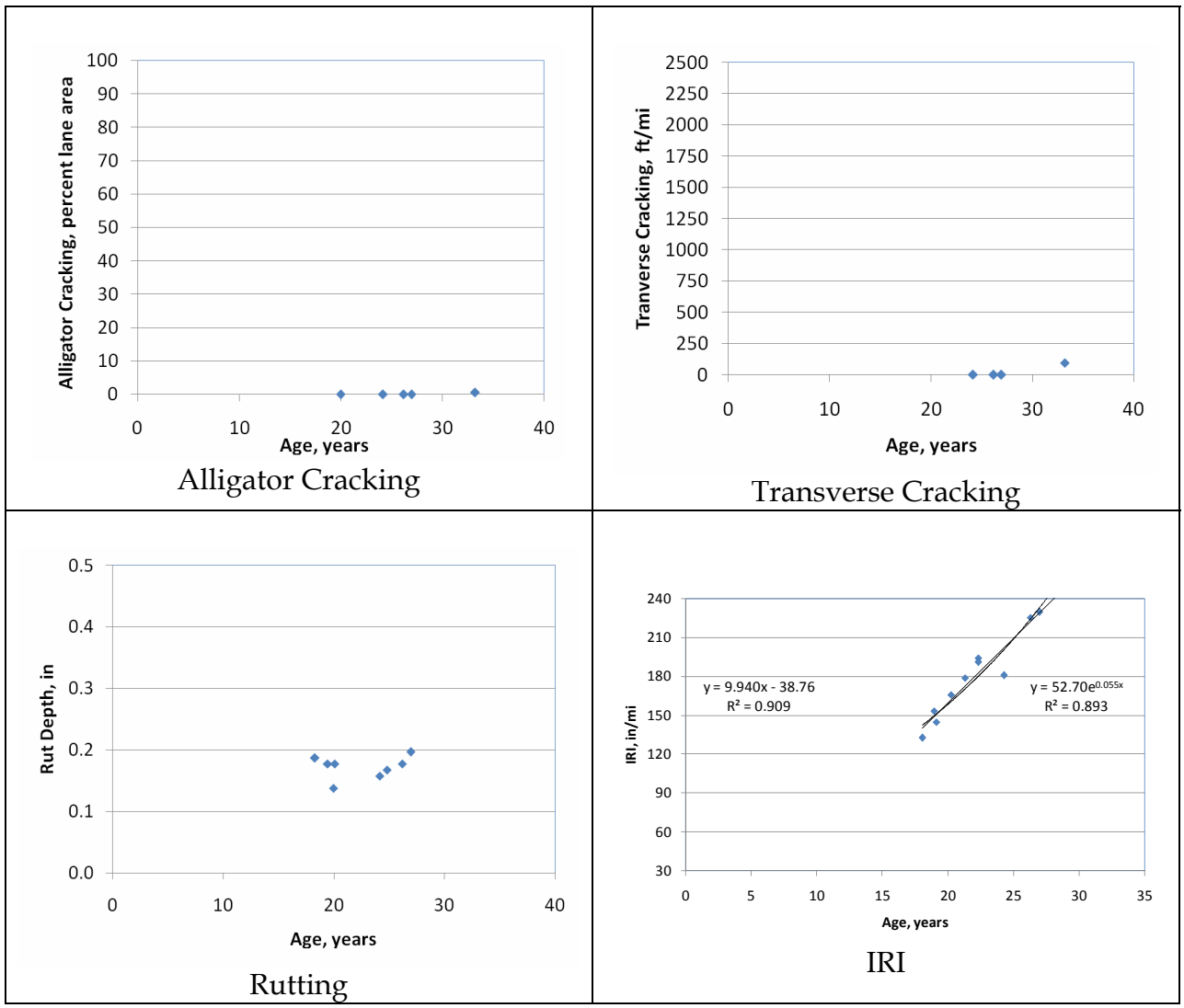

Figure A-4. Distress & IRI data plots for project LTPP 1004.

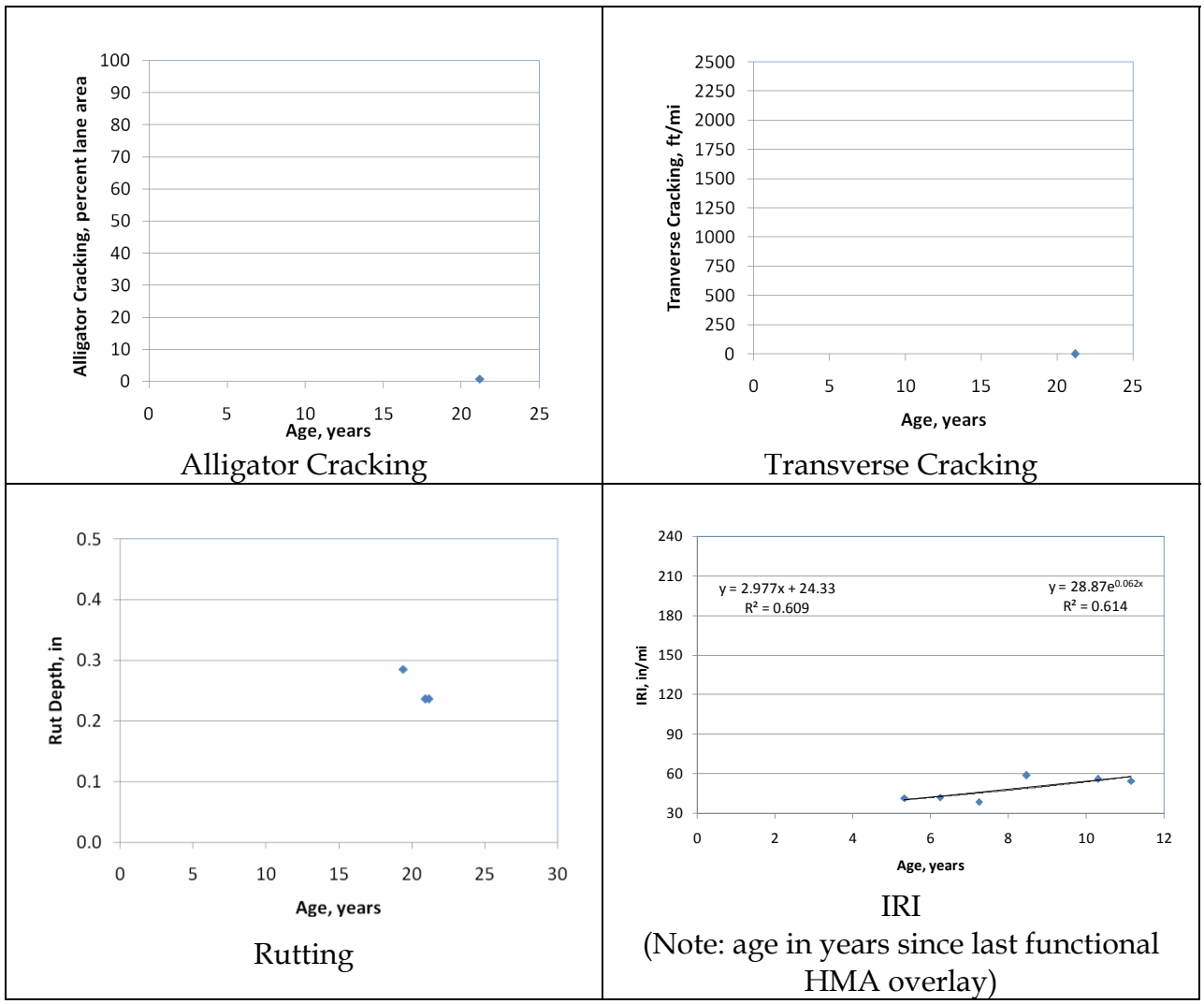

Figure A-5. Distress & IRI data plots for project LTPP 1005.

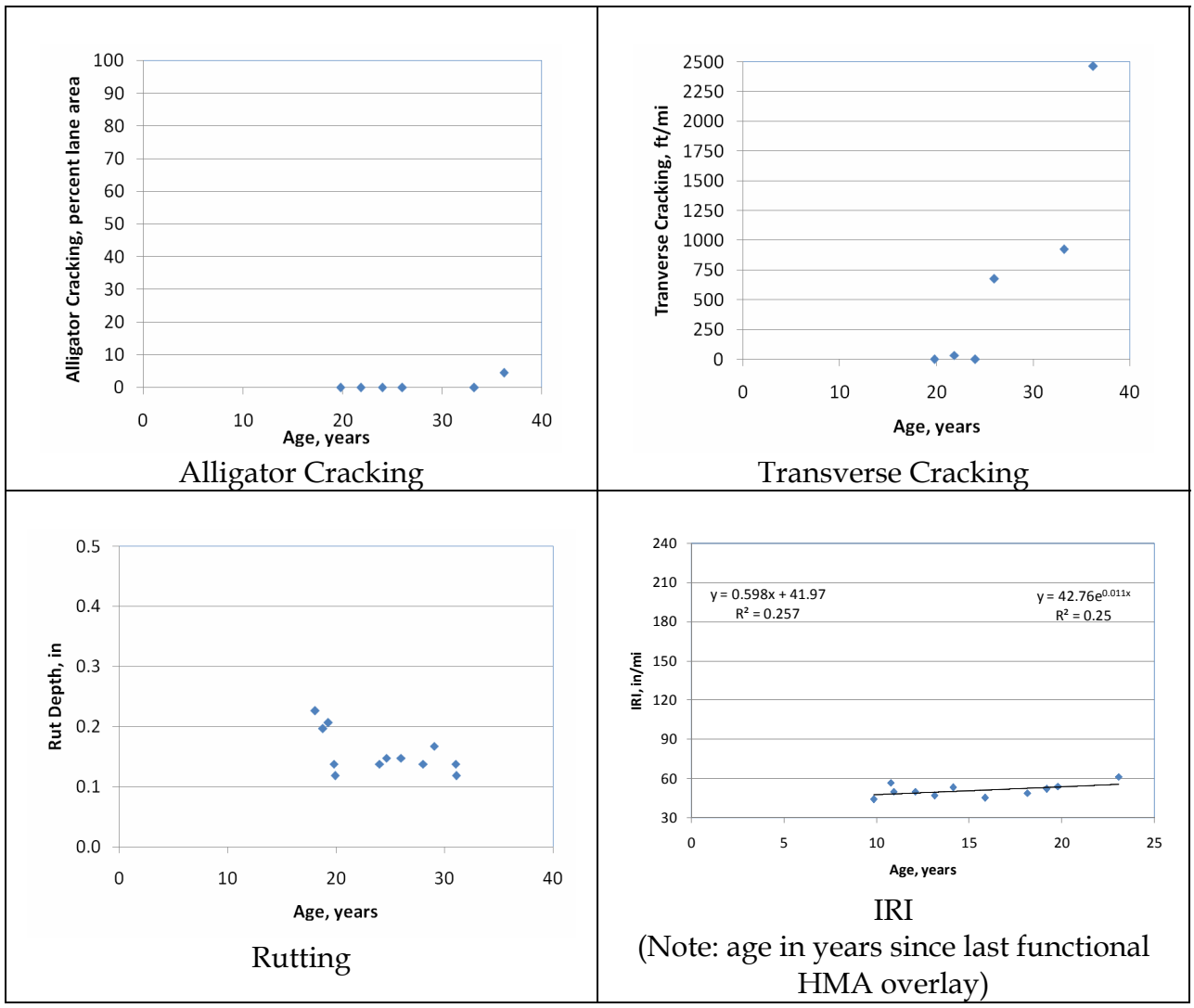

Figure A-6. Distress & IRI data plots for project LTPP 1006.

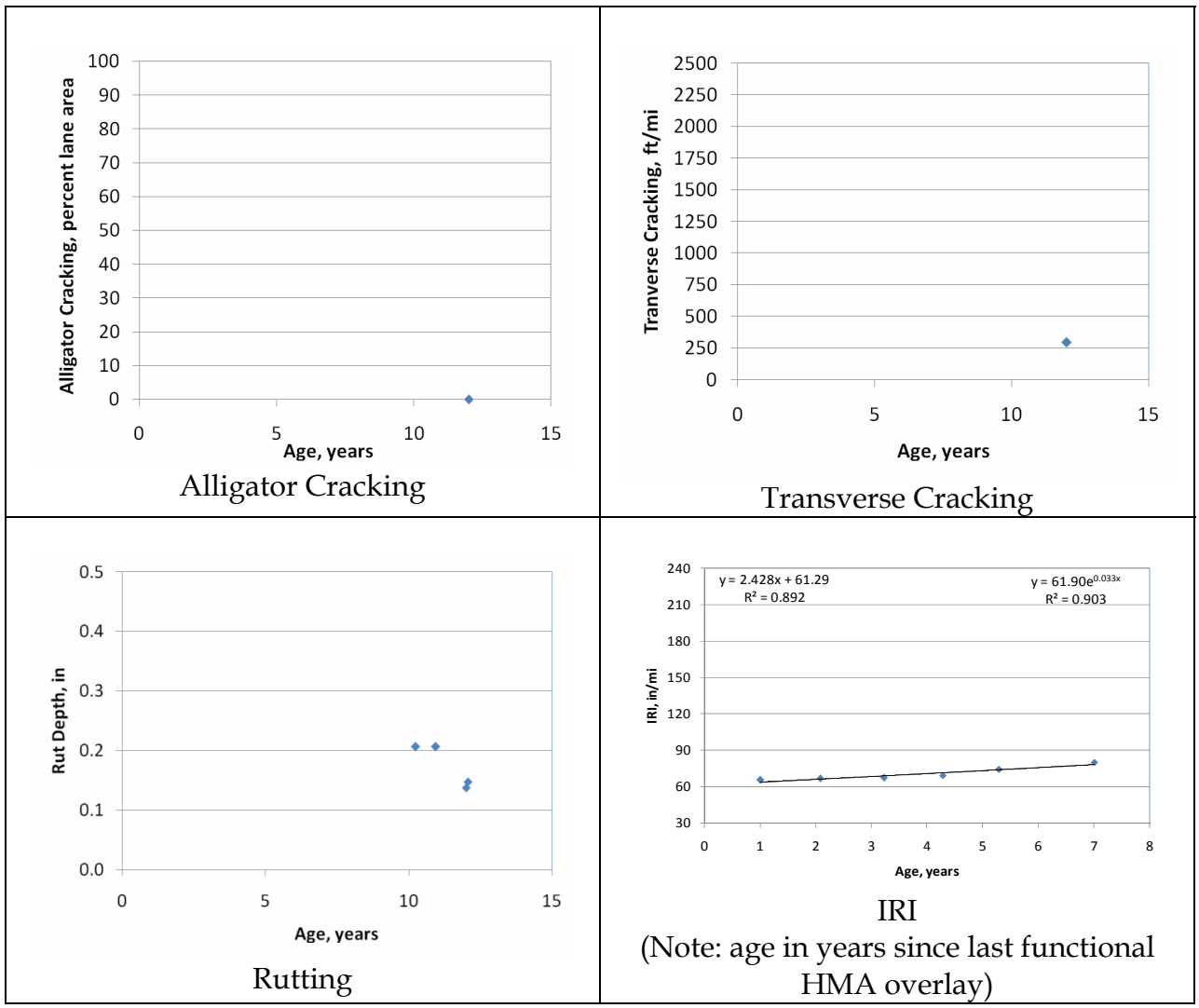

Figure A-7. Distress & IRI data plots for project LTPP 1007.

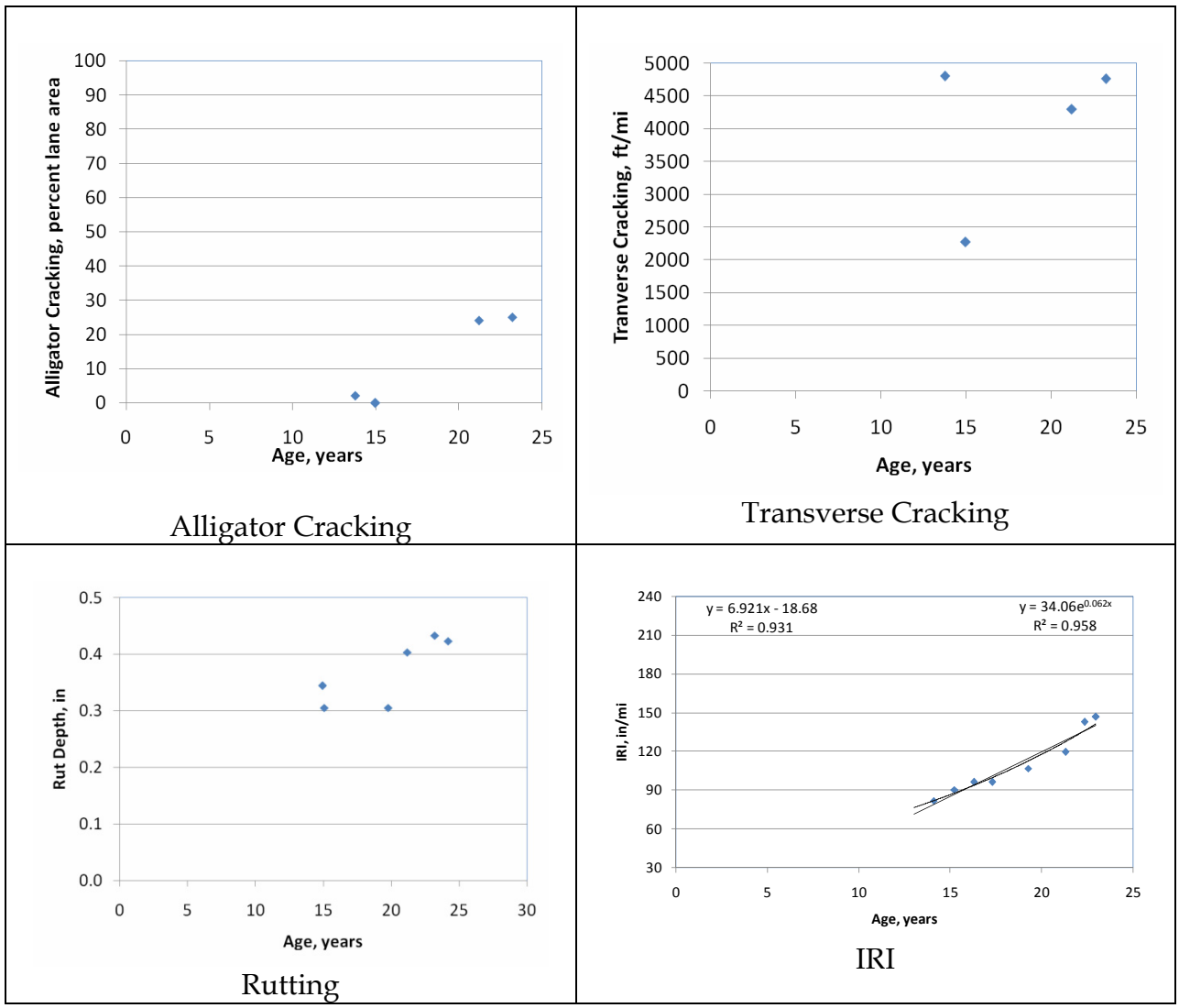

Figure A-8. Distress & IRI data plots for project LTPP 1008.

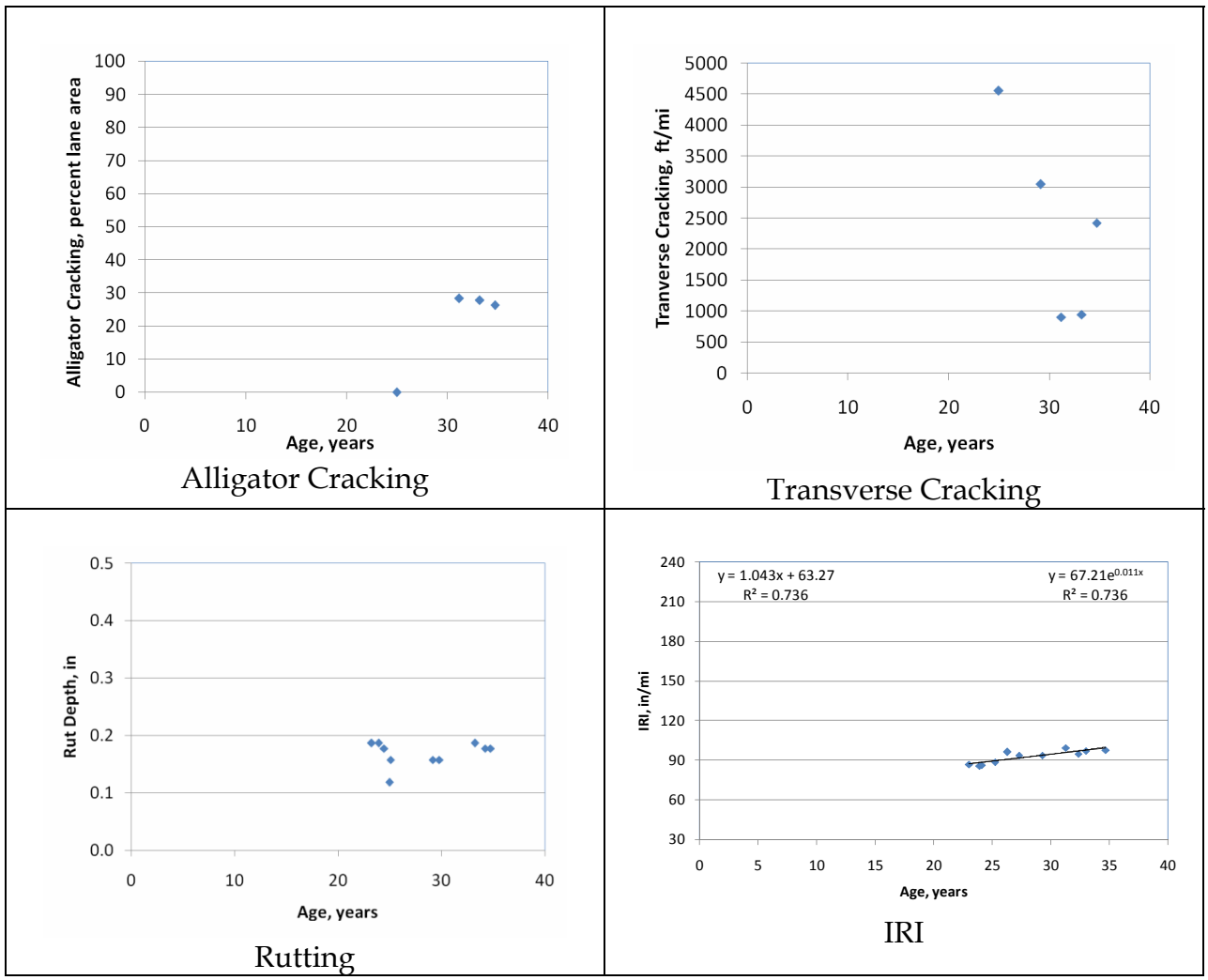

Figure A-9. Distress & IRI data plots for project LTPP 1017.

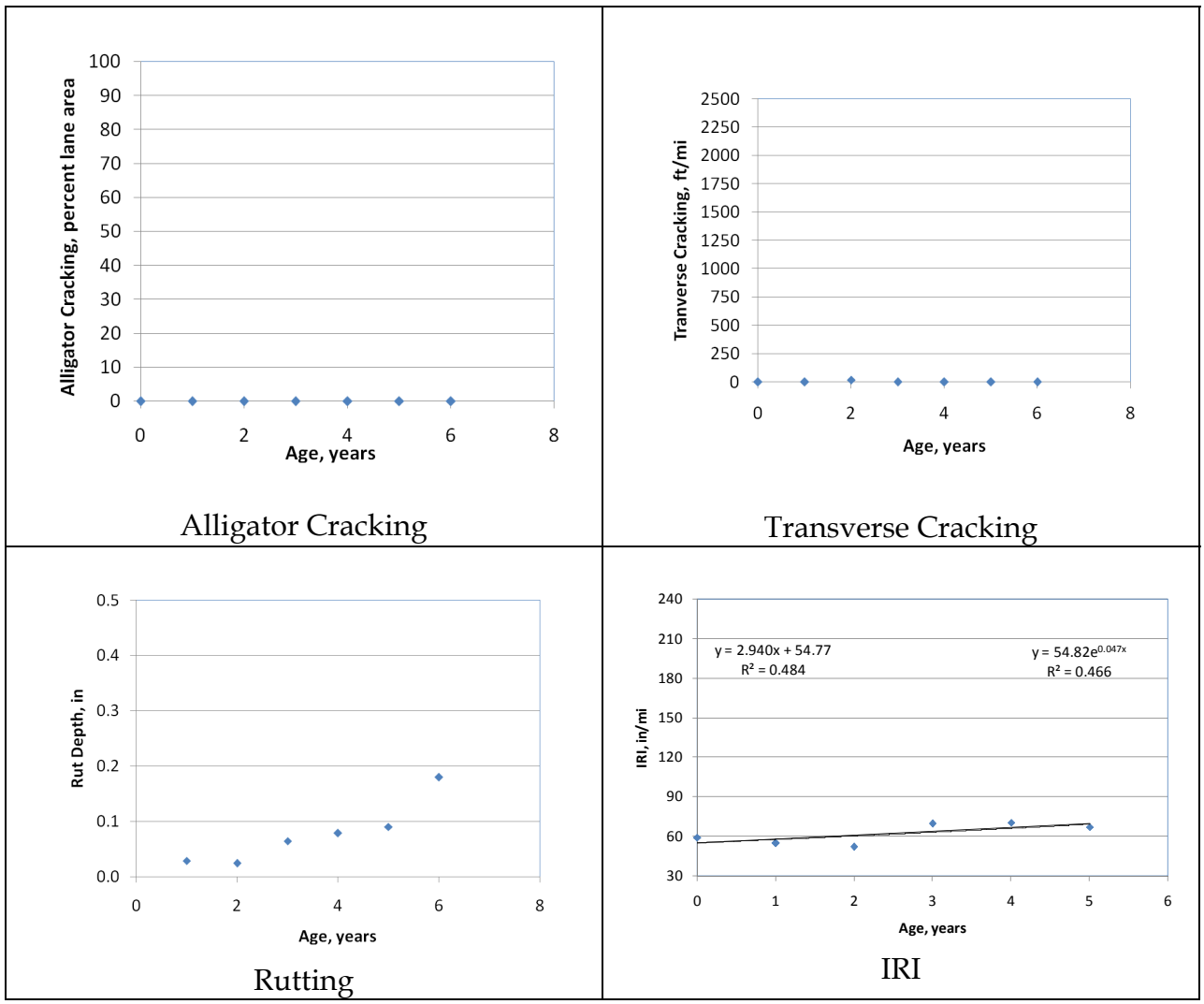

Figure A-10. Distress & IRI data plots for PMS HMA overlay project 2.

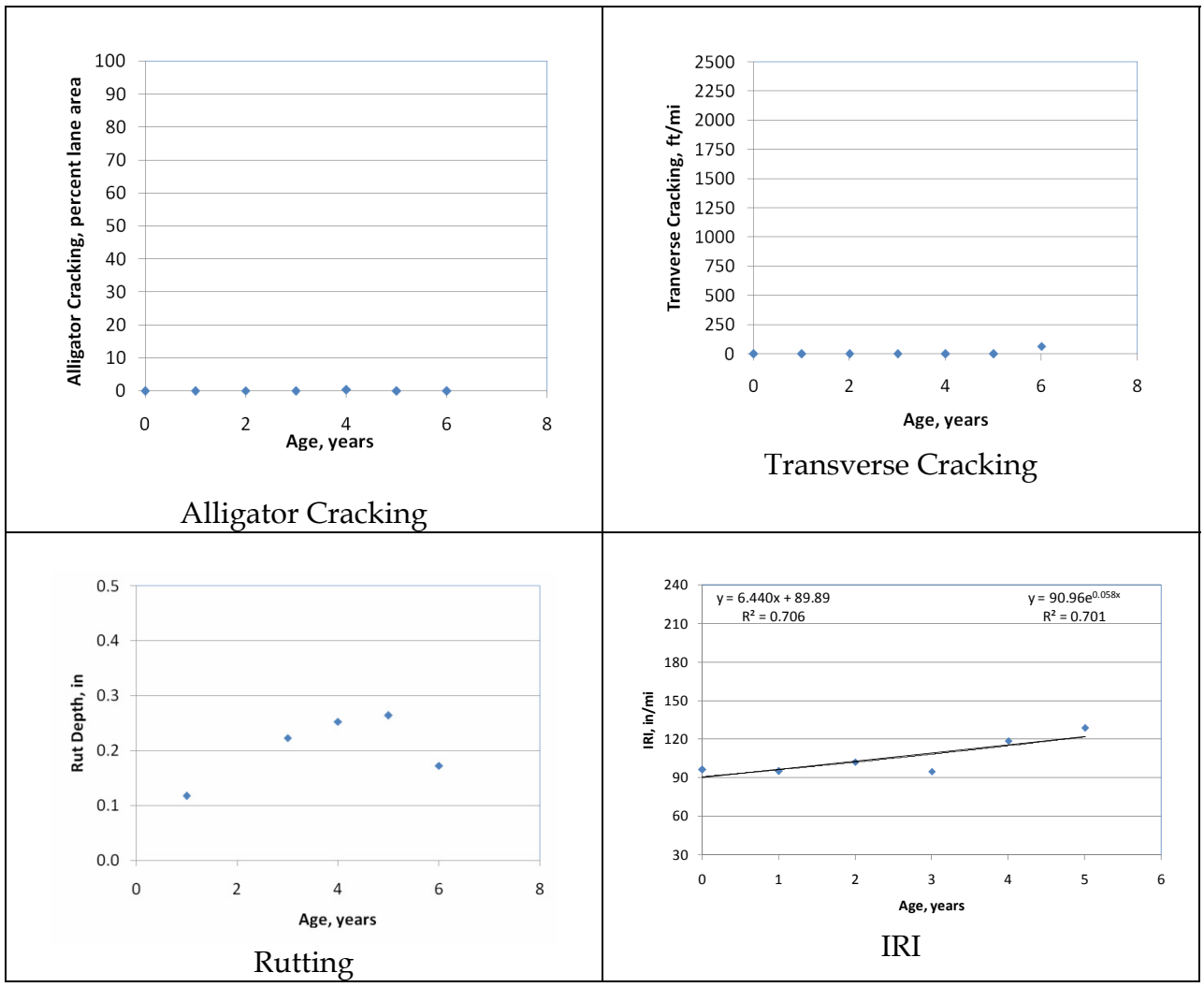

Figure A-11. Distress & IRI data plots for PMS HMA overlay project 3.

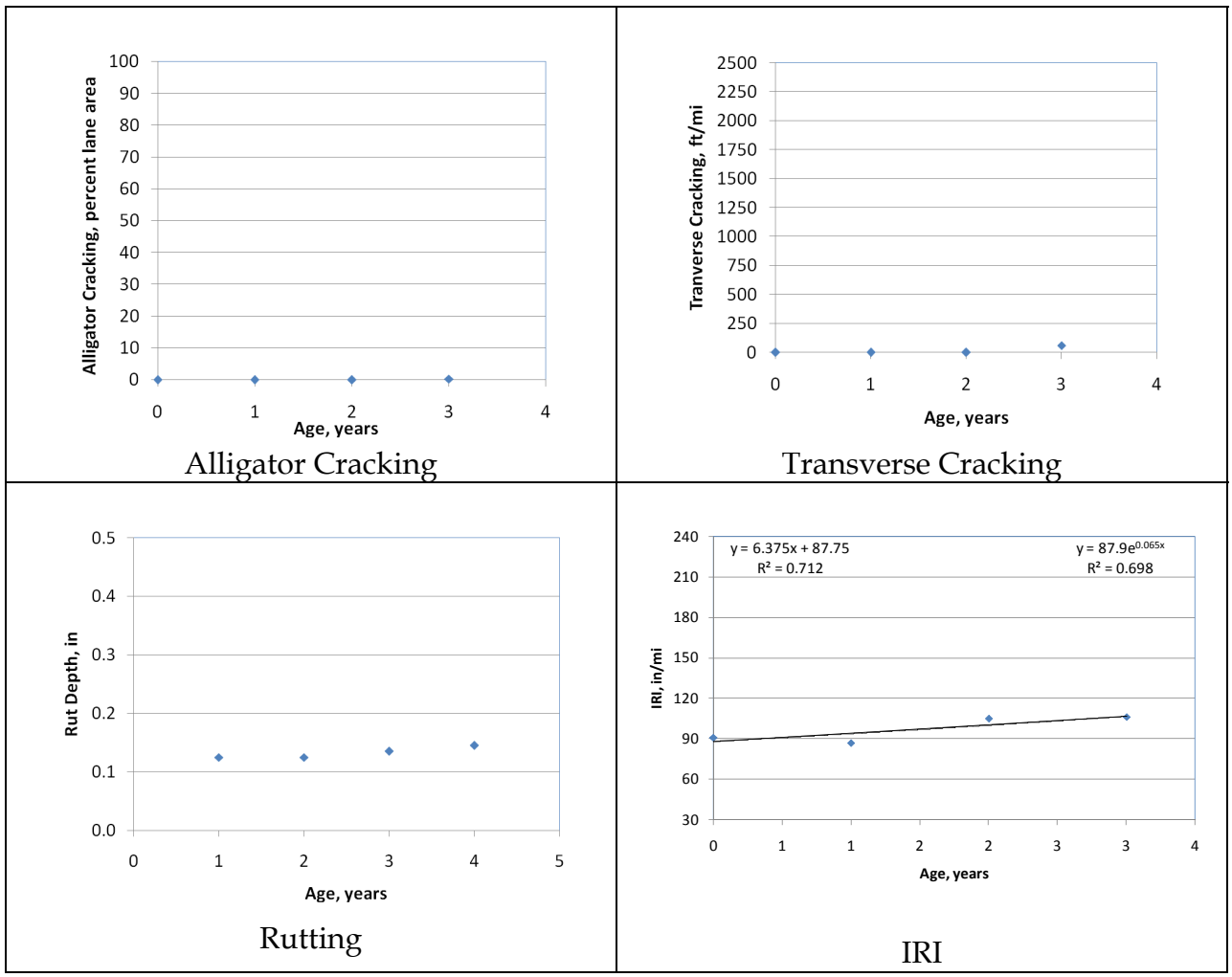

Figure A-12. Distress & IRI data plots for PMS HMA overlay project 4.

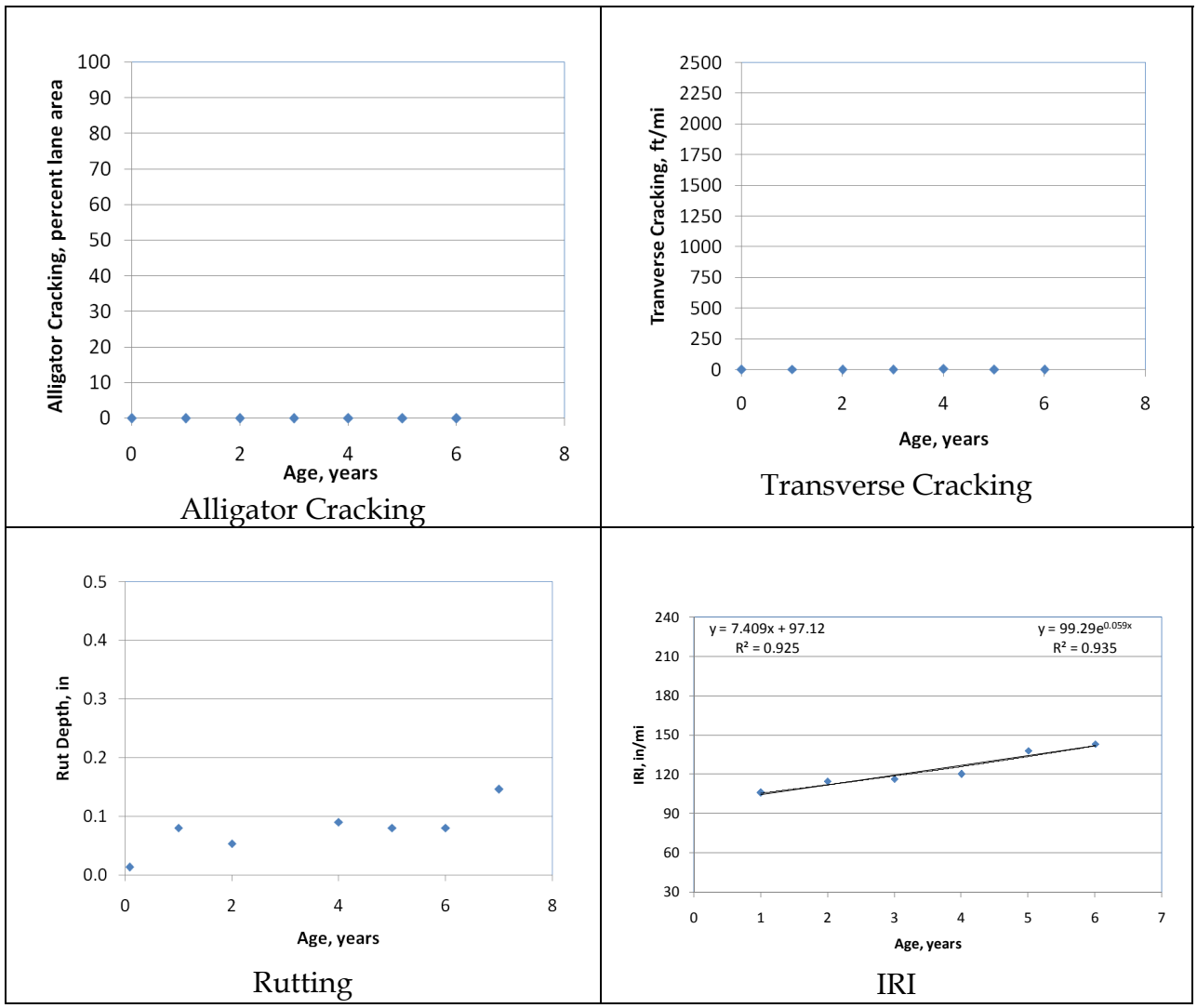

Figure A-13. Distress & IRI data plots for project PMS HMA R1 01.

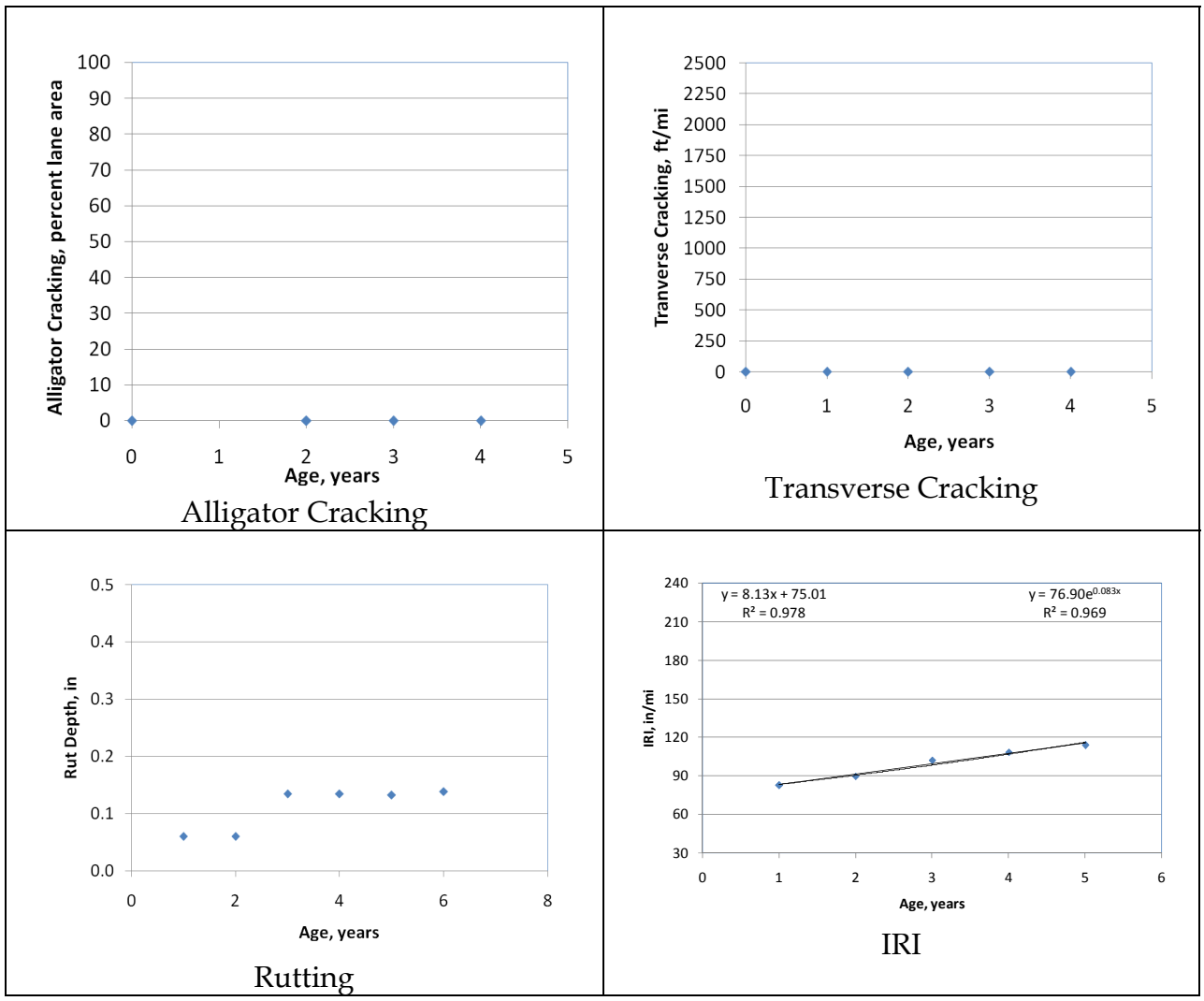

Figure A-14. Distress & IRI data plots for project PMS HMA R1 02.

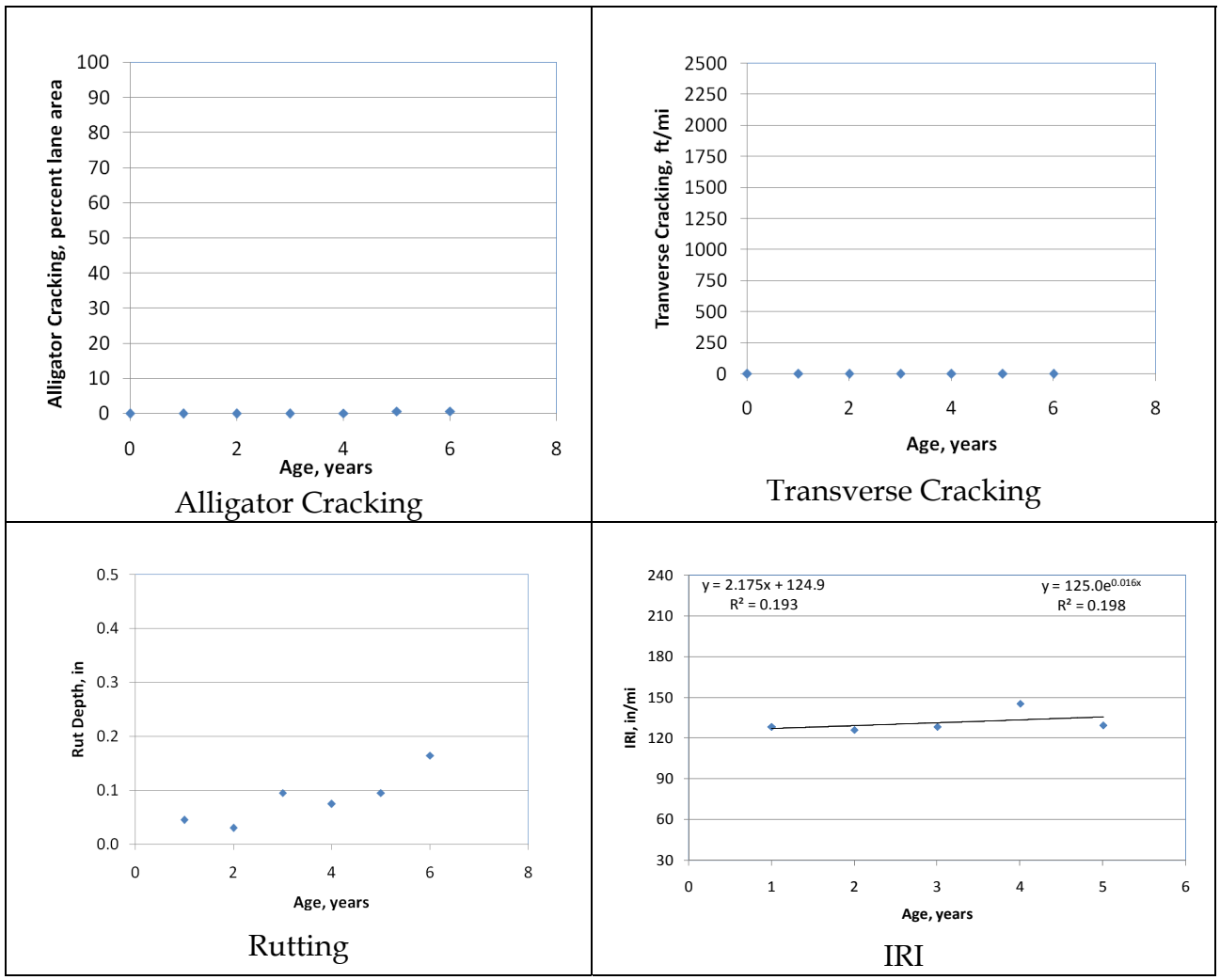

Figure A-15. Distress & IRI data plots for project PMS HMA R1 03.

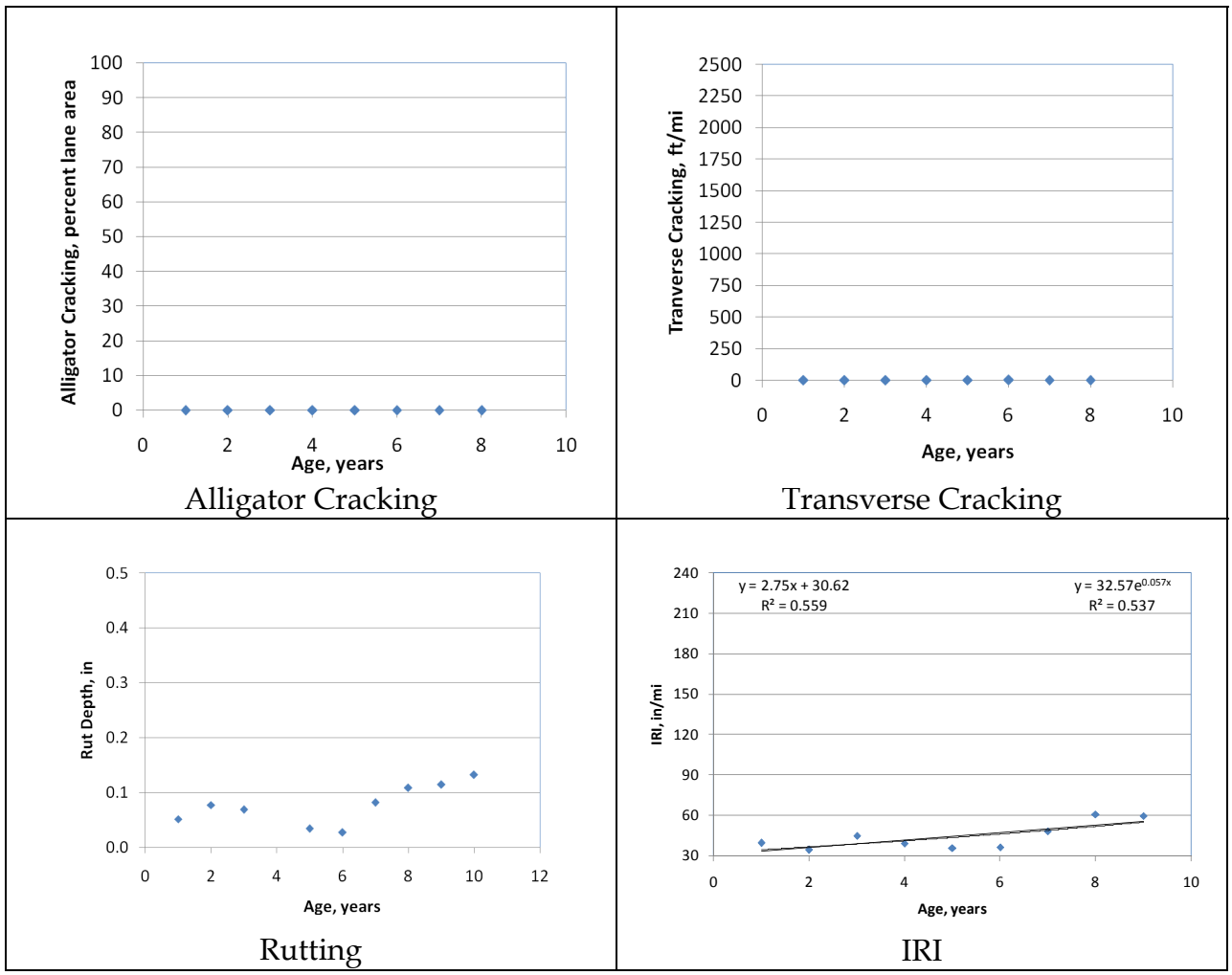

Figure A-16. Distress & IRI data plots for project PMS HMA R1 04.

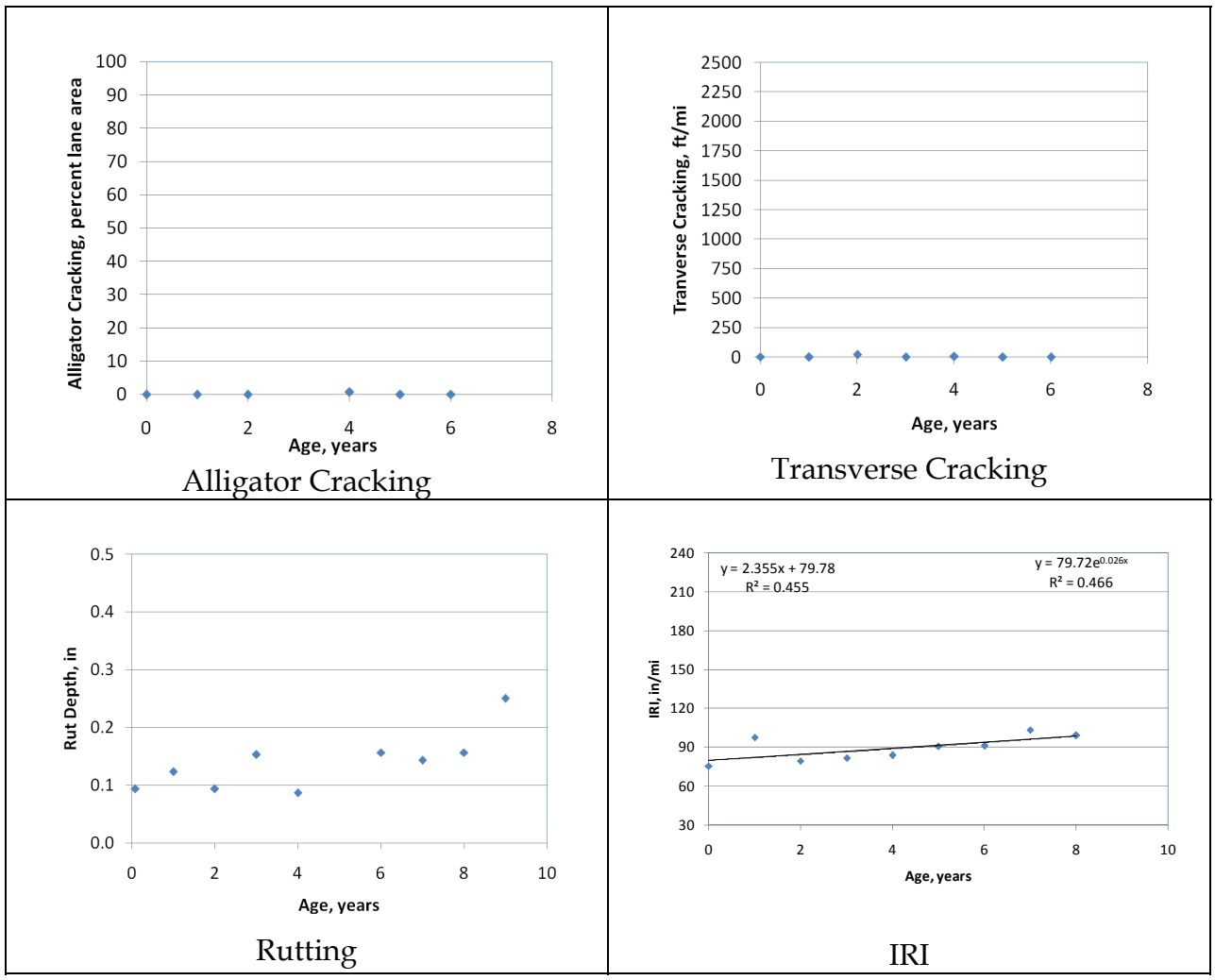

Figure A-17. Distress & IRI data plots for project PMS HMA R2 01.

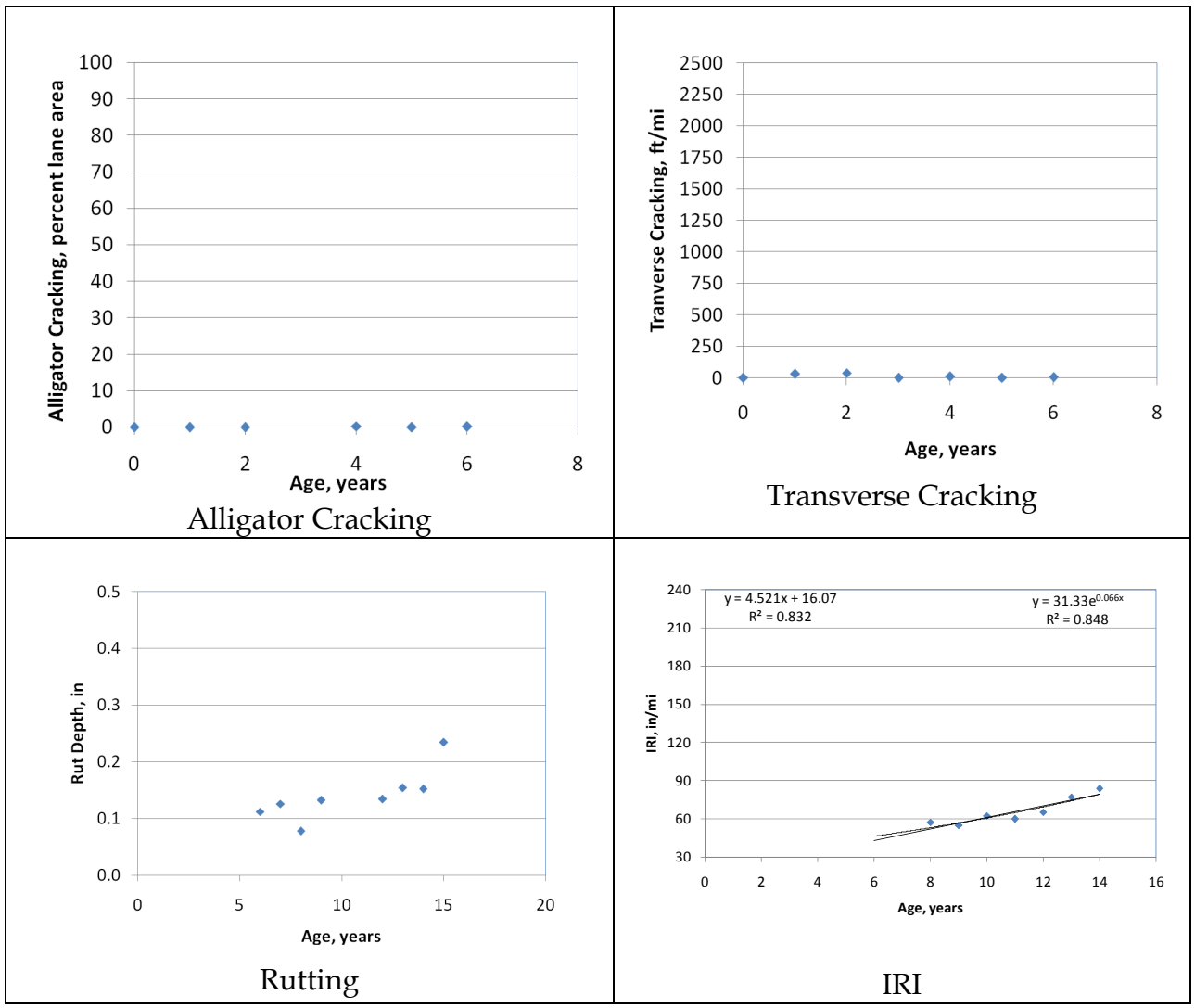

Figure A-18. Distress & IRI data plots for project PMS HMA R2 02.

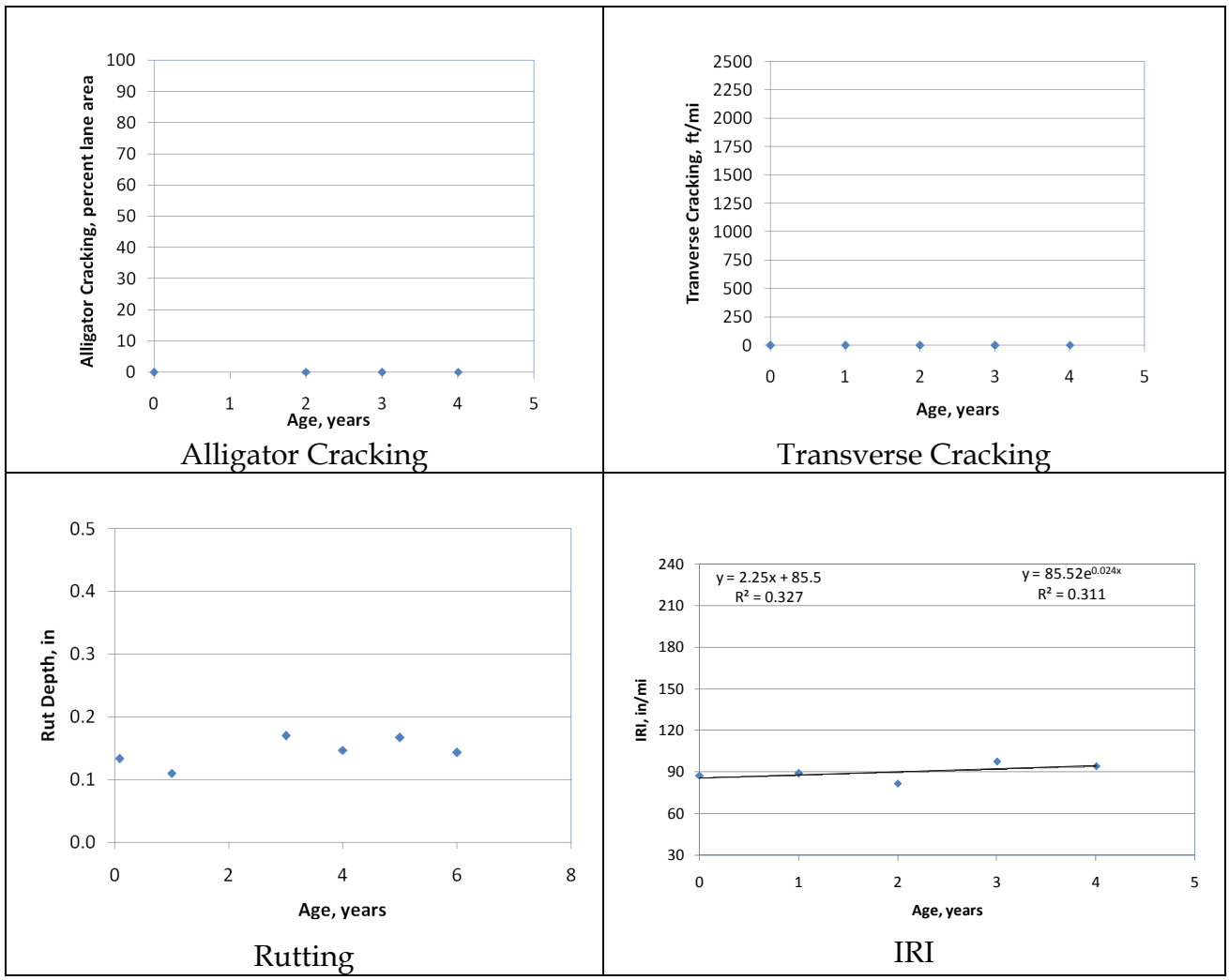

Figure A-19. Distress & IRI data plots for project PMS HMA R2 03.

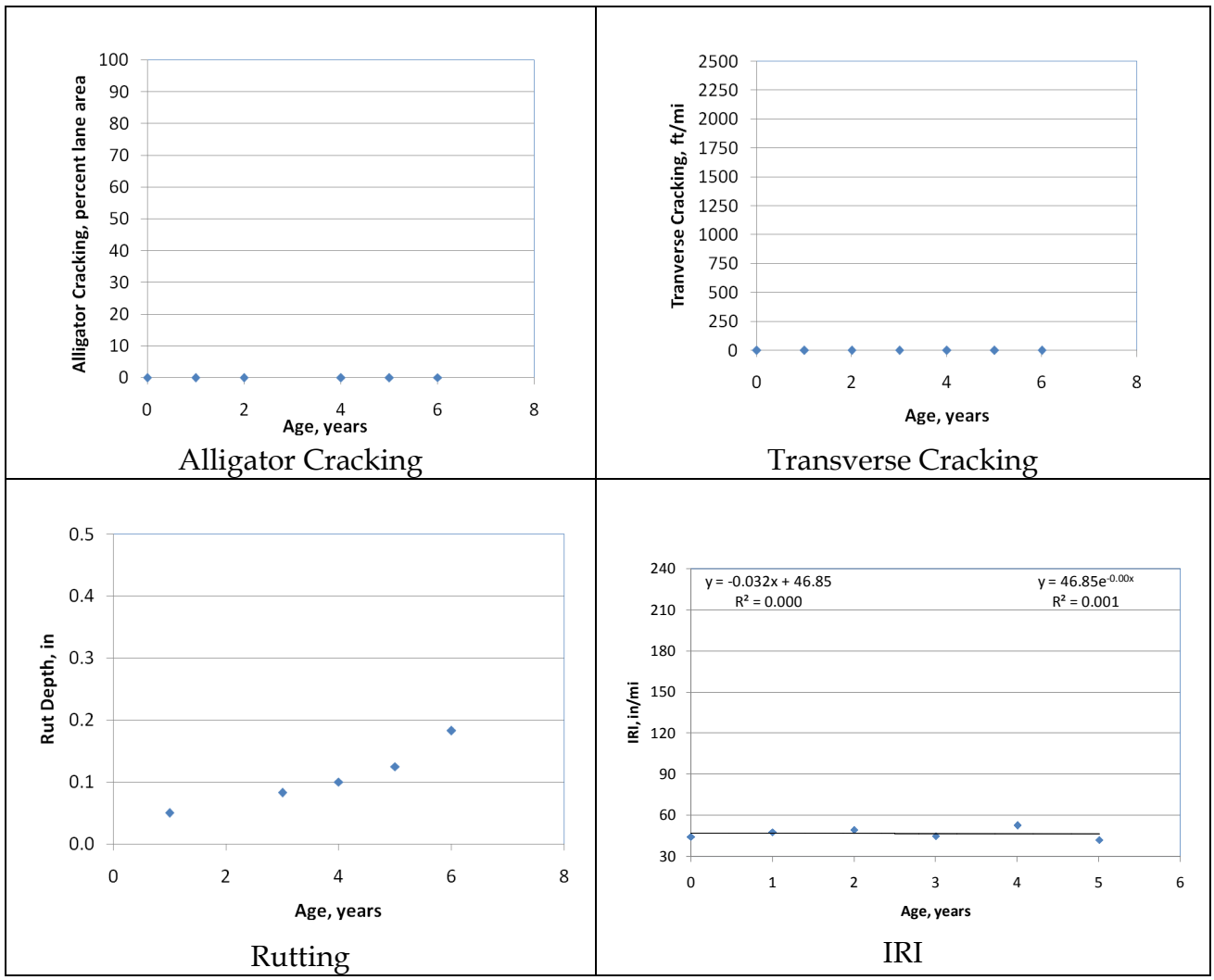

Figure A-20. Distress & IRI data plots for project PMS HMA R2 04.

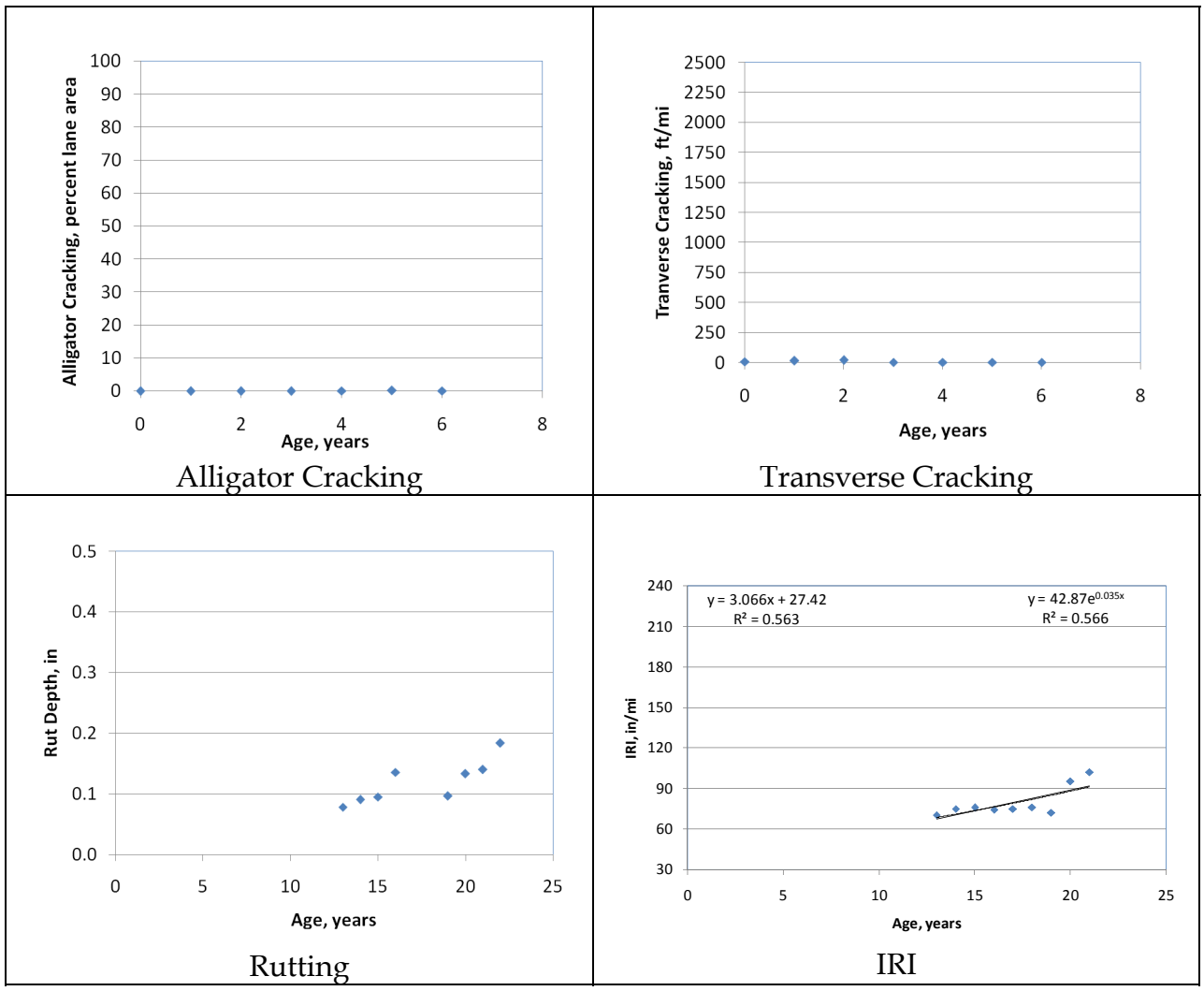

Figure A-21. Distress & IRI data plots for project PMS HMA R3 01.

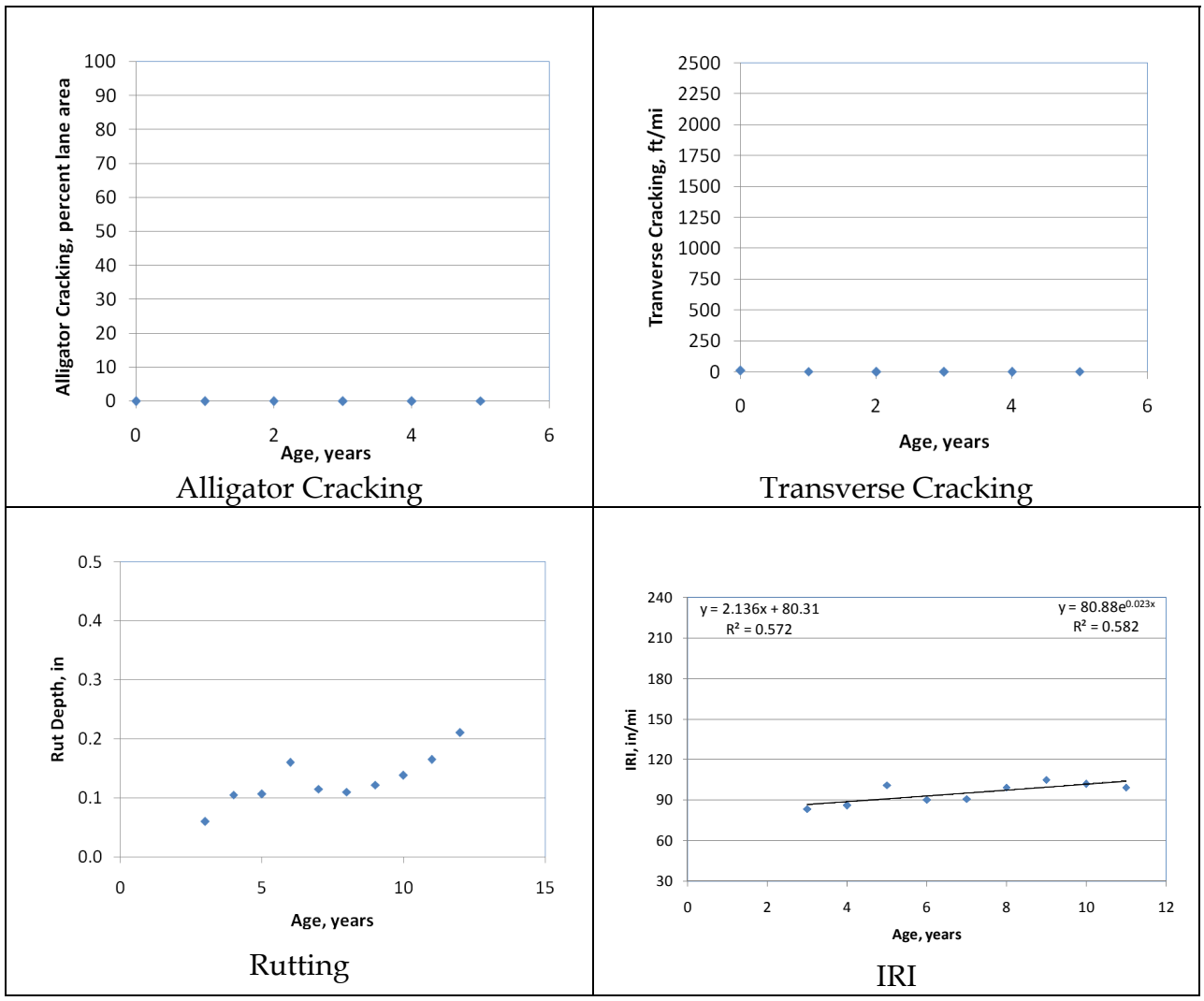

Figure A-22. Distress & IRI data plots for project PMS HMA R3 02.

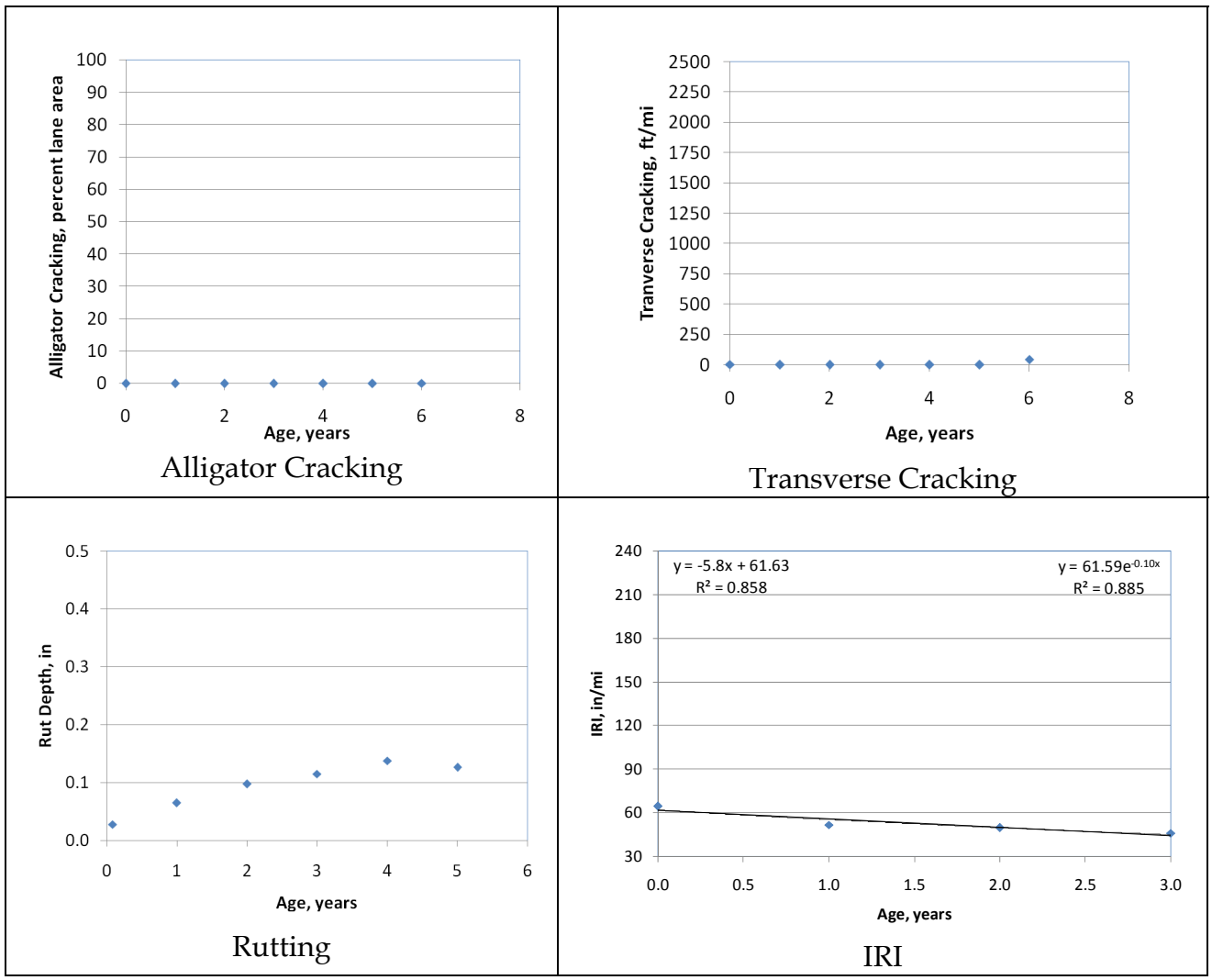

Figure A-23. Distress & IRI data plots for project PMS HMA R3 03.

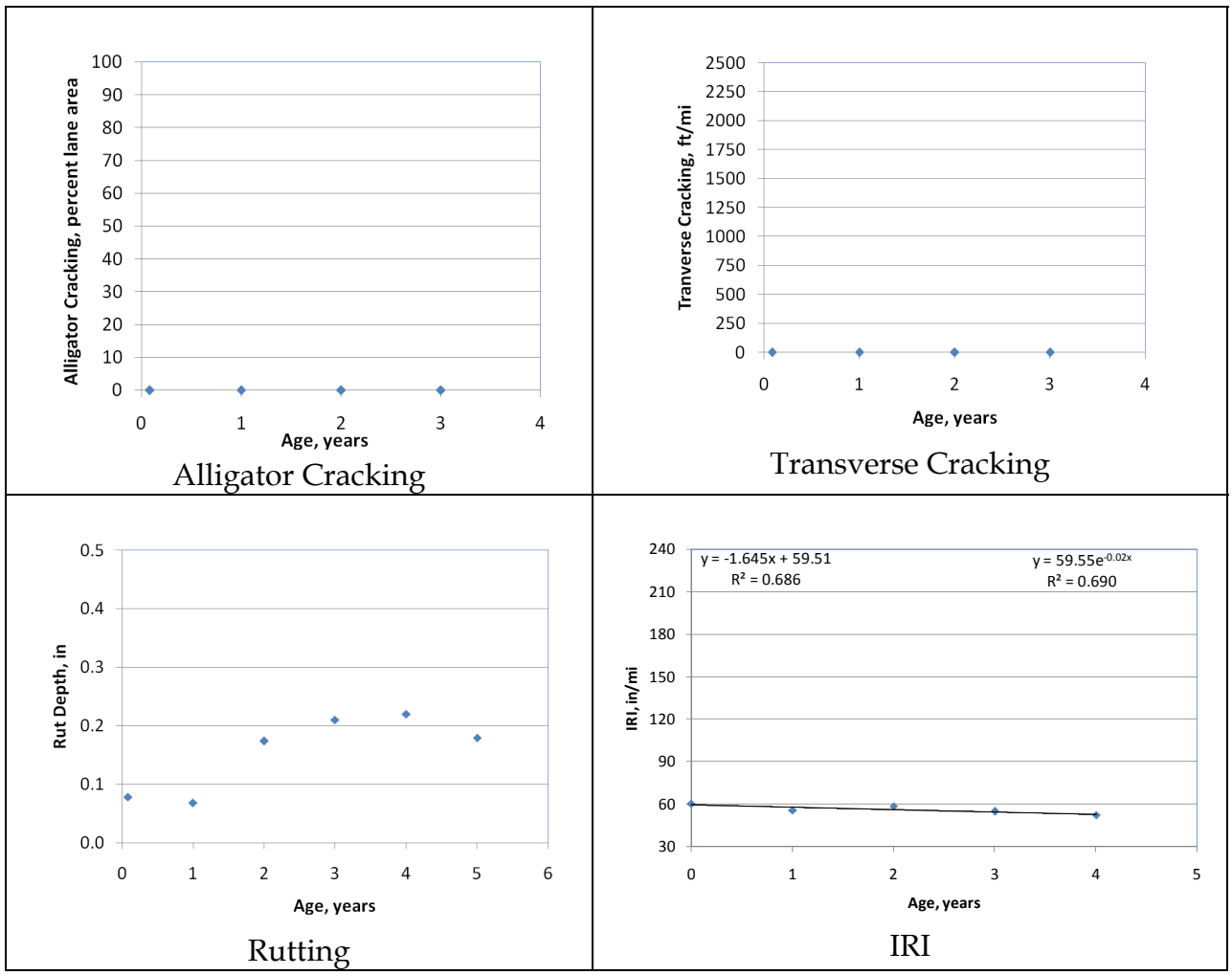

Figure A-24. Distress & IRI data plots for project PMS HMA R3 04.

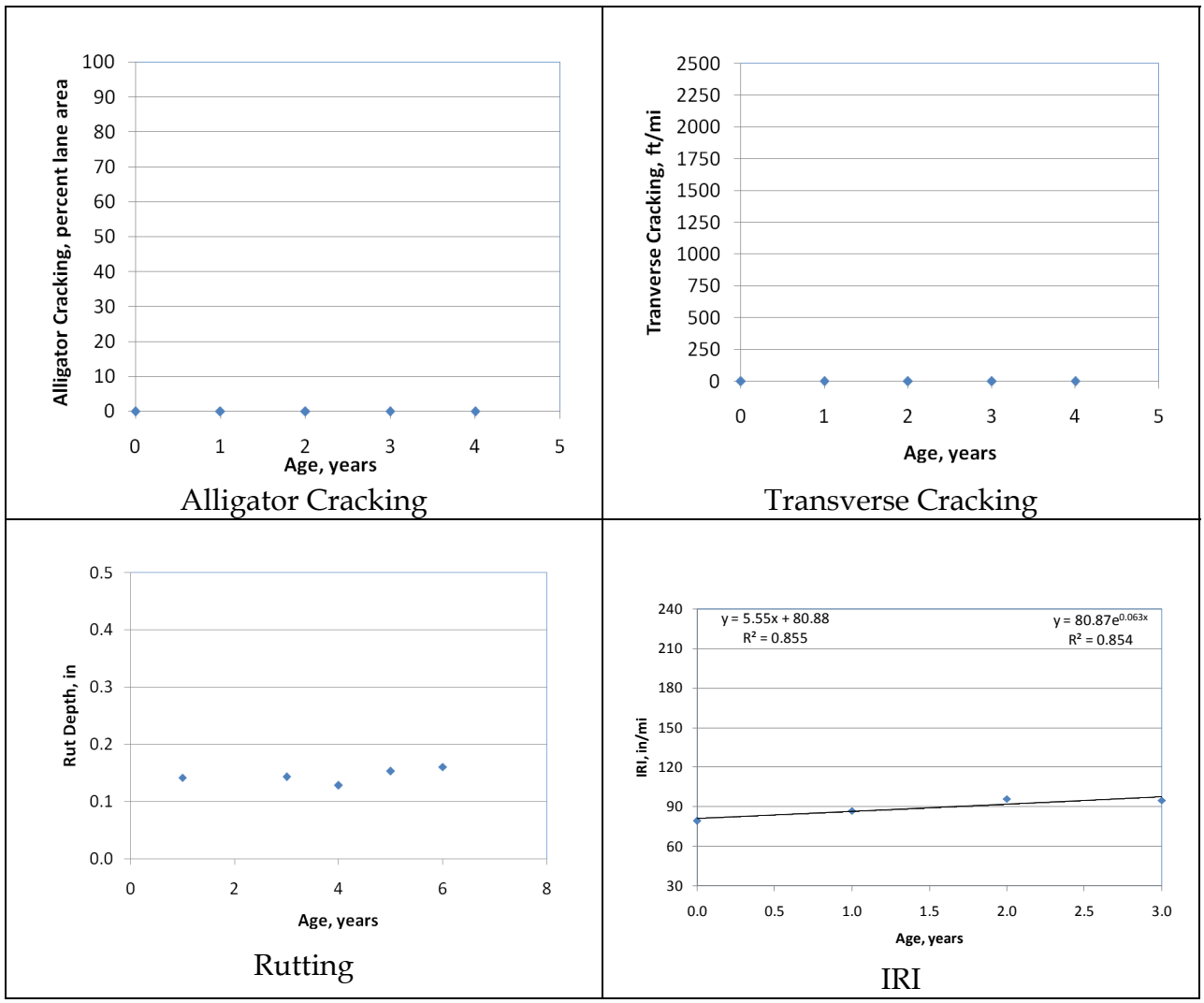

Figure A-25. Distress & IRI data plots for project PMS HMA R4 02.

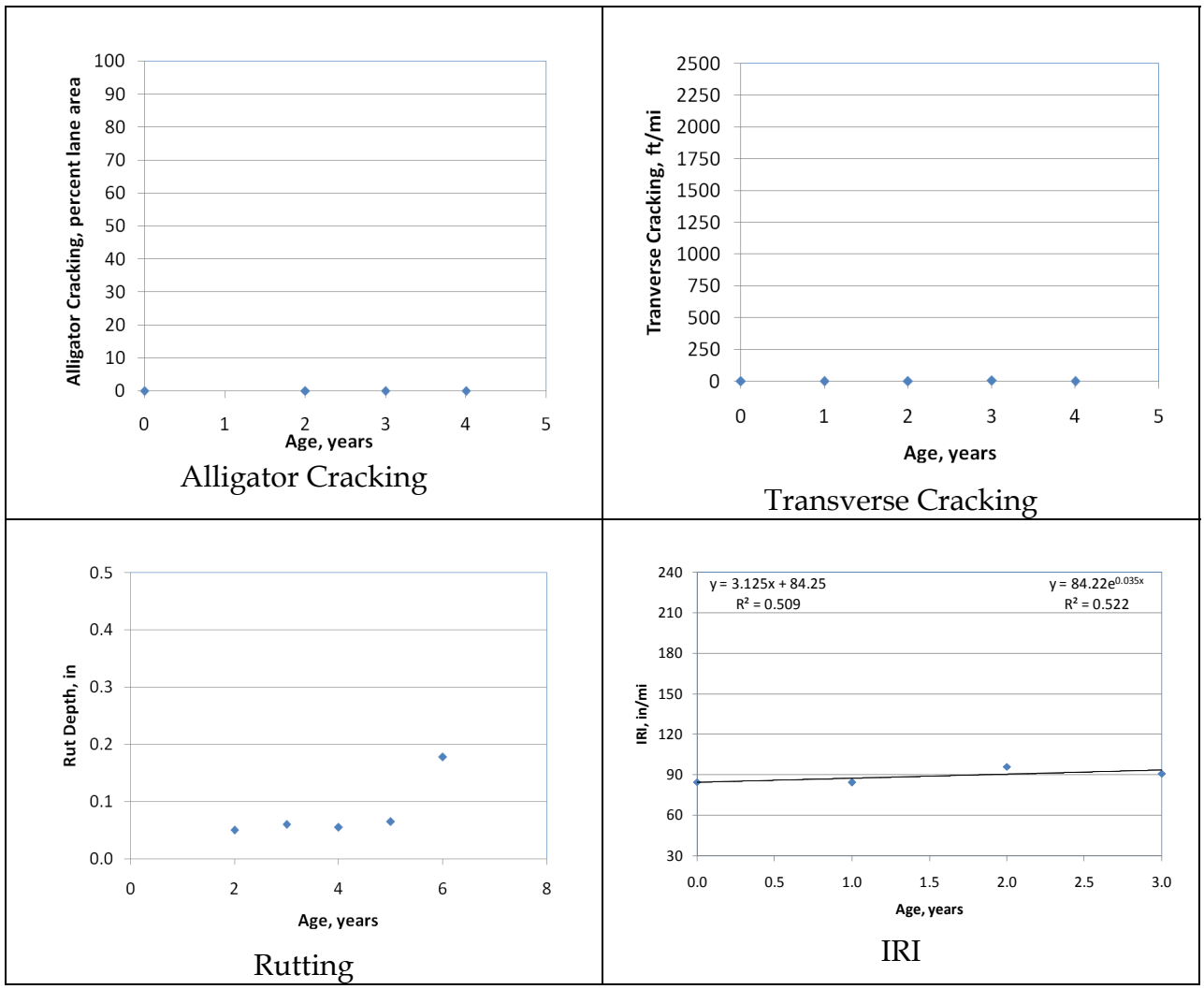

Figure A-26. Distress & IRI data plots for project PMS HMA R4 03.

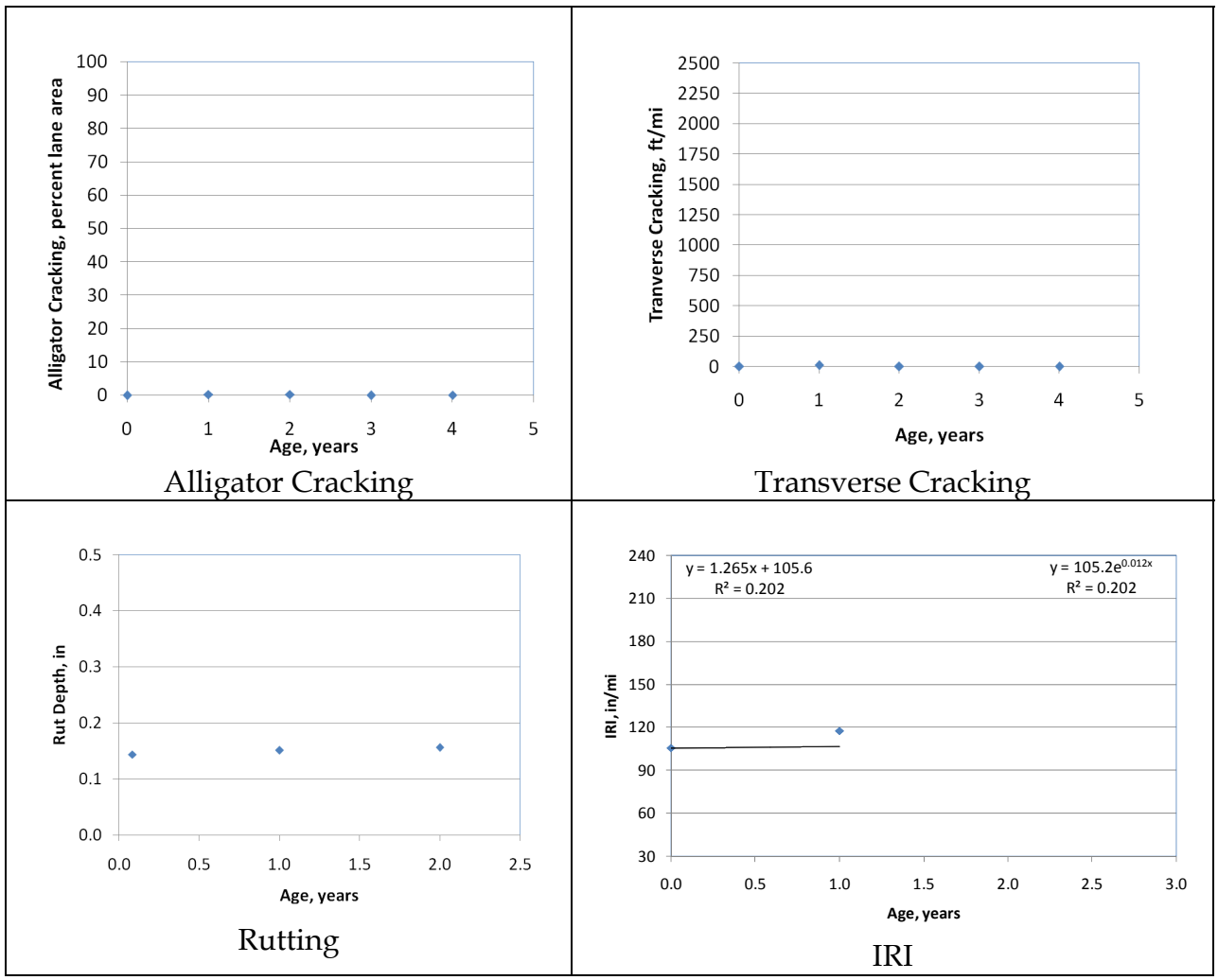

Figure A-27. Distress & IRI data plots for project PMS HMA R4 04(NB & SB).

THIS PAGE INTENTIONALLY LEFT BLANK

APPENDIX B. DISTRESS AND IRI DATA PLOTS FOR JPC SURFACED PAVEMENTS

Table B-1. Summary of UDOT distress/IRI data processing for JPCP.

<table>
<tr><th>Performance Indicator</th><th>Raw UDOT Measurement</th><th>Conversion Procedure & MEPDG Data Description</th></tr>
<tr><td>Transverse cracking</td><td>Reported as number of shattered panels or number of panels that have cracks that are predominantly perpendicular to the pavement centerline.</td><td>Convert to MEPDG reporting standards which is percentage of all slabs with transverse cracking of any severity as follows:
$$\text{PSlabsCracked} = \frac{(\text{NSP} + \text{NTCP})}{\text{TP}} * 100$$
where
PSlabsCracked = percent slabs cracked
NSP = number of shattered panels
NTCP = number of panels with transverse cracks
TP = total number of panels (typically 40 for UDOT)</td></tr>
<tr><td>Transverse joint faulting</td><td>Reported as the total number of joints with low, medium, and high severity faulting (i.e., categories 1, 2, and 3). Since UDOT profiler only records faults that are greater than or equal to 0.1 inch a fourth category of faulting (1*) was assumed representing joints with less than 0.1 inch faulting. Assumed mean joint faulting for all four categories are as follows:
<table>
<tr><th>Fault Cat.</th><th>Measured Faulting (Outer Wheelpath)</th><th>Assumed[1] Mean Faulting Value, in</th></tr>
<tr><td>1*</td><td>No. of joints with faulting < 0.1 in</td><td rowspan="2">0.067[2]</td></tr>
<tr><td>1</td><td>No. of joints with faulting > 0.1 in and < 0.3 in</td></tr>
<tr><td>2</td><td>No. of joints with faulting > 0.3 in and < 0.5 in</td><td>0.35</td></tr>
<tr><td>3</td><td>No. of joints with faulting > 0.5 in</td><td>0.5</td></tr>
</table>
[1]Weighted value for all joints any given category of faulting. Obtained through regression of LTPP measured faulting and UDOT PMS reported faulting categories.
[2]Represents the mean for all joints in category 1 and 1*</td><td>Convert to MEPDG reporting standards which is mean faulting in inches (for outer wheelpath) as follows:
$$MFLT = \frac{(N1_F * F1 + N2_F * F2 + N3_F * F3 + N4_F * F4)}{TJTS}$$
where
MFLT = mean transverse joint faulting, in
N1F = number of joints with faulting < 0.1 in
N2F = number of joints with faulting > 0.1 in and < 0.3 in
N3F = number of joints with faulting > 0.3 in and < 0.5 in
N4F = number of joints with faulting > 0.5 in
F1 = mean faulting for joints with low faulting (< 0.1 in), = 0.067 in
F2 = mean faulting for joints with low faulting (> 0.1 in), = 0.067 in
F3 = mean faulting for joints with moderate faulting, = 0.35 in
F4 = mean faulting for joints with high Faulting, = 0.5 in
TJTS = total number of joints = $N1_F + N2_F + N3_F + N4_F$</td></tr>
<tr><td>IRI</td><td>Reported as the average of both wheel paths IRI</td><td>No conversion needed</td></tr>
</table>

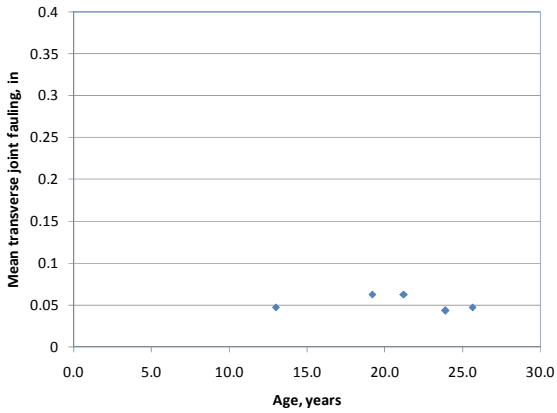

Transverse Joint Faulting

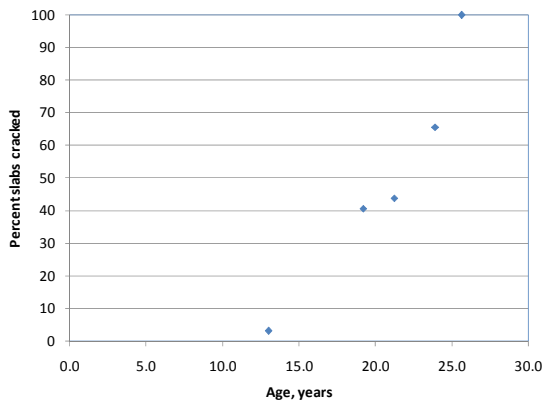

Transverse Cracking

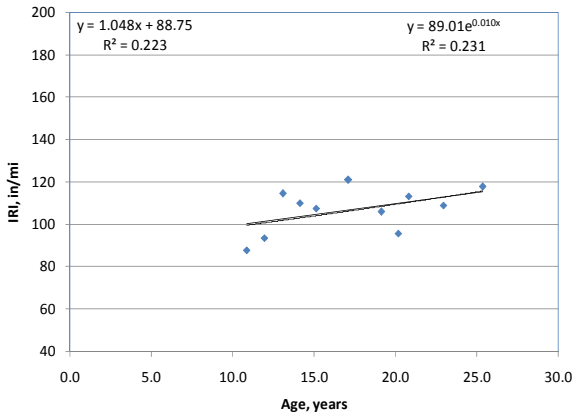

IRI

Figure B-1. Distress & IRI data plots for project LTPP 3010.

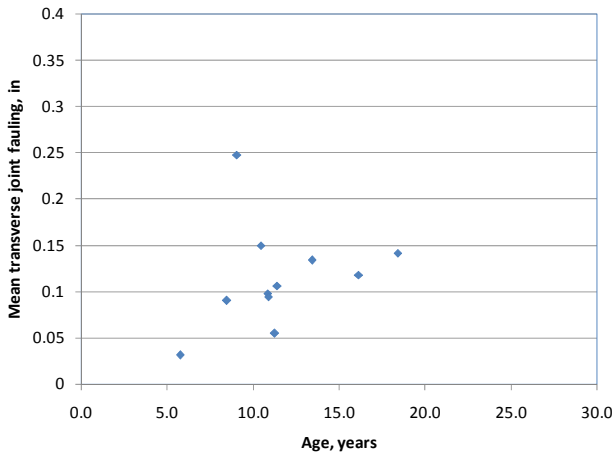

Transverse Joint Faulting

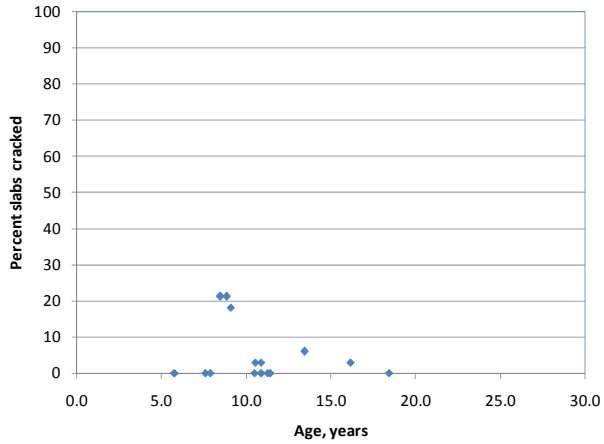

Transverse Cracking

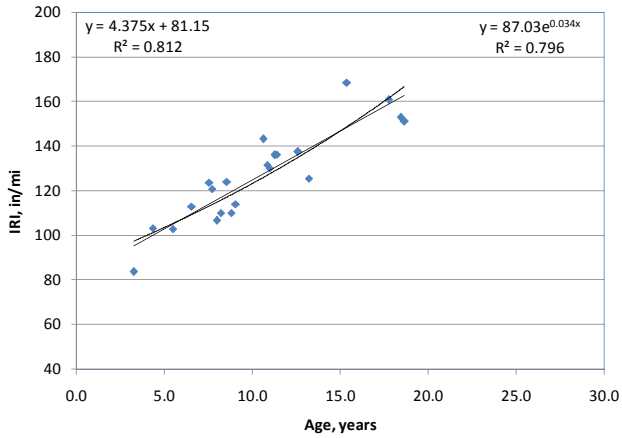

IRI

Figure B-2. Distress & IRI data plots for project LTPP 3011.

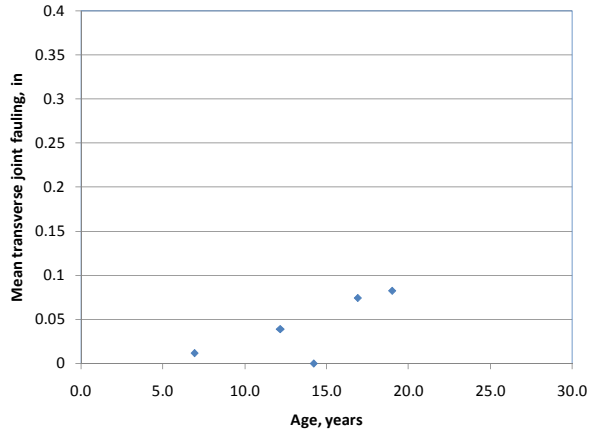

Transverse Joint Faulting

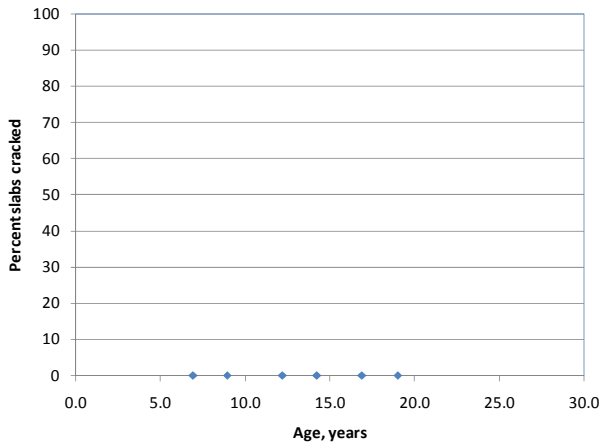

Transverse Cracking

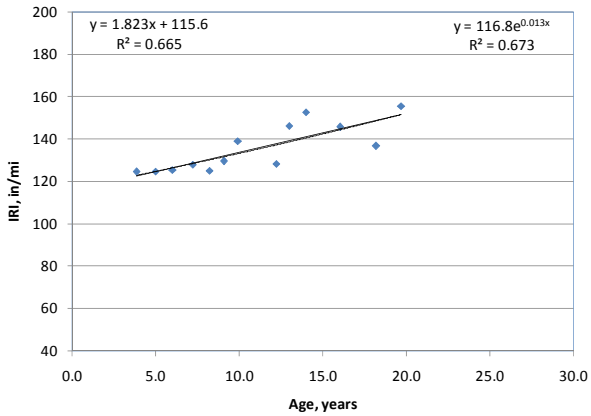

IRI

Figure B-3. Distress & IRI data plots for project LTPP 3015.

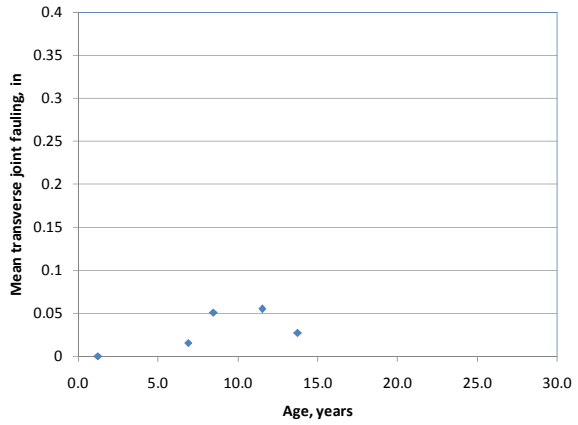

Transverse Joint Faulting

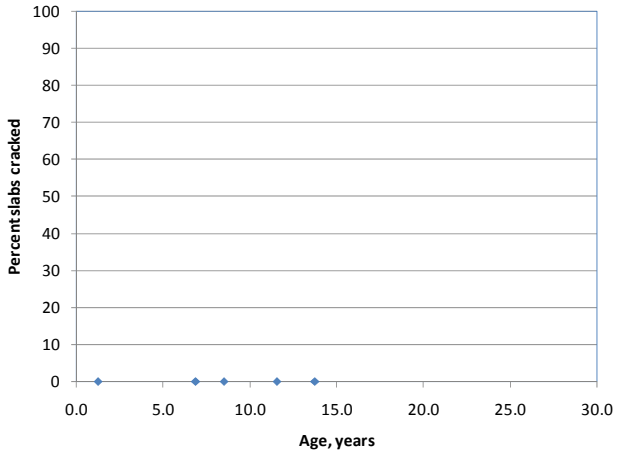

Transverse Cracking

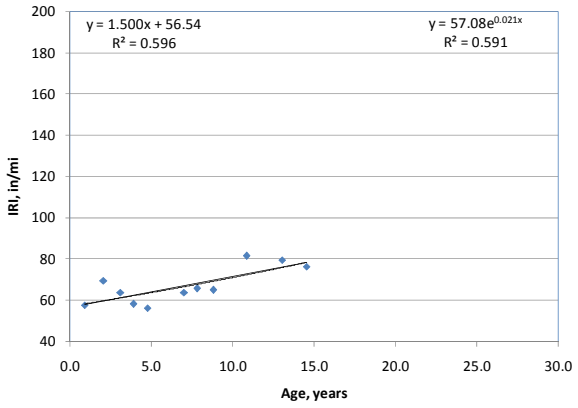

IRI

Figure B-4. Distress & IRI data plots for project LTPP 7082.

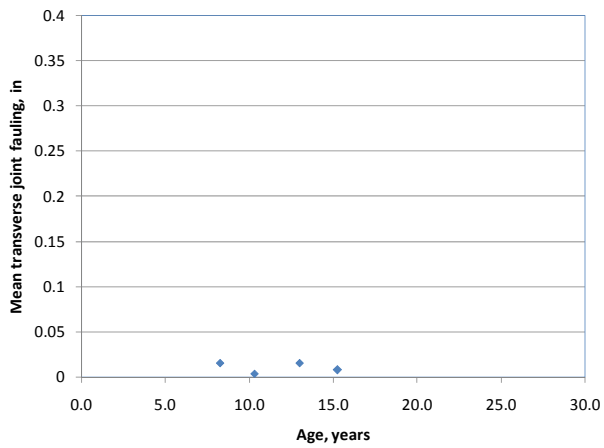

Transverse Joint Faulting

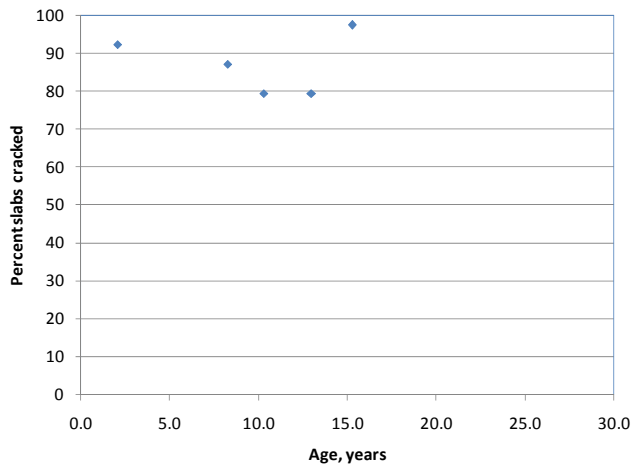

Transverse Cracking

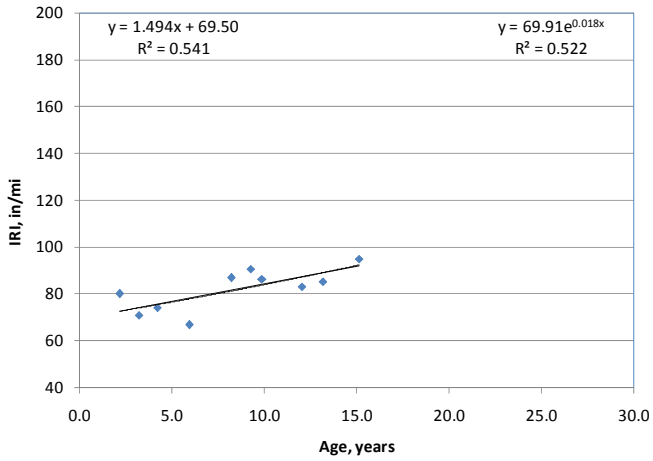

IRI

Figure B-5. Distress & IRI data plots for project LTPP 7083.

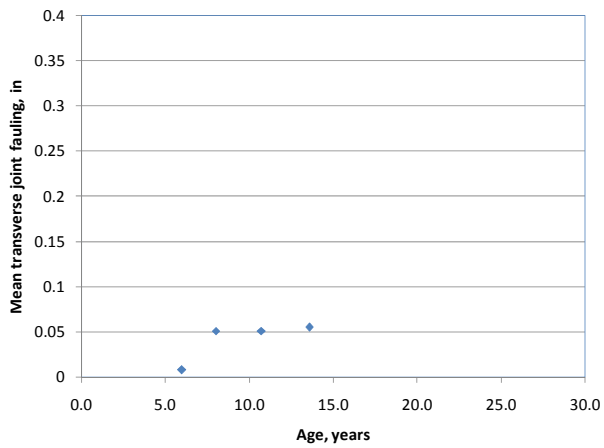

Transverse Joint Faulting

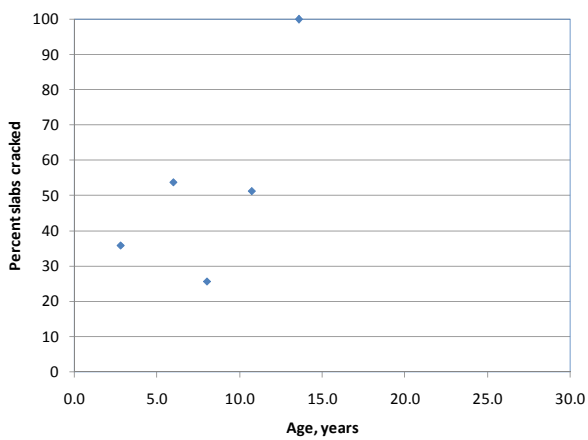

Transverse Cracking

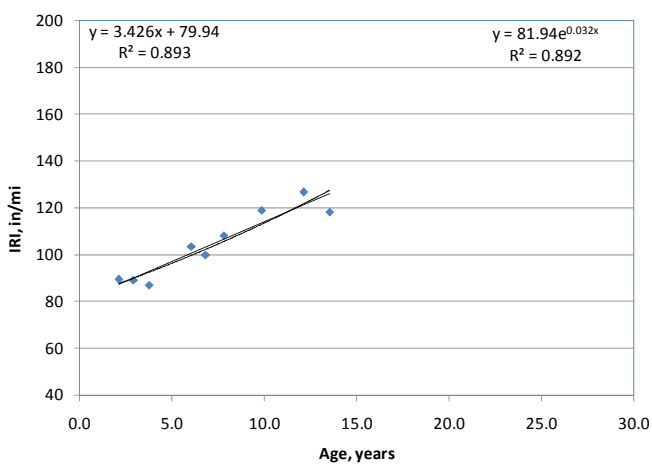

IRI

Figure B-6. Distress & IRI data plots for project LTPP 7085.

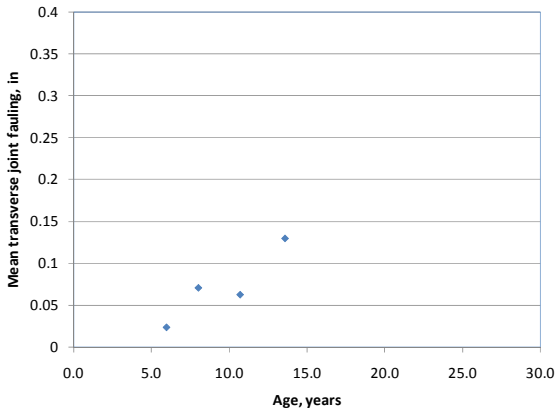

Transverse Joint Faulting

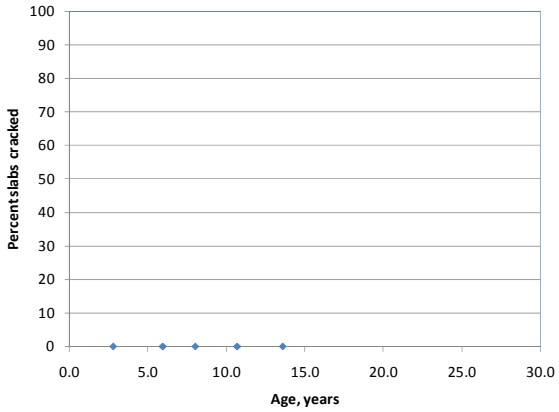

Transverse Cracking

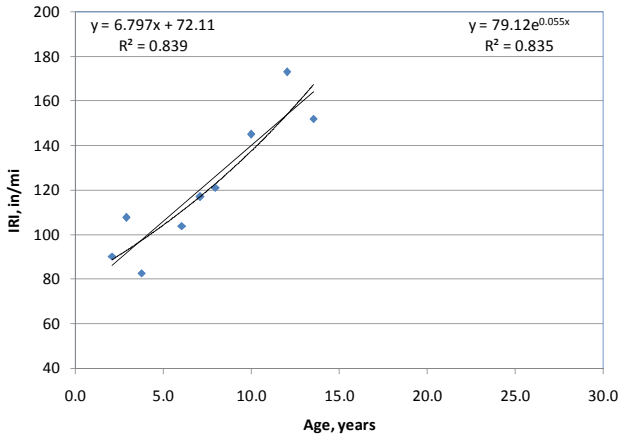

IRI

Figure B-7. Distress & IRI data plots for project LTPP 7086.

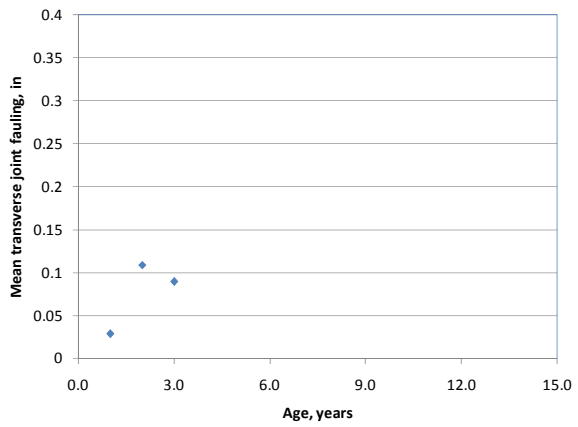

Transverse Joint Faulting

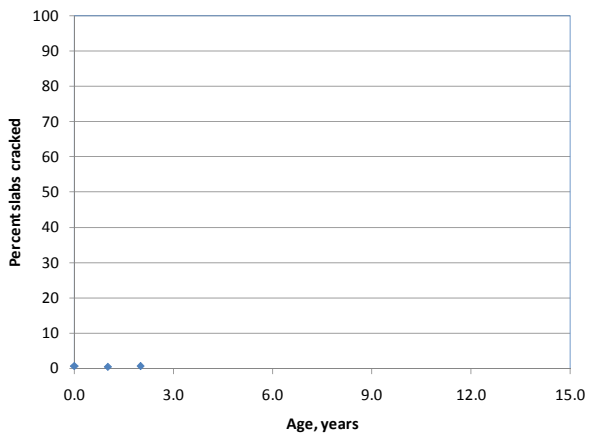

Transverse Cracking

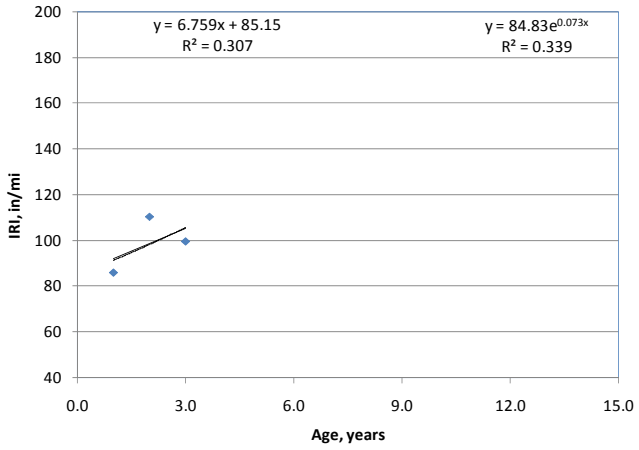

IRI

Figure B-8. Distress & IRI data plots for project UDOT PMS CPR2.

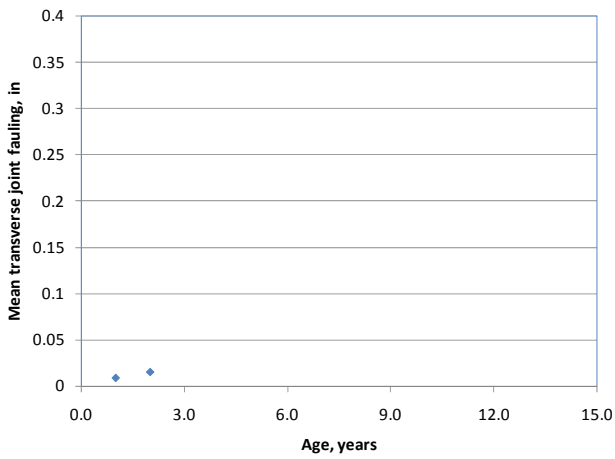

Transverse Joint Faulting

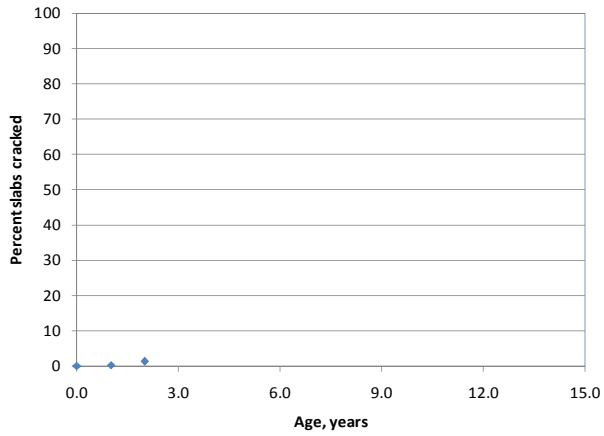

Transverse Cracking

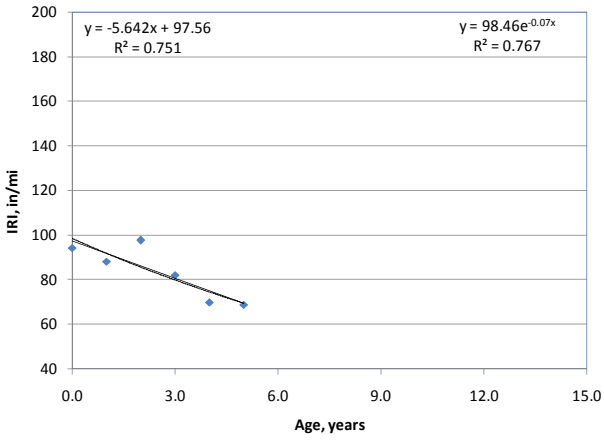

IRI

Figure B-9. Distress & IRI data plots for project UDOT PMS CPR3.

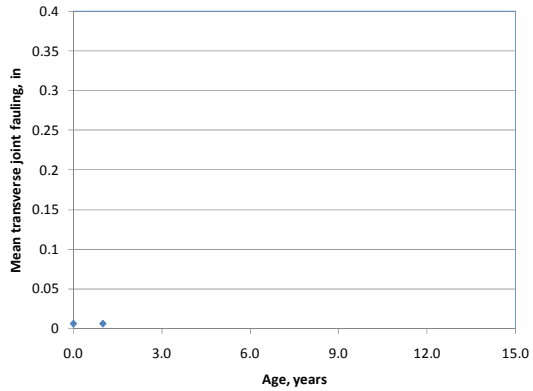

Transverse Joint Faulting

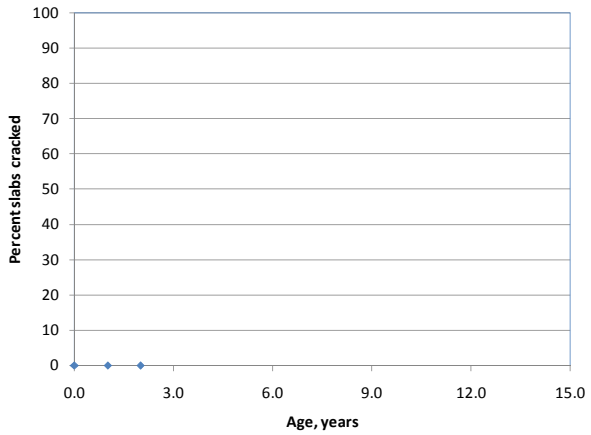

Transverse Cracking

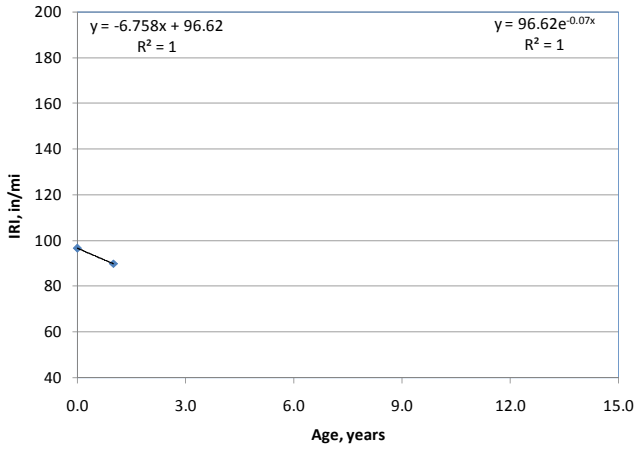

IRI

Figure B-10. Distress & IRI data plots for project UDOT PMS CPR4.

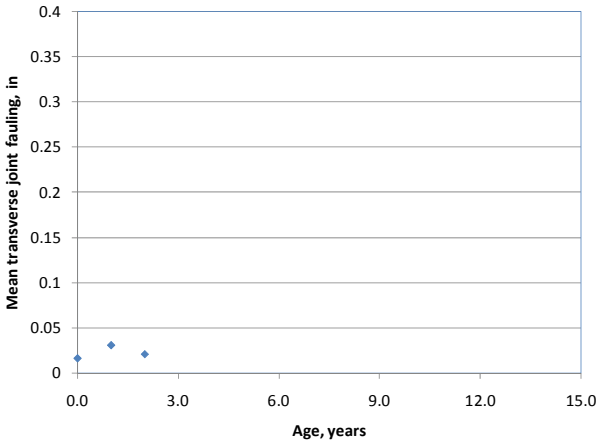

Transverse Joint Faulting

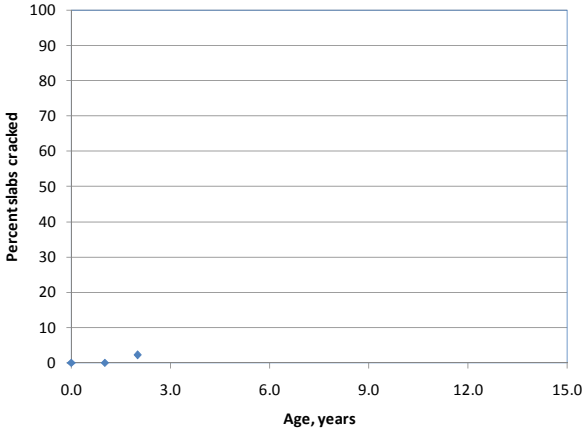

Transverse Cracking

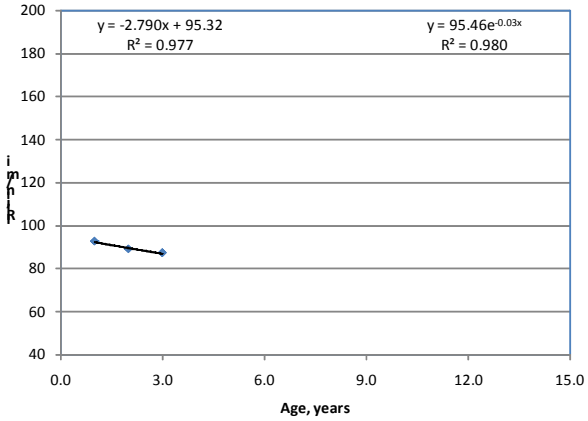

IRI

Figure B-11. Distress & IRI data plots for project UDOT PMS CPR5.

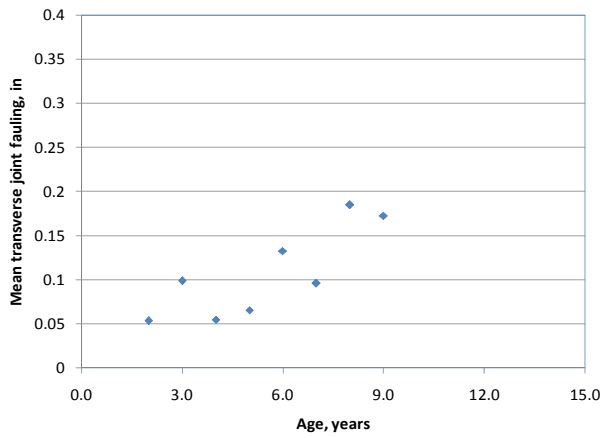

Transverse Joint Faulting

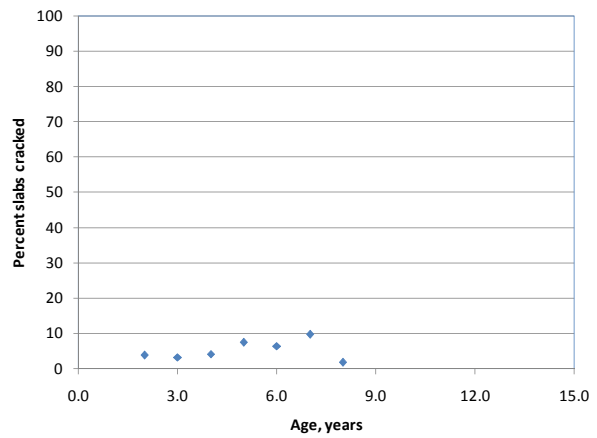

Transverse Cracking

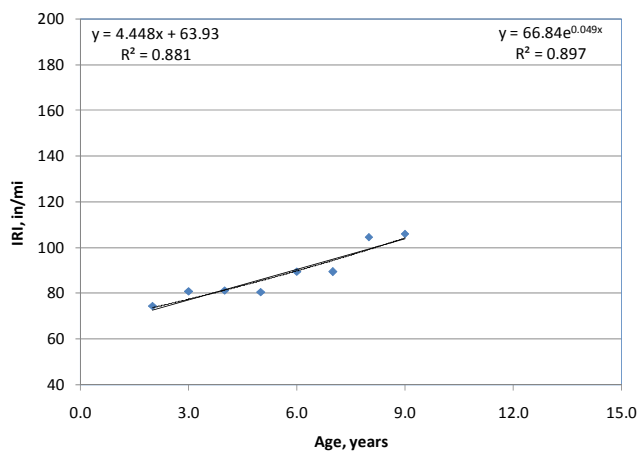

IRI

Figure B-12. Distress & IRI data plots for project UDOT PMS CPR6.

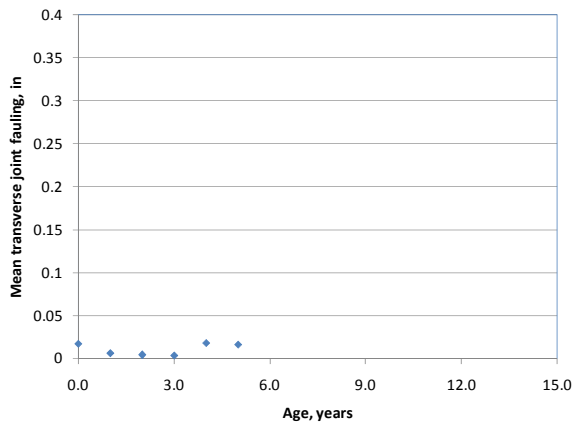

Transverse Joint Faulting

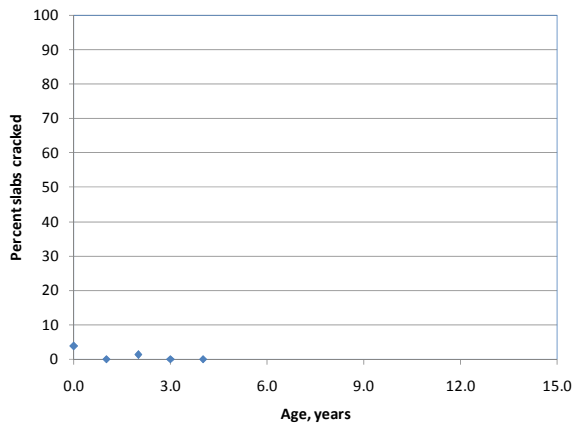

Transverse Cracking

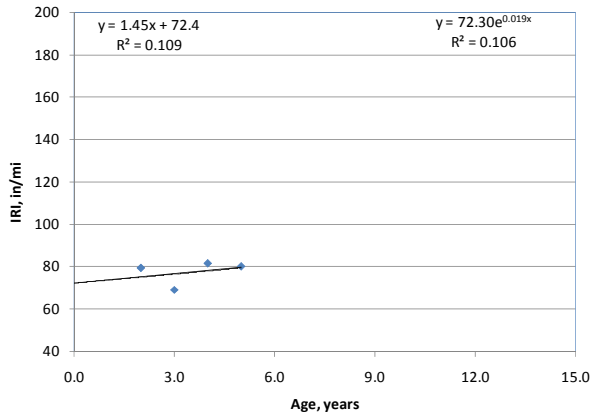

IRI

Figure B-13. Distress & IRI data plots for project UDOT PMS CPR7.

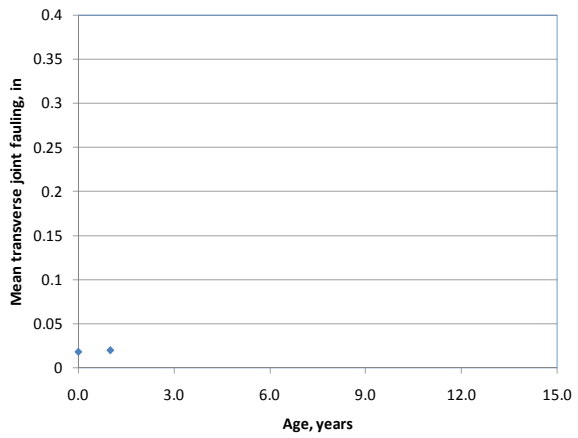

Transverse Joint Faulting

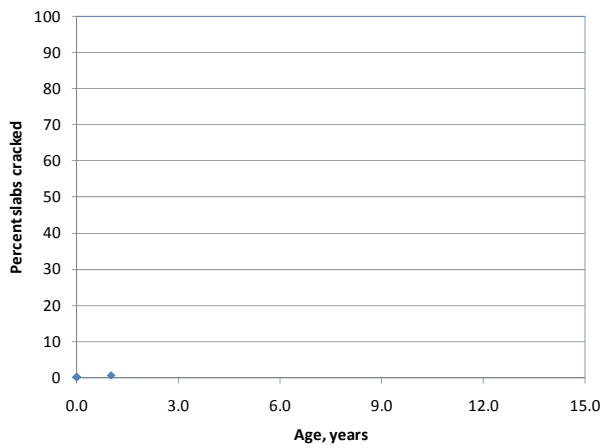

Transverse Cracking

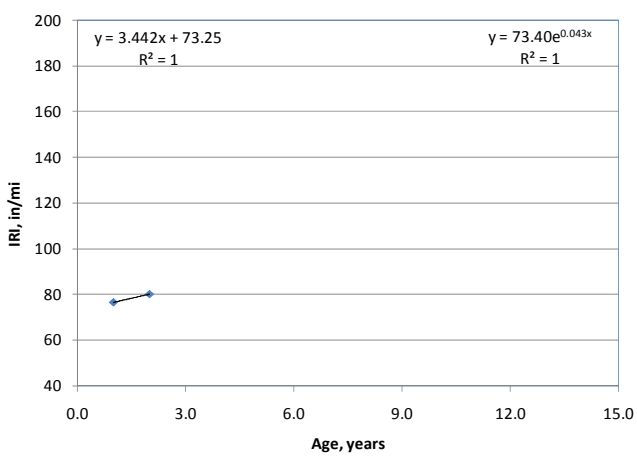

IRI

Figure B-14. Distress & IRI data plots for project UDOT PMS CPR8.

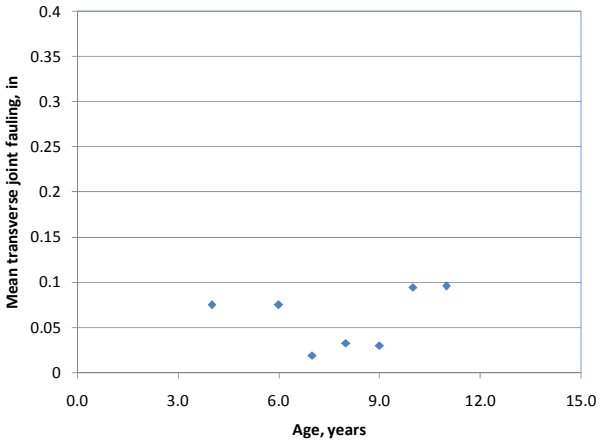

Transverse Joint Faulting

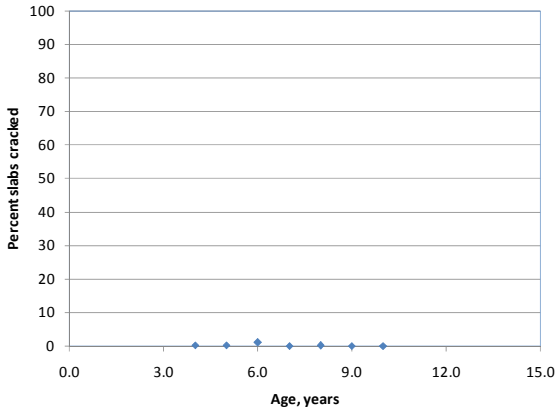

Transverse Cracking

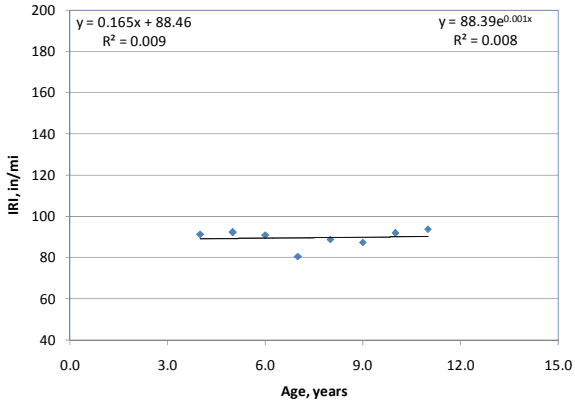

IRI

Figure B-15. Distress & IRI data plots for project UDOT PMS JPCP2.

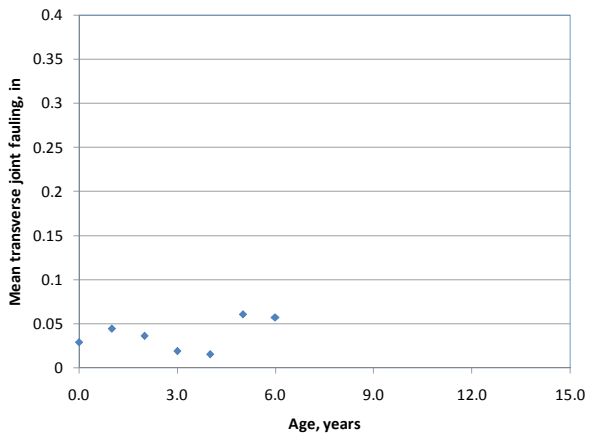

Transverse Joint Faulting

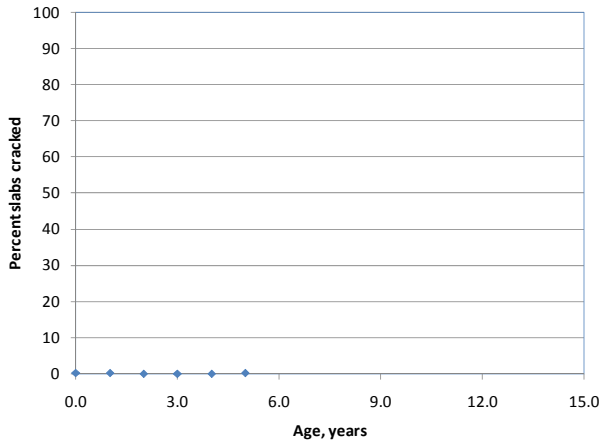

Transverse Cracking

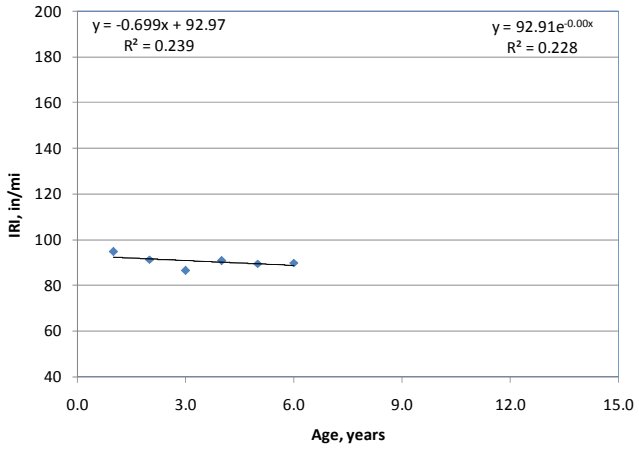

IRI

Figure B-16. Distress & IRI data plots for project UDOT PMS JPCP5.

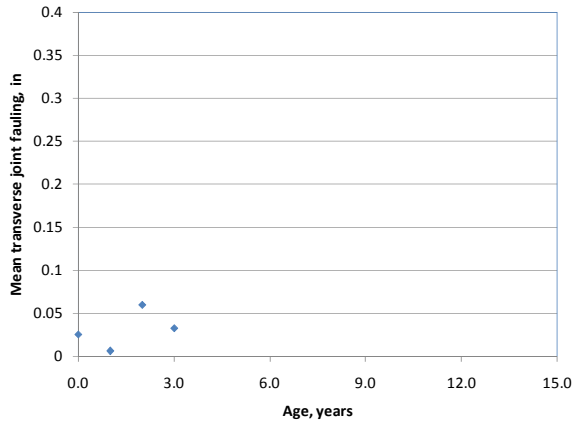

Transverse Joint Faulting

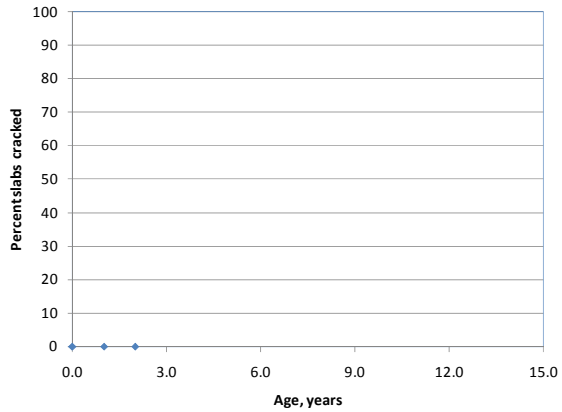

Transverse Cracking

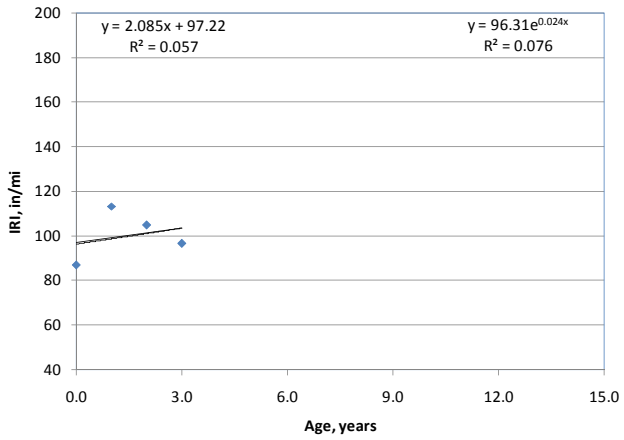

IRI

Figure B-17. Distress & IRI data plots for project UDOT PMS JPCP6.

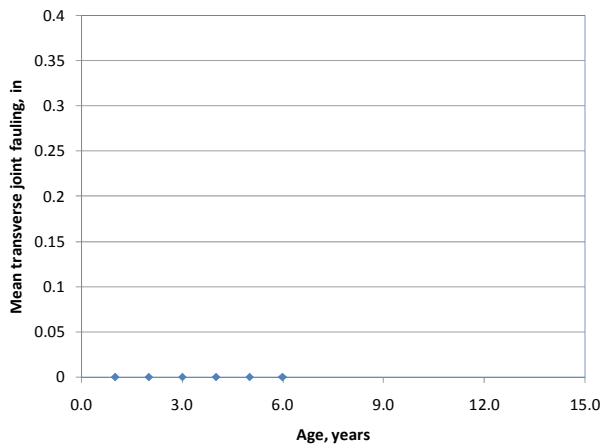

Transverse Joint Faulting

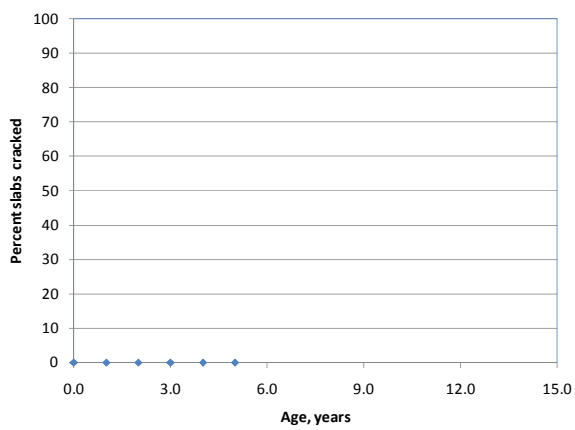

Transverse Cracking

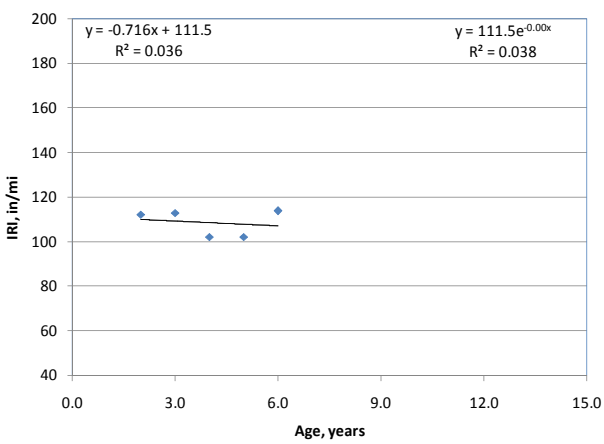

IRI

Figure B-18. Distress & IRI data plots for project UDOT PMS JPCP10.

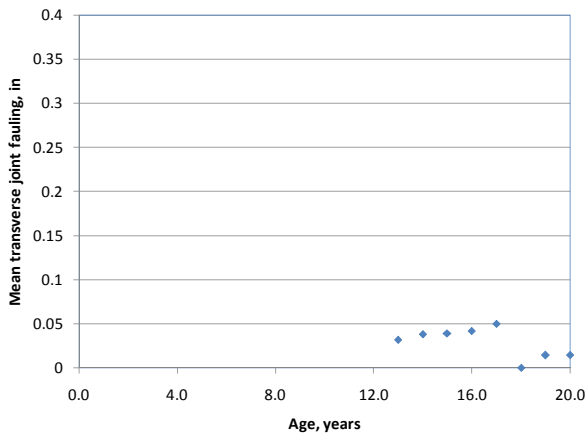

Transverse Joint Faulting

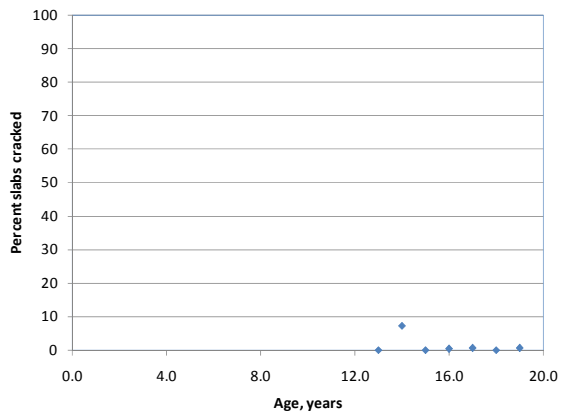

Transverse Cracking

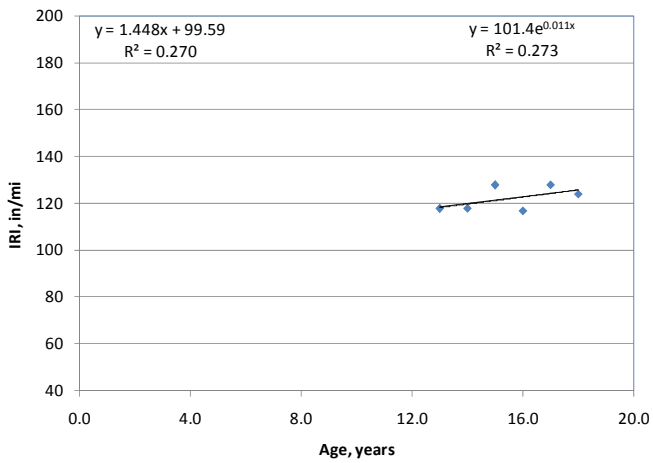

IRI

Figure B-19. Distress & IRI data plots for project UDOT PMS JPCP14.

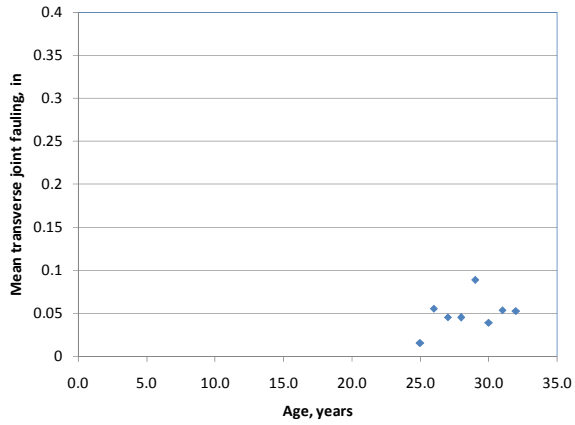

Transverse Joint Faulting

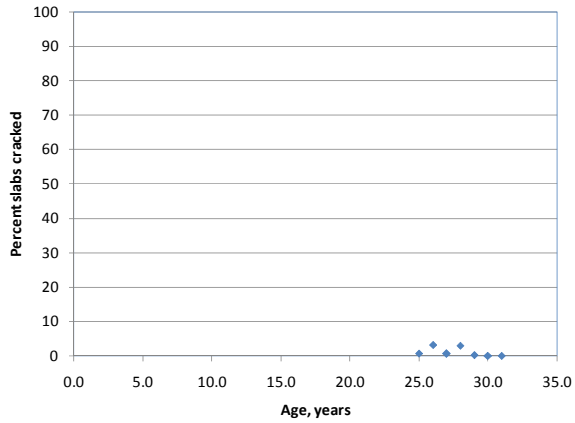

Transverse Cracking

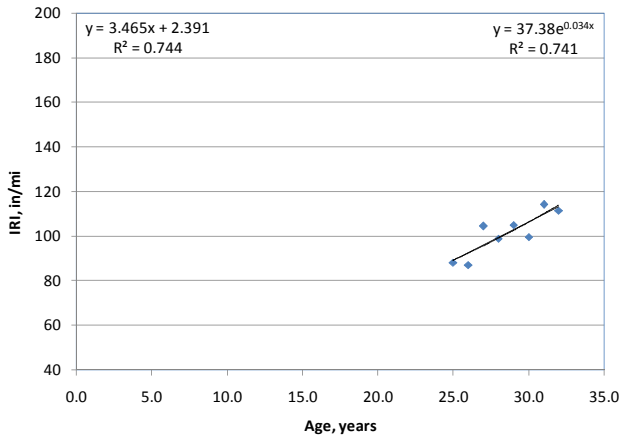

IRI

Figure B-20. Distress & IRI data plots for project UDOT PMS JPCP16.

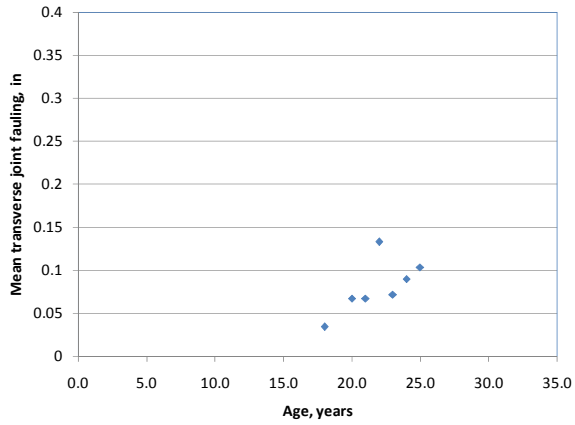

Transverse Joint Faulting

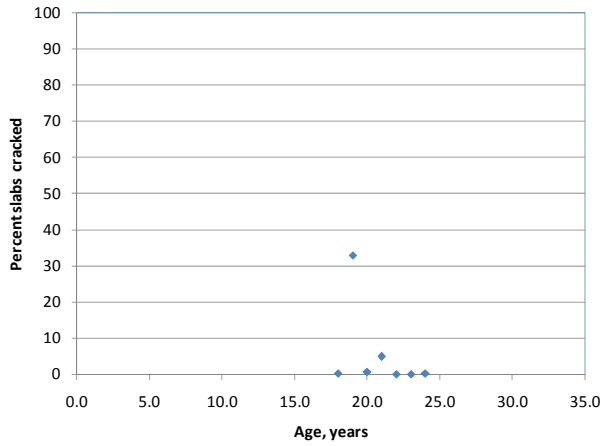

Transverse Cracking

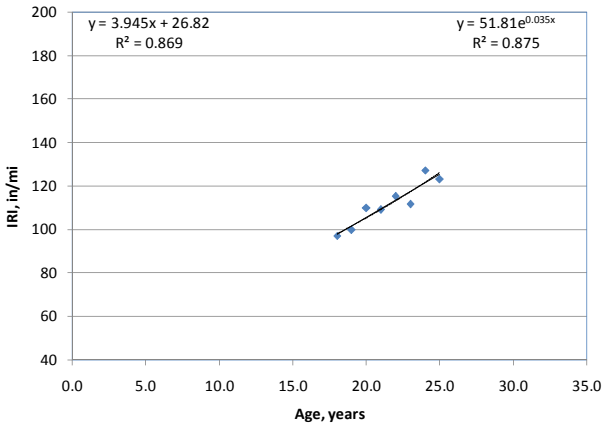

IRI

Figure B-21. Distress & IRI data plots for project UDOT PMS JPCP17.

APPENDIX C. MEPDG INPUT DATA

General Information, Site Identification, and Analysis Parameters

Key MEPDG inputs required under general information, site identification, and analysis parameters are:

- Pavement construction and traffic opening date.
- Location and other inventory information.
- Initial IRI.

A summary of general and site location information for all the projects included in analysis is presented in Table C-1. Tables C-2 and C-3 present estimates of initial IRI for HMA pavements and JPCP. It must be noted that for most projects, LTPP and UDOT performance databases do not contain the construction year IRI or initial IRI. Construction year IRI was thus computed backcasting using historical IRI information (see figures in Appendix A and B). An example of backcasting using a linear and non-linear model is presented in Figure C-1. Hierarchical input levels are not required for this input type.

Traffic

Key MEPDG traffic inputs required are:

- Initial AADTT and AADTT growth rate.
- Axle load distribution.
- Vehicle class distribution.
- Mean number of single, tandem, tridem, and quad axles per truck.

A summary of initial AADTT for the project construction year along with AADTT growth rate is presented in Table C-4. It must be noted that for most projects, LTPP and UDOT traffic databases do not contain the construction year AADTT. Construction year AADTT was thus computed backcasting using historical AADTT information (see Figure C-2). For the other traffic inputs such as axle load distribution, a general assumption made by the MEPDG was that there were no significant changes in traffic patterns over the analysis period. Thus, mean values of data collected for as many years as available was sufficient to estimate these inputs. Appendix D presents plots of AADTT versus age for selected LTPP projects.

Table C-1. Summary of general information, site identification, and analysis parameters information for all the projects included in analysis.

Project Name	New or Rehabilitation Construction Year	New or Rehabilitated Pavement Design Type	Project Location	Route No.	LTPP or UDOT Project ID	Begin Milepost	End Milepost
CPR1	2001	CPR of JPCP	State Street to 2300 East, Salt Lake County	I-80	SP-80-3(57)124	121.000	126.000
CPR2	2004	CPR of JPCP	Levan Ridge South of Nephi, Juab County	I-15	IM-15-5(33)211	211.186	216.000
CPR3	2005	CPR of JPCP	North Richfield to Sigard, Sevier County	I-70	IM-70-1(56)42	42.000	48.000
CPR4	2006	CPR of JPCP	MP 1 to MP 3, Junction SR-118 to State Canal Crossing, Sevier County	SR-120	STP-0120(3)1	0.976	3.380
CPR5	2005	CPR of JPCP	Riverdale to Uintah Junction, Weber County	I-84	IM-84-6(84)44	42.000	44.000
CPR6	1998	CPR of JPCP	Hot Springs to Brigham, Box Elder County	I-15	SP-15-8(32)355	354.200	364.800
CPR7	2002	CPR Dowels Bar and Diamond Grind	5600 S to 4500 S. Salt Lake East Side, Salt Lake County	I-215	IM-215-9(108)4	3.700	5.700
CPR8	2006	CPR of JPCP with Dowels, Grinding	S Nephi to N. Nephi, Juab County	I-15	IM-15-5(32)223	216.000	230.000
CPR9	2004	JPCP Const. 1983, diamond ground in 2004	Clear Creek Canyon MP 7 to 17, Sevier County	I-70	IM-70-1(51)7	7.000	17.000
JPCP1	1972	New JPCP	Pages Lane Lagoon, Davis County	I-15	I-15-7(85)315	315.000	321.000
JPCP10	2001	New JPCP	At intersection of US-89 & US-50 and W. Main Street, Salina, Sevier County	US-89 & US-50	NH-STP-9999(196)	194.800	195.550

Table C-1. Summary of general information, site identification, and analysis parameters information for all the projects included in analysis, continued.

Project Name	New or Rehabilitation Construction Year	New or Rehabilitated Pavement Design Type	Project Location	Route No.	LTPP or UDOT Project ID	Begin Milepost	End Milepost
JPCP11	1984	New JPCP	Scipio to Juab County, Millard County	I-15	–	188.000	194.000
JPCP13	1987	New JPCP	Belknap to Elsenor, Sevier County	I-70	I-ID-70-1(39)19	17.000	31.000
JPCP14	1987	New JPCP	Elsenor to South Richfield, Sevier County	I-70	I-ID-70-1(40)31	31.000	37.700
JPCP15	1986	New JPCP	25569, North Richfield to Sigard, Sevier County	I-70	I-70-1(24)40	37.800	46.800
JPCP16	1975	New JPCP	Plymouth to Idaho, Box Elder County	I-15	I-15-8(45)382	382.000	388.530
JPCP17	1982	New JPCP	Riverside to Plymouth, Box Elder County	I-15	I-15-8(19)376	386.970	396.730
JPCP2	1996	New doweled JPCP	Morgan to Summit County, Morgan County	I-84	IM-84-6(70)102	112.270	102.220
JPCP3	1976	New JPCP	Wahsatch to WY State line, Summit County	I-80	IM-STP-80-4(93)189	191.900	196.680
JPCP4	1976	New JPCP	Wahsatch to Castle Rock, Summit County	I-80	IM-STP-80-4(98)186	181.000	196.680
JPCP5	2001	New doweled JPCP over a permeable base	10800 South to 500 N. SLC valley, Salt Lake County	I-15	SP-15-7(135)296	293.000	309.000
JPCP6	2004	Unbonded JPCP overlay over existing JPCP	Redwood Rd. to 4700 South, Salt Lake West Side Belt, Salt Lake County	I-215	IM-BHF-215-9(112)14	13.320	17.010
JPCP7	–	New JPCP over existing HMA (considered new design)	Wyoming State Line to Castle Rock, Summit County	I-80	–	181.000	196.680
HMA_R1 01	2001	New HMA (reconstruction with asphalt pavement	Snow Basin Road, Weber County	SR-226	SP-0226(1)0	0.000	3.200

Table C-1. Summary of general information, site identification, and analysis parameters information for all the projects included in analysis, continued.

Project Name	New or Rehabilitation Construction Year	New or Rehabilitated Pavement Design Type	Project Location	Route No.	LTPP or UDOT Project ID	Begin Milepost	End Milepost
HMA_R1 02	2002	New HMA (reconstruction with asphalt pavement)	Logan Canyon; Tony Grove to Franklin Basin, Cache County	US-89	NH-0089(29)393	392.700	397.800
HMA_R1 03	2002	New HMA (reconstruction with asphalt pavement)	Wilson Lane in Ogden; SR-126 to I-15, Weber County	SR-104	STP-0104(2)0	0.000	0.700
HMA_R1 04	1998	New HMA (asphalt overlay over crack & seat PCC)	450 North to Hot Springs, Weber County	I-15	IM-15-8(92)49	346.885	352.028
HMA_R2 01	1999	New HMA (reconstruction with asphalt pavement)	High School to US-40, Summit County	SR-248	SP-0248(002)3	1.400	3.070
HMA_R2 02	1993	New HMA (reconstruction with asphalt pavement)	Bear Hollow to 248, Summit County	SR-224	HPP-NH-0036(6)63	6.040	9.390
HMA_R2 03	2002	New HMA (lane widening with asphalt pavement (to 4 lanes))	700 East; 6300 S. to 6000 S., Salt Lake County	SR-71	STP-0071(11)10	16.670	14.060
HMA_R2 04	2002	New HMA (lane widening with asphalt pavement (to 4 lanes))	Mills Junction to I-80, Tooele Co, Tooele County	SR-36	NH-0036(6)36	62.100	65.600
HMA_R3 01	1986	New HMA (reconstruction with asphalt pavement)	Tickville Wash to Fairfield, Utah County	SR-73	NF-57(1)	20.842	31.925
HMA_R3 02	1996	New HMA (reconstruction with asphalt pavement)	Tickville Wash to SR-68, Utah County	SR-73	SP-0073(1)32	31.540	36.540
HMA_R3 03	2003	New HMA (asphalt overlay of crack & seat JPCP)	Point of Mountain to Lehi, Utah County	I-15	IR-15-6(104)285	285.930	282.710

Table C-1. Summary of general information, site identification, and analysis parameters information for all the projects included in analysis, continued.

Project Name	New or Rehabilitation Construction Year	New or Rehabilitated Pavement Design Type	Project Location	Route No.	LTPP or UDOT Project ID	Begin Mile post	End Milepost
HMA_R3 04	2003	New HMA (asphalt overlay over rubblized of JPCP)	Sevier River to Mills, Juab County	I-15	IM-NH-15-5(31)200	200.070	211.170
HMA_R4 01	2002	New HMA (reconstruction with asphalt pavement)	Centerfield to Gunnison, Sanpete County	US-89	NH-0089(43)206	204.600	207.900
HMA_R4 02	2002	New HMA (lane widening with asphalt pavement (to 4 lanes))	Huntington to Poison Springs Bench, Emery County	SR-10	STP-0010( )48	48.400	53.400
HMA_R4 03	2002	New HMA (lane widening with asphalt pavement (to 4 lanes))	I-15 to Iron Springs, Iron Co, Iron County	SR-56	SP-0056(3)56	56.000	57.500
HMA_R4 04 (NB)	2006	New HMA (lane widening with asphalt pavement (to 4 lanes))	Moab to I-70 at Crescent Junction, Grand County	US-191	SP-0191(30)125	125.000	132.000
HMA_R4 04 (SB)	2006	New HMA (SB lane widening with asphalt pavement)	Moab to I-70 at Crescent Junction, Grand County	US-191	SP-0191(30)125	125.000	132.000
HMA_OVLY_1	1970/2006	HMA overlay of existing HMA	Arizona State Line to Bluff Street MP 0-6, Washington County	I-15	IM-15-1(63)0	0.000	6.000
HMA_OVLY_2	2002	HMA overlay of existing HMA	Dog Valley through Baker Canyon, Millard County	I-15	IM-15-4(39)138	138.600	143.900
HMA_OVLY_3	2002	HMA overlay of existing HMA	Intersection with SR-211 to RP 93 North of Monticello, San Juan County	US-191	NH-0191(12)87	86.000	89.000
HMA_OVLY_4	2004	HMA overlay of existing HMA	Fremont junction to Quitchupah Hill, Emery, Sevier County	SR-10	SP-0010(20)0	0.000	7.000
49_0803	1997	New HMA	Wolf Creek Road (0.6 miles east of bridge crossing Provo River), Wasatch County	SR-35	–	–	–
49_0804	1997	New HMA	Wolf Creek Road (0.6 miles east of bridge crossing Provo River), Wasatch County	SR-35	–	–	–

Table C-1. Summary of general information, site identification, and analysis parameters information for all the projects included in analysis, continued.

Project Name	New or Rehabilitation Construction Year	New or Rehabilitated Pavement Design Type	Project Location	Route No.	LTPP or UDOT Project ID	Begin Milepost	End Milepost
49_1001_1	1980	New HMA	Start of section is 2.4 miles north of the US-191 – US-163 intersection. The entrance to the Bluff UDOT Maintenance Yard is 1 mile northbound of the start of section, San Juan County	US-191	–	23.74	23.83
49_1004_2	1978	HMA overlay of existing HMA	The start of section is 6.0 miles north of junction SR-20 and 15.9 miles south of junction SR-62, Garfield County	US-89	–	147.81	147.90
49_1005_1	1984	HMA overlay of existing HMA	Start of section is 0.239 miles north of junction with SR-109, Davis County	US-89	–	339.97	340.06
49_1006	1988	HMA overlay of existing HMA	2.354 miles north of the junction with US-89 and 3.104 miles south of the entrance road to Fayette, Sanpete County	SR-28	–	2.37	2.46
49_1007_1	1988	HMA overlay of existing HMA	Start of section is 3.398 miles north of the 1st street north overcrossing in Price, and 0.158 miles south of the Price River Bridge, Carbon County	US-6	–	236.80	236.89
49_1008_1	1976	New HMA	0.852 miles north of the I-70 overcrossing and 0.571 miles south of Salina creek bridge, Sevier County	US-89	–	193.38	193.47
49_1008_2	1990	HMA overlay of existing HMA	0.852 miles north of the I-70 overcrossing and 0.571 miles south of Salina creek bridge, Sevier County	US-89	–	193.38	193.47
49_1017_1	1966	New HMA	Start of section is 0.275 miles North of Sevier River Bridge and 2.178 miles south of junction with SR-4, Sevier County	US-89	–	190.30	190.39

Table C-1. Summary of general information, site identification, and analysis parameters information for all the projects included in analysis, continued.

Project Name	New or Rehabilitation Construction Year	New or Rehabilitated Pavement Design Type	Project Location	Route No.	LTPP or UDOT Project ID	Begin Milepost	End Milepost
49_3010	1978	New JPCP	1.394 miles north of Paragonah overcrossing and 10.806 miles south of Panquitch overcrossing, Iron County	I-15	–	83.67	83.76
49_3011	1986	New JPCP	14.55 miles north of exit 207 (Mills overpass). Exit 222 (Nephi overpass) is 1.65 miles north of the start of section, Juab County	I-15	–	221.17	221.26
49_3015_1	1985	New JPCP	Start of section is 0.4 miles southbound of the RR overpass just after exiting I-15. Exit 28 (Redwood Road) is 0.6 miles southbound of the start of section, Salt Lake County	I-215	–	28.46	28.55
49_7082	1990	New JPCP	4.26 miles north of Riverside/Logan exit (exit 387, SR-30 east). Exit 394 (SR-13 south, Plymount) is 2.8 miles north of the start of section, Box Elder County	I-15	–	391.91	392.00
49_7083_1	1989	New JPCP	The start of section is 1.9 miles east of the west Richfield exit (exit 35) and 1.5 miles west of the east Richfield exit (exit 38), Sevier County	I-70	–	38.99	39.08
49_7085_1	1991	New JPCP	Start of section is approximately 8.2 miles Eastbound (South) of the Park City exit. The junction of US 40 and SR 19 is about 0.8 miles Eastbound (South) of the start of the section, Wasatch County	US-40	–	12.55	12.64
49_7086	1991	New JPCP	0.5 miles south of 2100 S. St. and 3100 S. St. is 0.7 miles south of the start of section, Salt Lake County	SR-154	–	19.00	19.09

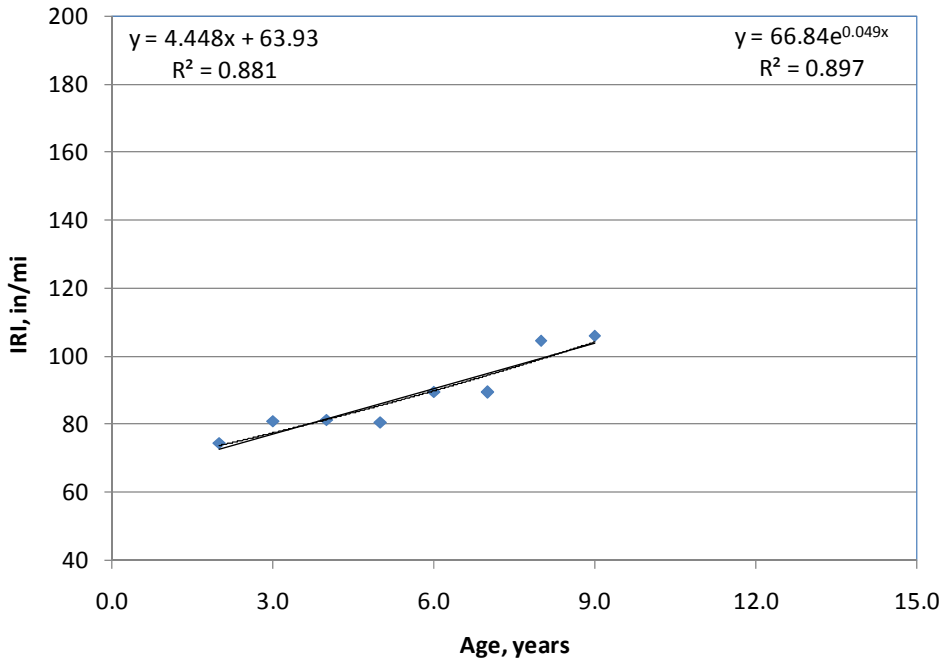

Figure C-1. Illustration of initial IRI backcasting for project CPR-6.

Table C-2. Summary of initial IRI information for all HMA surfaced pavements.

Project ID	Linear	Exponential	Initial IRI, in/mi	Comment
0803	63.7	63.7	63.7	OK
0804	57.6	57.43	53.5	Negative slope, average used
1001	38.88	46.31	42.6	OK, used mean
1004	-38.76	52.7	52.7	Negative linear estimate, exponential used
1005	24.33	28.87	26.6	OK, used mean
1006	41.97	42.76	42.4	OK, used mean
1007	61.29	61.9	61.6	OK, used mean
1008	-18.68	34.06	34.06	Negative linear estimate, exponential used
1017	63.27	67.21	65.2	OK, used mean
HMA_OVLY_2	54.77	54.82	54.8	OK, used mean
HMA_OVLY_3	89.89	90.96	90.425	OK, used mean
HMA_OVLY_4	87.75	87.9	87.825	OK, used mean
HMA R1 01	97.12	99.29	98.205	OK, used mean
HMA R1 02	75.01	76.9	75.955	OK, used mean
HMA R1 03	124.9	125	124.95	OK, used mean
HMA R1 04	30.62	32.57	31.595	OK, used mean
HMA R2 01	79.78	79.72	79.75	OK, used mean
HMA R2 02	16.07	31.33	23.7	OK, used mean
HMA R2 03	85.5	85.52	85.51	OK, used mean
HMA R2 04	46.85	46.85	46.77	Negative slope, average used
HMA R3 01	27.42	42.87	35.145	OK, exponential used
HMA R3 02	80.31	80.88	80.595	OK, used mean
HMA R3 03	61.53	61.59	52.93	Negative slope, average used
HMA R3 04	59.51	59.55	56.55	Negative slope, average used
HMA R4 02	80.88	80.87	80.875	OK, used mean
HMA R4 03	84.25	84.22	84.235	OK, used mean
HMA R4 04	105.6	105.6	105.6	OK, used mean

Table C-3. Summary of initial IRI information for JPC surfaced projects included in analysis.

Project ID	Linear	Exponential	Initial IRI, in/mi	Comment
3010	88.8	89.0	88.9	OK, used mean
3011	81.1	87.0	84.05	OK, used mean
3015	115.6	116.8	116.2	OK, used mean
7082	56.5	87.1	71.8	OK, used mean
7083	69.5	69.9	69.7	OK, used mean
7085	79.4	81.9	80.65	OK, used mean
7086	72.1	79.1	75.6	OK, used mean
CPR2	85.1	84.8	84.95	OK, used mean
CPR3	–	–	–	Not included in analysis
CPR4	–	–	93.2	Negative slope, average used
CPR5	–	–	89.7	Negative slope, average used
CPR6	63.9	66.8	65.35	OK, used mean
CPR7	72.4	72.3	72.35	OK, used mean
CPR8	73.2	73.4	73.3	OK, used mean
JPCP2	88.5	88.4	88.45	OK, used mean
JPCP5	–	–	90.5	Negative slope, average used
JPCP6	97.2	96.3	96.75	OK, used mean
JPCP10	–	–	108.7	Negative slope, average used
JPCP14	99.6	101.4	100.5	OK, used mean
JPCP16	–	37.4	37.4	Negative linear estimate, exponential used
JPCP17	–	51.8	51.8	Negative linear estimate, exponential used

Table C-4. Summary of construction year initial AADTT and AADTT growth rate information for all the projects included in analysis.

Project ID	Construction Year 2-Way Initial AADTT	Number of Lanes in Design Direction	Percent of Trucks in Design Direction	Percent of Trucks in Design Lane	Operational Speed, mph	AADTT Growth Type	AADTT Growth Rate, percent
49_0803	15	1	100	100	60	Compound	12.0
49_0804	15	1	100	100	60	Compound	12.0
49_1001_1	164	1	100	100	60	None	0.0
49_1004_1	131	1	100	100	60	None	0.0
49_1004_2	135	1	100	100	60	None	0.0
49_1005_1	278	1	100	100	60	None	0.0
49_1006	203	1	100	100	60	Compound	3.8
49_1007_1	190	1	100	100	60	Compound	8.4
49_1008_1	352	1	100	100	60	Compound	2.1
49_1008_2	469	1	100	100	60	Compound	2.1
49_1017_1	158	1	100	100	60	None	0.0
49_3010	306	1	100	100	60	Linear	18.9
49_3011	368	1	100	100	60	Linear	16.2
49_3015_1	208	1	100	100	60	Compound	13.8
49_7082	298	1	100	100	60	Compound	11.0
49_7083_1	60	1	100	100	60	Compound	20.6
49_7085_1	204	1	100	100	60	Compound	11.8
49_7086	706	1	100	100	60	None	0.0

Table C-4. Summary of construction year initial AADTT and AADTT growth rate information for all the projects included in analysis, continued.

Project ID	Construction Year 2-Way Initial AADTT	Number of Lanes in Design Direction	Percent of Trucks in Design Direction	Percent of Trucks in Design Lane	Operational Speed, mph	AADTT Growth Type	AADTT Growth Rate, percent
CPR2	3850	2	49.5	65	75	Compound	5.00
CPR3	3931	2	51.8	80	75	Compound	5.80
CPR4	2757	2	49.6	60	35	Compound	0.70
CPR5	4728	2	50	70	65	Compound	3.90
CPR6	6944	2	47.5	90	75	Compound	1.60
CPR7	2434	3	50.1	80	65	Compound	3.80
CPR8	5267	2	49.5	65	75	Compound	5.40
JPCP10	2878	2	50.6	100	45	Compound	2.70
JPCP14	967	2	53.1	90	75	Compound	4.20
JPCP16	707	2	50.8	90	75	Compound	3.90
JPCP2	2479	4	50	90	75	Compound	1.00
JPCP5	17021	5	54.4	35	65	Compound	2.30
JPCP6	4475	5	54.4	35	65	Compound	2.30
OVLY1	4929	2	50.3	90	75	Compound	4.70
OVLY2	3257	2	53.7	90	75	Compound	4.40
OVLY3	1278	2	49.7	100	65	Compound	0.90
OVLY4	901	2	50	100	65	Compound	5.70
HMA R101	70	1	50	100	35	Compound	0.60
HMA R102	956	1	50	100	45	Compound	3.60
HMA R103	3132	1	50	100	45	Compound	1.30
HMA R201	1842	2	50	90	75	Compound	2.70
HMA R202	2615	1	50	100	45	Compound	5.78
HMA R203	2653	3	50	75	40	Compound	0.40
HMA R204	5135	4	45.9	90	55	Compound	2.80
HMA R301	36	1	50	100	65	Compound	9.80
HMA R302	206	1	49.6	100	65	Compound	17.90
HMA R303	25915	4	50.1	80	65	Compound	2.50
HMA R401	2508	2	50	100	65	Compound	3.00
HMA R402	1846	4	50	90	65	Compound	2.40
HMA R403	983	2	50.5	100	65	Compound	4.80
HMA R404N	885	2	50.4	75	65	Compound	3.60
HMA R404S	821	2	50.4	75	65	Compound	3.60

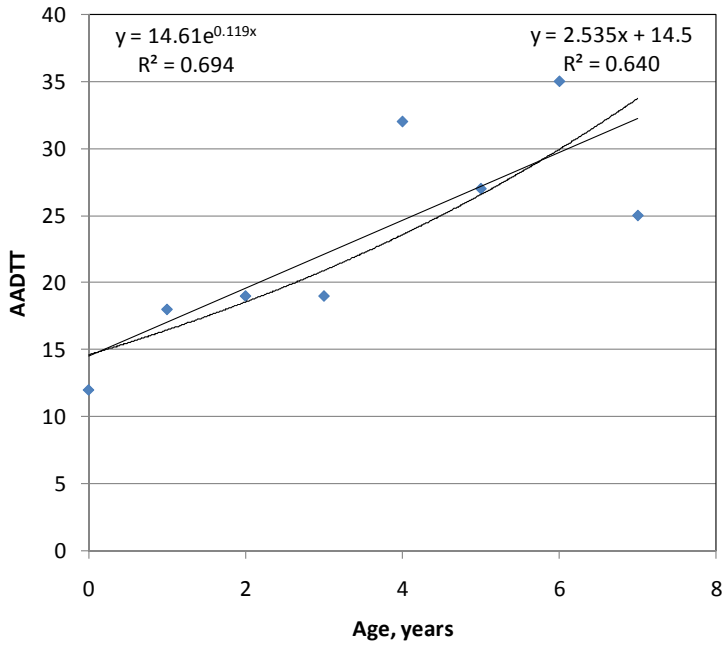

Figure C-2. Example computation of backcasting of initial AADTT and estimation of AADTT growth rate and type for projects 0803 & 0804 (initial AADTT = 15, AADTT growth type = compound, AADTT growth rate = 11.9 percent).

Climate

Pavement projects location described in terms of longitude, latitude, and elevation along with the depth of water table are the required MEPDG inputs for estimating climate related data. Using this information, the MEPDG identifies the five closest weather stations to the pavement project with climate data available. The weather stations with the most reliable data (selected by the project based on factors such as actual distance from the project site, number of months with data available, etc.) were then used to develop a project specific virtual weather station through interpolation. Climate data required for analysis was then derived from the project specific virtual weather station.

For this project, longitude, latitude, and elevation data was obtained directly from LTPP and UDOT pavement inventory databases. The depth of water table was not available in any of the LTPP or UDOT pavement databases. Very limited information available in the USDA-NRCS soil database was therefore reviewed in order to develop reasonable defaults for Utah as there were not enough projects with specific depth of water table information in the USDA-NRCS soil database. The typical reasonable depth of ground water table value adopted was 25-ft. Table C-5 provides a summary of project longitude, latitude, elevation, and depth of water table information used for analysis. Table C-6 presents detailed summary of weather stations locations from which data obtained from NCDC was processed by the MEPDG for use in analysis.

Table C-5. Summary of project longitude, latitude, elevation, and depth of water table information used for analysis.

Project Name	Latitude, degrees	Longitude, degrees	Elevation, ft	Depth to Water Table (Annual Average), ft
49_0803	40.6	-111.1	6485	25
49_0804	40.6	-111.1	6485	25
49_1001_1	37.3	-109.6	4384	25
49_1004_1	38.0	-112.4	6321	25
49_1004_2	38.0	-112.4	6321	25
49_1005_1	41.1	-111.9	4800	25
49_1006	39.2	-111.8	5132	25
49_1007_1	39.6	-110.9	5600	25
49_1008_1	39.0	-111.9	5200	25
49_1008_2	38.9	-111.9	5200	25
49_1017_1	38.6	-112.3	5600	25
49_3010	37.9	-112.8	5764	25
49_3011	40.5	-111.6	4221	25
49_3015_1	40.8	-111.9	4245	25
49_3015_2	40.8	-111.9	4245	25
49_7082	41.9	-112.2	4527	25
49_7083_1	38.8	-112.1	5113	25
49_7085_1	40.6	-111.4	5756	25
49_7085_2	40.6	-111.4	5756	25
49_7086	40.7	-112.0	4242	25
CPR1	40.7	-113.5	4168	25
CPR2	39.5	-112.0	5263	25
CPR3	38.8	-112.1	5264	25
CPR4	38.8	-112.1	5243	25
CPR5	41.7	-112.2	4288	25
CPR6	41.4	-112.0	4173	25
CPR7	40.8	-111.9	4163	25
CPR8	39.7	-111.8	5118	25
CPR9	38.6	-112.5	7044	25
HMA_OVLY_1	37.0	-113.6	2766	25
HMA_OVLY_2	38.7	-112.6	5639	25
HMA_OVLY_3	38.1	-109.3	6007	25
HMA_OVLY_4	38.8	-111.3	6433	25
HMA_R1 01	41.2	-111.9	6113.5	25
HMA_R1 02	42.0	-111.5	7170	25
HMA_R1 03	41.2	-112.0	4229	25
HMA_R1 04	41.3	-112.0	4222	25

Table C-5. Summary of project longitude, latitude, elevation, and depth of water table information used for analysis, continued.

Project Name	Latitude, degrees	Longitude, degrees	Elevation, ft	Depth to Water Table (Annual average), ft
HMA_R2 01	40.6	-111.3	6686	25
HMA_R2 02	40.6	-111.5	6739	25
HMA_R2 03	40.7	-111.9	4278	25
HMA_R2 04	40.7	-112.3	5856	25
HMA_R3 01	40.3	-112.1	4836	25
HMA_R3 02	40.4	-112.0	4957	25
HMA_R3 03	40.5	-111.9	4534	25
HMA_R3 04	39.4	-112.1	5073.5	25
HMA_R4 01	39.1	-111.8	5026	25
HMA_R4 02	39.3	-110.9	5633	25
HMA_R4 03	37.7	-113.2	5433	25
HMA_R4 04 (NB)	38.6	-109.6	4179	25
HMA_R4 04 (SB)	38.6	-109.6	4019	25
JPCP1	40.9	-111.9	4265	25
JPCP2	41.1	-111.5	5233	25
JPCP3	40.7	-112.2	4177	25
JPCP4	40.7	-112.5	4167	25
JPCP5	40.6	-111.9	4337	25
JPCP6	40.7	-112.0	4190	25
JPCP7	40.7	-112.2	4183	25
JPCP10	39.0	-111.9	5066	25
JPCP11	39.3	-112.1	5272	25
JPCP13	38.6	-112.3	5757	25
JPCP14	38.7	-112.2	5345	25
JPCP15	38.8	-112.1	5374	25
JPCP16	41.7	-112.2	4478	25
JPCP17	41.9	-112.2	4416	25

Table C-6. Summary of Utah climate stations locations used to obtain climate data for analysis.

Utah City Served	FAA Designation	Airport Name	Airport Use	Latitude, degrees	Longitude, degrees	Elevation, ft
Bryce Canyon	BCE	Bryce Canyon Airport	CS	37.70	-112.14	7590
Cedar City	CDC	Cedar City Regional Airport	CS	37.70	-113.09	5622
Logan	LGU	Logan-Cache Airport	GA	41.79	-111.85	4457
Milford	MLF	Milford Municipal Airport (Ben and Judy Briscoe Field)	GA	38.42	-113.01	5039
Moab	CNY	Canyonlands Field Airport	CS	38.75	-109.75	4557
Ogden	OGD	Ogden-Hinckley Airport	RL	41.19	-112.01	4473
Price	PUC	Carbon County Regional Airport (Buck Davis Field)	GA	39.61	-110.75	5957
Salt Lake City	SLC	Salt Lake City International Airport	PR	40.78	-111.97	4227
Vernal	VEL	Vernal Regional Airport (was Vernal-Uintah Co. Airport)	GA	40.44	-109.51	5278

1. PR: Commercial Service airport (Primary).
2. CS: Commercial Service airport (non-primary).
3. RL: Reliever airport.
4. GA: General Aviation airport.

Pavement Surface Properties

A surface shortwave absorptivity of 0.85 was assumed for both HMA and PCC surfaced pavements.

Pavement Structure/Layering

Pavement structure information (layer material types and thicknesses) was obtained from the LTPP materials database and UDOT project design and construction files. A summary of the raw pavement structural information is presented in Table C-7 for UDOT PMS projects and Table C-8 for LTPP projects.

Table C-7. Summary of raw pavement structural information for UDOT PMS projects.

Project Name	Layer No.	Layer Type	Material Type	Thickness, in
CPR2	1	JPCP	PCC	10
	2	Base	Lean concrete	4
	3	Subbase	Untreated base course	4
	4	Subgrade	A-6	Semi-infinite
CPR3	1	JPCP	PCC	10
	2	Base	Lean concrete	4
	3	Subbase	Untreated base course	4
	4	Subbase	Granular borrow	12
	5	Subgrade	A-6	Semi-infinite
CPR4	1	JPCP	PCC	8
	2	Base	Untreated base course	12
	3	Subgrade	A-6	Semi-infinite
CPR5	1	JPCP	PCC	9
	2	Base	Lean concrete	4
	3	Subbase	Untreated base course	4
	4	Subbase	Granular borrow	12
	5	Subgrade	A-6	Semi-infinite
CPR6	1	JPCP	PCC	9
	2	Base	Lean concrete	4
	3	Subbase	Untreated base course	4
	4	Subbase	Granular borrow	12
	5	Subgrade	A-7-6	Semi-infinite
CPR7	1	JPCP	PCC	9
	2	Base	Lean concrete	4
	3	Subbase	Untreated base course	4
	4	Subbase	Granular borrow	12
	5	Subgrade	A-1-b	Semi-infinite

Table C-7. Summary of raw pavement structural information for UDOT PMS projects, continued.

Project Name	Layer No.	Layer Type	Material Type	Thickness, in
CPR8	1	JPCP	PCC	10
	2	Base	Lean concrete	4
	3	Subbase	Untreated base course	4
	4	Subbase	Granular borrow	12
	5	Subgrade	A-2-4	Semi-infinite
JPCP10	1	JPCP	PCC	12
	2	Base	Untreated base course	6
	3	Subbase	Granular borrow	9
	4	Subgrade	A-6	Semi-infinite
JPCP14	1	JPCP	PCC	10
	2	Base	Lean concrete	4
	3	Subbase	Untreated base course	4
	4	Subbase	Granular borrow	12
	5	Subgrade	A-6	Semi-infinite
JPCP16	1	JPCP	PCC	9
	2	Base	Cement treated base	4
	3	Subbase	Untreated base course	4
	4	Subbase	Granular borrow	18
	5	Subgrade	A-6	Semi-infinite
JPCP2	1	JPCP	PCC	11
	2	Base	Cement treated base	4
	3	Subbase	Untreated base course	4
	4	Subbase	Asphalt treated base (Existing HMA)	4
	5	Subbase	Untreated base course	12
	6	Subgrade	A-4	Semi-infinite
JPCP5	1	JPCP	PCC	13
	2	Base	Untreated base course (permeable)	4
	3	Subbase	Granular borrow (less permeable)	6
	4	Subbase	Granular borrow	15
	5	Subbase	Borrow material	60
	6	Subgrade	A-6	Semi-infinite
JPCP6	1	JPCP	PCC	9
	2	Base	Asphalt concrete (separation layer)	2
	3	Subbase	Existing PCC (JPCP)	9
	4	Subbase	Lean concrete	4
	5	Subbase	Untreated base course	4
	6	Subgrade	A-7-6	Semi-infinite
HMA_R1 02	1	HMA	Asphalt concrete	5.5
	2	Base	Untreated base course	9.2
	3	Subbase	Granular borrow	12
	4	Subgrade	A-6	Semi-infinite

Table C-7. Summary of raw pavement structural information for UDOT PMS projects, continued.

Project Name	Layer No.	Layer Type	Material Type	Thickness, in
HMA_R1 03	1	HMA	Asphalt concrete	6.8
	2	Base	Untreated base course	6
	3	Subbase	Granular borrow	12
	4	Subbase	Fractured PCC	10
	5	Subgrade	A-4	Semi-infinite
HMA_R1 04	1	HMA	Asphalt concrete	7
	2	Base	Untreated base course	6
	3	Subbase	Granular borrow	12
	4	Subbase	Graded Cobble	12
	5	Subgrade	–	Semi-infinite
HMA_R2 01	1	HMA	Asphalt concrete	6
	2	Base	Untreated base course	8
	3	Subbase	Granular borrow	12
	4	Subgrade	A-2-4	Semi-infinite
HMA_R2 02	1	HMA	Asphalt concrete	6
	2	Base	Untreated base course	6
	3	Subbase	Granular borrow	12
	4	Subgrade	A-1-b	Semi-infinite
HMA_R2 03	1	HMA	Asphalt concrete	6
	2	Base	Untreated base course	6
	3	Subbase	Granular borrow	18
	4	Subgrade	A-2-4	Semi-infinite
HMA_R2 04	1	HMA	Asphalt concrete	6
	2	Base	Untreated base course	4
	3	Subbase	Granular borrow	12
	4	Subgrade	A-4	Semi-infinite
HMA_R3 01	1	HMA	Asphalt concrete	4.5
	2	Base	Untreated base course	6
	3	Subbase	Granular borrow	12
	4	Subgrade	A-4	Semi-infinite
HMA_R3 02	1	HMA	Asphalt concrete	5.5
	2	Base	Untreated base course	8
	3	Subbase	Granular borrow	12
	4	Subbase	Fractured PCC	9
	5	Subgrade	A-5	Semi-infinite
HMA_R3 03	1	HMA	Asphalt concrete	8
	2	Base	Untreated base course	5
	3	Subbase	Granular borrow	4
	4	Subbase	Fractured PCC	10
	5	Subgrade	A-4	Semi-infinite
HMA_R3 04	1	HMA	Asphalt concrete	9
	2	Base	Untreated base course	7.7
	3	Subgrade	–	Semi-infinite

Table C-7. Summary of raw pavement structural information for UDOT PMS projects, continued.

Project Name	Layer No.	Layer Type	Material Type	Thickness, in
HMA_R4 01	1	HMA	Asphalt concrete	7.5
	2	Base	Untreated base course	10
	3	Subbase	Granular borrow	15
	4	Subgrade	A-6	Semi-infinite
HMA_R4 02	1	HMA	Asphalt concrete	8
	2	Base	Untreated base course	6
	3	Subbase	Granular borrow	10
	4	Subgrade	A-6	Semi-infinite
HMA_R4 03	1	HMA	Asphalt concrete	6
	2	Base	Untreated base course	7
	3	Subbase	Granular borrow	12
	4	Subgrade	A-6	Semi-infinite
HMA_R4 04 (NB)	1	HMA	Asphalt concrete	7
	2	Base	Untreated base course	12
	3	Subbase	Granular borrow	12
	4	Subgrade	A-4	Semi-infinite
HMA_R4 04 (SB)	1	HMA	Asphalt concrete	5.5
	2	Base	Untreated base course	7
	3	Subbase	Granular borrow	12
	4	Subgrade	A-4	Semi-infinite
HMA_OVLY_1	1	HMA Ovly	Asphalt concrete	12
	2	Existing HMA	Cold in place recycled asphalt	4
	3	Subbase	Untreated base course	12
	4	Subgrade	A-2-4	Semi-infinite
HMA_OVLY_2	1	HMA Ovly	Asphalt concrete	4
	2	Existing HMA	Asphalt concrete	4
	3	Base	Untreated base course	12
	4	Subgrade	A-4	Semi-infinite
HMA_OVLY_3	1	HMA Ovly	Asphalt concrete	4
	2	Existing HMA	Asphalt concrete	7
	3	Base	Untreated base course	12
	4	Subgrade	A-4	Semi-infinite
HMA_OVLY_4	1	HMA Ovly	Asphalt concrete	4
	2	Existing HMA	Asphalt concrete	7
	3	Base	Untreated base course	12
	4	Subgrade	A-6	Semi-infinite

Table C-8. Summary of raw pavement structural information for LTPP projects.

Project Name	Layer No.	Layer Type	Material Type	Thickness, in
49_0803	4	Asphalt	Asphalt concrete	4.9
	3	Granular base	A-1-b	7.8
	2	Granular base	A-2-6	41.2
	1	Subgrade	A-6	Semi-infinite
49_0804	4	Asphalt	Asphalt concrete	7.1
	3	Granular base	A-1-b	12
	2	Granular base	A-2-6	41.2
	1	Subgrade	A-6	Semi-infinite
49_1001_1	3	Asphalt	Hot mixed, hot laid dense graded asphalt concrete	5.5
	2	Granular base	Soil-aggregate mixture (predominantly coarse-grained)	5.8
	1	Subgrade	Coarse-grained soil: silty sand	Semi-infinite
49_1004_1	4	Asphalt	Hot mixed, hot laid dense graded asphalt concrete	4.6
	3	Asphalt	Hot mixed, hot laid dense graded asphalt concrete	3.2
	2	Granular base	Crushed gravel	9.2
	1	Subgrade	Coarse-grained soil: silty sand with gravel	Semi-infinite
49_1004_2	5	Asphalt	Hot mixed, hot laid dense graded asphalt concrete	2
	4	Asphalt	Hot mixed, hot laid dense graded asphalt concrete	3.9
	3	Asphalt	Hot mixed, hot laid dense graded asphalt concrete	3.2
	2	Granular base	Crushed gravel	9.2
	1	Subgrade	Coarse-grained soil: silty sand with gravel	Semi-infinite
49_1005_1	6	Asphalt	Hot mixed, hot laid dense graded asphalt concrete	1.2
	5	Asphalt	Hot mixed, hot laid dense graded asphalt concrete	2.6
	4	Asphalt	Hot mixed, hot laid dense graded asphalt concrete	5.9
	3	Granular base	Crushed gravel	6.2
	2	Granular base	Soil-aggregate mixture (predominantly fine-grained)	7.8
	1	Subgrade	Coarse-grained soil: silty sand	Semi-infinite

Table C-8. Summary of raw pavement structural information for LTPP projects, continued.

Project Name	Layer No.	Layer Type	Material Type	Thickness, in
49_1006	5	Asphalt	Asphalt concrete	1.2
	4	Asphalt	Asphalt concrete	1.3
	3	Asphalt	Asphalt concrete	9.2
	2	Granular base	Soil-aggregate mixture (predominantly coarse-grained)	7.9
	1	Subgrade	Coarse-grained soil: clayey gravel with sand	Semi-infinite
49_1007_1	5	Asphalt	Hot mixed, hot laid dense graded asphalt concrete	1.0
	4	Asphalt	Hot mixed, hot laid dense graded asphalt concrete	1.0
	3	Asphalt	Hot mixed, hot laid dense graded asphalt concrete	9.4
	2	Granular base	Soil-aggregate mixture (predominantly coarse-grained)	3.2
	1	Subgrade	Coarse-grained soil: silty gravel with sand	Semi-infinite
49_1008_1	3	Asphalt	Asphalt concrete	9.1
	2	Granular base	Soil-aggregate mixture (predominantly coarse-grained)	4.7
	1	Subgrade	Fine-grained soils: sandy lean clay	Semi-infinite
49_1008_2	4	Asphalt	Hot mixed, hot laid dense graded asphalt concrete	1
	3	Asphalt	Asphalt concrete	9.1
	2	Granular base	Soil-aggregate mixture (predominantly coarse-grained)	4.7
	1	Subgrade	Fine-grained soils: sandy lean clay	Semi-infinite
49_1017_1	5	Asphalt	Hot mixed, hot laid dense graded asphalt concrete	1.1
	4	Asphalt	Hot mixed, hot laid dense graded asphalt concrete	3.9
	3	Granular base	Soil-aggregate mixture (predominantly coarse-grained)	5.6
	2	Granular base	Soil-aggregate mixture	6.8
	1	Subgrade	Clayey gravel with sand	Semi-infinite
49_3010	5	PCC	JPCP	9.4
	4	Chemically treated	Soil cement	4.8
	3	Granular base	A-1-b	5
	2	Granular base	A-2-6	9.2
	1	Subgrade	A-2-6	Semi-infinite

Table C-8. Summary of raw pavement structural information for LTPP projects, continued.

Project Name	Layer No.	Layer Type	Material Type	Thickness, in
49_3011	4	PCC	JPCP	10.2
	3	Chemically treated	Cement treated base	4
	2	Granular base	A-1-a	3.2
	1	Subgrade	A-4	Semi-infinite
49_3015_1	4	PCC	JPCP	11.2
	3	Chemically treated	Cement treated base	7.6
	2	Granular base	Crushed gravel	4.2
	1	Subgrade	Coarse-grained soil: silty sand with gravel	Semi-infinite
49_7082	5	PCC	JPCP	9.8
	4	Chemically treated	Cement treated base	4.2
	3	Granular base	A-1-a	4
	2	Granular base	A-1-a	18
	1	Subgrade	A-1-b	Semi-infinite
49_7083_1	5	PCC	JPCP	10.2
	4	Chemically treated	Cement treated base	4.4
	3	Granular base	Crushed gravel	4
	2	Granular base	Soil-aggregate mixture (predominantly coarse-grained)	10
	1	Subgrade	Clayey Gravel with Sand	Semi-infinite
49_7085_1	5	PCC	JPCP	9.7
	4	Chemically treated	Cement treated base	4.8
	3	Granular base	Crushed Gravel	4
	2	Granular base	Soil-aggregate mixture (predominantly coarse-grained)	18
	1	Subgrade	Coarse-grained soil: silty gravel with sand	Semi-infinite
49_7086	6	PCC	JPCP	10.1
	5	Chemically treated	Cement treated base	5.4
	4	Granular base	A-1-a	4
	3	Granular base	A-1-a	12
	2	Granular base	A-1-a	12
	1	Subgrade	A-6	Semi-infinite

It must be noted that it was not possible to model (1) very thick embankments separately or (2) granular materials sandwiched between non pervious HMA/asphalt treated or chemically treated materials using the MEPDG software due to (1) limitations in number of sublayers a thick unbound layer can be subdivided into and (2) limitations in modeling unbound material temperature and moisture profiles for sandwiched layers. Thus, for some situations as noted in Tables C-7 and C-8, the actual as constructed pavement structure was modified to make it possible to be analyzed by the MEPDG as follows:

- The sandwiched unbound granular material was replaced with a chemically stabilized material (e.g., soil cement) with the same resilient modulus as the original material. This modification does not affect pavement structure significantly as the new material will maintain a constant resilient modulus throughout the analysis period which would be the case of a granular material not subjected to moisture infiltration from groundwater or surface runoff.
- The embankment thickness was reduced to a minimum 12-in thick layer as the remaining embankment material merged with the subgrade.

Layer Material Properties

Key layer material properties were obtained from LTPP materials database and UDOT construction data files. Where data was not available in the UDOT project files, default values were assumed. A detailed description of all the key layer material properties required by the MEPDG used for analysis is presented in the following sections.

<u>HMA and Asphalt Treated Materials</u>

Key inputs for asphalt materials at hierarchal level 2 are (1) mix gradation, (2) binder type, (3) as-placed mix air void content, and (4) as-placed volumetric binder content. For both the LTPP and UDOT projects, information on mix gradation and binder type was mostly available for at least one asphalt layer. Where no data was available, typical defaults were developed using the data available for both LTPP and UDOT projects or defaults were obtained using as-designed specifications available in the UDOT Materials Specification manual. For all project types, there was no direct information available on as-placed mix air void content and as-placed volumetric binder content. Thus, typical UDOT and MEPDG national defaults were assumed or available laboratory mix values were used. A summary of this information for all the projects analyzed is placed in Table C-9.

Table C-9. Summary of MEPDG key HMA and asphalt treated materials inputs.

Project Name	Layer No	Layer Type	Cumulative Percent Retained			Pct Passing No. 200	Binder Grade	As-Placed Vol. Binder Content, percent	As-Placed Air Voids, percent
			3/4-in	3/8-in	No. 4				
49_0803	4	Asphalt	1	4	34	5.1	PG 58-34	11	8.5
49_0804	4	Asphalt	0	4	34	5.1	PG 58-34	11	8.5
49_1001_1	3	Asphalt	0	23	42	7.4	AC 10	11	8.5
49_1004_1	4	Asphalt	0	21	41	7	AC-10	11	8.5
49_1004_1	3	Asphalt	0	19	46	11	PEN 85-100	11	8.5
49_1004_2	5	Asphalt	0	12	48	8	AC-10	11	8.5
49_1004_2	4	Asphalt	0	21	41	7	AC-10	11	8.5
49_1004_2	3	Asphalt	0	19	46	11	PEN 85-100	11	8.5
49_1005_1	6	Asphalt	0	18	44	9	AC-20	11	8.5
49_1005_1	5	Asphalt	0	18	44	9	AC-20	11	8.5
49_1005_1	4	Asphalt	0	19	40	6	AC-12	11	8.5
49_1006	5	Asphalt	0	19	45	5.6	AC-20	11	8.5
49_1006	4	Asphalt	0	19	45	5.6	AC-10	11	8.5
49_1006	3	Asphalt	0	19	45	5.6	AC-10	11	8.5
49_1007_1	5	Asphalt	0	29	54	12	AC-20	11	8.5
49_1007_1	4	Asphalt	0	29	54	12	AC-20	11	8.5
49_1007_1	3	Asphalt	0	29	54	12	AC-10	11	8.5
49_1008_1	3	Asphalt	0	12	37.5	9.9	AC 10	11	8.5
49_1008_2	4	Asphalt	0	12	37.5	9.9	AC 10	11	8.5
49_1008_2	3	Asphalt	0	12	37.5	9.9	AC 10	11	8.5
49_1017_1	5	Asphalt	0	12	37.5	9.9	PEN 85-100	11	8.5
49_1017_1	4	Asphalt	0	12	37.5	9.9	PEN 85-100	11	8.5

Table C-9. Summary of MEPDG key HMA and asphalt treated materials inputs, continued.

Project Name	Layer No	Layer Type	Cumulative Percent Retained			Pct Passing No. 200	Binder Grade	As-Placed Vol. Binder Content, percent	As-Placed Air Voids, percent
			3/4-in	3/8-in	No. 4				
HMA_OVLY_1	1	HMA Overlay	0	28	50	6.4	AC 20	11	8.5
HMA_OVLY_1	2	Existing HMA	0	28	50	6.4	AC 20	11	8.5
HMA_OVLY_2	1	HMA Overlay	0	28	50	6.4	PG 64-34	11	8.5
HMA_OVLY_2	2	Existing HMA	0	28	50	6.4	PG 64	11	8.5
HMA_OVLY_3	1	HMA Overlay	0	28	50	6.4	PG 64	11	8.5
HMA_OVLY_3	2	Existing HMA	0	28	50	6.4	PG 64	11	8.5
HMA_OVLY_4	1	HMA Overlay	0	28	50	6.4	PG 64	11	8.5
HMA_OVLY_4	2	Existing HMA	0	28	50	6.4	PG 64	11	8.5

Table C-9. Summary of MEPDG key HMA and asphalt treated materials inputs, continued.

Project Name	Layer No	Layer Type	Cumulative Percent Retained			Pct Passing No. 200	Binder Grade	Lab Vol. Binder Content, percent	Lab Air Voids, percent
			3/4-in	3/8-in	No. 4				
HMA_R1 01	1	HMA	2	23	54	5.9	PG 64-34	9.5	3.9
HMA_R1 02	1	HMA	0	24.5	54.8	3.9	PG 64-34	10.68	3.92
HMA_R1 03	1	HMA	0	6	61	3.5	PG 64-34	9.54	3.86
HMA_R1 04	1	HMA	4.6	22.2	60.8	3.56	PG 64-34	9.56	6.24
HMA_R2 01	1	HMA	0	15	39	9	PG 64-34	9.5	4
HMA_R2 02	1	HMA	0	23.7	54.2	5.2	AC-20	10.7	4.7
HMA_R2 03	1	HMA	0	15	39	9	PG 64-28	10	5
HMA_R2 04	1	HMA	0	15	39	9	PG 64-28	9.7	3.8
HMA_R3 01	1	HMA	0	15	39	9	AC-10??	9.7	3.9
HMA_R3 02	1	HMA	0	15	39	9	AC-10	9.5	4
HMA_R3 03	1	HMA	0	25	49	5	PG 76-28	10.2	3.8
HMA_R3 04	1	HMA	4	44	67	4.1	PG 64-34	9.7	3.6
HMA_R4 01	1	HMA	0	32	60	5	PG 64-34	9.42	4.16
HMA_R4 02	1	HMA	4	24	52	4.7	PG 64-34	9.97	4.04
HMA_R4 03	1	HMA	0	21.7	57	5.2	PG 64-34	9.91	3.33
HMA_R4 04 (NB)	1	HMA	0	28	50	6.4	PG 64-34	10.25	3.36
HMA_R4 04 (SB)	1	HMA	0	28	50	6.4	PG 64-34	10.25	3.36

PCC Materials

The required MEPDG PCC properties include elastic modulus, E_{PCC}, flexural strength, MR, coefficient of thermal expansion (CTE), cementitious material content, and water-to-cement ratio among others. Appropriate values for Utah design conditions were established mostly using data from LTPP sites that were cored and tested. Very limited project specific data was obtained from UDOT material data files.

PCC strength and elastic modulus and other required information from the LTPP projects with data available at Levels 2 and 3 are summarized in Tables C-10 through C-13. The long term compressive strength, tensile strength, and modulus of elasticity as measured on the cores after they were cut from the pavements were converted to 28-day values using recommended MEPDG relationships. Also, compressive strength and tensile strength data was converted into MR as needed as MR data for these projects were not available in LTPP. Relationships used in the conversions described are as follows:

$$MR = 9.5\sqrt{f_c^{'}} \tag{C-1}$$

$$MR = \frac{f_t^{'}}{0.67} \tag{C-2}$$

where

MR	=	PCC flexural strength, psi
$f_c^{'}$	=	PCC compressive strength, psi
$f_t^{'}$	=	PCC tensile strength, psi

For the UDOT PMS projects, data was mostly not available and thus defaults computed using the LTPP data were developed and applied accordingly.

From the UDOT materials data files, flexural strength (third-point modulus of rupture) data from Region 2 were obtained. The results showed that for 186 tests run from 2004 through 2005 the average 28-day strength was 801 psi, with a standard deviation of 63 psi. The range was 650 to 970 psi. Lab tested CTE values from UDOT data files are presented in Table C-14.

Table C-10. Summary of Utah LTPP MEPDG key PCC materials inputs.

Project ID	Layer Type	PCC Unit Wt., pcf	PCC Poisson's Ratio	PCC Cement Type	PCC Cementitious Material Content, lb/yd³	Water-to-Cement Ratio	PCC Coarse Aggregate Type
49_3010	PCC	143.5	0.165	I	513	0.42	Basalt
49_3011	PCC	145	0.185	II	564	0.443	Quartzite
49_3015_1	PCC	152	0.11	II	585	0.39	
49_7082	PCC	142.5	0.21	II	612	0.39	Quartzite
49_7083_1	PCC	137.5	0.21	II	611	0.41	Diabase
49_7085_1	PCC	139.5	0.16	II	519	0.50	Quartzite
49_7086	PCC	139.5	0.185	II	611	0.381	Limestone

Table C-11. Summary of Utah PCC compressive and flexural strength and elastic modulus from LTPP sections.

Utah SHRP LTPP ID	Measured Comp. Strength, psi *	Measured Modulus Elasticity, psi *	Flexural Strength, psi *	Age of Concrete Years	Modulus Elasticity, psi (28-days)**	Flexural Strength, psi 28-days**	Comp. Strength, psi (28-days)**
3010	7,430	4,600,000	819	12.1	3,871,661	671	5,160
3010	7,000	4,450,000	795	12.1	3,745,412	651	4,861
3011		4,300,000		3.9	3,709,809		
3011		4,550,000		3.9	3,925,496		
3015		4,100,000		4.6	3,522,333		
3015		4,700,000		4.6	4,037,797		
7082	6,320	5,150,000	755	0.1	5,149,957	755	4,389
7082	8,310	5,400,000	866	0.1	5,399,955	866	5,771
7083	6,480	3,700,000	765	1.7	3,268,113	632	4,500
7083	6,860	4,100,000	787	1.7	3,621,422	650	4,764
7085	7,880	4,100,000	843		4,100,000	843	5,472
7085	7,110	3,650,000	801		3,650,000	801	4,938
7086	7,810	4,100,000	840	0.7	3,732,908	694	5,424
7086	7,180	3,950,000	805	0.7	3,596,339	665	4,986
Mean	7,238	4,346,429	808		3,952,229	723	5,027
Std Dev	629	504,009	35		601,071	87	437

* Measured at age of pavement when core was cut.
**Estimated from measured value.

Table C-12. Summary of Utah PCC CTE from LTPP sections.

UTAH SHRP LTPP ID	Measured CTE, per °C	Coarse Aggregate Type	Measured CTE, per °F
3010	8.60E-06		4.78E-06
3010	9.10E-06	Basalt	5.06E-06
3010	1.10E-05	Basalt	6.11E-06
3010	9.00E-06	Siliceous gravel	5.00E-06
3011	1.04E-05		5.78E-06
3011	1.03E-05		5.72E-06
3011	1.41E-05	Siliceous gravel	7.83E-06
3015	1.00E-05		5.56E-06
3015	1.04E-05		5.78E-06
3015	1.10E-05	Limestone	6.11E-06
7082	9.90E-06		5.50E-06
7082	1.00E-05	Limestone	5.56E-06
7083	9.00E-06		5.00E-06
7083	9.30E-06		5.17E-06
7083	8.60E-06	Diabase	4.78E-06
7083	1.11E-05	Siliceous gravel	6.17E-06
7085	1.40E-05		7.78E-06
7085	1.14E-05	Dolomite	6.33E-06
7085	1.18E-05	Sandstone	6.56E-06
7085	1.23E-05	Sandstone	6.83E-06
7085	9.20E-06	Quartzite	5.11E-06
7086	1.04E-05		5.78E-06
7086	1.27E-05	Limestone	7.06E-06
Mean			5.88E-06

Table C-13. Summary of Utah PCC tensile strength from LTPP sections.

SHRP_ID	Age, years	Long-Term Tensile Strength, psi	28-day Tensile Strength, psi	28-day Flexural Strength, psi (Computed from Tensile Str.)
3010	11.4	599	505	753
3010	11.4	501	422	630
3011	3.7	641	554	826
3011	3.7	708	611	913
3015	4.5	609	524	781
3015	4.5	640	550	821
7082	0.1	744	738	1101
7082	0.1	640	635	947
7083	1.6	471	416	621
7083	1.6	500	442	659
7085	0.1	634	634	946
7085	0.1	660	660	985
7086	0.7	440	401	598
7086	0.7	676	615	919

Table C-14. Summary of CTE values for UDOT PMS projects.

Project Location	Core No.	Test No.	PCC Expansion CTE, 10^{-6}/deg C	PCC Contraction CTE, 10^{-6}/deg C	Mean PCC CTE, 10^{-6}/deg C	Mean PCC CTE, 10^{-6}/deg F	Mean PCC CTE, 10^{-6}/deg F
Richfield Main St	Core 1	1	-10.7	10.8	10.8	6.0	5.8
	Core 1	2	-10.5	10.6	10.6	5.9	
	Core 1	3	-10.3	10.4	10.4	5.8	
	Core 2	1	-10.4	10.6	10.5	5.8	
	Core 2	2	-10.0	10.3	10.2	5.7	
	Core 2	3	-10.1	10.3	10.2	5.7	
I-70	Core 1	1	-9.5	9.7	9.6	5.3	5.3
	Core 1	2	-9.4	9.6	9.5	5.3	
	Core 1	3	-9.3	9.5	9.4	5.2	
	Core 1	4	-9.3	9.5	9.4	5.2	
	Core 2	1	-9.5	9.6	9.6	5.3	
	Core 2	2	-9.5	9.7	9.6	5.3	
	Core 2	3	-9.2	9.4	9.3	5.2	
	Core 2	4	-9.1	9.3	9.2	5.1	

Chemically Treated Materials

The commonly applied chemically treated material used in Utah was LCB. The key input for this material type was elastic modulus. For the LTPP database, long term compressive strength of LCB materials was available for most projects. The compressive strength values were used to estimate elastic modulus as recommended in the MEPDG Manual of Practice using equation C-3.

$$E = 57000\sqrt{f_c^{'}} \qquad \text{(C-3)}$$

where

E	=	elastic modulus, psi
$f_c^{'}$	=	LCB compressive strength, psi

For the UDOT projects compressive strength or elastic modulus information was not available. Thus, typical values obtained from the LTPP projects were applied. A summary of LCB compressive strength and elastic modulus values for the LTPP projects (with LCB compressive strength and elastic modulus data available) is presented in Table C-15.

Table C-15. Summary of Utah elastic modulus for chemically treated materials from LTPP sections.

UTAH SHRP LTPP ID	Measured Comp. Strength, psi	Modulus Elasticity, psi (Computed from Comp Str.)
7082	2400	2,792,418
7082	2500	2,850,000
7083	3300	3,274,401
7083	3060	3,153,084
7085	1420	2,147,925
7085	1630	2,301,276
7086	2910	3,074,832
7086	3040	3,142,763
Mean		2,842,087
Std Dev		414,911

Granular Materials and Subgrade Soils

Key MEPDG inputs for unbound granular and subgrade soils materials at hierarchal level 2 are (1) gradation, (2) Atterberg limits, and (3) resilient modulus at optimum moisture content. Descriptions of these key inputs are presented as follows:

- Granular base/subbase course materials (gradation, Atterberg limits, and resilient modulus).
    - For LTPP projects both gradation and Atterberg limits information was available as LTPP sampled most of these pavements and conducted laboratory tests to characterize the material properties such as plasticity index, liquid limit, and gradation. Although LTPP conducted extensive amounts of resilient modulus testing, there were no lab tests conducted to obtain the resilient modulus of the unbound base at optimum moisture. Thus, for the LTPP projects, MEPDG default resilient modulus values determined based on the material's AASHTO soil classification were adopted (see Table C-16).
    - For UDOT projects, only the material description (e.g., UTBC, granular borrow) was available. Thus, default as-designed recommendations of gradation and Atterberg limits available in the UDOT 2008 Standard Specification for Road and Bridge Construction were adopted (see Tables C-17 and C-18). UDOT specifies the following from granular borrow materials used as subbases and embankments:
        - Borrow (embankment): material meeting classifications A-1-a through A-4 as per AASHTO M 145.
        - Granular borrow (subbase): material meeting classification A-1-a. Additionally, material must be non-plastic, well-graded, with a 3-inch maximum aggregate size.

      Thus, for both thick embankments and subbases, AASHTO classification A-1-a was assumed. Again, MEPDG default resilient modulus values determined based on the material's AASHTO soil classification were adopted (see Table C-16).

Table C-16. Typical resilient modulus values for unbound granular and subgrade materials (modulus at optimum moisture content) (AASHTO 2008).

Material Classification	M_r Range	Typical M_r
A-1-a	38,500 – 42,000	40,000
A-1-b	35,500 – 40,000	38,000
A-2-4	28,000 – 37,500	32,000
A-2-5	24,000 – 33,000	28,000
A-2-6	21,500 – 31,000	26,000
A-2-7	21,500 – 28,000	24,000
A-3	24,500 – 35,500	29,000
A-4	21,500 – 29,000	24,000
A-5	17,000 – 25,500	20,000
A-6	13,500 – 24,000	17,000
A-7-5	8,000 – 17,500	12,000
A-7-6	5,000 – 13,500	8,000

Table C-17. Aggregate properties requirements for UDOT UTBC (UDOT 2008 Standard Specifications for Road and Bridge Construction).

Aggregate Properties				
	Aggregate Class			
	A	B	C	
Dry Rodded Unit Weight	Not less than 75 lb/ft^3			AASHTO T 19
Liquid Limit/Plastic Index	Non-plastic		PI $\leq$ 6	AASHTO T 89 AASHTO T 90
Aggregate Wear	Not to exceed 50 percent			AASHTO T 96
Gradation	Table C-18			AASHTO T 11 AASHTO T 27
CBR with a 10 lb surcharge measured at 0.2 inch penetration	70 percent minimum		N/A	AASHTO T 193
Two Fractured Faces	50 percent min.	N/A	N/A	AASHTO TP 61

Table C-18. UDOT UTBC gradation requirements (UDOT 2008 Standard Specifications for Road and Bridge Construction).

Gradation Limits		
Sieve Size	**Job Mix Gradation Target Band**	**Job Mix Gradation Tolerance**
1½ inch	100	
1 inch	90 - 100	±9.0
¾ inch	70 - 85	±9.0
½ inch	65 - 80	±9.0
⅜ inch	55 - 75	±9.0
No. 4	40 - 65	±7.0
No. 16	25 - 40	±5.0
No. 200	7 - 11	±3.0

- Subgrade soils (gradation and Atterberg limits).
    - For LTPP projects both gradation and Atterberg limits information was available as LTPP sampled most of these pavements and conducted laboratory tests to characterize the material properties such as plasticity index, liquid limit, and gradation.
    - For UDOT projects, subgrade information was not available in the UDOT pavement database. Thus, information available in county soil reports available through the USDA-NRCS soil database were utilized. Using project location information, the predominant soil types within the project location were determined. The engineering properties of all significant soil types (AASHTO soil class, gradation, Atterberg limits, etc.) were then obtained from the USDA-NRCS database. The most predominant AASHTO soil type was selected to represent the entire project. Default MEPDG gradation and Atterberg limits for the predominant AASHTO soil type was also utilized. An example of data obtained from the USDA-NRCS database and how it was utilized is presented in Appendix E.
- Subgrade soils (resilient modulus).
    - The MEPDG was calibrated in 2007 using subgrade resilient modulus inputs that were determined as follows:
        - Rigid Pavement: the subgrade k value was backcalculated from FWD deflections on top of the slab. The standard plate on springs model was used to obtain a dynamic k value for all available months. These dynamic k values were compared to the MEPDG output k-values for given months. The input Mr subgrade resilient modulus was adjusted until the FWD backcalculated k-value matched that k-value in the MEPDG output. This approach ensured that the Mr and k-value used to compute stresses and deflections were reasonable and generally matched the field. The adjusted input Mr values (lab values) were compiled into the

various AASHTO Classifications and the mean values published into a table of recommendations shown in Table C-19.

- Flexible Pavement: the subgrade elastic modulus was backcalculated from FWD deflections. The elastic modulus for each section was then adjusted to "reflect laboratory results at optimum conditions." The adjusted input Mr values (lab values) were compiled into the various AASHTO Classifications and the mean values published into a table of recommendations shown in Table C-20. The backcalculated elastic modulus, which would be at in situ moisture content, likely more than optimum, was adjusted upward to optimum moisture condition. The backcalculated elastic modulus was adjusted from a "field" elastic half space to a "lab" value using the following multipliers (as was used in the national calibration in 2007):
    - Fine grained soils: 0.55.
    - Coarse grained soils: 0.67.

Table C-19. Recommended resilient modulus input (at optimum density and moisture) for subgrades under rigid pavements and rehabilitation of rigid pavements (Darter et al. 2007).

Subgrade AASHTO Soil Class	Optimum Dry Density (mean, std. dev.)*	Optimum Moisture Content (mean)* %	Design Guide Input Resilient Modulus at Optimum Density/Moist. (mean, std. dev.)**	Design Guide Back-calculated Output Dynamic k-value (mean, std. dev.)**	Recommended Input Subgrade Resilient Modulus (Opt. Density/Moisture Content)
A-1-a	128 pcf, 17 pcf	11	13,228 psi, 3,083 psi	322 psi/in, 68 psi/in	18,000 psi
A-1-b	122, 9	11	14,760, 8,817	335, 92	18,000
A-3	NA	NA	NA	NA	16,500
A-2-4	119, 7	11	14,002, 5,730	256, 79	16,000
A-2-5	NA	NA	NA	NA	16,000
A-2-6	120, 6	12	16,610, 6,620	289, 51	16,000
A-2-7	NA	NA	NA	NA	16,000
A-4	119, 7	12	17,763, 8,889	270, 88	15,000
A-5	NA	NA	NA	NA	8,000
A-6	114, 5	14	14,109, 5,935	211, 54	14,000
A-7-5	103, 19	19	7,984, 3,132	148, 32	10,000
A-7-6	102, 8	20	13,218, 322	203, 53	13,000

*Information provided in these columns was obtained from the LTPP database (optimum density and moisture).
**Information was obtained from Design Guide back-calculation and from use of the Design Guide (input subgrade resilient modulus, Mr, at optimum density and moisture).

Table C-20. Recommended resilient modulus input (at optimum density and moisture) for subgrades under flexible pavements and rehabilitation of flexible pavements (Darter et al. 2007).

AASHTO Soil Classification	Mean Modulus (psi)*	Standard Deviation (psi)	Corrected Mean Modulus (psi)	Standard Deviation (psi)	Recommended Resilient Modulus at Optimum (psi)**
A-1-a	44,471	22,970	29,650	15,315	29,500
A-1-b	39,965	19,428	26,646	12,953	26,500
A-3	37,041	17,853	24,697	11,903	24,500
A-2-4	32,013	19,807	21,344	13,206	21,500
A-2-5	--	--	--	--	21,000
A-2-6	30,832	18,443	20,556	12,297	20,500
A-2-7	24,373	6,897	16,250	4,598	16,500
A-4	29,797	18,442	16,429	12,296	16,500
A-5	--	--	--	--	15,500
A-6	26,313	13,657	14,508	9,106	14,500
A-7-5	23,586	19,595	13,004	13,065	13,000
A-7-6	21,159	11,801	11,666	7,868	11,500

* Results are based on 594 back-calculated values extracted from the MON_FLX_BACKCAL_SECT table found in the Long-Term Pavement Performance (LTPP) database.
** Information obtained after correcting the NDT values to reflect laboratory results at optimum conditions.

The input for subgrade resilient modulus for each section in Utah was determined as follows:

- Rigid Pavement:
  - The AASHTO Soil Class was determined from county soil maps (USDA-NRCS soil database). This provided gradations and Atterberg limits.
  - The subgrade k value was backcalculated from FWD deflections on top of the slab.
  - The standard plate on springs model was used to obtain a dynamic k value for all available months.
  - The MEPDG program was run with default input Mr for the subgrade based on AASHTO Classification.
  - The MEPDG output k-values for given months were compared to the backcalculated k-values. The input Mr subgrade resilient modulus was adjusted until the FWD backcalculated k-value matched that k-value in the MEPDG output.
  - This approach is exactly what was done in the original 2007 MEPDG work under NCHRP 1-40D. It ensures that the Mr and k-value used to compute stresses and deflections were reasonable and generally matched the field.

- Flexible Pavement:
    - The subgrade elastic modulus was backcalculated from FWD deflections using the AASHTO 93 simple model.
    - The elastic modulus for each section was then adjusted to "reflect laboratory results at optimum conditions."
        - The backcalculated elastic modulus was adjusted from a "field" elastic half space to a "lab" value through a multiplier of 0.55 (for fine grained soils) and 0.67 (for coarse grained soils) to produce a laboratory adjusted Mr.
        - The MEPDG program was run with default input Mr for the subgrade based on AASHTO Classification.
        - The MEPDG output Mr for the subgrade was then compared to the lab adjusted Mr. If the two do not match, the MEPDG input Mr is adjusted until they match. This provides for an adjustment in Mr from in situ moisture content to optimum moisture content.
        - This approach is similar to the original 2007 MEPDG calibration under NCHPR 1-40D and should result in an array of input Mr for various Utah soils that can be used as defaults.
        - It also provides for a procedure to use for overlay design using the FWD to obtain the subgrade Mr input.

A summary of long-term, in situ field tested and MEPDG computed flexible subgrade resilient moduli and JPCP subgrade k-values are presented in Tables C-21 and C-22, respectively.

Table C-21. Field tested flexible pavement in-situ subgrade resilient modulus.

Data Source	Project ID	Route	Direction of Traffic	Soil Type	Backcalculated In-Situ Elastic Modulus, psi	Estimate of Lab Mr at Optimum Moisture, psi
LTPP	49_0803	SR-35	East	A-2-6	24,809	16,622
LTPP	49_0804	SR-35	East	A-2-4	30,024	20,116
LTPP	49_1001	US-191	North	A-2-4	11,364	7,614
LTPP	49_1004	US-89	North	A-1-b	21,306	14,275
LTPP	49_1005	US-89	South	A-2-4	24,994	16,746
LTPP	49_1006	SR-28	North	A-2-4	33,745	22,609
LTPP	49_1007	US-6	West	A-4	25,721	14,147
LTPP	49_1008	US-89	North	A-4	20,270	11,148
LTPP	49_1017	US-89	North	A-1-b	13,800	9,246
Utah	HMA_OVLY_1	I-15	North	A-2-4	74,452	49,883
Utah	HMA_OVLY_2	I-15	North	A-4	45,173	24,845
Utah	HMA_OVLY_3	US-191	–	A-4	37,997	20,898
Utah	HMA_OVLY_4	SR-10	North	A-6	15,827	8,705
Utah	HMA_R1 01	SR-226	–	A-7-5	25,945	14,270
Utah	HMA_R1 02	US-89	North	A-6	26,827	14,755
Utah	HMA_R1 03	SR-104	North	A-4	21,470	11,808
Utah	HMA_R1 04	I-15	North	A-6	27,694	15,232
Utah	HMA_R2 01	SR-248	North	A-2-4	23,876	15,997
Utah	HMA_R2 02	SR-224	North	A-1-b	27,506	18,429
Utah	HMA_R2 03	SR-71	North	A-2-4	19,564	13,108
Utah	HMA_R2 04	SR-36	North	A-4	21,782	11,980
Utah	HMA_R3 01	SR-73	North	A-4	21,245	11,685
Utah	HMA_R3 02	SR-73	North	A-5	18,139	9,977
Utah	HMA_R3 03	I-15	North	A-4	25,803	14,192
Utah	HMA_R3 04	I-15	North	A-4	36,827	20,255
Utah	HMA_R4 01	US-89	North	A-6	16,248	8,937
Utah	HMA_R4 02	SR-10	North	A-6	19,352	10,643
Utah	HMA_R4 03	SR-56	North	A-6	14,527	7,990
Utah	HMA_R4 04 (NB)	US-191	North	A-4	14,430	7,937
Utah	HMA_R4 04 (SB)	US-191	South	A-4	36,606	20,133

Table C-22. Field tested rigid pavement in-situ modulus of subgrade reaction (k-value).

Project ID	Backcalculated Modulus of Subgrade Reaction (k-value), psi/in
CPR2	569
CPR3	624
CPR4	591
CPR5	538
CPR6	501
CPR7	308*
CPR8	800
JPCP10	343
JPCP14	495
JPCP16	501
JPCP2	538
JPCP5	691
JPCP6	112*
LTPP3010	286
LTPP3011	211
LTPP3015	340
LTPP7082	372
LTPP7083	279
LTPP7085	343
LTPP7086	116

*Computed using default subgrade resilient modulus and MEPDG E to k models.

JPCP Design Data

The MEPDG requires both HMA and JPCP design features. For new HMA pavements, the relevant design feature is whether to consider an HMA endurance limit in fatigue analysis (applicable to the design of perpetual pavements). This was not considered in analysis, as the pavements being analyzed were not designed as perpetual pavements. For JPCP, the following design features are required:

- The temperature gradient during PCC placement and curing.
- PCC slab transverse joint spacing.
- Transverse joint sealant type.
- Slab width.
- Load transfer mechanism and properties.
- Slab edge support type.
- Base type and base erosion factor.
- PCC-base interface friction type and age at which friction is lost.

Details are presented in Tables C-23 and C-24 for LTPP and UDOT PMS projects, respectively.

Table C-23. Summary of design features for LTPP JPCP projects.

Project ID	Random Joint Spacing, ft	Random Joint?	Joint Skew, ft	Transverse Joint Dowel Bar Diameter, in	Tied PCC Shoulder?	Slab Width, ft
49_3010	12,13,17,18	Yes	2	0	Yes	12
49_3011	18,13,12,17	Yes	2	0	Yes	12
49_3015_1	10,11,14,15	Yes	2	0	Yes	12
49_7082	10,11,14,15	Yes	2	0	Yes	12
49_7083_1	10,11,14,15	Yes	2	0	Yes	12
49_7085_1	10,11,14,15	Yes	2	0	No	12
49_7086	10,11,14,15	Yes	2.2	0	No	12

- For skewed joints, the skew length was added to the joint spacing.
- For random joints, transverse cracking was analyzed for the mean of the long and short panels separately. Mean predicted percent slabs cracked was then used in analysis. For transverse joint faulting and IRI, the mean joint spacing was used directly for analysis.

Table C-24. Summary of design features for UDOT PMS JPCP projects.

Project ID	Random Joint?	Random Joint Spacing, ft				Dowel Diameter, in	Slab width, ft	Tied Shoulder	Joint Skew
		Joint Spacing #1	Joint Spacing #2	Joint Spacing #3	Joint Spacing #4				
CPR2	Yes	13	12	17	18	0	12	Yes	6:1
CPR3	Yes	10	11	15	15	0	12	Yes	6:1
CPR4	No	14				0	12	Yes	0
CPR5	Yes	13	12	17	18	0	12	No	6:1
CPR6	Yes	13	12	18	17	0	12	Yes	6:1
CPR7	Yes	12	13	19	17	1.5	12	Yes	6:1
CPR8	Yes	13'	12"	17'	18'	0	12	Yes	6:1
JPCP10	No	15				1.5	12	Yes	No
JPCP14	Yes	10	10	14	16	0	12	Yes	6:1
JPCP16	Yes	10	11	14	15	0	12	Yes	6:1
JPCP17	Yes	16	13	11	10	0	12	Yes	6:1
JPCP2	No	15				1.25	12	Yes	6:1
JPCP5	No	15				1.5	12	Yes	No
JPCP6	No	15				1.0	12	Yes	No

APPENDIX D. SUMMARY OF TRAFFIC DATA

Traffic data for MEPDG models validation and local calibration was obtained from the LTPP database (for LTPP projects) and UDOT (for UDOT PMS projects). Detailed listing of all traffic inputs required by the MEPDG along with data obtained for LTPP and UDOT is presented in Table D-1. Examples plots of traffic volume data provided by LTPP and used for determining initial AADTT and AADTT growth type and rate are presented in Figures D-1 through D-15. All of the traffic data provided could not be presented in this Appendix because of the size and extent of the data. MEPDG traffic data can be obtained from UDOT.

Table D-1. MEPDG input and Utah current practice.

MEPDG Input	Data Availability		
	LTPP Specific	UDOT Specific	MEPDG Default Applied?
Traffic open date	Yes	Yes	No
Number of lanes	Yes	Yes	–
Mean wheel load location and lateral traffic wander	No	No	Yes
Axle configuration	No	No	Yes
Wheelbase	No	No	Yes
Operational speed	No	Yes	Yes for LTPP projects
AADTT	Yes	Yes	No
AADTT growth type and rate	Yes	Yes	No
Direction distribution factor	Yes	Yes	No
Lane distribution factor	Yes	Yes	No
Monthly adjustment factors	No	Yes	Yes
Hourly distribution	No	Yes	Yes
Vehicle class distribution	Yes	Yes	No
Axle load distribution factors	Yes	Yes	No
Number of axles per truck	Yes	Yes	No

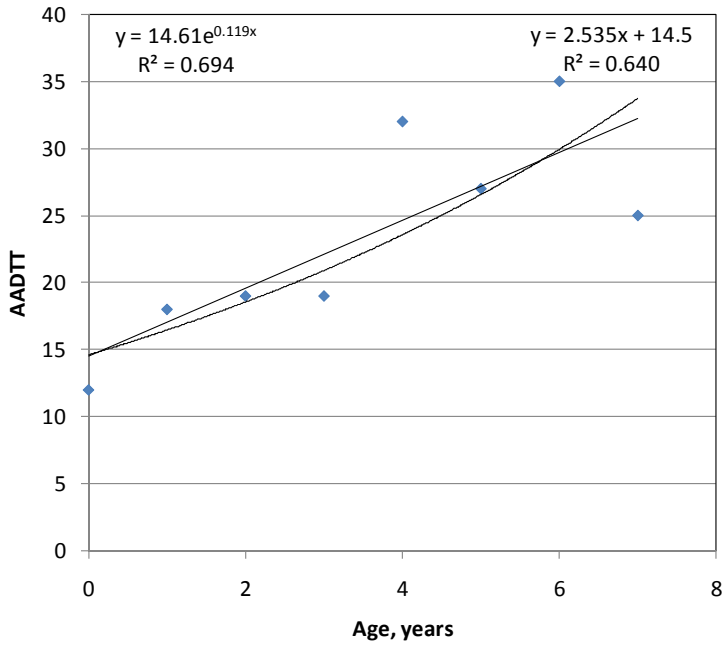

Figure D-1. Plot showing AADTT versus age for project LTPP 0800.

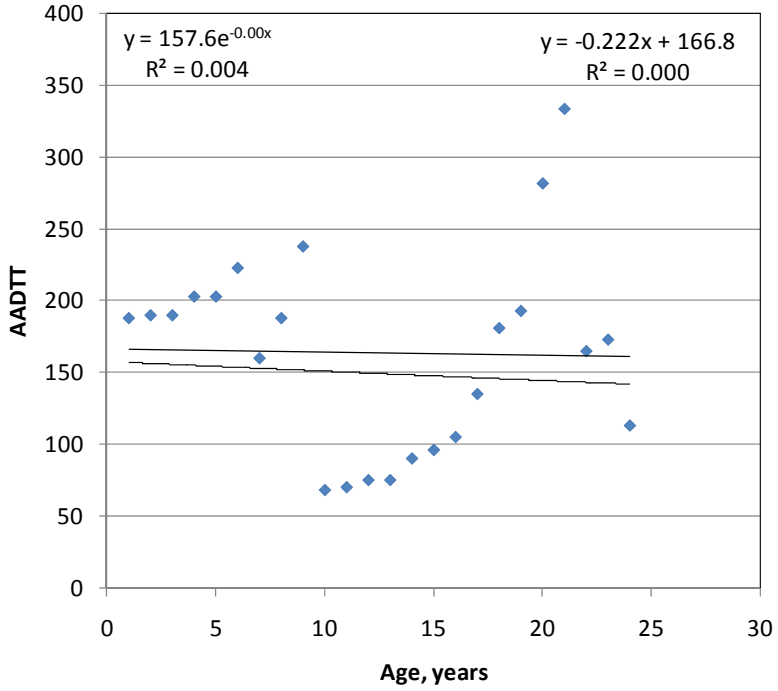

Figure D-2. Plot showing AADTT versus age for project LTPP 1001.

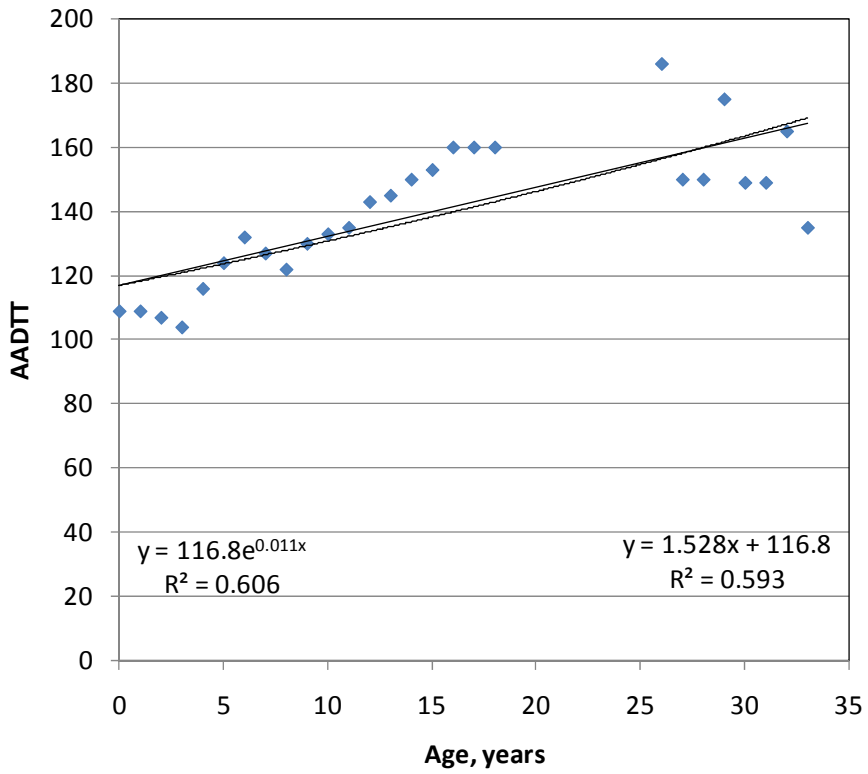

Figure D-3. Plot showing AADTT versus age for project LTPP 1004.

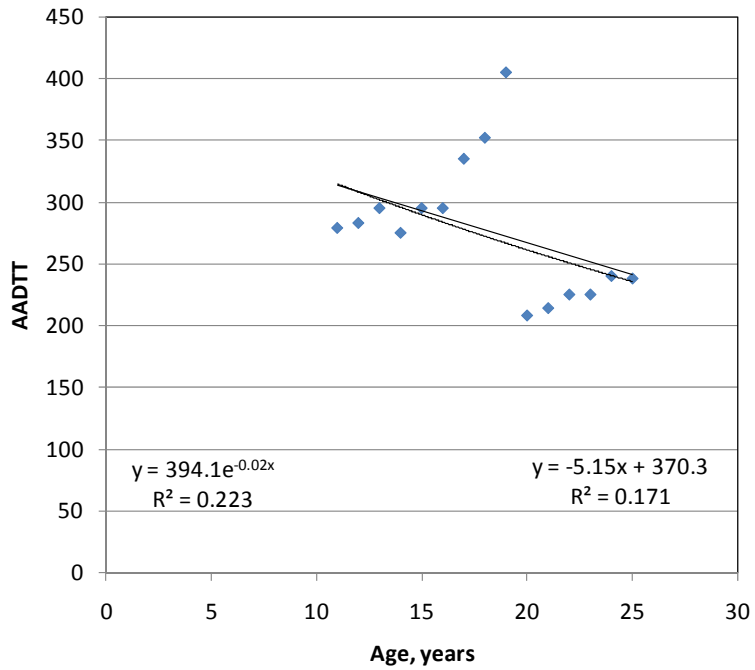

Figure D-4. Plot showing AADTT versus age for project LTPP 1005.

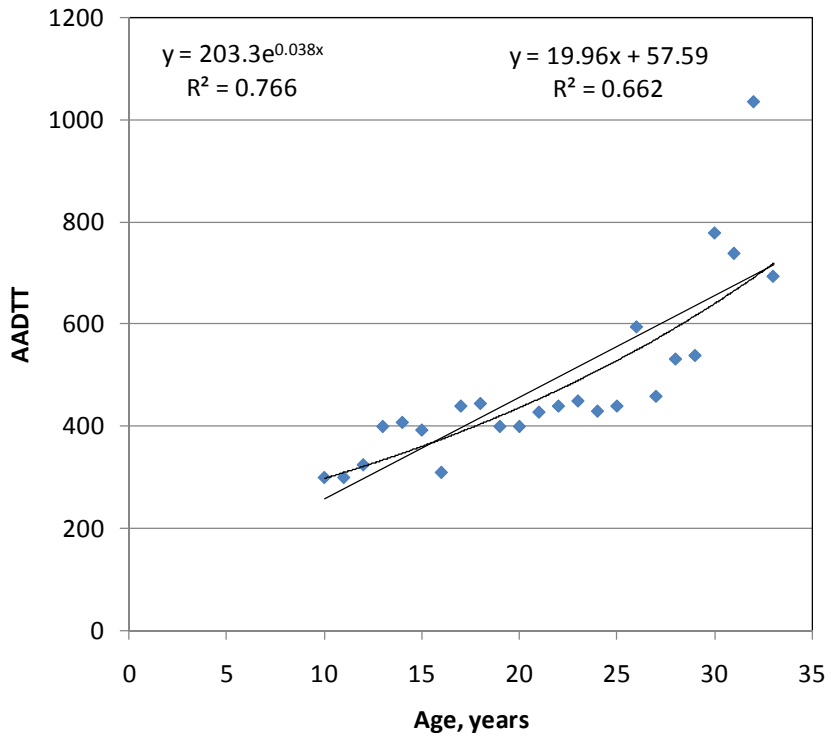

Figure D-5. Plot showing AADTT versus age for project LTPP 1006.

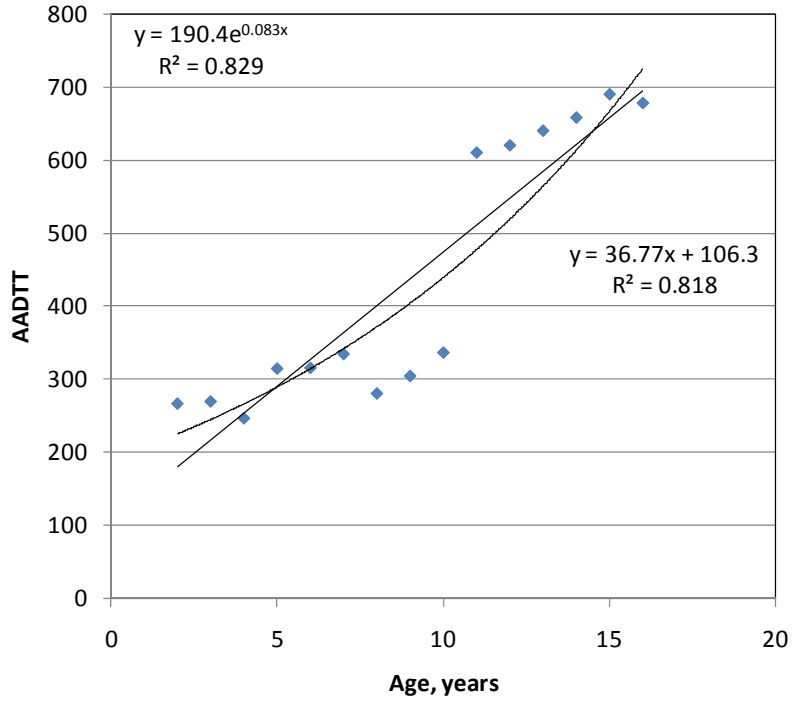

Figure D-6. Plot showing AADTT versus age for project LTPP 1007.

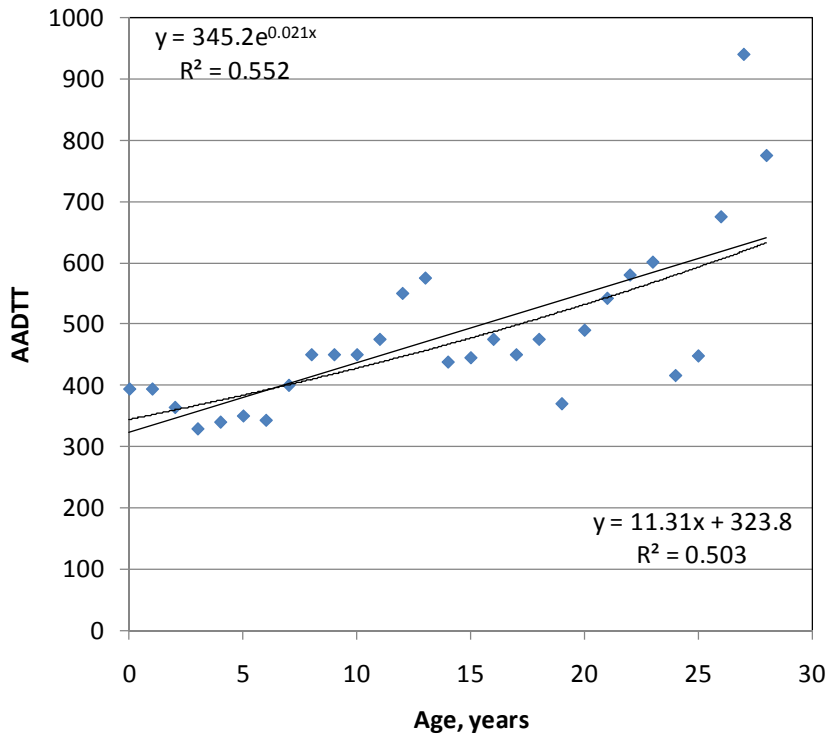

Figure D-7. Plot showing AADTT versus age for project LTPP 1008.

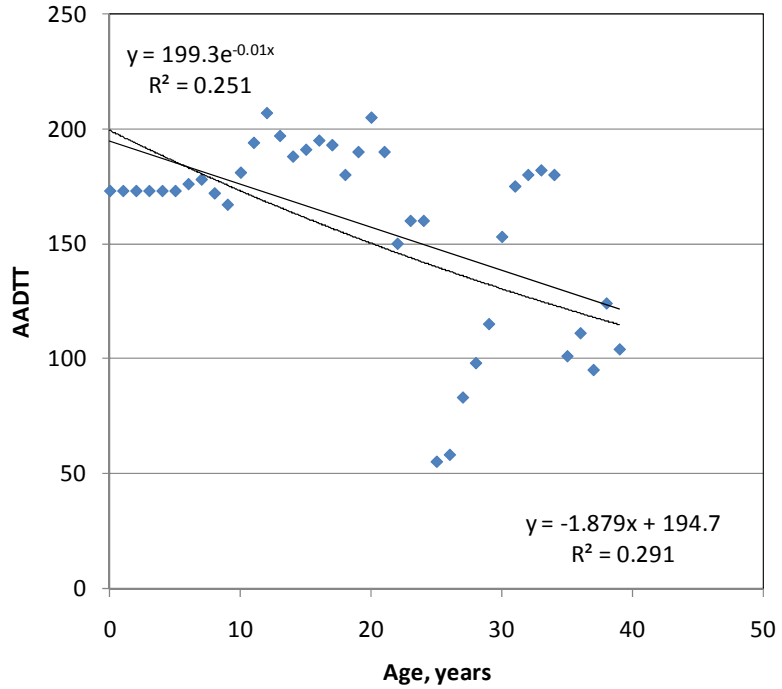

Figure D-8. Plot showing AADTT versus age for project LTPP 1017.

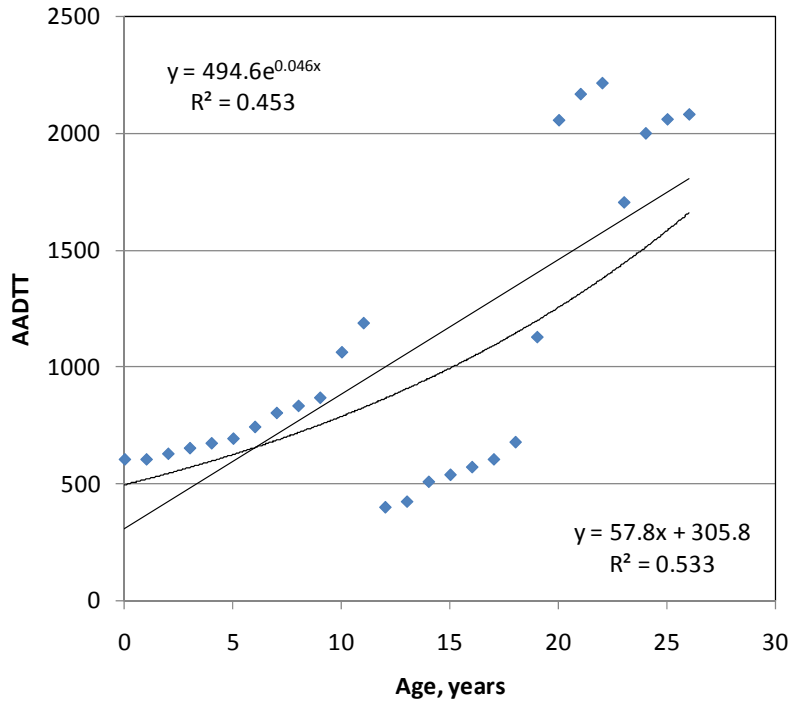

Figure D-9. Plot showing AADTT versus age for project LTPP 3010.

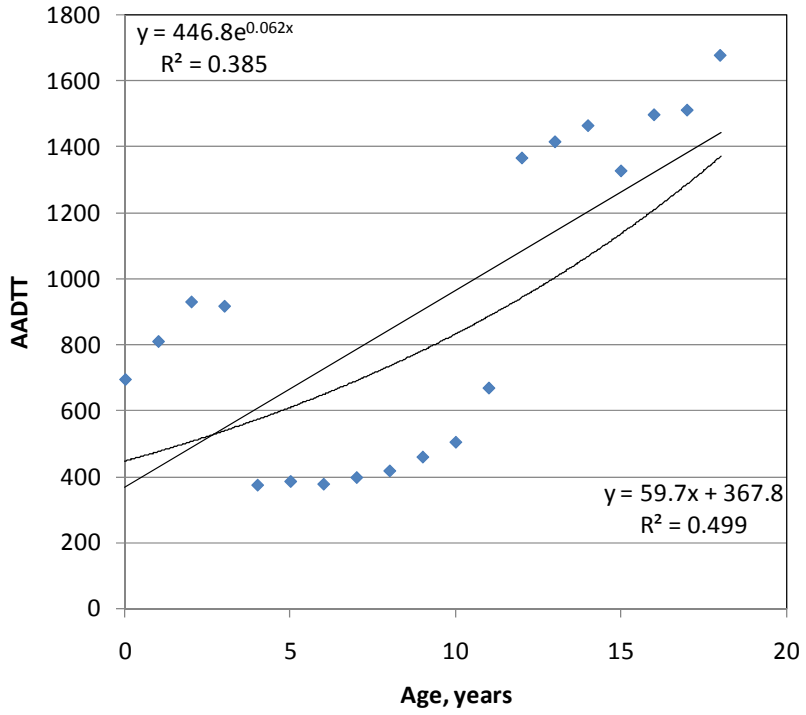

Figure D-10. Plot showing AADTT versus age for project LTPP 3011.

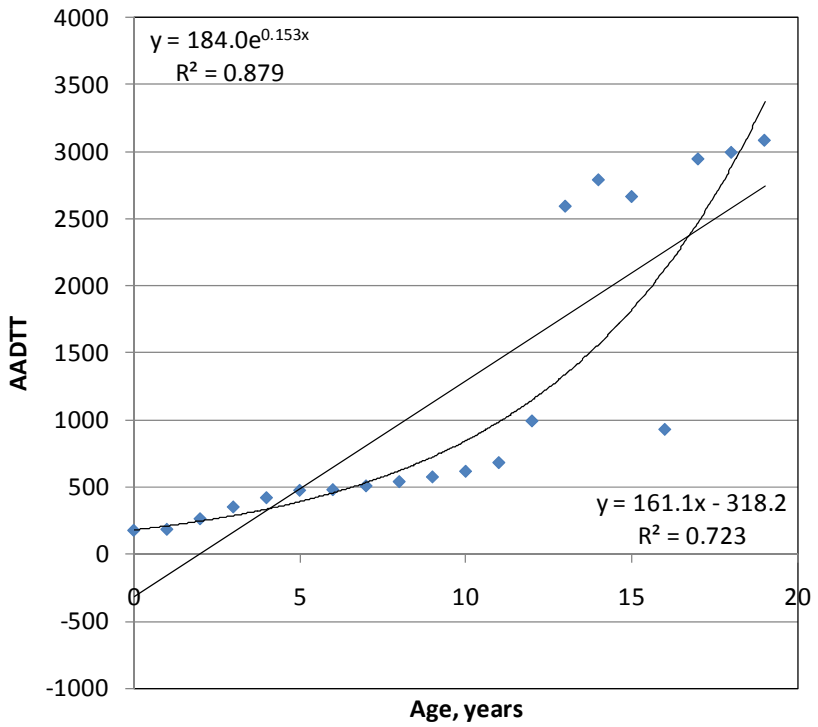

Figure D-11. Plot showing AADTT versus age for project LTPP 3015.

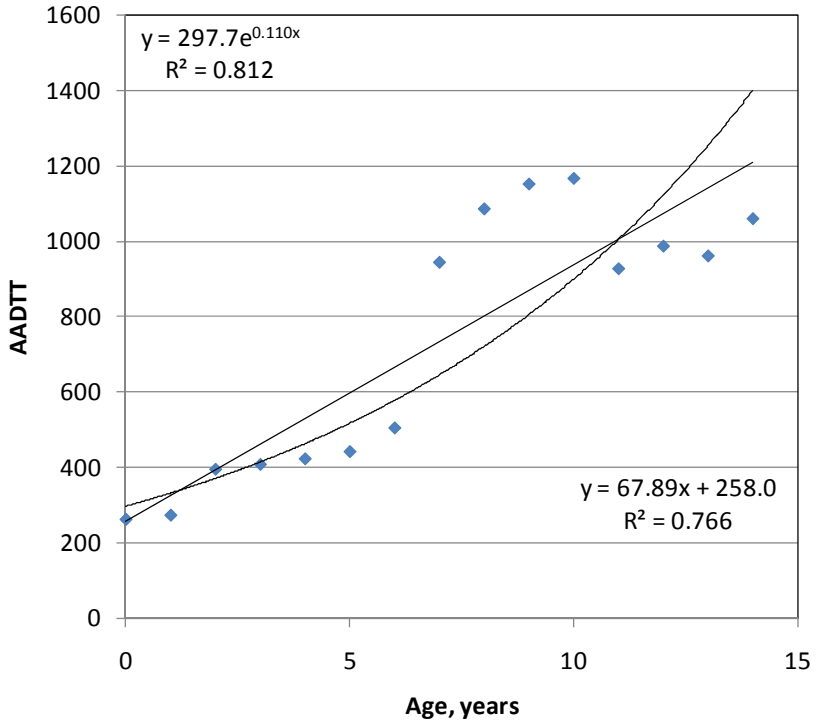

Figure D-12. Plot showing AADTT versus age for project LTPP 7082.

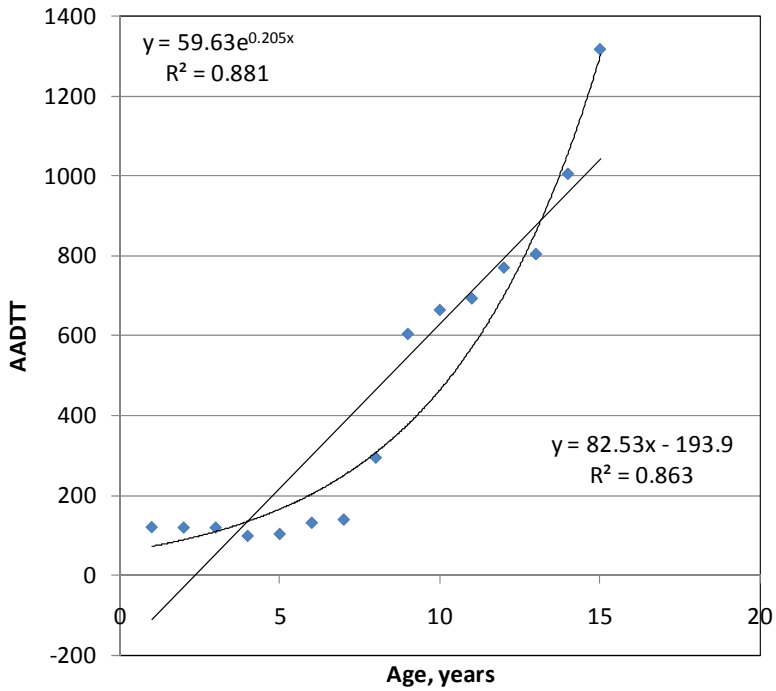

Figure D-13. Plot showing AADTT versus age for project LTPP 7083.

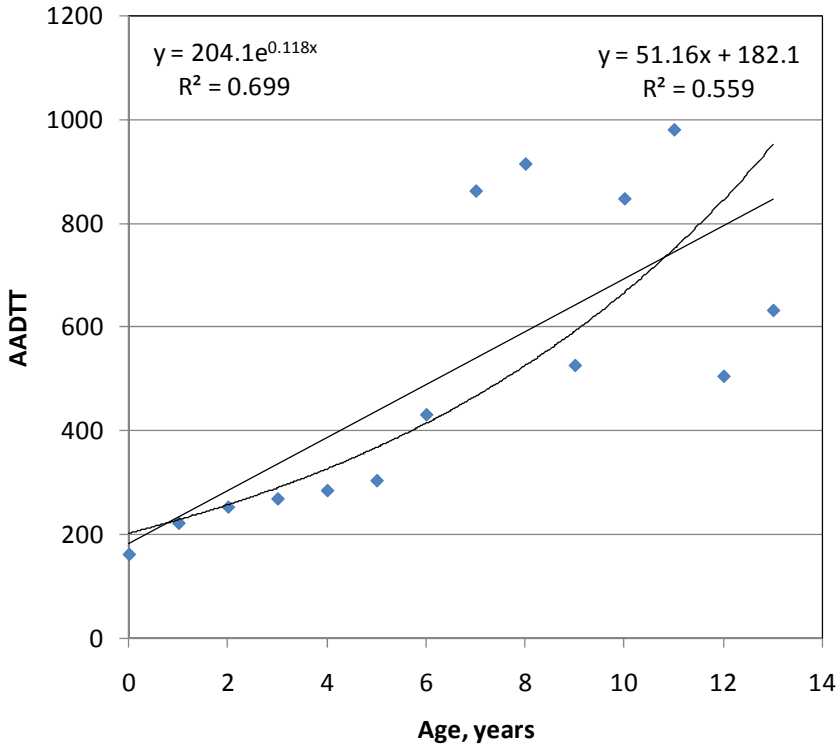

Figure D-14. Plot showing AADTT versus age for project LTPP 7085.

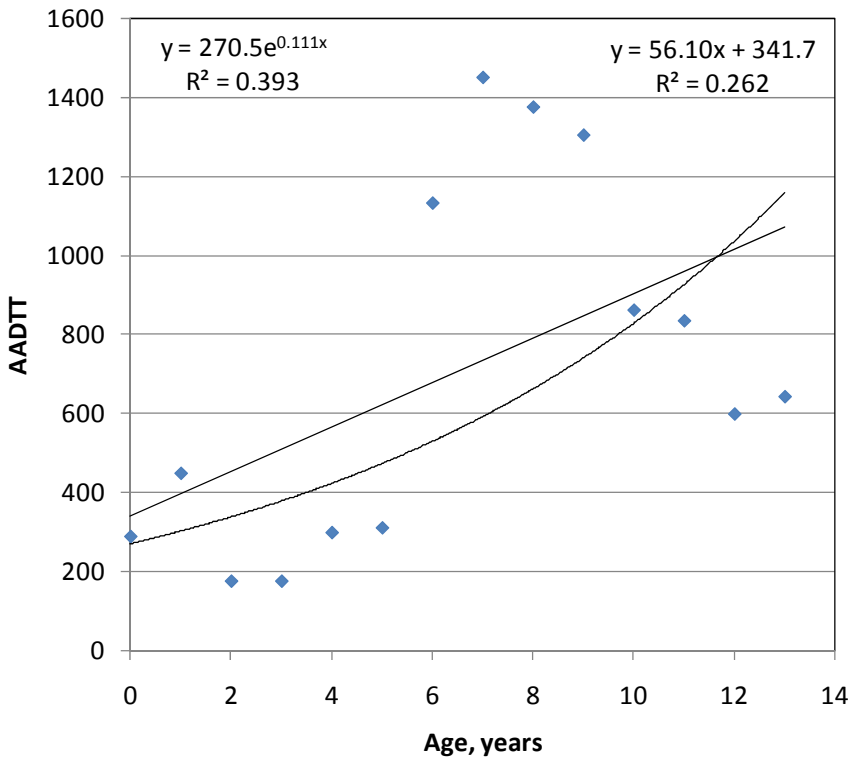

Figure D-15. Plot showing AADTT versus age for project LTPP 7086.

THIS PAGE INTENTIONALLY LEFT BLANK

APPENDIX E. SUBGRADE SOIL PROPERTIES CHARACTERIZATION

Minimum requirements for characterizing subgrade soil properties for use by the MEPDG (level 3) are as follows:

- Poisson's ratio
- Coefficient of lateral pressure, ko
- Resilient modulus at optimum moisture content
- Gradation
- Atterberg limits.

The MEPDG provides defaults for all of the key inputs listed above once the subgrade soil type is known (characterized using the AASHTO Soil Classification System or Unified Soil Classification System).

For the LTPP projects, detailed subgrade soil gradation and Atterberg limits information was obtained through soil sampling and laboratory testing (data was provided in the LTPP database). Also, the lab test information provided by LTPP was used to determine subgrade soil type (AASHTO Class) and default MEPDG soil properties as needed. For most LTPP projects, subgrade resilient modulus at optimum moisture content was determined through backcalculation using FWD deflection test data from LTPP. MEPDG default Poisson's ratio and coefficient of lateral pressure were assumed.

For the UDOT PMS projects, no lab test data was available. Subgrade soil type and AASHTO class were determined using project location information provided by UDOT (see Figure E-1) and soil properties data provided in the United States Department of Agriculture (USDA) SSURGO (Soil Survey Geographic) database. Subgrade soil type for a given UDOT PMS project was assumed based on the predominant subgrade soil type (see Figure E-2). The SSURGO database contains subgrade soils engineering and physical properties data among others. Specifically, the following subgrade soil engineering and physical properties were obtained from the SSURGO database (see Figure E-3):

- AASHTO classification.
- Clay content.
- Horizon depths (soil type layer thicknesses up to 120 inches).
- Liquid limit.
- Plasticity index.
- Sand content.
- Saturated hydraulic conductivity (Ksat).

- Silt content.
- Unified soil classification.
- Water table depth.

Using the data listed above, default MEPDG subgrade properties were determined and utilized. The SSURGO database is produced and distributed by the Natural Resources Conservation Service (NRCS).

Figure E-1. Project location information provided by UDOT for HMA_R2_03.

Map Unit Legend

Salt Lake Area, Utah (UT612)			
Map Unit Symbol	**Map Unit Name**	**Acres in AOI**	**Percent of AOI**
PsB	Preston sandy loam, 1 to 3 percent slopes	6.0	88.5%
Sd	Sandy alluvial lands	0.8	11.5%
Totals for Area of Interest (AOI)		6.8	100.0%

Figure E-2. Areal extent of soil types for HMA_R2_03 (note the predominant subgrade soil type is PsB).

HMA-R2-03

Engineering Properties

Salt Lake Area, Utah

[Absence of an entry indicates that the data were not estimated. This report shows only the major soils in each map unit]

Map symbol and soil name	Depth	USDA texture	Classification		Fragments		Percent passing sieve number--				Liquid limit	Plasticity index
			Unified	AASHTO	>10 Inches	3-10 Inches	4	10	40	200		
	In				*Pct*	*Pct*					*Pct*	
PsB:												
Preston	0-7	Sandy loam	SM	A-2, A-2-4, A-4	0	0	100	100	60-70	30-40	0-20	NP-5
	7-19	Loamy fine sand	SM	A-2, A-2-4, A-4	0	0	100	100	60-70	30-40	0-20	NP-5
	19-30	Loamy fine sand	SM	A-2, A-2-4, A-4	0	0	100	100	60-70	30-40	0-20	NP-5
	30-80	Sand	SM	A-2, A-2-4	0	0	100	100	50-70	5-15	0-20	NP-5

USDA Natural Resources Conservation Service

Survey Area Version: 4
Survey Area Version Date: 12/12/2006

Page 1

Figure E-3. Relevant soil properties obtained from the SSURGO database for HMA_R2_03.

THIS PAGE INTENTIONALLY LEFT BLANK